

**Patterns and Controls of CO₂ Fluxes in Wet Tundra Types
of the Taimyr Peninsula, Siberia - the Contribution of Soils
and Mosses**

**Muster und Steuerung von CO₂-Flüssen in nassen
Tundraformen der Taimyr Halbinsel, Sibirien - der Beitrag
von Böden und Moosen**

Martin Sommerkorn

**Ber. Polarforsch. 298 (1998)
ISSN 0176 - 5027**

Martin Sommerkorn

Institut für Polarökologie
Wischhofstr. 1-3, Geb. 12
D-24148 Kiel
Deutschland

Die vorliegende Arbeit ist die inhaltlich unveränderte Fassung einer Dissertation, die 1998 der Mathematisch-Naturwissenschaftlichen Fakultät der Christian-Albrecht-Universität zu Kiel vorgelegt wurde.

Contents

LIST OF ABBREVIATIONS	IV
1 SUMMARY AND CONCLUSIONS	1
1.1 ZUSAMMENFASSUNG UND SCHLÜßFOLGERUNGEN	5
2 INTRODUCTION	9
2.1 CO ₂ FLUXES, WHAT CAN THEY TELL?	9
2.2 TUNDRA ECOSYSTEMS: A CRITICAL FIELD FOR CO ₂ FLUX INVESTIGATIONS	11
2.3 OBJECTIVE OF THE STUDY	13
2.4 APPROACH	14
3 TAIMYR PENINSULA AND THE STUDY AREAS	17
3.1 TAIMYR PENINSULA, AN OVERVIEW	17
3.1.1 <i>The Area of Lake Labaz</i>	25
3.1.2 <i>The Area of Lake Levinson-Lessing</i>	27
4 METHODS	31
4.1 CO ₂ EXCHANGE	31
4.1.1 <i>Instrumentation Design</i>	31
4.1.2 <i>The Set-Up in the Field</i>	35
4.1.2.1 Soil Respiration Measurements	35
4.1.2.2 Soil-Moss System Measurements	38
4.1.2.3 Whole System Measurements	41
4.1.3 <i>The Set-Up in the Laboratory: Water Table Experiments</i>	43
4.1.4 <i>Data Handling</i>	45
4.1.5 <i>Modelling</i>	48
4.1.6 <i>Statistics</i>	53
4.2 MESO- AND MICROCLIMATOLOGICAL MEASUREMENTS	54
4.3 VEGETATION ANALYSIS AND SAMPLING FOR VASCULAR PLANT BIOMASS	54
4.4 ANALYSIS OF BACTERIAL BIOMASS	56
5 RESULTS	57

5	RESULTS	57
5.1	DESCRIPTIVE RESULTS	57
5.1.1	<i>Lake Labaz</i>	57
5.1.1.1	Mesoclimate of the Field-Season	57
5.1.1.2	Characteristics of the Experimental Sites	58
5.1.1.2.1	Tussock Tundra	58
5.1.1.2.1.1	Vegetation and Vascular Plant Biomass	58
5.1.1.2.1.2	Soils	61
5.1.1.2.1.3	Soil Microclimate	62
5.1.1.2.1.4	Bacterial Biomass	64
5.1.1.2.2	Wet Sedge Tundra	65
5.1.1.2.2.1	Vegetation and Vascular Plant Biomass	65
5.1.1.2.2.2	Soils	67
5.1.1.2.2.3	Soil Microclimate	68
5.1.1.2.2.4	Bacterial Biomass	69
5.1.2	<i>Lake Levinson-Lessing</i>	70
5.1.2.1	Mesoclimate of the Field Season	70
5.1.2.2	Characteristics of the Experimental Sites	71
5.1.2.2.1	Low-Centre Polygonal Tundra	71
5.1.2.2.1.1	Vegetation and Vascular Plant Biomass	71
5.1.2.2.1.2	Soils	75
5.1.2.2.1.3	Soil Microclimate	76
5.1.2.2.1.4	Bacterial Biomass	78
5.2	EXPERIMENTAL RESULTS	80
5.2.1	<i>Soil Respiration Studies</i>	80
5.2.1.1	Experiments in the Field	80
5.2.1.1.1	Lake Labaz	81
5.2.1.1.2	Lake Levinson-Lessing	87
5.2.1.2	Experiments in the Laboratory	90
5.2.1.3	Modelling of Soil Respiration in Tundra Systems	94
5.2.1.3.1	Balancing the CO ₂ Efflux of Soil Respiration	96
5.2.1.3.2	Performance of the Soil Respiration Process	99
5.2.1.3.2.1	Temperature Response	100
5.2.1.3.2.2	Relative Temperature Sensitivity	102
5.2.1.3.2.3	Response to Depth to Water Table	104
5.2.1.3.2.4	Identifying Patterns	106
5.2.1.3.3	Simulating Scenarios for Soil Respiration	108
5.2.2	<i>Studies on CO₂ Fluxes of the Soil-Moss System Considering Moss Photosynthesis</i>	114
5.2.2.1	Experiments in the Field	115
5.2.2.1.1	Lake Labaz	115
5.2.2.1.2	Lake Levinson-Lessing	122
5.2.2.2	Moss Photosynthetic Performance	130
5.2.2.3	Balancing the CO ₂ Fluxes of the Soil-Moss System	132
5.2.3	<i>Studies on CO₂ Fluxes of the Whole System</i>	134
5.2.4	<i>Connecting the Subsystems</i>	138

6	DISCUSSION	143
6.1	CONTROL OF SOIL RESPIRATION IN TUNDRA SYSTEMS	143
6.1.1	<i>Microsite and Efflux Patterns</i>	144
6.1.2	<i>The Factor Water Table</i>	148
6.1.3	<i>The Factor Temperature</i>	151
6.1.4	<i>Microsite and Soil Respiration Potential</i>	154
6.2	THE ROLE OF MOSS ASSIMILATION AS A BUFFER FOR CO ₂ EFFLUXES FROM TUNDRA	155
6.2.1	<i>Microsite and Moss Photosynthesis</i>	156
6.2.2	<i>Microsite and Quantitative Aspects of Buffering</i>	164
6.3	TUNDRA SYSTEM CO ₂ FLUXES: CONTRIBUTIONS OF THE SUBSYSTEMS	167
6.4	TUNDRA CARBON BUDGETS: A MATTER OF SCALING	169
7	REFERENCES	173
8	ACKNOWLEDGEMENTS	188
9	APPENDIX	190

List of abbreviations

CO ₂	carbon dioxide
DW	dry weight
GMP	gross photosynthesis of mosses
LAI	leaf area index
max.	maximum value
min.	minimum value
NSF	net system flux
PD	depression microsite in the low-centre polygonal tundra
PH	high apex microsite in the low-centre polygonal tundra
PL	low apex microsite in the low-centre polygonal tundra
PPFD	photosynthetic photon flux density
Q ₁₀	temperature quotient
SMR	respiration of the soil-moss system
ST2	soil temperature at 2 cm depth
TD	depression microsite in the tussock tundra
temp.	temperature
TH	moss hummock microsite in the tussock tundra
TT	tussock microsite in the tussock tundra
WS	wet sedge tundra
WT	soil water table
WW	wet weight

1 Summary and Conclusions

The goal of this study was to gain an understanding of the small-scale variability of CO₂ fluxes in wet tundra types. The investigation aimed at showing the spatial variability of the magnitude of CO₂ fluxes and at explaining differences in the mode of operation of their driving forces. Due to the fine-grained heterogeneity of the tundra, an understanding of the small-scale patterns can increase the insight into functional interrelations of the ecosystem. The study focused on the CO₂ fluxes from soils and the soil-covering moss layer. The CO₂ efflux from the soil to the atmosphere (soil respiration) describes the mobilization of carbon from the soil organic matter, the largest carbon store of the tundra. Mosses form the extensive interface between soil and atmosphere in tundra. Via their photosynthesis, they function as a filter for the CO₂ efflux originating from soil respiration.

To accomplish the overall goal, an existing measuring-technique was refined and a new method was developed: The application of CO₂ gas-exchange in dynamic differential mode resulted in the high-resolution capture of the CO₂ fluxes both in time and space. Continuous *in situ* measurements of the soil-moss system were accomplished by means of a transparent and conditioned chamber. The model used for describing the temperature response of soil respiration (Lloyd and Taylor 1994) allowed for a changing temperature sensitivity of the process across the temperature range. This provided an additional parameter for the description of CO₂ flux control. Individually fitted models describing the CO₂ fluxes of each investigated microsite permitted the identification of spatial differences with respect to the mode of operation of the controlling factors. Correlating the obtained model parameters with biotic and abiotic site characteristics of the microsities allowed to describe the control of CO₂ fluxes on a higher level.

Field experiments were carried out at seven microsities in three tundra types of the Taimyr Peninsula, North Siberia, during July and August of 1995 and 1996. At the intensive study site "Lake Labaz" within the belt of the "Southern Arctic Tundra", a tussock tundra and a wet sedge tundra were investigated. Within the belt of the "Typical Arctic Tundra", measurements were carried out in a low-centre polygonal tundra at Lake Levinsson-Lessing.

The diurnal course of soil respiration of all microsities was determined by depth to water table and soil temperature at two centimetres depth. The position of the water table controlled the total level of soil respiration by determining the soil volume available for aerobic processes.

The soil temperature modified this signal level. The high correlation of soil respiration with a temperature close to the soil surface indicates the source for the bulk of the respired CO₂ to be in the uppermost horizon. An individually fitted soil respiration model on the basis of the position of the water table and soil temperature at two centimetres depth was capable to explain more than 90 % of the variations of soil respiration. Differences in the magnitude of the CO₂ fluxes were much greater between directly adjacent microsites than between the different study areas. The highest daily means of soil respiration of 10.9 g CO₂*m⁻²*d⁻¹ were obtained at the comparatively dry microsites in the tussock tundra (tussock, moss hummock). These microsites also showed the lowest positions of the water table and the highest soil temperatures. The lowest daily means of soil respiration were measured at the wet and cold depressions of the tussock tundra and the polygonal tundra, as well as in the wet sedge tundra. When focusing on the relative potential of soil respiration instead of on the absolute magnitude of fluxes, a contrasting pattern was found. The wet and cold microsites showed a much greater relative response to changes in water table position and soil temperature than the dryer, warmer microsites. Two factors were responsible for this pattern. First, the Q_{10} , as a measure of the relative temperature sensitivity, ranged from 2.2 to 3.0 at the wet microsites, in combination with the mean soil temperature. Furthermore, the increase of the Q_{10} with decreasing temperature was much more pronounced at the wet microsites. Second, the response of soil respiration to water table position was much stronger at positions close to the soil surface, in particular at the wet microsites. The correlation analysis revealed that both parameters - high Q_{10} values and strong response to changes in depth to water table - can be explained by the availability of carbon for metabolic purposes.

The described process patterns of soil respiration also determined the response of the three different tundra types to scenario simulations with altered water table and soil temperature regimes. The calculation of the CO₂ efflux for the tundra types on the basis of the relative area shares of the microsites showed that the greatest relative response of soil respiration occurred in the homogeneously wet area of the wet sedge tundra. However, the tussock tundra showed the highest absolute CO₂ effluxes for all scenario calculations.

The mosses of the investigated communities showed high water contents during the experimental periods, indicating that they were capable of using the soil water as water supply. From the observation that soil respiration exceeded moss photosynthesis during extended periods of the day, a CO₂-enriched immediate environment of the mosses is inferred.

The temperature of the photosynthetically active parts of the mosses was affected by the degree of vascular plant coverage and the position of the water table. The *in situ* measuring method of CO₂ fluxes of the soil-moss system developed in the scope of this study guaranteed the maintenance of the natural conditions (water content, CO₂ concentration, light and temperature gradients) over the experimental periods. The photosynthetic capacity of the moss communities was higher at the dryer microsites as compared to the wet microsites. The mosses of the dry microsites achieved maximum gross photosynthetic rates of 450 mg CO₂*m⁻²*h⁻¹ with saturating irradiances of 450 μmol*m⁻²*s⁻¹. In contrast, the mosses of the wet microsites showed maximum rates of 80 mg CO₂*m⁻²*h⁻¹ and they were light saturated already at 100 μmol*m⁻²*s⁻¹.

The soil-moss systems of all microsites investigated showed a net loss of CO₂ to the atmosphere on the daily scale. The absolute net effluxes ranged from 0.07 g CO₂*m⁻²*d⁻¹ to 4.65 g CO₂*m⁻²*d⁻¹. The highest relative reductions of the CO₂ efflux originating from soil respiration by the photosynthesis of the mosses were achieved at the low-apex of the polygonal tundra. Here, the mosses assimilated 99 % of the soil-respired CO₂ on a daily scale. The lowest relative reduction rates were obtained in the wet sedge tundra, with also 35 % of the CO₂ efflux assimilated again. Neither the relative reduction of the CO₂ efflux nor the absolute net CO₂ flux of the soil-moss system could be linked to an overall pattern. Both were determined by the microsite dependent interplay of microclimatic parameters.

The whole system (soil, moss, vascular plants) of the depression of the polygonal tundra at Lake Levinson-Lessing was a strong sink for atmospheric carbon during the experimental periods. Carbon was accumulated with rates of 4.8 and 5.7 g CO₂*m⁻²*d⁻¹. The bulk of the CO₂ gain was contributed by the vascular plants, mosses accounted for 26 and 31 % of the total assimilation. Total assimilation rates at the microsite may be reduced by low irradiance levels, since the photosynthesis of the vascular plants was not light-saturated until 700 μmol*m⁻²*s⁻¹. The contribution of the aboveground portion of the vascular plants to the total system respiration was only 10 %. Therefore, the water table determined the total system respiration through its control of soil respiration. Thus, the position of the water table controlled the net CO₂ flux of the whole system over a wide range of irradiance conditions.

Conclusions

- Differences in magnitude and controls of CO₂ fluxes in the tundra were assigned to the microsite scale of the tundra. Therefore, measurements on this scale are especially useful for the revelation of functional interrelations in this ecosystem.
- The method of CO₂ exchange in dynamic mode was especially capable for the high resolution capture of data both in time and space. This proved to be important for the correlation of the observed fluxes with the controlling variables and therefore for the revelation of process differences. This was in particular valid for measurements of moss photosynthesis, because irradiance changes within short intervals. The newly developed soil-moss system chamber permitted measurements of the CO₂ fluxes of the structurally intact system for the first time.
- The application of a soil respiration model which was individually fitted to each microsite allowed the quantification of process parameters and their correlation with microsite characteristics. In particular the use of a temperature model which allowed for a changing temperature sensitivity of the process across the temperature range (Lloyd and Taylor 1994) provided an important additional process parameter.
- Soil water table is the primary controlling factor for the carbon balance of wet tundra types. On the one hand, it directly controls the aerated soil volume and thus the total magnitude of soil respiration. On the other hand, it affects the water content of the soil-covering moss layer, which can assimilate major portions of the soil-respired CO₂ in hydrated state. Because soil respiration contributes about 90 % of the total CO₂ efflux from a wet tundra type, the position of the water table determines the total magnitude of the net-system flux of the whole system as well.
- Sites with permanently high positions of water table comprise a great potential of soil respiration to change with altered water table positions and soil temperatures. High Q_{10} values at low temperatures, a strong increase of Q_{10} with decreasing temperatures, and a steep response of soil respiration to a falling water table are features of the soil respiration process at these sites. They can be explained by the availability of carbon for metabolic purposes.

1.1 Zusammenfassung und Schlußfolgerungen

Ziel dieser Studie war es, ein Verständnis der kleinräumigen Variabilität von CO₂-Flüssen in nassen Tundraformen zu erlangen. Die räumliche Variabilität in der Größenordnung der CO₂-Flüsse sollte aufgezeigt, und Unterschiede in der Wirkungsweise der sie steuernden Faktoren sollten beschrieben und erklärt werden. Durch ein Verständnis der kleinräumigen Muster ist in Tundren, mit der ihnen eigenen feingestreuten Heterogenität, Einsicht in ökosystemare Gesamtzusammenhänge möglich. Besonders berücksichtigt wurden in dieser Studie die CO₂-Flüsse der Böden und der bodenbedeckenden Moosschicht. Der CO₂-Fluß vom Boden zur Atmosphäre (Bodenatmung) beschreibt die Mobilisierung von Kohlenstoff aus der organischen Bodensubstanz, dem größten Kohlenstoffspeicher von Tundren. Moose bilden in Tundren flächendeckend die Grenzschicht zwischen Boden und Atmosphäre. Über ihre Photosynthese üben sie eine Filterfunktion auf das aus der Bodenatmung stammende CO₂ aus. Um das angestrebte Ziel zu erreichen, wurde eine bestehende Meßmethode verfeinert und eine neue Meßmethode entwickelt: Die Anwendung der CO₂-Gaswechsel-Methode im dynamischen System führte zu einer zeitlich und räumlich hochauflösenden Erfassung der CO₂-Flüsse. Eine neuentwickelte transparente, klimatisierte Kammer ermöglichte die kontinuierliche *in situ* Messung am ungestörten Boden-Moos-System. Das zur Beschreibung der Temperaturabhängigkeit der Bodenatmung verwendete Modell erlaubte eine Änderung der Temperaturempfindlichkeit des Prozesses über den Temperaturbereich. Diese Eigenschaft stellte einen zusätzlichen Faktor für die Beschreibung der Steuerung der CO₂-Flüsse zur Verfügung. Durch eine individuelle Modellierung der CO₂-Flüsse der untersuchten Kleinstandorte konnten räumliche Unterschiede in der Wirkungsweise der Steuerfaktoren quantifiziert werden. Die Korrelation der Modellparameter mit den biotischen und abiotischen Charakteristika der Kleinstandorte erlaubte Aussagen über die Kontrolle der CO₂-Flüsse auf einem höheren Niveau.

Während der Monate Juli und August 1995 und 1996 wurden Messungen an sieben Kleinstandorten in drei Tundraformen der Taimyr-Halbinsel in Nord-Sibirien durchgeführt. Am Standort „Labaz-See“ in der „südlichen arktischen Tundra“ wurden die „Tussock-Tundra“ und die „Wet-Sedge-Tundra“ untersucht, in der „typischen arktischen Tundra“ am Standort „Levinson-Lessing-See“ wurden Messungen in der „Low-Centre-Polygon-Tundra“ durchgeführt.

Der Tagesgang der Bodenatmung aller Kleinstandorte wurde durch den Bodenwasserstand und die Bodentemperatur in zwei Zentimeter Tiefe bestimmt. Indem er die Mächtigkeit des für aerobe Prozesse zur Verfügung stehenden Bodenvolumens bestimmte, gab der Bodenwasserstand die Größenordnung der Bodenatmung vor. Auf dieses Niveau konnte die

Bodentemperatur modifizierend einwirken. Die hohe Korrelation der Bodenatmung mit einer Bodentemperatur nahe der Bodenoberfläche zeigt, daß der Großteil des CO_2 aus dem obersten Bodenhorizont freigesetzt wird. Ein auf der Grundlage von Bodenwasserstand und Bodentemperatur in zwei Zentimeter Tiefe individuell an die einzelnen Kleinstandorte angepaßtes Bodenatmungsmodell konnte mehr als 90 % der Variationen der Bodenatmung erklären. Die Unterschiede der Stoffflüsse zwischen den unmittelbar benachbarten Kleinstandorten waren wesentlich größer als zwischen den unterschiedlichen Untersuchungsgebieten. Die höchsten Tagesmittel der Bodenatmung von $10,9 \text{ g CO}_2 \cdot \text{m}^{-2} \cdot \text{d}^{-1}$ wurden an den trockeneren Kleinstandorten der „Tussock-Tundra“ („Tussock“, „Moss-Hummock“) gemessen. Diese Kleinstandorte wiesen auch die niedrigsten Bodenwasserstände und die höchsten Bodentemperaturen auf. Die niedrigsten täglichen Bodenatmungsraten von $2,6 \text{ g CO}_2 \cdot \text{m}^{-2} \cdot \text{d}^{-1}$ wurden an den nassen und kalten Depressionen von „Polygon-Tundra“ und „Tussock-Tundra“, sowie in der „Wet-Sedge-Tundra“ gemessen.

Im Gegensatz zu den absoluten Stoffflüssen stand das relative Potential der Bodenatmung der Kleinstandorte. Die nassen, kalten Kleinstandorte zeigten eine wesentlich stärkere relative Reaktion der Bodenatmung auf Änderungen der Bodenwasserstände und Bodentemperaturen als die trockeneren, wärmeren Kleinstandorte. Zwei Faktoren verursachten dieses Muster. Erstens lag der Q_{10} -Wert, das Maß für die relative Temperaturempfindlichkeit, bei den mittleren Bodentemperaturen der nassen Standorte zwischen 2,2 und 3,0, bei den trockeneren Standorten hingegen nur zwischen 1,2 und 1,6. Außerdem war die Zunahme des Q_{10} mit fallender Temperatur bei den nassen Standorten wesentlich ausgeprägter als bei den trockeneren Standorten. Zweitens zeigte die Wasserstandsabhängigkeit der Bodenatmung einen sehr viel steileren Verlauf bei Wasserständen nahe der Geländeoberfläche verglichen mit Wasserständen in tieferen Horizonten, vor allem bei den nassen Kleinstandorten. Die Korrelationsanalyse zeigt, daß beide Faktoren - hoher Q_{10} und steile Reaktion auf Wasserstandsschwankungen - standortübergreifend durch die Verfügbarkeit von umsetzbarem Kohlenstoff erklärt werden können.

Die beschriebenen Reaktionsmuster der Bodenatmung bestimmten auch das Verhalten der drei unterschiedlichen Tundraformen auf die Simulation von Szenarien mit geänderten Wasserstands- und Temperaturregimen. Berechnet auf der Grundlage der relativen Flächenanteile der Kleinstandorte waren die größten relativen Veränderungen der Bodenatmung in der homogen nassen Fläche der „Wet-Sedge-Tundra“ zu verzeichnen. Bei allen Szenarien zeigte die „Tussock-Tundra“ jedoch die höchsten absoluten CO_2 -Verluste.

Die Moosgesellschaften der untersuchten Kleinstandorte zeigten über den Untersuchungszeitraum hohe Wassergehalte, da sie fähig waren, das Bodenwasser als Wasserquelle zu nutzen. Aus der Tatsache, daß die Bodenatmung über weite Teile des Tages

die Moosphotosynthese übertraf, wird auf eine CO₂-Anreicherung der unmittelbaren Umgebung der Moose geschlossen. Die Temperatur der photosynthetisch aktiven Moosteile war standortabhängig vom Bedeckungsgrad der Gefäßpflanzen und der Position des Bodenwasserstandes beeinflusst. Durch die in dieser Arbeit entwickelte Methode der *in situ* Messung des Boden-Moos-Systems waren die natürlichen Rahmenbedingungen (Wassergehalt, CO₂-Absolutkonzentration, Licht- und Temperaturgradienten) über den Versuchszeitraum gewährleistet. Die Photosynthesekapazität der Moosgesellschaften der trockeneren Kleinstandorte war größer als die der nassen Kleinstandorte. Die Moose der trockeneren Standorte erreichten maximale Bruttphotosyntheseraten von 450 mg CO₂*m⁻²*h⁻¹ bei Sättigungslichtstärken von 450 μmol*m⁻²*s⁻¹. Dagegen zeigten die Moose der nassen Standorte maximale Raten von 80 mg CO₂*m⁻²*h⁻¹ und waren schon bei 100 μmol*m⁻²*s⁻¹ lichtgesättigt.

Alle untersuchten Boden-Moos-Systeme zeigten im Tagesgang eine Nettofreisetzung von CO₂ an die Atmosphäre. Die absoluten Nettoausträge lagen zwischen 0,07 g CO₂*m⁻²*d⁻¹ und 4,65 g CO₂*m⁻²*d⁻¹. Die Moosphotosynthese erreichte die höchsten Reduktionen des durch die Bodenatmung freigesetzten CO₂ am „Low-Apex“ Kleinstandort in der „Polygon-Tundra“. Hier wurden im Tagesgang bis zu 99 % des durch die Bodenatmung freigesetzten CO₂ in der Mooschicht refixiert. Die niedrigsten Refixierungsraten wurden in der „Wet-Sedge-Tundra“ gemessen, aber auch hier betrug die relative Reduktion der CO₂-Freisetzung 35 %. Weder die relative Reduktion der CO₂-Freisetzung, noch der absolute Nettofluß des Boden-Moos-Systems ließen ein standortübergreifendes Muster erkennen, sondern waren standortabhängig und von der tagesspezifischen Kombination der mikroklimatischen Parameter bestimmt.

Das Gesamtsystem (Boden, Moos, Gefäßpflanzen) der Depression der Polygon-Tundra am Levinson-Lessing See stellte im Versuchszeitraum eine starke Senke für atmosphärisches CO₂ dar. Kohlenstoff wurde mit Raten von 4,8 und 5,7 g CO₂ m⁻²*d⁻¹ festgelegt. Der Hauptanteil des CO₂-Gewinns wurde von den Gefäßpflanzen getragen, Moose steuerten 26 und 31 % der Assimilation bei. Da die Photosynthese der Gefäßpflanzen erst bei Lichtstärken über 700 μmol*m⁻²*s⁻¹ gesättigt war, können die Assimilationsraten durch niedrige Einstrahlung begrenzt werden. Der Beitrag der überirdischen Pflanzenteile zur Gesamtrespiration des Systems war nur 10 %. Der Bodenwasserstand bestimmte damit durch die Bodenatmung die Respiration des Gesamtsystems. Über einen weiten Bereich von Lichtverhältnissen kontrolliert somit der Bodenwasserstand die Größenordnung des Netto-CO₂-Flusses des Gesamtsystems.

Schlußfolgerungen

- Da sich die Unterschiede in der Qualität und Quantität der CO₂-Flüsse in der Tundra auf dem Maßstab der Kleinstandorte erklären lassen, sind Messungen auf diesem Maßstab besonders dafür geeignet, funktionale Zusammenhänge in diesem Ökosystem aufzuzeigen.
- Die Methode des CO₂-Gaswechsels im dynamischen System war besonders dafür geeignet, zeitlich und räumlich hochauflösende Daten zu erfassen. Das war wichtig für die Korrelation der CO₂-Flüsse mit den Steuerfaktoren und damit für die Herausarbeitung von Prozessunterschieden. Dies gilt insbesondere für die Erfassung der Moosphotosynthese, da sich Änderungen der Einstrahlung sehr kurzfristig vollziehen. Der Einsatz der neukonstruierten Boden-Moos-Küvette erlaubte erstmals die Beobachtung der CO₂-Flüsse des strukturell intakten Systems.
- Die Anwendung eines individuell an den Kleinstandort angepaßten Bodenatmungsmodells erlaubte die Quantifizierung von Prozessparametern und deren Korrelation zu Charakteristika der Kleinstandorte. Insbesondere die Verwendung eines Temperaturmodells mit der Möglichkeit einer über den Temperaturbereich wechselnden Temperaturempfindlichkeit des Prozesses (Lloyd und Taylor 1994) erbrachte eine wichtige zusätzliche Steuergröße.
- Der Bodenwasserstand ist der bestimmende Parameter für die Kohlenstoffbilanz nasser Tundraformen. Er kontrolliert einerseits unmittelbar den für aerobe Umsatzprozesse zur Verfügung stehenden Bodenraum und damit das absolute Niveau der Bodenatmung. Zum anderen wirkt er mittelbar auf den Wassergehalt der den Boden bedeckenden Moosschicht. Die Moose können im nassen Zustand große Teile des durch die Bodenatmung freigesetzten CO₂ refixieren. Da die Bodenatmung etwa 90 % des CO₂ Verlustes des Gesamtsystems einer nassen Tundraform ausmacht, bestimmt der Bodenwasserstand ebenfalls mittelbar den Netto-CO₂-Fluß dieses Systems.
- An Standorten mit dauerhaft hohem Bodenwasserstand ist das relative Potential der Bodenatmung auf eine Veränderung von Bodenwasserständen und Bodentemperaturen zu reagieren wesentlich größer als an trockeneren und wärmeren Standorten. Hohe Q_{10} Werte bei kalten Temperaturen, eine starke Steigerung der Q_{10} -Werte mit sinkender Temperatur, und ein steiler Anstieg der Bodenatmung bei sinkendem Wasserstand sind Prozesseigenschaften der Bodenatmung der nassen Standorte und können mit der Verfügbarkeit von umsetzbarem Kohlenstoff erklärt werden.

2 Introduction

2.1 *CO₂ Fluxes, What Can They Tell?*

Two contrarotating fluxes describe the CO₂ exchange between ecosystems and the atmosphere: The assimilation of plants driven by light leads to a flux from the atmosphere into ecosystems, and a variety of respiratory processes drive the flux in the opposite direction. As suggested by the relatively stable concentration of CO₂ in the atmosphere, these fluxes were tending towards an equilibrium during extended periods of biologically affected times of our planet. However, when referring to single ecosystems, the equilibrium can be widely shifted: Whereas an overweight of respiratory losses from the ecosystem to the atmosphere will sooner or later lead to a destruction of the system itself, an overweight of assimilation results in the development of carbon stocks. Measuring CO₂ fluxes of ecosystems or parts of them can thus lead to insights into the carbon balance of these systems. But extending the insight towards an understanding and quantification of the carbon balance of a system requires exact knowledge of all factors controlling all processes that result or may result in carbon fluxes. Moreover, the mode of operation of these factors has to be appointed to its relevant time scale. In present times, even with quite well understood and comparably simple systems like e.g. taiga “attempts to estimate the carbon balance are rudimentary at best“ (Oechel and Lawrence 1985). Since it is the character of science that problems of this kind result in motivation rather than surrender, considerable effort has been undertaken in recent years to clarify the contributions and control of subsystems to the carbon balance of ecosystems.

An important part of the mentioned respiratory losses of a system takes place in the soil by means of microbial respiration and root respiration. These processes, whose combination has been defined as soil respiration, are of particular interest in the scope of control of ecosystem CO₂ fluxes, because their response is already determined by the quality and quantity of input of organic carbon and thus by parameters of the ecosystem itself. Furthermore, in particular the microbial respiration is often characterized by a considerable time lag to plant assimilation and thus describes the mobilisation of a carbon stock. Currently, about 80 % of the organic carbon in the world's terrestrial ecosystems is estimated to be present in soils (Post *et al.* 1985).

The determination of CO₂ fluxes, in particular soil respiration is a comparatively old story in nature sciences. Already Lundegårdh (1921) measured soil respiration in the field, and moreover, he did so using the “inverted-box-method“, a technique which is, though mostly modified, still in use in our times. It was his credit to define the term “soil respiration“ as the *in situ* CO₂ flux from the soil to the atmosphere which originates from microbial respiration as well as root respiration. His primary interest in soil respiration, however, was the supply of plants with CO₂, but this way of thinking proofs his ecological understanding of CO₂ fluxes. The measurement of soil respiration has gone multiple ways since then. Haber (1958) already differed between three different lines of investigations: The “physiological line“ contributes to an understanding of the efficiency of microbial populations (and partly also plant roots), and their reaction on biotic, abiotic and man-made factors (e.g. Domsch 1961, Anderson and Domsch 1978, Edwards 1989). Most of these studies were performed in the controlled environment of the laboratory by means of soil samples. The field of the “physical line“ is aiming on the factors controlling the emission of CO₂ from the soil into the atmosphere. While the process was already explained to be of diffusive character by Romell (1922), meteorological, hydrological and soil physical modifications of pure diffusion processes in various special cases were elaborated later (e.g. Albertsen 1977). The third line Haber distinguished is the “ecological line“, meaning the assessment of soil respiration in an ecosystem context. In particular in the applied agricultural science, this field of research solved questions of fertilisation and turnover ratios of organic matter. But also the characteristics of soil respiration of natural systems with respect to different soils and climates was a field of intensive research (summarized in Singh and Gupta 1977, Raich and Schlesinger 1992). In the last decades, in particular studies on natural ecosystems have contributed to an understanding of soil respiration in the context of ecosystem processes and their control (e.g. Cernusca 1991, Shaver 1996). The identification and mode of operation of factors controlling soil respiration, and their relevance for the CO₂ fluxes of the whole ecosystem was a primary aim of these studies, and thus measurements of CO₂ fluxes became the field of physiological ecologists. The extensive efforts to come to an assessment of CO₂ fluxes of ecosystems has -besides their contribution to a fundamental understanding of ecosystem function- of course to be seen in the context of predicting ecosystem processes in the scope of the anticipated climate change.

2.2 Tundra Ecosystems: a Critical Field for CO₂ Flux Investigations

*"...and they call the tundra places overgrown with moss."
Lomonosov, "On Wintry Paths"*

Tundra is the common term for the landscape which is situated north of the treeline along the coast of the Arctic Ocean, and stretches out to the polar desert (Chernov 1985). Tundra covers about $5.71 \cdot 10^6$ km² world-wide (Miller *et al.* 1983). Already the origin of the word tundra, which is derived from the Sami word "tunturi" (completely treeless height) explains an essential character of this region, and furthermore reminds that this term is also used to denote a special type of vegetation. Tundra can be characterized as treeless landscape where communities of shrubs, dwarf-shrubs, herbaceous perennials, mosses, and lichens dominate on wet soils with gleyic features (Aleksandrova 1980). The most obvious floristic property of tundra is the dominance of mosses, representing the "environment-forming building-blocks of the vegetation" (Chernov 1985). The moss carpet covering nearly the whole surface of the tundra serves as an insulator, effectively restricting the warming of the soil below during summer (Kershaw 1978). It also has a key role in evaporation and thus for the whole energy budget of tundra (Tenhunen *et al.* 1992).

On the side of the abiotic components, the most important characteristic of tundra soils is the occurrence of permafrost, meaning that parts of the ground are perennially frozen. Summer season leads to the development of an active layer, the uppermost centimetres to decimetres which thaw and freeze annually. The phase transition results in phenomena as solifluction and sorting of soil material, and due to the resulting frost patterns of various kind, a considerable microrelief is developed in many cases (summarized in Washburn 1979).

Although precipitation is mostly quite limited in tundra regions, evaporation is restricted due to low temperatures (Barry *et al.* 1981). Furthermore, the occurrence of permafrost restricts drainage in tundra soils to lateral movement only, so that 85 to 90 % of tundra soils are very wet (Rieger 1974). Particularly in levelled areas, the water table is situated directly below the soil surface throughout the growing season (Kane *et al.* 1992).

The wet and cold conditions in the soils have led to the above mentioned shift between the main CO₂ fluxes of the tundra ecosystem: Because decomposition is widely restricted under the unfavourable conditions of the soils, assimilation has exceeded respiration approximately since the last glaciation, thus leading to the development of huge carbon stocks (Gorham 1991). 90 to 98 % of the total carbon of the tundra ecosystem is located in the soils (Miller *et*

al. 1983). These carbon stocks are mostly present as thick organic surface-layers of poorly decomposed plant material, densely interwoven with the moss carpet (Everett *et al.* 1981). Of the world-wide estimate of organic carbon located in soils, 21 % (Raich and Schlesinger 1992) to 27 % (Post *et al.* 1982) is believed to be present in soils of tundra and taiga.

Until recently the main motivation for research in physiological ecology in arctic areas has been to understand how organisms cope with the environment, rather than questioning the role of the organisms in controlling ecosystem processes (Chapin *et al.* 1992). But, as indicated by the majority of current state-of-the-art reports of arctic projects, we often still know least about those physiological processes, that are most critical in determining controls over ecosystem function (Billings 1997). The Arctic, however, provides favourable conditions for an understanding of ecosystem processes with the approaches of physiological ecology, since the low stature and fine grained spatial heterogeneity of arctic soil-vegetation systems make it practical to measure both physiological and ecosystem responses on the same scale. The link between physiological ecology and ecosystem processes was actively developed during the International Biological Programme (IBP), from 1966 to 1974 (e.g. Rosswall and Heal 1975, Tieszen 1978a, Bliss *et al.* 1981), but has been logically picked up by several recent research projects and scientific programs (e.g. Oechel *et al.* 1997, Reynolds and Tenhunen 1996). Thus, physiological ecology has widely contributed to a progressing understanding of ecosystem processes in the Arctic in the last 20 years. There are, however, considerable gaps in knowledge: The tundra of the former Soviet Union covers an area of $3.21 \cdot 10^6$ km² (Tikhomirov *et al.* 1981), which represents about 56 % of the world-wide tundra. Until the beginning of this decade, only sparse information on CO₂ fluxes and carbon balance of Siberian tundra were available for the scientific community. It was due to the process of political opening of the former Soviet Union that it became possible for scientists to arrange for research projects in these vast areas.

Another gap in knowledge exists due to the lack of field studies on the intact system *in situ*, which are widely hampered due to logistical and technical constraints. Although considerable effort has been undertaken in recent years in Alaskan tundra (e.g. Poole and Miller 1982, Peterson *et al.* 1984, Grulke *et al.* 1990, Oberbauer *et al.* 1996b), there is still a great demand for research, in particular in the tundra regions of the former Soviet Union.

In our rapidly changing world, scientists can not deny their responsibility to make statements on the effect of the anticipated climate change on their field of research (although summary trials may have led to increased confusion rather than being a valuable contribution). This is particularly valid in the case of ecosystem research in the Arctic: The increase of the atmospheric CO₂ concentration mainly caused by the burning of fossil carbon and massive deforestation will most presumably warm the globe most strongly around the poles (Solomon *et al.* 1985). This will have widespread effects on other components of the arctic climate, such as evaporation, cloudiness, and precipitation (Maxwell 1992). The climate in turn determines the thermal and hydrological regimes of soils, and vegetation determines the degree of coupling between climate and soils. In combination with the large carbon pools present in arctic soils this is believed to lead to a particularly strong positive feedback of arctic areas to the increase of atmospheric CO₂ (Oechel and Billings 1992). Deeper active layers, thermokarst erosion, and lower water table can lead to better conditions for decomposition, resulting in a pronounced efflux of CO₂ from arctic soils (Billings *et al.* 1982, 1983, 1984).

2.3 Objective of the Study

The overall objective of this study was to clarify the role of soil respiration and moss photosynthesis in wet tundra types of Taimyr Peninsula in the context of site characteristics. Special emphasis was given to factors controlling both processes, and to differences in the mode of operation of these factors with reference to the spatial heterogeneity. The following questions drove the study:

- Which differences exist between microsites and tundra types with respect to soil respiration?
- What are the factors controlling soil respiration in these tundra types, and are there differences in the mode of operation of the controlling factors between microsites?
- To which extent can moss photosynthesis buffer the CO₂ efflux originating from soil respiration to the atmosphere?
- What is the contribution of both processes regarding the CO₂ flux of the whole system?

Additionally, a technical aim was the refinement of a measuring technique which allows the most precise correlation of CO₂ effluxes from soil with the controlling factors, and the development of a mode of measurement for the CO₂ fluxes of the soil-moss system *in situ*.

The study was part of the multidisciplinary project “Environmental Development of Central Siberia during Late Quaternary“ (German Ministry of Science and Technology (BmBF) grant 03PLO14B), involving the Alfred Wegener Institute of Polar and Marine Research, Potsdam, the Institute of Soil Science, University of Hamburg, the Institute for Polar Ecology, University of Kiel, as well as the Institute for Arctic and Antarctic Research, St. Petersburg. This investigation was embedded in the research fields investigating recent processes in soils and soil microbial communities. In order to cover the great variety of climatic regions apparent on Taimyr Peninsula, research in the scope of the project was carried out along an approximately 1400 km long north to south transect extending from the high arctic desert of Severnaya Semlya to the taiga zone near Norilsk. Three expeditions to Taimyr Peninsula were performed in the years 1994-1996, two field-seasons (July-August 1995, July-August 1996) could be used as experimental campaigns within the scope of this thesis. Investigations were carried out at two localities, Lake Labaz, situated within the southern tundra zone, and Lake Levinson-Lessing, situated within the typical tundra zone.

2.4 Approach

This study aimed at explaining differences of magnitude and potential of CO₂ efflux at various microsites on the basis of their individual process performance as determined by site characteristics. In order to examine the system in the most authentic way possible, the study was performed as a field study.

There are several possibilities to assess process performance and controls of intact systems. Although trends in arctic research during recent years were leading towards manipulation studies (e.g. Oechel *et al.* 1992), which contributed to an increasing knowledge of ecosystem controls and reactions, this kind of studies bear some intrinsic constraints: By applying an altered parameter to a site which represents an integral of other than the changed conditions, these kind of studies tend to describe the short-term influence of a disruptive factor on a steady state system. This approach allows the triggering of system reactions and provokes the revelation of internal controls. However, manipulation studies does not describe steady states, but pathways between them. Moreover, the full effect of the disruptive factor on all levels of the manipulated system is hardly seen, because of time lags of reactions between levels (in particular within the “normal“ three years project period). In contrast, gradient or microsite studies describe processes on the basis of the whole sum of parameters which represent the investigated site in a more consistent way. The danger with this kind of approach is that the

study can develop to a “just-so story“ (biological processes run the way they do because the organisms are adapted to do so), so results may lack new knowledge and insight (Gould and Lewantin 1979). On the other hand, it seems most reasonable that the shift of ecosystem structure and function in response to climate change will occur on axes that are predictable from existing patterns and gradients (Tenhunen *et al.* 1992).

In this study the microsite approach was chosen to reveal differences of process properties determining the CO₂ fluxes as well as differences of factors controlling these processes. The disadvantages described above were avoided by the use of several methods which were not applied before in tundra ecosystem research and which are thus capable to offer new insights in the mode of operation of factors controlling CO₂ fluxes:

- The use of open system gas exchange instrumentation offered the chance to continuously capture CO₂ fluxes with high resolution in time. This allowed the most precise correlation of the observed response with controlling parameters and thus the revelation of process properties.
- The development of a method capable to measure the CO₂ fluxes of the soil-moss system *in situ* facilitated the observation of an intact system, which had to be separated for analysis in previous field-studies.

In order to keep the advantages of the high resolution of the captured data and in particular to allow the assessment of differences of process properties, the use of individually fitted models describing CO₂ fluxes was another important point of this study. This way of data evaluation helps to refine the results of experiments by filtering the mode of operation of single factors out of a whole set of factors affecting a process. Doing so can provide an understanding of the process itself (Jarvis 1993).

3 Taimyr Peninsula and the Study Areas

3.1 Taimyr Peninsula, an Overview

Geography

By stretching out from Middle-Siberia into the Arctic Ocean to nearly 78°N, the Taimyr Peninsula forms the northernmost outpost of the Eurasian continent (Fig. 2.1). From the river Jenessej (86°E) in the West to the river Khatanga (115°E) in the East, from the Plateau of Putorana (70°N) in the South to Cape Tscheljuskin in the North it covers an area of about 400 000 km² and thus equals Sweden in size (Matveyeva 1994). Franz (1973) even defines the river Olenjok (125°E) as the eastern border.

From South to North, the 1750 km of Taimyr Peninsulas' length can be divided into three main geographical units (Fig. 2.1): The North Siberian Lowland is a gently rolling plain, representing 50 % of the surface area of the peninsula. Its homogenous character is characterized by heights rarely exceeding 150 m a.s.l. and a dense hydrological network including smaller lakes of glacial origin as well as thermokarst-lakes. Bordering the North Siberian Lowland in the north the Byrranga Mountains stretch more or less east-west over nearly 1000 km with a width of about 50 to 180 km. They reach heights of 300 to 400 m a.s.l. in the western, and up to 1100 m in the eastern parts of the range. Partly within the Byrranga Mountains, partly adjacent to their southern flanks the Lake Taimyr covers an area of about 6000 km², thus representing the largest arctic freshwater lake. North of the mountain range a coastal plain stretches out to the Kara Sea on the western side and the Laptev Sea on the eastern side of Taimyr Peninsula (Franz 1973).

Man and Taimyr Peninsula

The first news the western world received about Taimyr Peninsula was published in the book "Reise in den äußersten Norden und Osten Sibiriens" by the Baltic natural scientist Alexander Middendorf (1867, c.f. Brunckhorst 1994). He travelled all Taimyr Peninsula on dog-sledge and small boats. The next contact with the inner parts of Taimyr Peninsula was established 1931 by the Arctic journey of the airship "Graf Zeppelin" (described in Eckener and Italiaander, 1979), which delivered first aerial photographs of low-centre polygons.

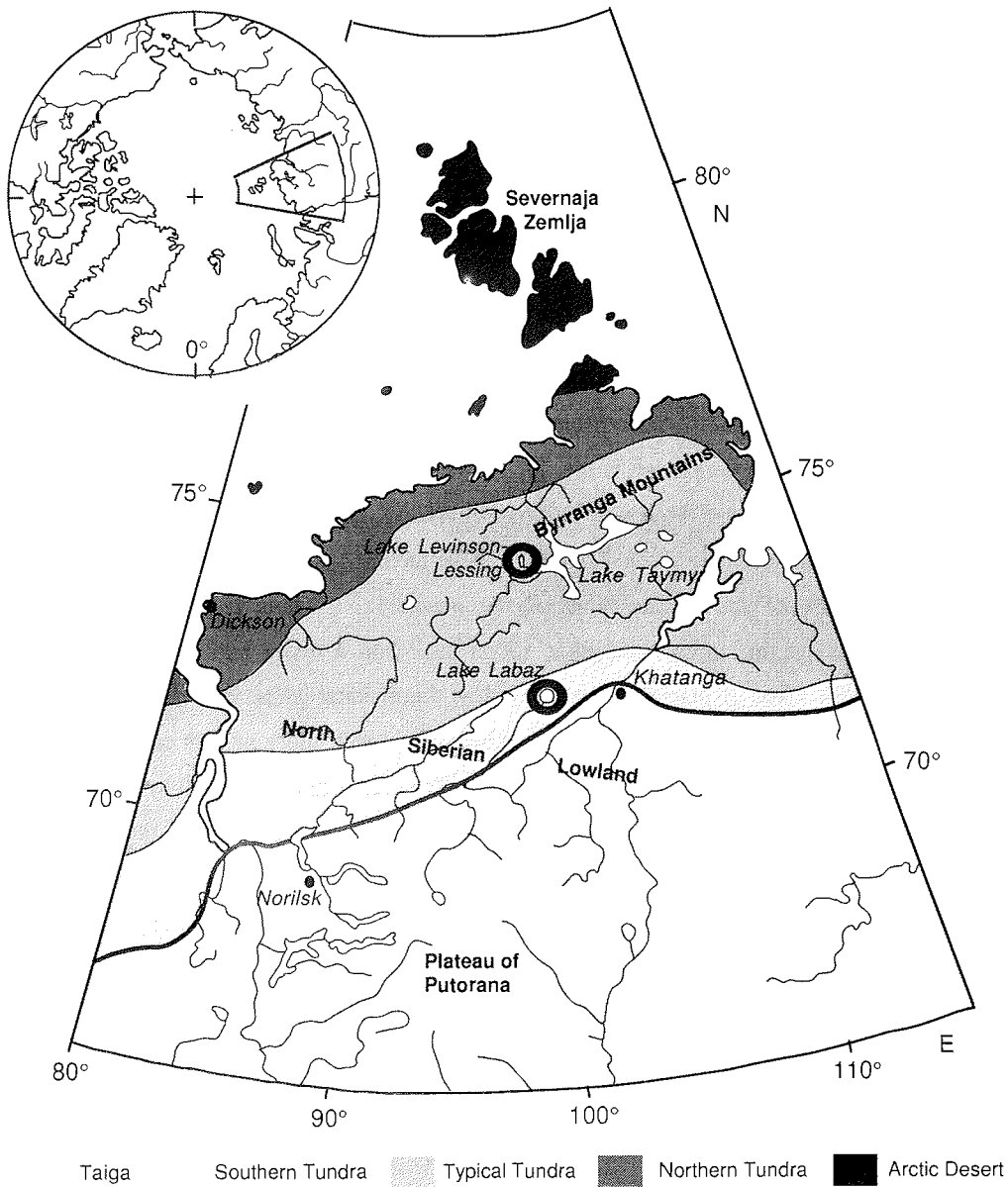


Fig. 2.1. Map of Taimyr Peninsula showing geographical and geobotanical units. The study areas Lake Labaz and Lake Levinson-Lessing are encircled. Borders of geobotanical units refer to Aleksandrova (1980), see paragraph "Vegetation" for details.

Although Taimyr Peninsula still belongs to the least settled and infrastructurally least developed areas of Siberia, lots of intensive research has been carried through in the second part of our century, in particular by Russian scientists. Since the beginning of the sixties a research station at the shores of Lake Taimyr ("Taimyr Lake Station") has been especially used for floristical and zoological research (e.g. Ignatenko 1971, Matveyeva 1971, Parinkina and Dokichayev 1979, Bab'yeva and Chernov 1983, Safronova and Sokolova 1989). During the IBP-project at the beginning of the seventies a total of four field sites on Taimyr Peninsula were under elaboration (Rosswall and Heal 1975). Besides these biologically-focused programmes, geological research and prospecting represents a major field (e.g. Samoilov 1995, Vernikosky 1996, Romanenko 1996).

Since the beginning of the nineties the Russian policy resulted in an opening of Siberian tundra-regions for scientists from western countries. Some initial expeditions by members of the WWF focused mainly on bird-protection and the declaration of protected areas (see below). Since then, several expeditions in particular by German and Scandinavian researchers have been carried through, mainly organized as cooperation between Russian and foreign scientists (e.g. Melles *et al.* 1994, Grönlund and Melander 1995, Siegert and Bolshiyarov 1995, Bolshiyarov and Hubberten 1996, Melles *et al.* 1997).

Ethnologists believe that man colonised the tundra landscape of Taimyr Peninsula during the early Palaeolithic period about 7-8000 years before present (Chernov 1985). Hunting reindeer was their main food source, although hunting birds and catching fish was also practised. It is more or less still these foodsources the indigenous people of the roughly 3000 "Dolgans", 1000 "Ngasans" and some few descendants of the "Nentsens" and "Evenkens" use in our times. Organized in Sowchos during the period of the USSR, these people were providing foodsupply for the regional mining-settlements, particularly Norilsk. In this way, they were able to continue parts of their traditional life and keep their identity, in particular during winter hunting trips for arctic fox and during summer-life in family-groups out in the tundra. With helicopter transportation of their harvest from their remote villages to the mining-settlements getting unaffordable during present times the fate of Taimyr Peninsula's indigenous people as tundra-people is increasingly uncertain.

Man's pressure on Taimyr Peninsulas tundra areas is immense in our times. The mining settlement of Norilsk with its smelters and 300000 inhabitants (Taimyr Peninsula as a whole: 350000) represents a major source of pollutants. Prospecting, exploration and exploitation in

the Russian Arctic is not at all a story of sustainability. Moreover, garbage treatment, hunting tourism and increasing scientific activities all add their share of pressures (Prokosch and Hötger 1995). An outline of threats for and recovery chances of arctic terrestrial ecosystems is given in Crawford (1997).

There is, however, also positive news. With parts of it already protected in 1979 and 1986, the "Great Arctic Reserve" on Taimyr Peninsula was inaugurated in 1993 covering an area roughly the size of Switzerland. It has the status of a "Sapovetnik", the most strictly protected area known in Russia. The main supporters for this reserve were the WWF and the Russian local authorities, the main goal is the protection of those areas on Taimyr Peninsula which are acting as a cradle for the majority of waders, ducks and geese using the "East Atlantic Flyway" and wintering in the Dutch-German-Danish Wadden Sea (Müller *et al.* 1993, Nowak 1995, Prokosch 1995).

Geology

From the geological point of view the North Siberian Lowland is part of the Jenessej-Chatanga-Trough. The Byrranga Mountains and the northern plain on the other side belongs to the Taimyr-Severnaja-Zemlja-Folded-Zone.

The North Siberian Lowland was lowered during the Jura, Palaeocene and Neocene and filled up to a thickness of 9000 m by sediments of shallow water- and continental origin consisting of sand and clay. During the Pleistocene transgressions, brackish and limnic sediments were added, the cold periods resulted in regressions and glaciation. Some authors (e.g. Isayeva 1984) state, that during the Sartan (= late Weichsel (Europe) or late Wisconsin (North America)) the North Siberian Lowland was an icefree periglacial area. Within the geological part of this project some more evidence was found that also the lowland was covered by glaciers during that period (C. Siegert, personal communication), which has been stated before (e.g. Grosswald 1989). Quaternary deposits reach thicknesses of up to 150 m.

The area of the present Byrranga Mountains formed a trough during the Carboniferous to Trias which functioned as a shallow water sedimentation area. Material mainly consists of clay, but also calcareous and coal deposits can be found. The thickness of these sedimentation layers reach up to 8000 m. The Byrranga Mountains as such were lifted up during the Pliocene, and nowadays their morphological character appears mainly shaped by the last glaciation periods as well as by present erosion caused by frost and solifluction. Marine

terraces found as high as 270 m a.s.l. strongly support the theory that the area is still lifted upwards (Khain 1985).

The maximum extent of permafrost can be found in the Byrranga Mountains and the adjacent lowland areas with depths reaching up to 800 m (Williams and Smith 1989).

Climate

The North of Middle-Siberia is generally characterized by a cold-dry-continental climate. The mean annual temperature is about -13°C . Heading northwards on Taimyr Peninsula, mainly the average summer temperatures vary according to latitude: Whereas the mean value for July is 12°C in the western parts of the North Siberian Lowland, it is only 4°C near Cape Tschelyuskin. Thus, the number of days above 0°C differs by around 20 days per year across Taimyr Peninsula, with 40-50 days in the South and 20-30 days in the North. Winter temperatures are more homogenous showing a mean value for January of around -31 to -34°C both in the North and the South (Matveyeva 1994).

Precipitation also varies from South to North: While the annual amount adds to 350 mm in the North Siberian Lowland, it only reaches values of 200 mm at the north coast (Matveyeva *et al.* 1975, Vasilyevskaja *et al.* 1975).

Additional to the South-North gradients, pronounced West-East gradients both in temperature and precipitation are observed across the Taimyr Peninsula. This reflects the fact that the western parts are still under the influence of relatively warm and moist atlantic low-pressure-systems, while the eastern parts are already governed by central-asiatic high-pressure-systems (Franz 1973). This explains the mean annual temperature of Dudinka (West-Taimyr) and Olenek (East-Taimyr) to be -10 and -15°C , respectively, though situated more or less on the same latitude. The same gradient is evident for annual precipitation, with values decreasing from 350 mm in the Southwest to 250 mm in the Southeast of Taimyr Peninsula (Norin and Ignatenko, 1975).

40 to 50 % of the precipitation falls during the short summer season, often as spray. Due to the limited winter precipitation, snow cover only accumulates to 40-60 cm as an average, with local gale-force winds (Burane) creating either considerable snowfree ground or massive packed snowdrifts.

The climate of Taimyr Peninsula is as well determined by the general principles of the Polar climate: First, the radiation climate is characterized by the pronounced difference between summer and winter. Second, evaporation is restricted because of low temperatures, resulting

in wet ground and -due to restricted drainage because of the underlying permafrost- massive flooding-events, in particular during snow-melt. An explanation of general principles of tundra climates can be found in Barry *et al.* (1981).

Vegetation

The most important fact characterising Taimyr Peninsula in terms of vegetation is the development of an undisturbed climatological determined sequence of vegetation units from the taiga to the polar desert (Aleksandrova 1980, Walter and Breckle 1986, Matveyeva 1994). Taimyr Peninsula is the only place on earth where this sequence can be observed over such an extent. Even throughout the Byrranga Mountains the zonal vegetation is continuous throughout the valley system (Walter and Breckle 1986). When the definitions of vegetation-units and of their limits are compared, it becomes obvious that classifying systems are not uniform (Table 2.1).

Table 2.1. Selected vegetation-classification systems of the northern polar landscape north of the tree-line.

	SOUTH		NORTH	
Aleksandrova (1980)	Subarctic Tundra Southern-, Middle-, Northern- (hyarctic shrubs characteristic (creeping <i>Betula</i> spp.); southern limit: treeline)		Arctic Tundra Southern-, Northern- (arctic dwarf-shrubs dominate (<i>Salix</i> spp), no shrub thickets, roots still form an inter-connected network; southern limit: 6°C July- isotherm)	Polar Desert Southern-, Northern- (roots do not form an inter- connected network; southern limit: 2°C July- isotherm)
Walter and Breckle (1986)	Southern Arctic Tundra (hyarctic shrubs dominate, bushes up to 1 m height occur; southern limit: treeline)	Typical Arctic Tundra (arctic and arctic-alpine species dominate over the hyarctic ones, still 100 % coverage southern limit: 10-11°C July-isotherm)	Northern Arctic Tundra (patchy plant cover of mostly arctic and arctic-alpine species; southern limit: 4-5°C July-isotherm)	Arctic Desert (single plants; southern limit: 2°C July- isotherm)
Yurtsev (1994)	Hyparctic Tundra (northern taiga and southern tundra; hyarctic shrubs dominate)		Arctic Tundra (arctic and arctic- alpine shrubs dominate)	High Arctic Tundra (lichens dominate; southern limit: 2°C July- isotherm)

Depending on the researcher's viewpoint the Russian authors (Aleksandrova 1980, Yurtsev 1994) generally refer to vegetation-history and -composition whereas the western authors mostly tend to use a combination of climatological and vegetational criteria to differentiate between subsystems (Walter and Breckle 1986). Although the numerous subdivisions suggest that the most complex system is the one of Aleksandrova (1980), in this study the terminology of Walter and Breckle (1986) will be adopted. The latter system ranks the present ecological conditions highest and therefore is the most simple in defining limits and terms. Both systems are actually quite similar, and the main difference is expressed by the fact that Aleksandrova uses the term "subarctic" for all vegetation zones influenced by boreal species, whereas Walter and Breckle restrict this term to wooded territory north of the taiga zone, the forest tundra. They therefore characterize all the landscapes north of the treeline as "arctic". Both systems allow a circumpolar comparison between study sites.

On Taimyr Peninsula the **Southern Tundra** is represented by a narrow belt of 100-150 km width. Prostrate and krummholz growth forms of *Larix sibirica* can be found extrazonal on well drained river terraces. The zonal vegetation under the mesic conditions of the watersheds consists of bush thickets of *Alnus fruticosa* and *Salix lanata* reaching heights of 1 m and 0.5 m, respectively. Mostly, a hummocky ground pattern is developed covered by dense stands of *Betula nana*. Other subarctic dwarf-shrubs (*Vaccinium* spp., *Ledum decumbens*, *Empetrum nigrum*, *Arctostaphylos alpinus*) characterize the lower layer together with a dense cover of mosses. On wet places a *Carex* spp. and *Eriophorum* spp. dominated tundra is developed, often with a tussocky character. Boreal species account for as much as 20 % of the total species number.

The belt of the **Typical Tundra** stretches out over the widest distance of Taimyr Peninsulas tundra range. Its 300-350 km latitudinal range covers huge parts of the North Siberian Lowland as well as the shores of Lake Taimyr and the valleys of the Byrranga Mountains. The zonal vegetation still appears closed, but the high bushes of the Southern Tundra are missing. Instead, the zonal vegetation on mesic sites is formed by a moss-tundra with *Carex* spp. (particular *C. bigelowii*) and arctic- as well as arctic-alpine dwarf-shrubs (*Salix reptans*, *Dryas punctata*, *Cassiope tetragona*). On wet sites the *Carex* spp. are accompanied by *Dupontia fisheri* and *Arctophila fulva* as well as *Eriophorum scheuchzeri*, at places blown snowfree

during winter polygonal ground has developed, mainly occupied by *Dryas punctata* and *Cassiope tetragona*.

The main difference between Typical- and **Northern Tundra** is that in the latter the zonal vegetation in mesic habitats is not closed anymore but shows patchy coverage. Solifluction and ground heaving processes constrain the total cover of the surface by vegetation. The only dwarf-shrubs still frequent are the arctic and arctic-alpine species *Salix arctica*, *S. polaris* and *Dryas punctata*. On the plains, plants are restricted to topographically favourable microsites to establish and grow. In wet areas extensive moss-carpet can be found, often lacking additional vascular plant cover.

In the **Arctic Desert** bare ground covers much more area than does vegetation, which represents only 5-25 %. Strong solifluction processes limit plant establishment and growth. Only arctic and arctic-alpine species can be found here, mainly revealing cushion growth form. They consist of single plants or small groups using cracks and depressions to shelter against wind and snowdrift. Lichens are the dominating life form. On the Taimyr Peninsula itself the belt of the Arctic Desert is restricted to the vicinity of Cape Tscheljuskin.

It is noteworthy that the climatic West-East-gradient over Taimyr Peninsula is reflected also by the species composition of the vegetation. From the Southwest a floristical wedge of what Aleksandrova (1980) named the "Yamal-Gydan-West Taimyr subprovince of the subarctic tundras" (which still belongs to the "East European-West Siberian province of the subarctic tundras") stretches out towards Lake Taimyr. The south-eastern parts of the Taimyr Peninsula, on the other hand, belong to the "Khatanga-Olenek subprovince of the subarctic tundras", already a part of the "East Siberian province of the subarctic tundras". The floristic history of the provinces is different from each other resulting in different species of the same genera replaced by each other (e.g. *Betula nana* <-> *Betula exilis*, *Diapensia lapponica* <-> *Diapensia obovata*) as well as species missing in the adjacent province (e.g. *Trollius europaeus*).

3.1.1 The Area of Lake Labaz

Lake Labaz is situated in the North Siberian Lowland and inside the belt of the Southern Tundra at 47.5 m a.s.l. (Fig. 2.1). It has a diameter of about 30 km and is quite shallow with depths of less than 5 m at most locations. The intensive study site "Lake Labaz" was established at the northern shore of the lake at 72°23'N and 99°43'E. It is situated in a rolling plain with maximum elevations of 115 m (Fig. 2.2). Numerous thermokarst lakes and creeks as well as wet depressions characterize the area. A watershed between two main river systems -both tributaries of Khatanga River- exists in close distance to a cliff at the northern shore of Lake Labaz, which reaches heights up to 30 m above the lake surface. Due to the extremely low relief-energy of the surrounding landscape these two rivers reach Khatanga River approximately 350 km from each other.

The Prae-Labaz lake was formed as a melt-water lake during the last glacial maximum (Isayeva 1984). The northern shore is dominated by marine terraces dating from the Kazantsev period ($125-75 \cdot 10^3$ years b.p., Fisher *et al.* 1990). Single peat lenses with thicknesses of up to 2 m can be dated to the Karginsk period ($50-25 \cdot 10^3$ years b.p., C. Siegert, personal communication).

More than 90 % of the investigated area is covered with clayey to loamy parent material. The predominant gley soils are characterized by high water content, low thaw depth (*i.e.* <60 cm), a pergelic temperature regime and free reduced iron (Pfeiffer and Hartmann 1995, Pfeiffer *et al.* 1996). An obvious gradient in vegetation-soil-complexes from wet to dry is best correlated with the position in meso-relief and thus drainage conditions (Fig. 2.2). Restricted to some hilltops and lobes, drier soils derived from more coarse-grained material can be found. Only in these well-drained soils active layer depths of more than 1 m do occur. The vegetation at these sites is comparably sparse. Chionophobous (e.g. *Cetraria nivalis*) or ruderal species (e.g. *Carex rupestris*) dominate. Mesic sites in areas with some inclination are dominated by nonsorted patterned ground, like earth-hummocks up to 2 m in diameter. Position in microrelief appears to be the outstanding factor for plant and soil development here. The hummock surface itself shows a high frequency of lichens, the slopes are dominated by dwarf-shrubs, and the depressions over the ice-wedges are mainly occupied by mosses. On the extensive more levelled and therefore wet habitats which are representative for most of the

study area a tussock tundra has developed, dominated by *Eriophorum vaginatum*, subarctic dwarf-shrubs as well as mosses. At the totally levelled areas of silted-up lakes and interconnecting watertracks, a wet sedge tundra can be found. Sometimes large low centred ice wedge polygons with diameters of up to 15 m have developed. While the vegetation in the watertracks and depression of the polygons is characterized by cotton grass, sedges and mosses, on the apices of the polygons dwarf-shrubs and mosses (sometimes *Sphagnum* spp.) can be found. In the two latter tundra types that thick organic layers (up to 30 cm) dominate the character of the soils, whose mineral parts are of pronounced gleyic character.

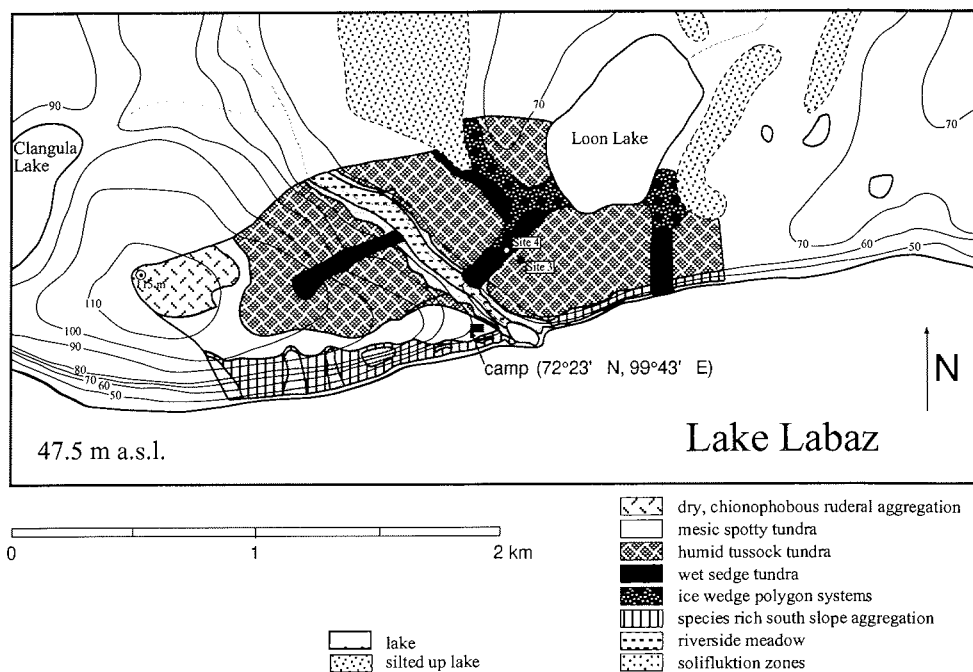


Fig. 2.2. Map of the intensive study area "Lake Labaz", showing the main vegetation units. "Site 3" depicts the position of the experimental site in the tussock tundra, "Site 4" the position of the experimental site in the wet sedge tundra.

There is no station or village at or near Lake Labaz, so in order to present longer-term climate data, those of Khatanga, approximately 100 km due East of the study area, are used (Table 2.2). Data show a yearly temperature amplitude on a monthly basis of 46.9°C, with monthly maxima of 13.1°C and minima of -33.8°C, occurring in July and January, respectively (Norin and Ignatenko 1975). A frostfree period of 35-45 days can be observed in July and August. Precipitation during that period adds to about 76 mm, representing 31 % of the total yearly amount.

Table 2.2. 25 year average values of monthly temperature and precipitation from the station Khatanga (modified from Norin and Ignatenko 1975).

	<i>J</i>	<i>F</i>	<i>M</i>	<i>A</i>	<i>M</i>	<i>J</i>	<i>J</i>	<i>A</i>	<i>S</i>	<i>O</i>	<i>N</i>	<i>D</i>	<i>Year</i>
temp.(°C)	-33.8	-32.6	-27.5	-18.4	-7.7	-5.4	13.1	8.9	1.6	-12.2	-26.1	-29.2	-13.2
prec.(mm)	9.9	9.4	10.0	9.9	13.2	30.3	40.5	35.3	27.1	22.1	17.9	17.3	243

It should be noted that because of the climatological West-East gradient (see above), Khatanga generally receives less precipitation and shows lower temperatures on an annual basis as compared to Lake Labaz. On the other hand Khatanga is situated at Khatanga River still inside the tree limit, so that a slightly warmer climate than at Lake Labaz can be expected. Due to the dominance of *Cetraria cucullata* over *Cladonia* species in mesic habitats around the Lake Labaz study site there is evidence that the area is part of the “Khatanga-Olenek subprovince of the Subarctic Tundras” (Aleksandrova 1980).

3.1.2 The Area of Lake Levinson-Lessing

Lake Levinson-Lessing is situated in the western part of the Byrranga Mountains inside the belt of the Typical Tundra at 40 m a.s.l. (Fig. 2.1). It is a long narrow lake (15 km*2 km) and reaches depths up to 108 m (Bolshiyarov and Anisimov 1995). Lake Levinson-Lessings drainage basin stretches North and West into the Byrranga Mountains, its outflow is the river “Protochny”, which connects it to Lake Taimyr in the Southwest. The intensive study site “Lake Levinson-Lessing” is situated at 74°32’N, 98°36’E at the lakes northern shore, close to the inflow of the main tributary “Krasnaya”. The area can be characterized as a low mountain region with elevations of up to 560 m.

The area has developed from Permian terrigenous rocks with intrusions of dolerites (Bolshiyarov and Anisimov 1995). An ancient deep valley was overformed by various marine- and denudation terraces indicating repeated transgressions. In recent times, the area appears mainly shaped by erosion processes. Deep V-shaped valleys in the surroundings indicate that the responsible erosional factor is water rather than ice.

Vegetation as well as soil characteristics of the area show pronounced differences between sites in mesorelief (Fig. 2.3). In the valley, soils showed a pergelic temperature regime, an aquic soil moisture regime, and a histic epipedon (Pfeiffer *et al.* 1996, Gundelwein *et al.* 1997). Their substrate derived from loamy to sandy sediments of fluvial origin. Organic layers of weakly decomposed organic material reached thicknesses of up to 10 cm. Maximum active layer depths did not exceed 30-45 cm. Thermokarst frequently occurs, either as shallow lakes or at the riversides. The dominant vegetation in mesic habitats of the valleys is such of the Typical Tundra of Taimyr Peninsula: Dwarf-shrubs like *Salix reptans*, *Dryas punctata*, and *Cassiope tetragona* are associated with *Carex* ssp and cover a dense moss carpet dominated by *Tomentypnum nitens*. Bush thickets are missing. At the more wet sites of the extensive levelled areas polygonal structures, mainly low-centre-polygons have developed. The diameter of the polygons ranges from 6 to 12 m and the apices with underlying ice wedges are 10 to 60 cm high. Whereas their apices with the underlying icewedges show a vegetation composition similar to the mesic sites, their wet depressions lack dwarf-shrubs and are dominated by *Carex stans* and *Dupontia fisheri*.

In contrast to the valley, the soils of the slopes are characterized by both a considerably better drainage as well as strong impact of solifluction. Thus, the horizontal profile differentiation often exceeds the vertical one. The active layer can reach thicknesses of up to 80 cm. Soils are built of skeletal material and are weakly developed. As a result of the strong movement due to solifluction and cryoturbation processes, organic layers are restricted to steps, stripes and lobes, and bare ground is widespread. Due to the same constraints, plant coverage rarely exceeds 60 % of the slope area, and is, in most localities, restricted to the surface of the organic layers. The main contributor to the vegetation of the slopes is a community formed by *Dryas punctata*, *Carex arctosibirica*, *Novosiversia glacialis* and mosses.

The elevated plains of the higher valleys are formed of fellfields with undeveloped soils and plant coverage not exceeding 10 % of the surface. Single cushion plants as well as moss carpets lacking vascular plant cover are the only representatives of vegetation here. Sorted and unsorted frost patterns characterize the surface. Active layer depths of up to 60 cm can be found.

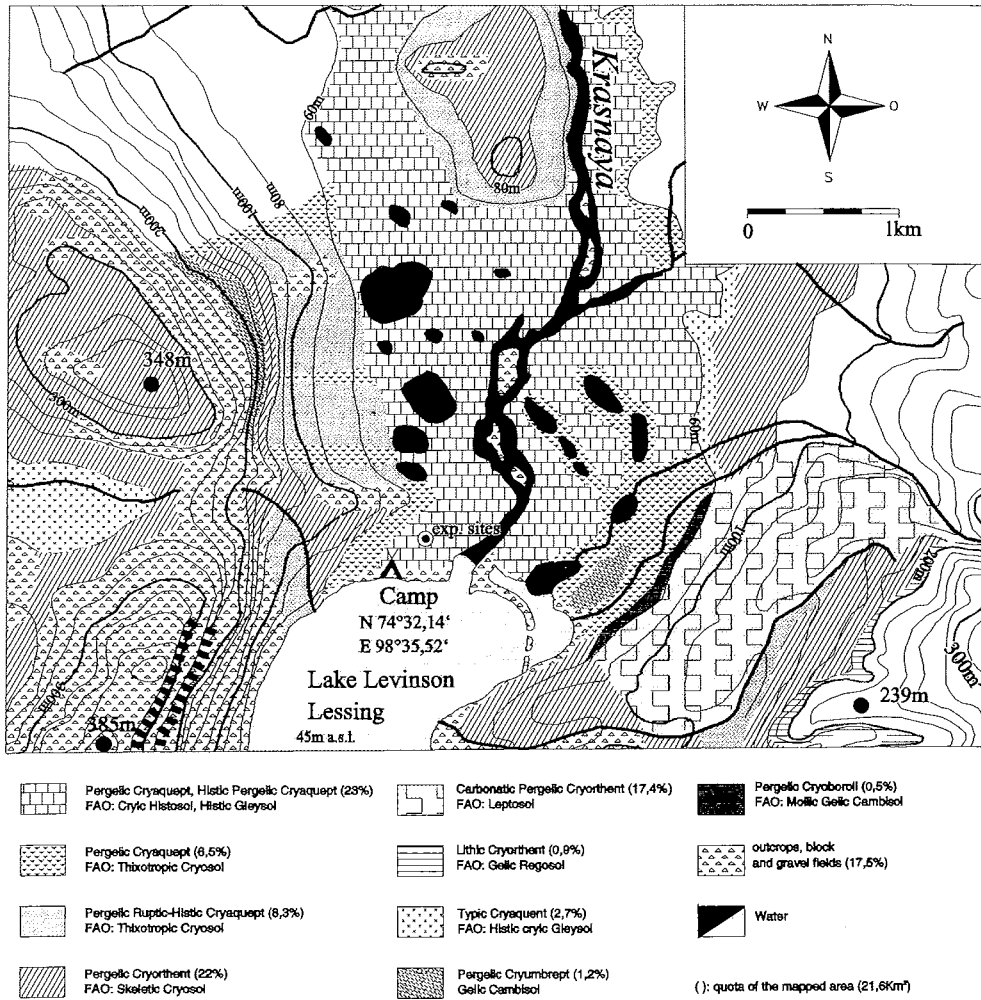


Fig. 2.3. Map of the intensive study area "Lake Levinson-Lessing", showing the main soil types and their distribution. The area with soils characterized as "Pergelic Cryaquept and Histic Pergelic Cryaquept" comprises high or low centre polygonal tundra. "exp. sites" depicts the experimental site in the low centre polygonal tundra (from Gundelwein *et al.* 1997).

Similar to the situation at Lake Labaz, no permanent station or settlement is situated nearby Lake Levinson-Lessing. Therefore, long-term climatological data had to be taken from Taimyr Lake Station, about 70 km to the East (Table 2.3). Data reveal a temperature amplitude of the monthly average of 39.5°C, which is 7.4°C less than at Khatanga. Monthly minima, occurring in January and February, show values of about -33°C, which is comparable to the corresponding values at Khatanga. A monthly maximum of only 6.6°C at Lake Taimyr (Khatanga 13.1°C), occurring in July, is thus responsible for the attenuated yearly amplitude at the northern station. The considerably lower summer temperatures at Lake Taimyr Station result in a frostfree period of only 35 days, which is about 10 days shorter than at the more southerly station. Precipitation during July and August amounts to 73 mm, representing for 26 % of the total yearly amount.

Table 2.3. 30 year (1962-1992) average values of monthly temperature and precipitation from Taimyr Lake Station (Dickson Regional Administration 1993).

	<i>J</i>	<i>F</i>	<i>M</i>	<i>A</i>	<i>M</i>	<i>J</i>	<i>J</i>	<i>A</i>	<i>S</i>	<i>O</i>	<i>N</i>	<i>D</i>	<i>Year</i>
Temp.(°C)	-32.9	-32.9	-29.6	-20.9	-10.2	-0.5	6.6	6.1	-0.5	-12.6	-24.8	-28.9	-15.0
Prec.(mm)	16.4	16.0	18.9	20.7	13.8	23.1	35.0	38.1	30.5	27.8	19.8	21.1	281

It has to be considered that Lake Taimyr Station is situated in a hilly lake-shore area outside the Byrranga Mountains, so in the narrow valley of Lake Levinson-Lessing inside the Byrranga mountains in particular summer-temperatures can be expected to be somewhat lower and the frost-free period shorter than at the long-term monitoring site.

4 Methods

4.1 CO₂ Exchange

4.1.1 Instrumentation Design

As manifold as the applications and questions behind the different aspects of soil respiration (see chapter 1) are the techniques for measuring these fluxes. A review of methods for the determination of soil respiration in the field is given in de Jong *et al.* (1979) and Wötzel (1993). Basically one has to distinguish two possibilities to determine the CO₂-flux from the soil:

- The determination of soil respiration from CO₂-profiles in the soil and the atmosphere near to the soil surface (e.g. Woodwell and Dykeman 1966, de Jong and Schappert 1972).
- The „inverted-box method“ (Lundegård 1921), in which a chamber open towards the ground is set on the soil surface in such way that it is sealed to the surrounding atmosphere. CO₂ emerging from the soil is accumulated in the chamber and the CO₂-efflux can be calculated as the increase of the CO₂-concentration per time unit in various ways. A “static accumulation method“, where the level of CO₂ inside the chamber increases for the period of the measurement (e.g. Koepf 1951, Frercks 1954, Parkinson 1981) can generally be distinguished from a “dynamic differential method“, where a permanent gas stream passes the chamber and is compared with an identical gas stream unaffected by a sample (e.g. Witkamp and Frank 1969, Edwards and Sollins 1973). While in the case of the static accumulation method the measuring periods have to be short to avoid artefacts, in the case of the dynamic differential method the mode of measurement can be continuous.

The dynamic differential measuring mode of the inverted-box method, however, bears some difficulties due to the open construction of the chambers („open-system-CO₂-exchange“ is a synonym for the dynamic differential method). Pressure changes caused by wind can significantly alter the CO₂-diffusion into the chamber. Several studies dealt with chamber designs in order to solve the problem (Wötzel 1993, Kutsch 1994, Fang and Moncrieff 1996). This thesis presents a solution suitable for wet and humid environments (see chapter 3.1.2.1). In order to check for quality of measurements, Wötzel (1993) tested a dynamic differential

CO₂ exchange device in combination with a chamber construction similar to the one used in this study to clarify the following points:

- Can a change in CO₂-concentration inside the chamber be detected to the full extent and with an acceptable time-lag at the analyser?
- Is the air inside the chamber well mixed by the gas flow through it, or is there a need for additional stirring by a fan?
- Does the increased CO₂-concentration inside the chamber alter the diffusion rate of CO₂ from the soil?
- How do pressure changes inside the chamber disturb the CO₂-diffusion and thus the CO₂-signal?

Wötzel (1993) showed that any given pulse of CO₂ could be recognised to the full extent and with an acceptable time-lag of seconds to a few minutes at the analyser (depending on volume of the tubing and the flow-rate). Additional stirring of the air inside the chambers was not necessary to provide homogeneity. The changes in diffusion rates due to the increased CO₂-concentration inside the chamber were negligible. Pressure changes of only a few μ bar, in fact, had an extremely high effect on the measured CO₂-signal. It can thus be suggested that under the condition that pressure artefacts are excluded, the dynamic differential measuring mode in combination with the inverted-box method is the best possible way of performing *in situ* CO₂-flux studies. The chamber system of this study shows a design avoiding pressure irregularities inside the chamber (see below).

One innovative characteristic of this study was the simultaneous measurement of soil respiration and moss photosynthesis in one chamber. Since changes in photosynthetic rates are subject to much faster changes than changes in soil respiration, the instrumentation had to be designed to keep track of rapid changes in the CO₂-concentration of the measured gas. This was taken into account for the design of the gas-streams as well as for the design of analyser and data storage. This kind of measurement could only be realized with the dynamic differential measuring technique.

From the above mentioned facts and the scope of this study it was clear that the instrumentation should be designed as an inverted-box method, operating in dynamic differential mode. At the beginning of this project, no CO₂-exchange device was available in the working-group, so that opportunities for several different kinds of applications should be included in the design. Furthermore, also within the scope of this work a whole range of

different measuring techniques were planned to be carried out. The device was thus designed to meet the following requirements:

- operation based on automatic programming and automatic data storage
- continuous, high resolution measurements of time series to make it possible to correlate the observed CO₂-fluxes with the controlling variables
- sufficient number of replicates to capture the small scale heterogeneity of the processes
- potential selection between suction- and pressure- mode of chamber operation
- potential selection between dynamic differential- and static accumulation mode of operation
- suitability for use under field conditions

The CO₂-exchange device was designed by the author, on the basis of experiences outlined in Wötzel (1993) and Kutsch (1994), and constructed by Walz (Germany). In order to obtain a construction suitable for such a broad range of applications and also to permit transportability, a modular design was chosen. The instrument consisted of the following units (see also Fig. 3.1):

- The analyser unit with the CO₂-analyser (Binos, Rosemount, Germany), consisting of an absolute CO₂-channel (0-2500 ppm) and a differential CO₂-channel (-50 to +50 ppm). This unit also included the control components of the magnetic valves as well as the “measuring-gas cooler“ for the removal of water vapour from the measured gases.
- The pump unit, consisting of 7 pumps for chamber-channels and 1 pump for the reference-channel. The unit included needle valves and flow-meters for each channel, which allowed regulation and monitoring of the gas flow. The magnetic valves which control the channel from which the actual measuring gas originates were situated in this unit as well.
- The temperature control unit, which contained a double regulation electronic. The first one was responsible for the conditioning of the “measuring-gas cooler“, which was constantly running at 2°C. The second one was responsible for the climate control of the “minicuvette“ chamber (see below).
- A programming and storage unit. Basically a datalogger, this unit could be programmed in a way that measuring periods and frequency of storing could be selected for every single channel in a measuring program. The unit was capable to store 1002 datasets.
- The „minicuvette“-chamber with some modified features (see chapter 3.1.2.2)

- The soil respiration chambers (see chapter 3.1.2.1)
- The whole-system chambers (see chapter 3.1.2.3)
- The laboratory chambers for water table changes in microcosms (see chapter 3.1.3)

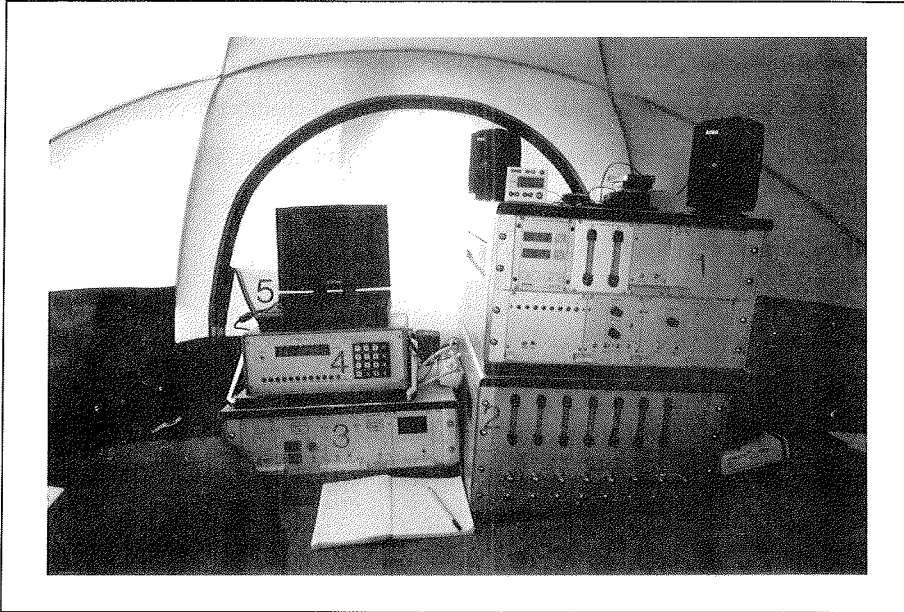


Fig. 3.1. The CO₂ exchange instrumentation in the field: analyser unit (1), pump unit (2), temperature control unit (3), programming and storage unit (4), laptop computer (5); see text for details.

An important and, with respect to measuring-artefacts, critical part of the instrumentation was the chamber system. Several features of the chamber construction in this study which, together with the conditions of the experiment localities proofed to avoid the irregularities observed in the above mentioned studies, were the following:

- Soil water table in wet and humid tundra types is found close (i.e. <20 cm) to the soil surface over the whole vegetation period. By inserting soil frames into the ground in such way that their lower sections were in contact with the soil water, the chamber attached to the soil frame was sealed towards the outer atmosphere, even if the soil showed low bulk density and/or high porosity. On the other hand the chamber was still open towards any diffusion of CO₂ from lower layers.
- Another feature of the chamber construction used in this study was the wide supplier tubing to the chambers including buffer containers (see chapter 3.1.2), which effectively buffered pressure irregularities. Additionally, this construction made it possible to directly

and parallelly remove both reference- and measuring-gas from a buffer volume. To avoid errors of the differential signal at the analyser, a volume of the same size as the chambers for measurement was inserted into the reference gas-stream, which consisted of exactly the same length of tubing as the measuring gas-streams.

During the field season at Lake Labaz some soil respiration rates exceeded the measuring range of the analyser. Already in the field a construction enabling the measurements of these high fluxes was added to the instrumentation with spare parts, which was later exchanged by some extra parts for the field season 1996. The construction consists of a needle valve and an additional flow meter, which makes it possible to analyse an aliquot volume only (The rest of the measuring gas is blown off). The ratio of the flow through the chamber to the flow through the analyser has to be considered for the calculations of CO₂ fluxes.

4.1.2 The Set-Up in the Field

In the field, a tent was used to house the instrumentation. Measurements were performed within a radius of 5 m around the instrumentation. A portable 1 kW generator was used as electrical power supply. The generator was placed about 100 m downwind of the experimental sites.

4.1.2.1 Soil Respiration Measurements

Measurements of soil respiration were carried out in continuous differential mode of operation. The chambers were operated in suction mode, meaning that the air was sucked through the chambers by the pumps (Fig. 3.3). The design of the chambers for the measurements of soil respiration was based on a commercial PVC pipe-system (Fig. 3.2). The pipes of this system had a sleeve at one end, so that they could be stacked into each other. A rubber seal included in the sleeve provided sealing of the pipe-system. The chamber system consisted of soil frames permanently anchored in the ground from the beginning of the field period, and chambers which were placed on the soil frames and sealed during measuring periods. For the soil frames, pipes with a sleeve at one end were taken to the field and cut to length according to water table conditions of the specific measuring plot. For chamber construction, pipe pieces of 10 cm length were cut and closed at one end with a blind-end cap,

thus forming the top of the chamber. One gas outlet was drilled at the centre of the chambers' top, four gas inlets were drilled near the base of the side-walls in 90°-angles to each other.



Fig. 3.2. The setup for the measurements of soil respiration in the field (tussock tundra). Chambers (red-brown), distributor containers (white, on top of the chambers), reference chamber on top of the transport box, which served as buffer volume.

To minimise pressure problems on one hand and irregularities in the volume and origin of measuring- and reference-gas stream on the other (as described in Wötzel 1993 and Kutsch 1994), a tubing construction of comparably large volume was attached to the gas inlets of the chamber. Four tubings with a diameter of 11 mm and a length of 30 cm were leading towards a plastic box with a volume of about half a litre. It served as a distributor to the four tubing as well as a buffer volume against pressure changes caused by wind. From this distributor-box, about 1 m of tubing with 2.4 cm diameter lead into a transport box (60*40*40 cm) which served to buffer rapid changes of the absolute CO₂-concentration in the air. The gas inlet of the box was always pointing towards the lee side. During the 1995 field season a chamber system with a diameter of 19 cm (2.835 litre volume, 284 cm² surface area) was used, which was replaced by a system with 10 cm diameter (0.785 litre volume, 79 cm² surface area) for the field season of 1996.

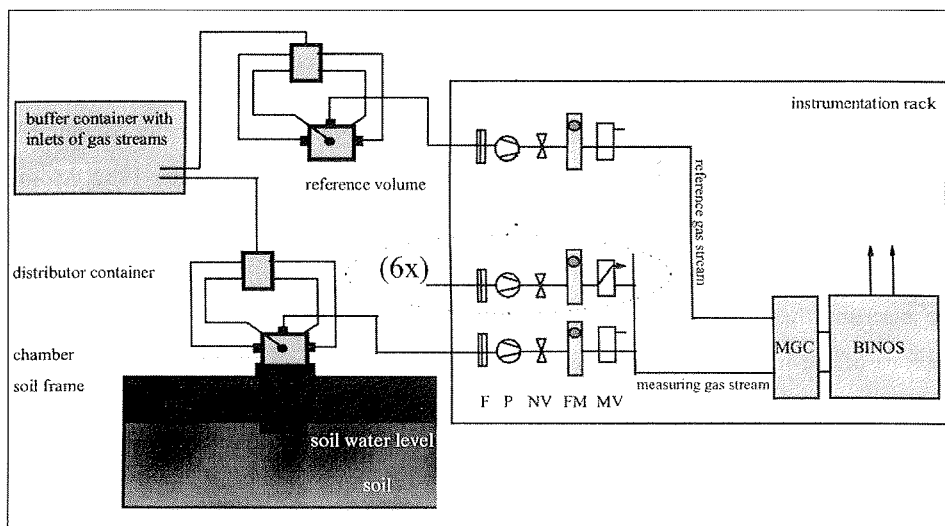


Fig. 3.3. Pneumatic set-up for the measurement of *in situ* soil respiration in the field. F=filter, P=pump, NV=needle valve, FM=flowmeter, MV=magnetic valve, MGC=measuring-gas cooler, BINOS=CO₂-analyser.

For the measurement of soil respiration, plots were chosen where no, or as little as possible, aboveground vascular plant biomass had to be clipped for insertion of the soil frames. If clipping was unavoidable, microsites with only herbs were chosen. Plants were clipped off directly at surface level in those cases (the avoidance of clipping was the main reason for the construction of a chamber system requiring less surface area in the second year of the study).

The mosslayer was never clipped, due to several reasons:

- Living and dead moss tissue is difficult to separate from each other. While the microbial biomass indicating decomposition activity reaches high values already in the green layer of the mosses (Flanagan and Bunnell 1980), living moss cells with the capability to produce new shoots were observed, for example, in *Polytrichum alpestre* up to 25 cm below the moss surface (Longton 1972).
- When the moss layer is clipped at sites with a water table right below the green parts of the moss, the whole balance of aeration and gas-diffusion is affected negatively. Furthermore, the thermal regime of the soil is disturbed because the clipped zone is much darker than the intact moss and thus absorbs more radiative energy.
- After the clipping of the green parts of the moss layer in pilot-experiments, an outburst of CO₂ was observed, which after a while leveled out again. The final level was observed to

be higher than the original CO₂-flux of the intact moss in some cases, in some cases it was lower.

- Nearly all authors who have measured soil respiration in tundra areas have not clipped off any moss inside their chambers, so that the results of this study will be directly comparable (e.g. Peterson and Billings 1975, Billings *et al.* 1982, 1983, Pool and Miller 1982, Moore 1986, Moore and Knowles 1989, Oberbauer *et al.* 1991, 1992, 1996).

Before inserting the soil frames into the ground, the organic layer was carefully cut in the dimensions of the frames, so that the insertion caused no compression of the organic layer. Measurements did not start until 2 days after insertion to avoid artefacts due to cutting and insertion (see also Fig 3.6).

4.1.2.2 Soil-Moss System Measurements

As pointed out in the introduction, soil and moss forms a densely interwoven system in wet and humid tundra types (Everett *et al.* 1981), which can hardly be separated without changing essential structural characteristics of both components. One objective of the study was thus to measure CO₂ fluxes of the intact soil-moss system *in situ*. The measurements of the soil-moss system were carried out by means of the “minicuvette“ (Walz, Germany), which was part of the CO₂-exchange device. This temperature-controlled one litre chamber consists of a transparent part, in which the sample is placed, and a part with peltier-elements, where conditioning of the air takes place (Fig. 3.5). The air is circulated between these parts by means of an adjustable fan. Several sensors measure chamber temperature and humidity, sample temperature and PPFD at sample level, as well as PPFD and temperature outside the chamber. One of the outstanding features of the “minicuvette“-device is the possibility to measure the external temperature at a chosen place within 1 m distance from the chamber, and, by means of an external control-unit, adjust this temperature inside the chamber with a negligible time-lag. This “track-mode“ was used for all experiments in the scope of this work. The external sensor was placed at the nearest unaffected microsite of the same type as the analysed one, so that in combination with the dynamic differential mode of the CO₂-exchange device a continuous long-term operation under natural conditions was possible.

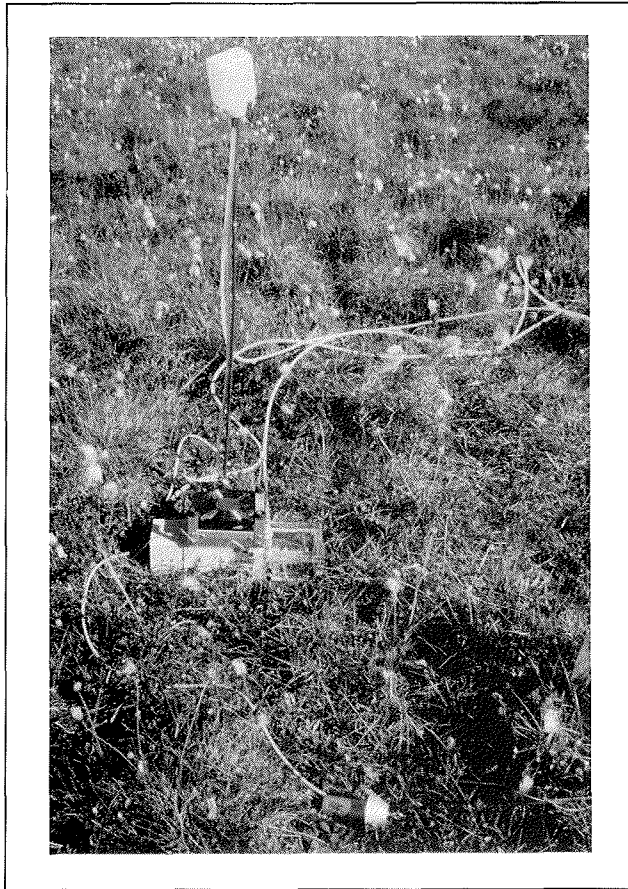


Fig. 3.4. The “minicuvette”-chamber for measurements of the CO₂ fluxes of the soil-moss system in the field. See text for details.

The original “minicuvette” was modified by the author and the company Walz in such way that the original construction was inverted. An additional opening for access to the interior was applied to the original base, and a soil frame was attached to the original top opening (Fig. 3.4). These modifications permitted the operation of the “minicuvette” directly on ground level, with the soil frame lowered into the ground down to the soil water level. The lengths of the soil frames used in this study were 7 cm and 13 cm, both covered a surface area of 7 cm * 8 cm. When lowered into the ground, the green parts of the moss were situated in the transparent part of the chamber, separated from the neighbouring, unmeasured moss-shoots only by a thin layer of acryl-glass.

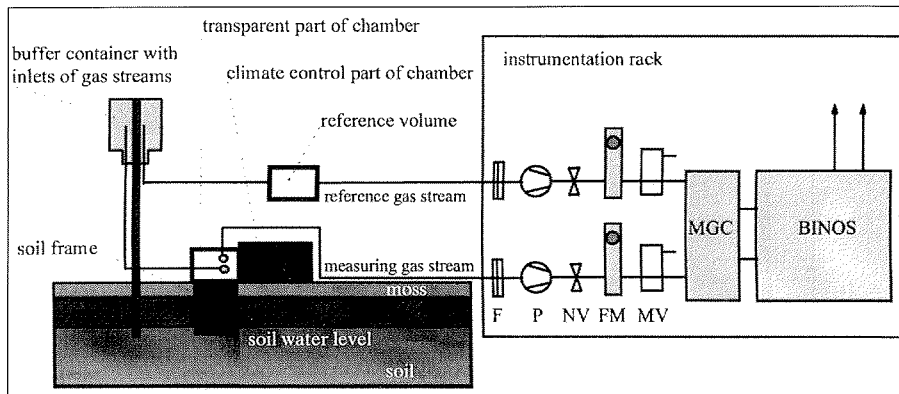


Fig. 3.5. Pneumatic set-up for the CO₂ measurements on the soil-moss system in the field. F=filter, P=pump, NV=needle valve, FM=flowmeter, MV=magnetic valve, MGC=measuring-gas cooler, BINOS=CO₂-analyser.

Measurements were carried out in continuous differential mode of operation. The „minicuvette“ was operated in suction-mode (Fig. 3.5). The gas-inlet of the chamber was connected to a tubing of about 60 cm length, which was fixed to a small pole 50 cm in height directly adjacent to the chamber together with the inlet of the tubing for the reference gas-stream. The inlets of both tubings were placed inside a small buffer container of about half a litre volume.

It should be noted that the operation of this device is restricted to locations where the soil frame can reach down to the water table, or other soil features (e.g. grain structure and bulk density) providing an airtight seal to the surrounding. In all other cases, air is at least partly sucked into the chamber through the ground, instead of through the inlet tube, which leads to highly artificial results.

The „minicuvette“ was established at each measurement plot by carefully cutting the organic layer with a sharp knife in the dimensions of the chambers' soil frame. Measurement did not start until 6 hours after cutting of the organic layer and insertion of the chamber. After this period, the CO₂-exchange of the plot was tested continuously to determine whether it had stabilised. Fig. 3.6 shows the course of the CO₂ efflux of the soil-moss system during the hours following insertion. In the figure, the surface temperature was also plotted, for some of the changes in CO₂-efflux were due to the trend towards lower temperatures the afternoon when the experiment was performed. The chamber was covered the whole time to prevent photosynthesis of the moss.

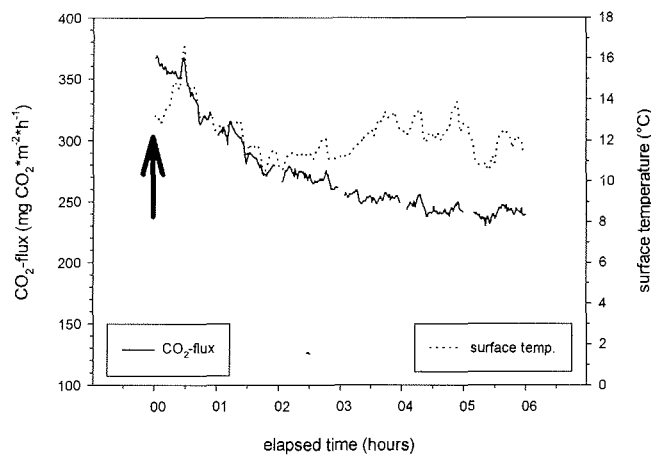


Fig. 3.6. CO₂-flux and surface temperature after cutting of the organic layer and insertion of the “minicuvette”-chamber. The arrow marks the time of insertion. The experiment was performed at the depression of the polygonal tundra.

4.1.2.3 Whole System Measurements

To show the contribution of the CO₂ fluxes of the soil and the moss to the CO₂ flux of the whole system (including soil, moss, and vascular plants), measurements were carried out by means of a chamber including all three subsystems (Fig.3.7). The experiments for the analysis of the whole-system CO₂-fluxes were carried out in static accumulation mode of the gas-exchange device. In this mode of operation, the air was sucked from the chamber to the analyser and returned into the chamber (Fig. 3.8). The change in the CO₂-concentration per time unit in this closed loop was used to calculate the CO₂-fluxes. The absolute channel of the CO₂ -analyser was connected to a 30*30*30 cm chamber made of acrylic-glass. The air was reinserted into the chamber near to its base by means of a “gas-comb” (a multi-punctured tube fixed around the chambers’ inner wall) to provide mixing of the returned air with the air inside the chamber. The outlet for the gas was situated near the top of the chamber. A soil frame of 30*30 cm, made of stainless steel, was carefully cut into the ground to about 2-4 cm deep and levelled out several days before the experiments. On top of this soil frame a ditch for carrying the chamber was situated, which could be filled with water. When the chamber was

placed in the waterfilled ditch, the whole system consisting of chamber, frame and the enclosed system was sealed towards the outer atmosphere and the measurements were started. Measurements were carried out once an hour over a diurnal course at each site measured.

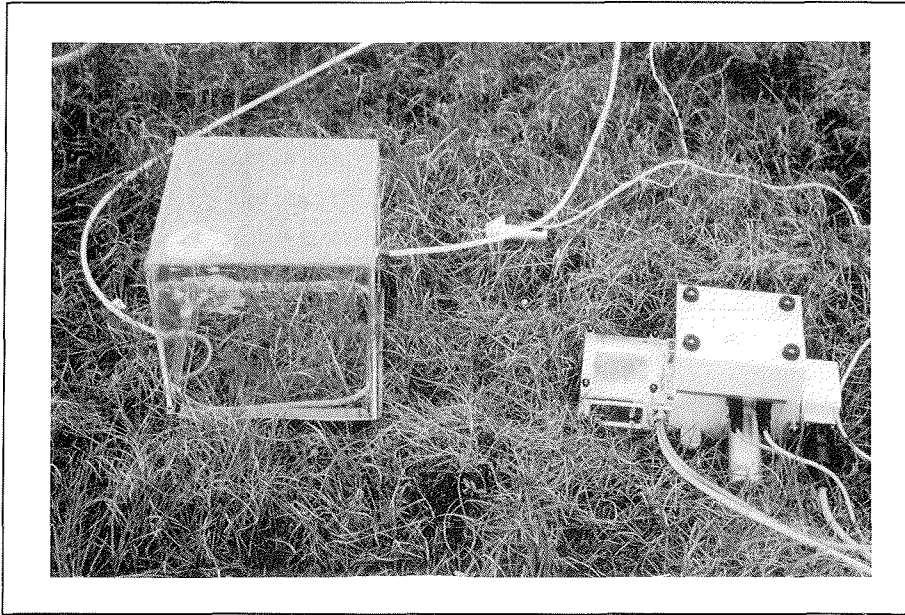


Fig. 3.7. The chamber for measurements of CO_2 fluxes of the whole system in the field (left). See text for details.

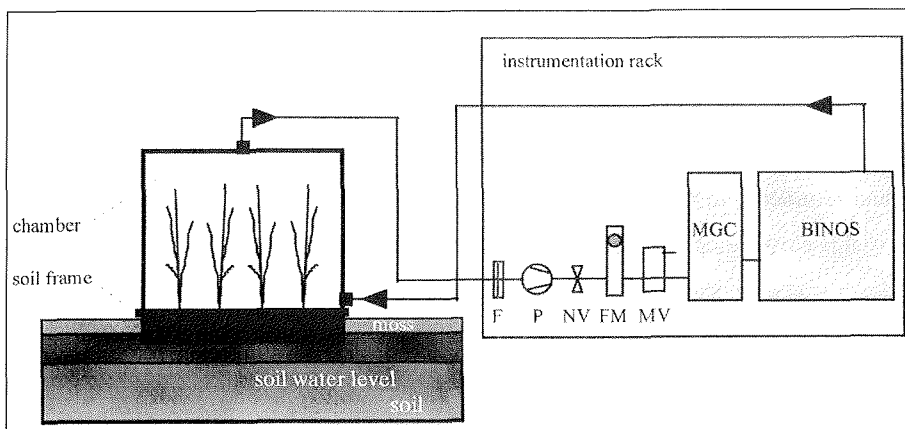


Fig. 3.8. Pneumatic set-up for the experiments on the whole system in the field. F=filter, P=pump, NV=needle valve, FM=flowmeter, MV=magnetic valve, MGC=measuring-gas cooler, BINOS= CO_2 -analyser.

The advantage of the static accumulation measuring mode is the avoidance of any pressure differences and associated problems. A second advantage is the short measuring period of only a few minutes or less. For this reason, no temperature regulation (which would be very costly for a chamber of this size) is needed. The assumption for the use of an unconditioned transparent chamber is, that the temperature inside the chamber is more or less constant over the short measuring period. This was not the case. Temperature measured in the centre of the chamber increased by about 4°C during a 3 min measuring period in full radiation, but was more or less constant over the equivalent shaded period. One consequence could have been to increase the ratio of biomass per chamber volume in order to reduce measuring periods. This was not possible in the case of a whole-system chamber due to the height of the vegetation. Another disadvantage of the static accumulation method, in particular for the measurement of photosynthesis, was the discontinuous character of the obtained CO₂-fluxes, which led to a limited database when observing light response relationships.

4.1.3 The Set-Up in the Laboratory: Water Table Experiments

In order to obtain systematic data on the relationship between soil respiration and position of the water table, laboratory experiments with material from all microsites were performed. Small microcosms of 10 *10 cm surface area and about 30 cm height were cut out with a knife and hand-spade in the nearest possible vicinity of the chambers for soil respiration experiments in the field (Fig. 3.9). Samples were airdried in the field under cool conditions, transported to Kiel and stored at 0°C until analysis. A cubic type of chamber was constructed from PVC-plates, with inner dimensions equivalent to those of the microcosms, except for the height. An air-volume of about half a litre over the microcosms was used for inlet and outlet of gas-tubes. By means of a sealable opening at the bottom of the chamber, water could be taken out of the chamber. A transparent tube, whose beginning and end opened into the chamber at the bottom and in the free gas volume on top of the microcosm, respectively, was fixed at the outside of the chamber in order to provide information on the water table inside. The chambers were connected to the CO₂-exchange device in pressure-mode of operation (i.e. the air was pushed through the chamber by the pumps, Fig. 3.10). All chambers and the reference chamber (half a litre volume) were placed in a "Climatic Test Chamber" (Heraeus-Vötsch, Germany), which was conditioned at 5°C.

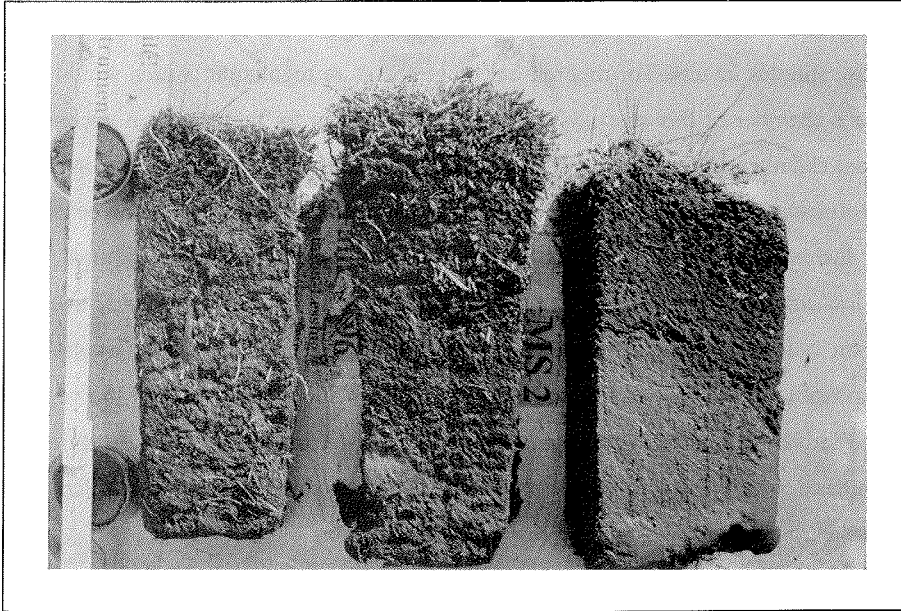


Fig. 3.9. Microcosms from the polygonal tundra at Lake Levinson-Lessing directly after removal from the ground (left: depression microsite, centre: low apex microsite, right: high apex microsite).

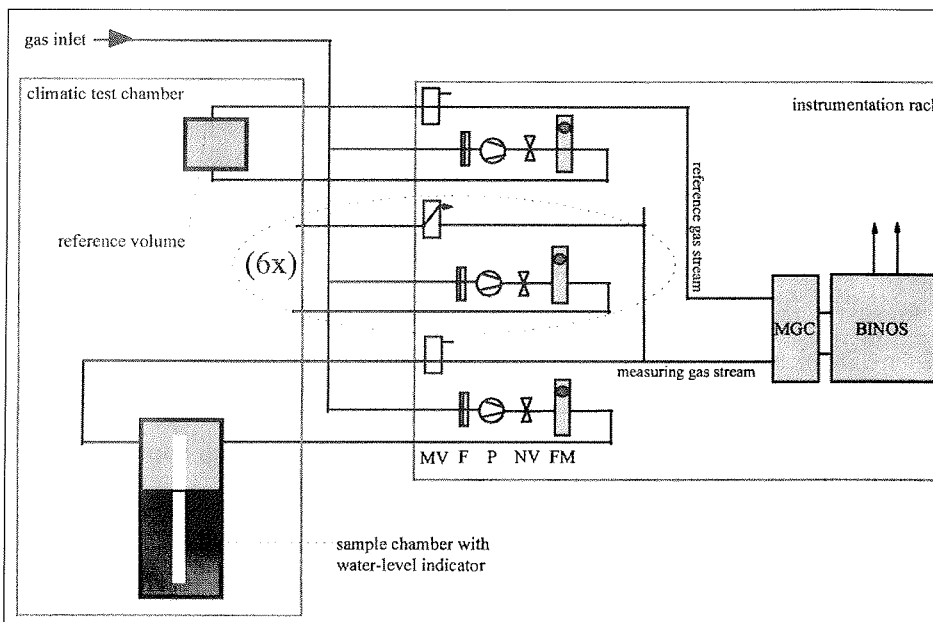


Fig. 3.10. Pneumatic set-up for the microcosm experiments in the laboratory. F=filter, P=pump, NV=needle valve, FM=flowmeter, MV=magnetic valve, MGC=measuring-gas cooler, BINOS=CO₂-analyser.

The microcosms were placed in the sample chambers, water-saturated with demineralised water and kept so for five days. After this period, the chambers were opened at the bottom, so that all water exceeding the maximal saturation of the microcosms was drained. This procedure took about a day. The experiment started by first measuring this state and then successively adding water from top of the chambers to increase the water table in 5 cm steps. It took about 12 hours until the water table was exactly adjusted. Soil respiration at every step was analysed for about a day. After the experiment with the water table 5 cm below the surface of the microcosms, two experiments with water tables of 1 cm below and 1 cm above the surface were performed in order to reach higher resolution in this most sensitive range.

4.1.4 Data Handling

Values from the CO₂ analyser were recorded every 10 seconds and averaged and stored in the program and storage module. The averaging period was 5 min for soil respiration measurements and 1 min for the measurements of the soil-moss-system. No averaging was made of the data of the whole-system measurements.

Since a maximum of three soil respiration-chambers were measured successively and hourly values for each chamber were required, three 5 min values per chamber were stored every hour. Also of the reference gas three 5 min values per hour were taken. The mean value of the three was taken for further analysis, so that all calculations of soil respiration were based on 15 min average values. Since all meso- and microclimatological parameters were taken as 15 min averages as well (see chapter 3.2), a direct correlation between all values was possible. Soil respiration experiments lasted for at least one day, mostly for longer periods.

Measurements of the soil-moss-system with the Walz "minicuvette" were performed as 24-36 h experiments whenever possible. 35-40 min of light, 15-20 min of shading and 5 min of reference gas were measured every hour. Because the main principle of the CO₂-measurements in an open system is the steady-state condition of the measured object, only the final plateau of the respiration values obtained during shading of the chamber were averaged for further analysis (three to five 1 min-values). For the same reason, about 5-20 min of data in light were omitted after a shading period, until about the same CO₂-value as before the shading period was reached again. The duration of the omitted period was depending on the

signal level (the magnitude of CO₂-turnover of the measured object) and the gas-flow through the system. Because in the worst cases the described procedure led to a limited database of net system flux and moss photosynthesis (i.e. less than 15-20 min of usable light values per hour) shading was performed only every second hour over most periods of the 1996 field-season. The soil respiration data were linearly interpolated between the measured datapoints and gross moss photosynthesis was calculated by subtraction of the net system flux values from this baseline.

For the whole-system experiments, CO₂-data were measured and stored every 10 s. Data from a first period of about 30 s at the beginning of each experiment were omitted. During this time, only the air of ambient CO₂-concentration being in the tubing reached the analyser. For calculation of the CO₂-flux, five sets of three 10 s-values were obtained in most cases. For each of the sets the slope of the CO₂-decrease or -increase was determined and averaged over the five sets. Including the omitted period, the light-phase of a single experiment had a duration of 3 min. After the chamber was shaded, the procedure was repeated. Altogether, a single experiment took about 6 min and led to one net-system-flux value and one whole-system-respiration value. Due to an unexpectedly short fieldstay during the expedition of 1996, where this type of measurements was carried out, only four diurnal experiments were performed.

An overview of the calculation of CO₂-exchange rates was introduced by Šestak *et al.* (1971). In order to calculate CO₂-fluxes from the differential ppm-values of the analyser, the following formula was used:

$$FCO_2 = (DCO_2 * F * RCO_2 * c) / A \quad \text{(Equation 1)}$$

where: **FCO₂** is the CO₂-flux rate [mg CO₂*m⁻²*h⁻¹],

DCO₂ is the differential value from the analyser [ppm],

F is the flow rate of the air through the system [l*h⁻¹],

RCO₂ is the density of CO₂ in air at 273 K, 1013 mbar,

c is a constant for unit conversion,

A is the surface area covered by the chamber.

CO₂-fluxes from experiments in static absolute mode were calculated using the formula:

$$\mathbf{FCO_2=(\Delta CO_2 * H * RCO_2 * c) / \Delta T} \quad \mathbf{(Equation 2)}$$

where: **FCO₂** is the CO₂-flux rate [mg CO₂*m⁻²*h⁻¹],

ΔCO₂ is the change of the absolute CO₂-concentration over the period ΔT [ppm],

H is the height of the chamber [m],

RCO₂ is the density of CO₂ in air at 273 K, 1013 mbar,

c is a constant for unit conversion,

ΔT is the time interval over which the change in CO₂-concentration ΔCO₂ is observed.

Three kinds of corrections were applied to the raw CO₂-data:

1. Temperature correction: The density of CO₂ in air is temperature dependent. Correction was applied according to the formula:

$$\mathbf{RCO_{2Tcorr}=RCO_2 * (273 / (273 + T_{act}))} \quad \mathbf{(Equation 3)}$$

where: **RCO_{2Tcorr}** is the temperature-corrected density of CO₂ in air,

RCO₂ is the density of CO₂ in air at 273 K, 1013 mbar,

T_{act} is the actual temperature of the measured gas [°C].

The temperature of the air some centimetres above the ground (as read from the minicuvettes external sensor) was taken for nearest matching the temperature of the measuring gas.

2. Pressure correction: The density of CO₂ in air is pressure dependent. Correction was calculated from the values of the barometer in the climate station according to the formula:

$$\mathbf{RCO_{2Pcorr}=RCO_2 * (P_{act} / 1013)} \quad \mathbf{(Equation 4)}$$

where: **RCO_{2Pcorr}** is the pressure-corrected density of CO₂ in air,

RCO₂ is the density of CO₂ in air at 273 K, 1013 mbar,

P_{act} is the actual air pressure [mbar].

3. Absolute CO₂-concentration correction: The signal of the differential channel of the CO₂-analyser is dependent on the absolute CO₂-concentration. The correction of this error was calculated following the specifications of the analysers' individual data-sheet.

4.1.5 Modelling

"Picasso defined art as "the lie that helps us to see the truth". I believe that it is the same with scientific theories: a lie that helps us to see something new will survive; a truth that we do not see will be forgotten. Therefore, a simple and beautiful theory -albeit wrong- that can be understood is better than a more complex one -even if less wrong- that cannot be understood."

T. Fagerström (1987)

Models in the sense of being "a simplified picture of reality" have been used since mankind has been able to think (Joergensen 1988). Mathematical modelling of biological processes, in particular, has to be regarded as a tool which can help to refine the results of experiments (Jarvis 1993): First, the use of models makes it possible to filter the effect of single parameters out of a whole set of parameters affecting a process. Doing so can provide an understanding of the process itself. Second, a calibrated model will allow the most precise interpolation of the measured datapoints and can thus be taken for balancing over a given time period. As a last point, modelling has an essential role in developing an understanding of process, community and ecosystem responses to changes of the environment (Dahlman 1985, Reynolds and Acock 1985). In this context, "the judicious use of modelling will allow a limited body of empirical knowledge to be greatly extended through simulations of complex combinations of environmental-biotic interactions" (Reynolds *et al.* 1993). However, mathematical models in ecology have to be treated with great care. First of all, one has to be aware of the fact that a model represents only a simplified picture of reality. Processes described by means of mathematical expressions will always be determined by more processes and factors than included in the model: According to the theory of hierarchy (Allen and Hoekstra 1990) the observed layer is always nested in a whole set of lower and higher layers which it controls and by which it is controlled. Koestler (1967) defined a given structure as the interface between processes driven from below and structural constraints imposed from above. As a consequence for mathematical modelling this calls for the application of mechanistic bottom-up models, ideally containing a consistent, interlocking, interdependent set of processes that represent a coherent description of the way the system functions (Jarvis 1993). It can thus be

suggested that a mathematical model describing only one process should be used with great care with respect to extrapolation in time, space or parameter range.

Numerous studies have been performed on the temperature dependency of soil respiration (reviewed e.g. in Singh and Gupta 1977, Raich and Schlesinger 1992), but within recent years there has been growing evidence that the process neither follows either simple exponential- nor conventional Arrhenius-relationships (Jenkinson *et al.* 1991, Lloyd and Taylor 1994, Kirschbaum 1995, Kutsch and Kappen 1997). Instead, the response of soil respiration was observed to change over the measured temperature ranges beyond its exponential relationship. To speak in exponential terms, the Q_{10} -value and therefore the efficiency of the process increases with decreasing temperature. This principle has been described already much earlier for biochemical reactions (Slator, 1906, Kanitz 1915), but has not gained much attention since then. Oechel (1976) described the phenomenon for moss respiration as well, suggesting that it does not only apply for physiologically heterogeneous processes like soil respiration. Lloyd and Taylor (1994) have introduced an expression that incorporates these changes of process efficiency with temperature. Their equation, which was also adopted for modelling the temperature dependency of soil respiration in this study is:

$$SR = k * z * (\exp(-E_0 / (T - T_0))) \quad (\text{Equation 5})$$

where: **SR** is the soil respiration rate [$\text{mg CO}_2 * \text{m}^{-2} * \text{h}^{-1}$],

k is a constant for unit conversion,

T is the actual temperature [K],

z, **E₀**, **T₀** are regression parameters.

The equation was fitted to the field data in the program Sigma-Plot, using non-linear least-square regression. It is evident from the character of the expression that various combinations of E_0 and T_0 may lead to an appropriate fit over the observed temperature range. In order to later correlate the approximated values with site characteristics (see below, chapter 3.1.6), the E_0 -parameter was set to the value which Lloyd and Taylor (1994) have calculated for a world-wide comparison of soil respiration datasets. In this case, the T_0 -parameter is a value for the change of process efficiency across the temperature range (the higher the T_0 -value, the higher the Q_{10} at low temperatures). The size of the z -parameter, however, is an unbiased value of the increase of soil respiration with temperature.

The Q_{10} values for single degree C intervals were calculated from the approximated temperature models using the formula of Hochachka and Somero (1984):

$$Q_{10} = (SR2/SR1)^{10/(T2-T1)} \quad \text{(Equation 6)}$$

where: Q_{10} is the temperature coefficient,

SR1 and **SR2** are soil respiration rates

measured at **T1** and **T2**.

Due to the dynamic differential technique, which was used for the analysis of soil respiration in this study, as well as due to the observation of considerable temperature amplitudes in the field, sufficient data for a temperature correlation were available. For water table changes, which are oscillating much slower and with less amplitude, no sufficient database could be produced in the field. In order to obtain a systematic result, laboratory experiments had to be performed (see chapter 3.1.3). On the basis of the laboratory experiments, an empirical expression was sought to describe the dependence of the soil respiration on water table changes. Oberbauer *et al.* (1992) have introduced such an equation which uses a slightly sigmoidally-modified asymptotic function. The empirical expression is based upon experiments showing that changes of water table position over some depths (below about 20 to 40 cm) have nearly no influence on soil respiration values, whereas such changes closer to the surface result in strong increase or decrease of this process. Water table changes very close (i.e. <2 cm) to the surface, or even beyond the surface, have a smaller effect on soil respiration again. Ostendorf (1996) and Reynolds *et al.* (1996) have already used this model to explain carbon-turnover on the watershed-scale. The equation according to Oberbauer (1992) which was also used in this study to describe the reaction of soil respiration to water table changes, is:

$$SR = k * \exp((a * WT) / (WT + b)) \quad \text{(Equation 7)}$$

where: **SR** is the soil respiration rate [$\text{mg CO}_2 \cdot \text{m}^{-2} \cdot \text{h}^{-1}$],

WT is the depth to water table [cm]

k is a constant for unit conversion,

a, **b** are regression parameters.

The “a”-parameter determines the upper level of insensitivity of soil respiration to water table changes. “b” is a measure of the slope of the water table response curve. It also determines the shape of the curve at water tables above the soil surface. The lower the value of “b”, the higher soil respiration rates are reached already with water tables close below the soil surface. The model was fitted to the laboratory data as described above. When evaluating the combined temperature- and water model for the field data, the parameters from the corresponding laboratory experiment were given as the starting parameters. When applying this model, in particular when extrapolating towards higher water tables without approximation of the parameters, special attention has to be given to the fact that at the depth to water table “b” above the soil surface, “SR” jumps to artificially high values, due to the exponential character of the function. For this reason, a sigmoid expression of the form:

$$SR = k \cdot \frac{a}{1 + \exp(-(\text{WL} - x_0)/b)} \quad (\text{Equation 8})$$

where: **SR** is the soil respiration rate [$\text{mg CO}_2 \cdot \text{m}^{-2} \cdot \text{h}^{-1}$],

WT is the depth to water table [cm]

k is a constant for unit conversion,

a, x₀, b are regression parameters,

was tested with the laboratory data with success. The equation describes a more robust model of the process for its double asymptotic character and should thus be considered for applications such as larger scale modelling. However, it results in slightly lower regression coefficients than Equation 7, due to its symmetric character (Fig. 3.11). For this reason, and because the aim of this study was to approximate coefficients for every single data set, Equation 7 instead of Equation 8 was chosen for data analysis.

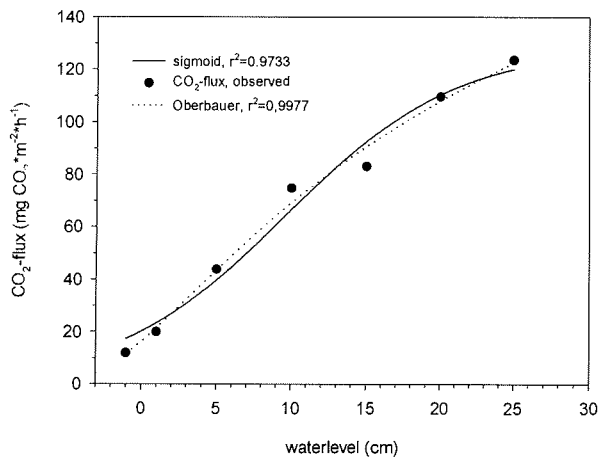


Fig. 3.11. Comparison of Equation 7 (Oberbauer) and Equation 8 (sigmoid) on soil respiration data during water table changes in the laboratory. Material was a microcosm from the depression of the polygonal tundra.

Gross moss photosynthesis from the soil-moss experiments was modelled using an empirical expression for light dependency and an Arrhenius function for temperature dependency. The expression for light dependency has been previously introduced to describe the photosynthesis of lichen, in particular at low light-levels (Kappen *et al.* 1995):

$$\mathbf{GP(L)=(a+c*L)/(1+b*L)} \quad \mathbf{(Equation\ 9)}$$

where: **GP** is the gross photosynthetic rate [$\text{mg CO}_2 \cdot \text{m}^{-2} \cdot \text{h}^{-1}$],

L is the PPFD [$\mu\text{mol} \cdot \text{m}^{-2} \cdot \text{s}^{-1}$]

a, b, c are regression parameters,

Arrhenius relationships have frequently been used to describe the temperature dependency of biological processes (Arrhenius 1915, Precht *et al.* 1973):

$$\text{GP}(T)=\exp(d*T-e) \quad \text{(Equation 10)}$$

where: **GP** is the gross photosynthetic rate [$\text{mg CO}_2 \cdot \text{m}^{-2} \cdot \text{h}^{-1}$],

T is the temperature [$^{\circ}\text{C}$]

d, **e** are regression parameters,

Since only a very restricted temperature range was observed during field experiments of moss photosynthesis, the models evaluated in the scope of this study should not be extrapolated to a wider temperature range. Modelling of moss photosynthesis in this study was primarily performed to calculate daily balances as well as to reveal differences in the light response of the observed moss-species or -communities of the microsites. Another goal was to show the contribution of the mosses to the whole-system CO_2 -flux. For these cases a more extended validation of the models as obtained e.g. by laboratory experiments was not necessary.

4.1.6 Statistics

As pointed out already in chapter 3.1.5, one of the advantages of modelling is the parameterisation of reaction properties. Statistical methods can then be applied to correlate the approximated model parameters with factors determining the reaction on a higher level than the one directly included in the model. This facilitates at least the delimitation of factor combinations or patterns responsible for an observed type of response, in the best case it can lead to the formation of indexes. In this study, the correlation of the approximated model parameters will be restricted to site characteristics, in order to identify patterns responsible for certain types of response. To circumnavigate constraints regarding the number of n and the assumption of normal distribution, as well as scale and character of the compared values, Spearman rank analysis was chosen. This method allows unproblematic correlation of heterogeneous, non-normally distributed datasets of any character (e.g. linear, exponential), by not comparing absolute values of the variables, but differences in their ranks (Spearman 1904, c.f. Sachs 1984).

Spearman rank analysis was also applied to identify those soil microclimatic parameters explaining most of the daily variation of soil respiration prior to presentation of datasets and

modelling. The parameters identified were then used for incorporation in the soil respiration model (see chapter 3.1.5).

4.2 Meso- and Microclimatological Measurements

Mesoclimatological measurements were carried out by means of a prefabricated climate station (Driesen und Kern, Germany) comprising a datalogger (Grant, UK), a PPFD-sensor (Skye, UK), a temperature- and humidity-sensor (Humicap, Vaisala, Finland), wind-speed and -direction equipment (Vector, UK), and a barometric pressure-sensor (Driesen und Kern, Germany). All sensors were fixed to a mast in 2 m height above the ground. Data were recorded every minute and averaged and stored every 15 minutes.

Soil microclimate was analysed by means of thermistors (Driesen und Kern, Germany) fixed to a wooden pole of 5 mm diameter in 20 cm, 10 cm, 5 cm, 2 cm depth and at the soil surface. A steel rod (also used to test for the depth of the active layer) was used to prepare a hole, in which the thermistor chain was inserted. A datalogger (Grant, UK) was used to record the data taken in 15 min intervals. Depth to water table was measured in holes in the ground, mostly those resulted from the sampling of the microcosms for the water table-experiments (see above). A set of both, a soil temperature-measuring unit and a water table indicator was established near to every chamber for CO₂-measurements.

Water content of soil- and moss- samples for correlation with the CO₂-measurements was analysed by means of a moisture analyser (Sartorius MA30, Sartorius, Germany). In this device, subsamples of about 7 g-15 g WW are dried with infrared radiation at 105°C while situated on a balance. Since this method is destructive, samples from the nearest suitable microsite with equal conditions were taken.

4.3 Vegetation Analysis and Sampling for Vascular Plant Biomass

Vegetation analysis and sampling for biomass/production values was undertaken at identical sites, except for the low-centre polygonal tundra at Lake Levinson-Lessing, where harvesting for the latter analysis was performed in the scope of a diploma-thesis (Becker 1997). The sites were situated in close vicinity (i.e. less than 2 m distance) of the soil profiles as well as in the neighbourhood (i.e. less than 10 m distance) to the CO₂-measurements.

For vegetation analysis, 1 m² plots were chosen and analysed for coverage on the basis of a 10 *10 cm grid. Analysis of coverage was chosen because it provides the most neutral registration of species in the sense of structural shares (Londo 1975, c.f. Dierßen 1990), an important fact for comparisons between sites. Lichens were counted for frequency of thalli instead of coverage. Mosses representing less than 5 % of coverage were not assessed.

Sampling for biomass/production values was undertaken as late as possible during the field stay: at Lake Labaz on 20.8.1995 and at Lake Levinson-Lessing on 28.8.1996 (Becker 1997). Aboveground biomass was clipped off directly at the ground, separated immediately according to origin, and air-dried (For a detailed list of fractions of aboveground biomass see Sommerkorn 1996). At Kiel University, samples were dried at 105°C for at least 24 h until constant dry weight. It should be mentioned that sampling for aboveground biomass was performed of vascular plants only. Mosses were left in place, since it is complicated to determine the lower border of living moss tissue. The same is valid for aboveground production of mosses, which was not sampled for as well. Aboveground annual production of vascular plants was determined without the share of the annual increase of leaves of evergreen dwarfshrubs and also without the annual increment of the woody part of all dwarfshrubs. Sampling of belowground biomass of vascular plants was undertaken at the same days as for aboveground biomass. At Lake Levinson-Lessing, belowground biomass was determined by soil cores with a volume of 250 cm³. Becker (1997) took samples down to 15 cm depth, since 85-90 % of the belowground biomass of vascular plants is situated in this layer in wet tundra (Dennis and Johnson 1970, Dennis 1977, Dennis *et al.* 1978). At Lake Labaz, samples of 100 cm² and 30 cm depth were taken with knife and spade (Pfeiffer *et al.* 1996). Samples from both localities were washed with water several times over a sieve with 2 mm mesh size to remove mineral and humus particles. Additionally, an ultrasonic bath was used for the last cleaning-step in the laboratory. As a last step, the samples were dried in the oven at 60°C to constant dry-weight. No separation of living and dead roots was possible, so that the realistic values for belowground living biomass may, in fact, be lower than those presented in this study.

4.4 Analysis of Bacterial Biomass

Bacterial biomass from the soils investigated in the scope of this study were analysed by epifluorescence microscopy (M. Bölder, unpublished data). Sampling from different layers of soil profiles was carried out in July 1995 at Lake Labaz, and in July 1996 at Lake Levinson-Lessing. While sampling at Lake Labaz was performed in steps of several cm, sampling steps at Lake Levinson-Lessing were defined by soil horizons. Samples were air-dried immediately after sampling and taken to the laboratory in Kiel where they were stored under freezing conditions until analysis. Samples were rewetted prior to laboratory analysis. Analysis of microbial communities was performed by epifluorescent microscopy using acridine orange as stain and blue light for excitation. Cells were counted and measured by image analysis equipment (Leitz Aristoplan and Quantimed 500). The spheric parameters of the cells as well as their carbon content were calculated from planimetric diameters (of cocci) or length and width (of rods) using appropriate geometrical formulas (Bölder *et al.* 1993). Until the completion of this thesis, only the bacterial share of the microbial community was fully elaborated for the investigated soils. Therefore in the according paragraphs it will be referred to bacterial biomass instead to microbial biomass.

5 Results

5.1 Descriptive Results

In the scope of this study, CO₂ flux measurements were performed at seven microsites of three different tundra types. In this chapter, the biotic and abiotic characteristics of these tundra types and their microsites, as well as the mesoclimatic conditions of the field-seasons will be presented. Most of the data were taken by the author, some by colleagues within the project, some are joint work. All data of foreign origin will be identified accordingly. Data taken by the author will not appear specifically marked.

5.1.1 Lake Labaz

5.1.1.1 Mesoclimate of the Field-Season

Compared with the summer of the field season in 1994, when a pre-expedition had surveyed the area (Sommerkorn 1995), the summer of 1995 was warmer (Table 4.1.1), but still within the range of the long-term July to August values of Khatanga (Table 2.2). Mean ambient temperature for the field-season from 20.7. to 25.8. was 11.2°C, and daily averages ranged between 3.9 and 16.2°C. The bulk of the high temperatures were contributed by about 10 days at the beginning of the field-season with daily maximum temperatures often found above 20°C (for graphs of mesoclimate and a table of daily values of mesoclimatic parameters see appendix, Fig. A1, Table A1). But also after that particular warm period, daily mean temperatures ranged around 9°C and radiation was high due to relatively little cloud cover. Consequently, maximum daily totals of PPFD were as high as 40.3 mol*m⁻²*d⁻¹, with a mean value of 23.3 mol*m⁻²*d⁻¹. Minimum daily totals of PPFD during overcast days were as low as 6.8 mol*m⁻²*d⁻¹. Precipitation for the recorded period of 36 days was 38.2 mm in total, which is comparable to the corresponding value from Khatanga.

Table 4.1.1. Mesoclimate of the field-season at Lake Labaz, 20.7.-25.8.1995.

	<i>total campaign (20.7.-25.8.)</i>		<i>equivalent period to Lake Levinson-Lessing campaign (27.7.-12.8.)</i>	
	<i>ambient temp. (°C)</i>	<i>daily total PPFD (mol*m⁻²*d⁻¹)</i>	<i>ambient temp. (°C)</i>	<i>daily total PPFD (mol*m⁻²*d⁻¹)</i>
mean	11.2	23.3	10.5	22.9
max.	23.2	40.3	23.2	33.1
min.	-2.6	6.8	1.5	12.8
max. daily average	16.2		13.6	
min. daily average	3.9		6.9	

total precipitation 38.2 mm

5.1.1.2 Characteristics of the Experimental Sites

At the intensive study site “Lake Labaz“, CO₂-flux-measurements were obtained at sites of two dominating tundra types, tussock tundra and wet sedge tundra (see also Fig. 2.2). Both tundra types showed a well defined border to each other. The distance between the investigated sites of both tundra types was about 15 m. While the wet sedge tundra appeared homogeneous, several microsites could be distinguished in the tussock tundra on the scale of a square metre.

5.1.1.2.1 Tussock Tundra



Fig. 4.1.1. The tussock tundra at Lake Labaz in the surrounding of the experimental sites.

5.1.1.2.1.1 Vegetation and Vascular Plant Biomass

Of the 1 m² of tussock tundra analysed within the scope of this study, a total of 0.6 m² could be characterized as wet depressions (TD) and low parts of slopes, whereas 0.4 m² were hummock- (TH) and tussock- (TT) area. Hummocks appeared as frostpatterns but were additionally shaped by moss cushions as well as tussocks of *Eriophorum vaginatum*.

Generally, the slopes and some parts of the depressions as well as the lower parts of the tussocks and hummocks were the realm of the dwarf-shrubs, which accounted for 51 % of coverage (Table 4.1.2), whereas the higher parts of the tussocks and hummocks were mainly covered by the monocotyledons (45 % of coverage) and lichens. The distance between the investigated microsites was about 1 m.

Table 4.1.2. Vegetation and coverage of the tussock tundra. Plot size was 1 m² (0.5 m*2 m):

	frequency (thalli/m ²)		
<i>Cetraria cucullata</i>	145		
<i>Cladina arbuscula</i>	25		
<i>Cladonia uncialis</i>	24		
<i>Cetraria islandica</i>	21		
<i>Bryocaulon divergens</i>	8		
<i>Dactylina arctica</i>	5		
<i>Nephroma arctica</i>	2		
		total = 229	
	coverage (%)	group coverage (%)	total coverage (%)
<i>Betula nana</i>	13		
<i>Salix pulchra</i>	10		
<i>Vaccinium vitis-idea</i>	10		
<i>Cassiope tetragona</i>	8		
<i>Vaccinium uliginosum</i>	5		
<i>Dryas punctata</i>	4		
<i>Pyrola rotundifolia</i>	3		
<i>Pedicularis lapponica</i>	2		
<i>Polygonum viviparum</i>	1		
<i>Salix glauca</i>	1		
<i>Saxifraga hierculus</i>	1		
<i>Saxifraga nelsoniana</i>	1		
		59	
<i>Eriophorum vaginatum</i>	24		
<i>Carex bigelowii ssp. arctosibirica</i>	18		
<i>Arctagrostis latifolia</i>	3		
		45	
<i>Tomentypnum nitens</i>	18		
<i>Drepanocladus uncinatus</i>	15		
<i>Kiaeria starkii</i>	12		
<i>Hylocomium splendens</i>	10		
<i>Polytrichum strictum</i>	7		
<i>Aulacomnium turgidum</i>	5		
<i>Plagomnium elatum</i>	4		
		71	175

Mosses, which represented 71 % of coverage in this tundra type, occupied nearly all sites of the micro-relief, though they were only sparsely found between the shoots of *Eriophorum vaginatum* on the most elevated parts of the tussocks. Extensive moss cushions could be found on moderately high parts of the hummocks, adjacent to the *E. vaginatum* tussocks. The total degree of coverage in the tussock tundra was 175 %, the total number of species observed was 29.

Biomass values and annual production rates differed between the microsites of the tussock tundra (Table 4.1.3). The depression was the least productive site as well as the one with the least aboveground biomass. Compared with the tussock it accounted for only 35 % of the aboveground biomass and 38 % of the aboveground production. This fact, however, is not reflected by the belowground biomass, which was approximately equal sized at both locations. The aboveground production/biomass-ratio was about the same at both microsites, showing values of 0.33 at the depression and of 0.3 at the tussock. In contrast, the ratio of aboveground/belowground biomass differed considerably between both microsites: The ratio was 0.03 for the depression, but 0.09 for the tussock. The value of the depression microsite, however, has to be regarded with some care and may, in fact, be higher, since it was obvious when sampling that the belowground biomass at this site mainly crept in from the sides. Belowground biomass formed an interconnected network in the whole tundra type and was distributed more or less homogeneous, as also indicated by the absolute values of belowground biomass.

Table 4.1.3. Biomass and annual production of the tussock (TT) and of the depression (TD) microsite of the tussock tundra in g dry weight (DW) per m² (joint work, modified from Sommerkorn 1996 and Pfeiffer *et al.* 1996).

	biomass (g DW*m ⁻²)		production (g DW*m ⁻² *a ⁻¹)
	aboveground	belowground	aboveground
tussock (TT)	370	4239	111
depression (TD)	129	4310	42

5.1.1.2.1.2 Soils

The soils of the tussock tundra derived from loamy-clayey parent material and had gleyic features. They could be classified as Pergelic Cryaquept (Soil Taxonomy), or Cryic Histosol (FAO)(Pfeiffer *et al.* 1996). The soils showed pronounced differences between sites in micro-relief (Fig. 4.1.2, Tables 4.1.4, 4.1.5, description of the unfrozen horizons of profiles). Whereas a thick organic layer of poorly decomposed plant material was developed in the depressions, the tussocks lack these mats. Also, the gleyic mineral horizon below the organic layer at the depression microsite was still characterized by high humus content, a feature not evident at the tussock microsite. As a consequence, the total carbon content of the uppermost horizon of the depression microsite was very high, about 7 times higher than at the tussock microsite. The same was evident for nitrogen content, which was found to be 6 times higher at the uppermost horizon of the depression microsite than at the corresponding layer of the tussock microsite. Both parameters, however, were comparable between microsites at the lower horizons. When comparing the C/N-ratio between sites in micro-relief, the uppermost horizons showed values of 16 at the tussock microsite and 19.8 at the depression microsite. The C/N-ratios of the lower horizons ranged between 11.5 and 13.3 at both sites in micro-relief. If it is assumed that most of the organic material produced in the tussock tundra will gather in the depressions, and that the depression is by far cooler and wetter than the tussock microsite (see chapter 4.1.1.2.1.3), the huge total carbon content as well as the wide C/N-ratio is readily explained.

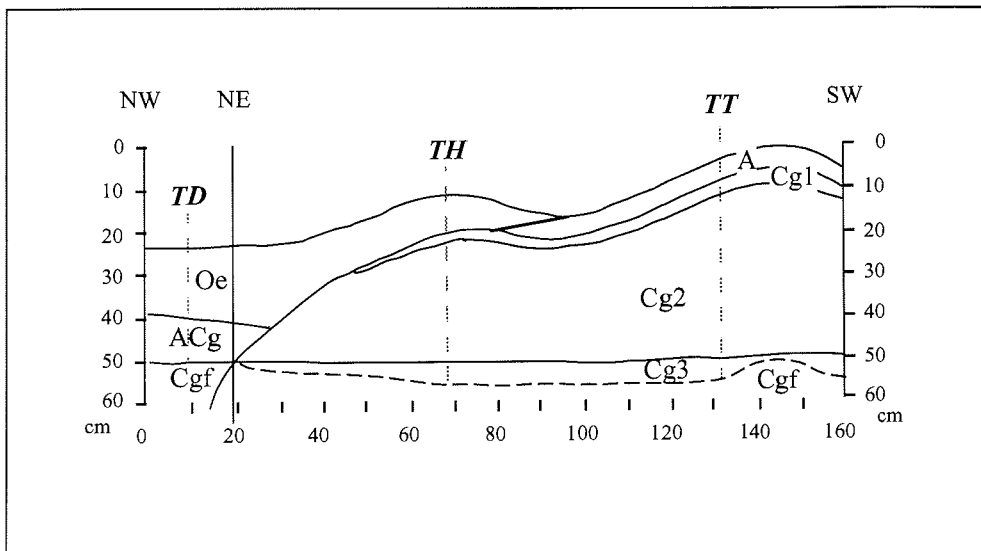


Fig. 4.1.2. Soil profile of the tussock tundra showing the cross sections of the three microsites: tussock (TT), mosshummock (TH); depression (TD).

Table 4.1.4. Soil characteristics of the tussock tundra, tussock (**TT**) (modified from Pfeiffer *et al.* 1996).

<i>horizon</i>	<i>depth</i> [cm]	<i>pH</i> (CaCl ₂)	<i>C</i> [% DW]	<i>N</i> [% DW]
A (mineral surface horizon with high humus content)	0-5	4.8	4.8	0.3
Cg1 (less developed mineral subsurface horizon with gleyic features)	5-8	5.3	2.3	0.2
Cg2	8-44	5.5	2.3	0.2
Cg3	44-50	5.3	4.0	0.3

Table 4.1.5. Soil characteristics of the tussock tundra, depression (**TD**) (modified from Pfeiffer *et al.* 1996).

<i>horizon</i>	<i>depth</i> [cm]	<i>pH</i> (CaCl ₂)	<i>C</i> [% DW]	<i>N</i> [% DW]
Oe (intermediately decomposed plant material)	0-17	5.6	33.6	1.7
ACg (less developed mineral horizon with gleyic features and high humus content)	17-27	5.5	3.8	0.3

5.1.1.2.1.3 Soil Microclimate

Depth to permafrost in the tussock tundra increased by 9-10 cm over the field season (20.7.-25.8.), resulting in maximum active layer depths of 59 cm and 48 cm by mid-August for tussock and depression, respectively (Tables 4.1.6, 4.1.7, for graphs of soil microclimate see appendix, Figs. A3, A4). Water table at the depression was observed to be between 2 cm and 6 cm below soil surface over the observed period, whereas it was found between 20 cm and 24 cm below soil surface at the tussock. Thus, the amplitude of water table changes was the same at both microsites. Differences in the position of water table between the two microsites reflected the height of the tussock, which was elevated about 18 cm over the depression.

Mainly as a consequence of micro-relief, expressed by distance to permafrost and distance to water table, the soil temperatures at various depths showed pronounced differences between the two microsites. Surface temperature values at some microsites of this study appeared to be influenced by radiation errors, so that in the following paragraphs the soil temperature at 2 cm depth will be discussed as the uppermost temperature in the profile. Average soil temperature at 2 cm depth was 13.4°C at the tussock, but only 8.6°C at the depression. Even more extreme was the difference between the maximum temperature at 2 cm depth: While a maximum temperature of 42.4°C could be observed at the tussock, the depression only reached a

maximum of 18.8°C. Minimum temperatures, in contrary, were comparable between microsites, with the tussock even showing a slightly colder value. Consequently, the soil temperature at 2 cm depth showed a much higher amplitude at the tussock (41.2°C), than at the depression (16.8°C). Another microclimatic property distinguishing the microsites of the tussock tundra from each other, was attenuation of soil temperature towards deeper horizons. The difference between the mean soil temperature at 2 cm depth and the one at 10 cm depth was 3.8°C for the tussock, but only 2.7°C for the depression. The amplitude of soil temperature in 10 cm depth was still as high as 14.4°C at the tussock, whereas it only showed a value of 6.4°C at the depression.

Depth to water table appeared responsible for attenuation of temperature and temperature amplitude at the depression. Horizons below the water table (i.e. lower than 5 cm at the depression) showed attenuated mean values and amplitude of soil temperatures. None of the soil temperatures observed at the tussock have been affected by the water table, so that the comparably less attenuated soil temperature at deeper horizons becomes readily explained.

Table 4.1.6. Soil temperatures, depth to permafrost and to water table in the tussock tundra, tussock (TT), during the field-season at Lake Labaz, 20.7-25.8.1995. Negative distances from soil surface indicate layers below soil surface.

	soil temperatures (°C)					distance from soil surface (cm)	
	surface	2 cm	5 cm	10 cm	20 cm	permafrost	water table
mean	14.6	13.4	11.0	9.6		-55.2	-21.9
max.	52	42.4	22.8	16.8		-59	-20
min.	-2.4	1.2	1.2	2.4		-50	-24

Table 4.1.7. Soil temperatures, depth to permafrost and to water table in the tussock tundra, depression (TD), during the field-season at Lake Labaz, 20.7-25.8.1995. Negative distances from soil surface indicate layers below soil surface.

	soil temperatures (°C)					distance from soil surface (cm)	
	surface	2 cm	5 cm	10 cm	20 cm	permafrost	water table
mean	12.9	8.6	7.5	5.9	2.8	-43	-3.7
max.	50.0	18.8	12.4	9.2	4.4	-48	-2
min.	1.2	2.0	2.4	2.8	1.6	-38	-6

5.1.1.2.1.4 Bacterial Biomass

Bacterial counts by epifluorescence microscopy were performed by M. Bölter (unpublished data). At the tussock microsite of the tussock tundra the total bacterial biomass decreased with depth (Table 4.1.8). A maximum value of $7.1 \mu\text{g C}^*\text{g DW}^{-1}$ was observed in the uppermost sample from 0-2 cm. Bacterial biomass from 2-5 cm depth was only about 31 % of the value from the uppermost sample. With the transition from the organic layer to the mineral horizon, the bacterial biomass decreased to values below $1 \mu\text{g C}^*\text{g DW}^{-1}$. A small increase of biomass values below 30 cm depth could be observed again.

Table 4.1.8. Total bacterial biomass (TBB) in various depths of the soil profile in tussock tundra, tussock (TT) (Bölter, unpublished data). Description of horizons from Pfeiffer *et al.* 1996.

sample / depth (cm)	horizon	TBB ($\mu\text{g C}^*\text{g DW}^{-1}$)
0-2	A	7.08
2-5	A	2.23
5-10	Cg1	0.99
10-20	Cg2	0.97
20-30	Cg2	0.63
30-40	Cg2	0.74
40-50	Cg3	0.99

While the bacterial biomass value of the uppermost sample (0-2 cm) at the depression microsite of the tussock tundra was about the same as the one observed at the tussock microsite, much higher values up to $33.11 \mu\text{g C}^*\text{g DW}^{-1}$ occurred in deeper layers (5-10 cm) of the organic horizon (Table 4.1.9). At the lower end of this horizon, the values for bacterial biomass were about similar to those of the uppermost sample. The mineral horizon from 20-27 cm depth showed a biomass value of $1.72 \mu\text{g C}^*\text{g DW}^{-1}$, considerably lower than any value of the organic layer.

Table 4.1.9. Total bacterial biomass (TBB) in various depths of the soil profile in tussock tundra, depression (TD) (Bölter, unpublished data). Description of horizons from Pfeiffer *et al.* 1996.

sample / depth (cm)	horizon	TBB ($\mu\text{g C}^*\text{g DW}^{-1}$)
0-2	Oe	7.02
2-5	Oe	13.23
5-10	Oe	33.11
10-20	Oe	5.84
20-27	ACg	1.72

5.1.1.2.2 Wet Sedge Tundra



Fig. 4.1.3. The wet sedge tundra at Lake Labaz in the surrounding of the experimental sites.

5.1.1.2.2.1 *Vegetation and Vascular Plant Biomass*

In contrast to the tussock tundra, the wet sedge tundra (WS) was homogeneous in the sense of vegetation cover. Although the total degree of coverage of the wet sedge tundra (200 %) was within the range of the corresponding value of the tussock tundra, the species-composition showed pronounced differences (Table 4.1.10). The total number of species observed in the wet sedge tundra was 14 species, only half the amount of the tussock tundra. A thick mosslayer consisting of a dense carpet of interwoven species covered the ground completely. It was only interrupted by the shoots of the monocotyledons which occupied 89 % of this type of tundra. Dwarfshrubs were represented by only three species with a total of 14 % coverage. Lichens were absent.

Table 4.1.10. Vegetation and coverage of the wet sedge tundra (WS). Plot size was 1 m² (0.5 m*2 m).

	coverage (%)	group coverage (%)	total coverage (%)
<i>Salix pulchra</i>	10		
<i>Ranunculus affinis</i>	4		
<i>Betula nana</i>	3		
<i>Salix glauca</i>	1		
<i>Rumex arcticus</i>	1		
<i>Potentilla palustris</i>	1		
		20	
<i>Carex stans</i>	78		
<i>Eriophorum angustifolium</i>	6		
<i>Arctagrostis latifolia</i>	5		
		89	
<i>Drepanocladus uncinatus</i>	59		
<i>Tomentypnum nitens</i>	18		
<i>Plagomnium elatum</i>	11		
<i>Hylocomium splendens</i>	2		
<i>Polytrichum strictum</i>	1		
		91	200

The belowground biomass of the wet sedge tundra was exceeding 8.3 kg*m⁻² (Table 4.1.11), which was about twice the amount sampled in the tussock tundra. Aboveground biomass was found to be about 180 g*m⁻², less than half the value of the tussock microsite, but more than at the depression microsite of the tussock tundra. The aboveground production/biomass-ratio of the wet sedge tundra showed a value of 0.89, which was about triple the corresponding values from the tussock tundra. The main reason for this can be found in the high percentage of monocotyledons in the wet sedge tundra. The ratio of aboveground/belowground biomass was 0.02, representing the lowest ratio observed among the investigated sites at Lake Labaz.

Table 4.1.11. Biomass and annual production of the wet sedge tundra (WS) in g dry weight (DW) per m² (joint work, modified from Sommerkorn 1996 and Pfeiffer *et al.* 1996).

biomass (g DW*m ⁻²)		production (g DW*m ⁻² *a ⁻¹)
aboveground	belowground	aboveground
177	8360	157

5.1.1.2.2.2 Soils

The soil of the wet sedge tundra could as well be characterized as Pergelic Cryaquept (Soil Taxonomy) or Cryic Histosol (FAO) (Pfeiffer *et al.* 1996), deriving from loamy-clayey parent material. It was characterized by a water table permanently situated close to the surface. A thick organic surface layer, where the majority of soil-carbon was stored, covered the mineral horizon (Fig. 4.1.4, Table 4.1.12, description of the unfrozen horizons of the profile).

In contrast to the soils of the tussock tundra, the soil of the wet sedge tundra was homogeneous. The thick organic surface layer of the wet sedge tundra consisted of poorly decomposed organic material. The mineral horizon showed a high humus content and gleyic features. The carbon content of the organic surface layer was about half that of the depression of the tussock tundra. In the wet sedge tundra, a nitrogen content of only about a third of that measured at the tussock tundra depression resulted in a C/N-ratio of 28, the widest ratio analysed. In the lower horizon this ratio exceeded the range observed in the tussock tundra, by showing a value of 13.5. As with the depression of the tussock tundra, the comparatively high C/N-ratios can be taken as an indication of low turnover-rates of organic matter at this coldest and wettest site of the three analysed at Lake Labaz (see chapter: 4.1.1.2.2.3).

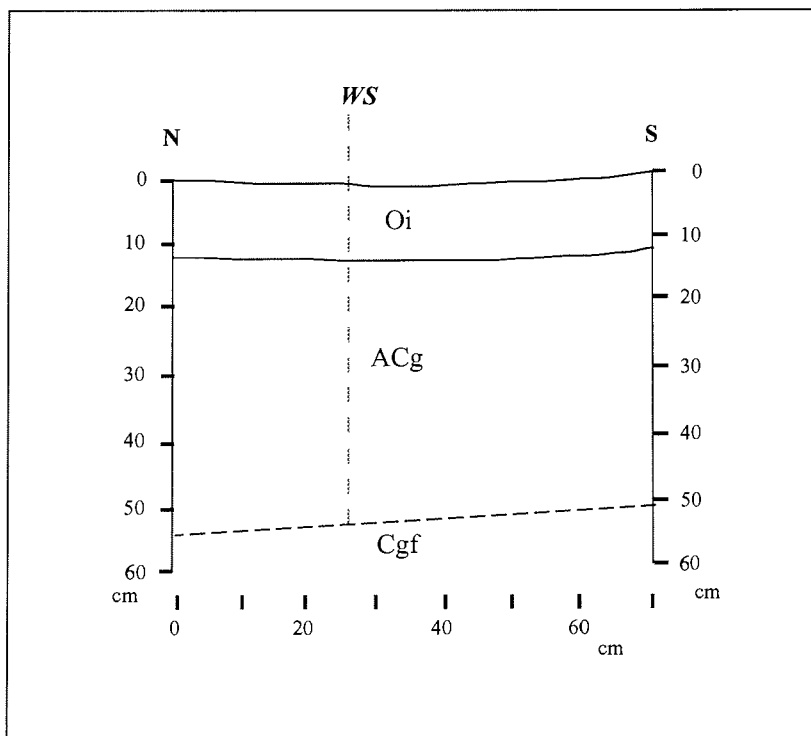


Fig. 4.1.4. Soil profile of the wet sedge tundra showing the cross section of the microsite WS.

Table 4.1.12. Soil characteristics of the wet sedge tundra (WS) (modified from Pfeiffer *et al.* 1996).

<i>horizon</i>	<i>depth</i> [cm]	<i>pH</i> (CaCl ₂)	<i>C</i> [% DW]	<i>N</i> [% DW]
Oi (poorly decomposed plant material)	0-12	4.1	16.8	0.6
ACg (less developed mineral horizon with gleyic features and high humus content)	12-54	5.7	2.7	0.2

5.1.1.2.2.3 Soil Microclimate

Depth to permafrost in the wet sedge tundra increased by 10 cm over the field season (20.7.-25.8.), resulting in a maximum active layer depth of 54 cm during the second half of August (Table 4.1.13, for graphs of soil microclimate see appendix, Fig. A5). The amplitude of water table changes was restricted in this type of tundra; oscillations of only 2 cm were observed. Mean water table position was found at about 2 cm below soil surface, representing the highest position of the sites investigated at Lake Labaz. The reason for the constantly high water table can be found in the fact that the area around the experimental site served as a watertrack.

The mean soil temperature at 2 cm depth was 8°C, which was the lowest value observed at Lake Labaz. With a maximum soil temperature at 2 cm depth of 13.6°C and a minimum temperature of 2.4°C, the wet sedge tundra showed the lowest amplitude of soil temperature at this depth, as compared to the corresponding values from the tussock tundra microsites. The dense and homogeneous vegetation cover of the monocotyledons reduced warming of upper soil layers by direct radiation. Due to the constantly high water table in the wet sedge tundra, the temperatures at 2 cm depth were already determined by the cold regime of the soil water. Soil temperatures of layers below the water table were comparable between wet sedge tundra and depression of the tussock tundra, both in terms of absolute values and amplitudes.

The difference between the mean soil temperature value at 2 cm depth and the one at 10 cm depth was 2.2°C, which was the lowest value observed among the investigated sites at Lake Labaz. Consequently, the temperature distribution between soil surface and permafrost was most homogeneous in this tundra type.

Table 4.1.13. Soil temperatures, depth to permafrost and to water table in the wet sedge tundra (WS) during the field-season at Lake Labaz, 20.7-25.8.1995. Negative distances from soil surface indicate layers below soil surface.

	soil temperatures (°C)					distance from soil surface (cm)	
	surface	2 cm	5 cm	10 cm	20 cm	permafrost	water table
mean	9.2	8.0	7.0	5.8	4.1	-50	-2.1
max.	26.8	13.6	11.6	8.8	6.4	-54	-1
min.	2.4	2.4	2.4	2.4	2.4	-44	-3

5.1.1.2.2.4 Bacterial Biomass

The values for bacterial biomass in the profile of the wet sedge tundra (Bölter, unpublished data) showed a pronounced decrease with depth (Table 4.1.14). The highest bacterial biomass of 29.4 $\mu\text{g C}^*\text{g DW}^{-1}$ was observed in the sample from 0-2 cm depth, the lowest layer of the organic horizon still showed a value of 7.3 $\mu\text{g C}^*\text{g DW}^{-1}$. Biomass values constantly decreased throughout the mineral horizon as well. The lowest value of 0.5 $\mu\text{g C}^*\text{g DW}^{-1}$ was found in the lowest sample of the active layer (30-50 cm). It accounted for only 1.8 % of the bacterial biomass of the uppermost sample.

Table 4.1.14. Total bacterial biomass (TBB) in various depths of the soil profile in wet sedge tundra (WS) (Bölter, unpublished data). Description of horizons from Pfeiffer *et al.* 1996.

sample / depth (cm)	horizon	TBB ($\mu\text{g C}^*\text{g DW}^{-1}$)
0-2	Oi	29.38
2-5	Oi	16.21
5-10	Oi	7.34
10-20	ACg	2.48
20-30	ACg	1.47
30-50	ACg	0.52

5.1.2 Lake Levinson-Lessing

5.1.2.1 Mesoclimate of the Field Season

Mesoclimatic data for the field season at Lake Levinson-Lessing (20.7.-12.8.) are somewhat incomplete due to a malfunction of the precipitation gauge and a one week data loss in the period 20.7.-27.7.. The first half of that particular week was rainy and stormy with permanent overcast, the second half led over to a sunny and warm period, whose end was recorded again (for graphs of mesoclimate and a table of daily values of mesoclimatic parameter see appendix, Fig. A2, Table A2). The rest of the field-season was characterized by cool, cloudy and humid weather. Fog was frequent, because Lake Levinson-Lessing was covered by ice until the second week of August. The first snow fell on 11.8.. Compared with the equivalent period of the Lake Labaz field season of 1995 (Table 4.1.1), ambient temperatures for the field season at Lake Levinson-Lessing in 1996 were lower (Table 4.1.15). Mean temperature for the first half of August was about 2.5°C lower (minimum temperature 0.5°C lower, maximum temperature 3°C lower) than at the more southerly site. Whereas the maximum daily average at Lake Levinson-Lessing was recorded as 13.7°C and was thus almost identical with the corresponding value at Lake Labaz, the minimum daily average was 2.2°C at the northern site, which is as much as 4.7°C lower than at the southern site. On the other hand, the mean temperature of the recorded period at Lake Levinson-Lessing was about 2°C warmer than the long-term monthly average of August from Lake Taimyr Station (1.5°C warmer than the average for July), indicating a warm summer for this area of Taimyr Peninsula in 1996. The mean daily total PPFD value for Lake Levinson-Lessing was low ($15 \text{ mol} \cdot \text{m}^{-2} \cdot \text{d}^{-1}$), as compared to the corresponding value of Lake Labaz, due to extensive and persistent cloud cover. This can also be seen from the minimum daily total, which was as low as $4.5 \text{ mol} \cdot \text{m}^{-2} \cdot \text{d}^{-1}$. The corresponding values for Lake Labaz were $23 \text{ mol} \cdot \text{m}^{-2} \cdot \text{d}^{-1}$ and $12.8 \text{ mol} \cdot \text{m}^{-2} \cdot \text{d}^{-1}$, respectively.

Table 4.1.15. Mesoclimate of the field-season at Lake Levinson-Lessing, 1996.

	<i>recorded period of campaign (27.7.-12.8.)</i>	
	<i>ambient temp. (°C)</i>	<i>daily total PPFD ($\text{mol} \cdot \text{m}^{-2} \cdot \text{d}^{-1}$)</i>
mean	8.2	15.0
max.	20.2	28.3
min.	0.9	4.5
max. daily average	13.7	
min. daily average	2.2	

5.1.2.2 Characteristics of the Experimental Sites

At the intensive study site “Lake Levinson-Lessing“, CO₂-flux-measurements were obtained at three microsites of a low-centre polygonal tundra, the dominating tundra type of the study area (see also Fig. 2.3). The three microsites investigated were situated within 2 m distance. Due to logistic constraints on the duration of the field-stay, one microsite was not fully elaborated.

5.1.2.2.1 Low-Centre Polygonal Tundra



Fig. 4.1.5. The polygonal tundra at Lake Levinson-Lessing. Experimental sites were situated close to the tent (centre of the picture). High apices appear brown, low apices yellow, and depressions green in this view.

5.1.2.2.1.1 Vegetation and Vascular Plant Biomass

In terms of vegetation, spatial heterogeneity in the low-centre polygonal tundra occurred on a wider scale than in the tussock tundra at Lake Labaz. Microsite differentiation was obvious between the wet central depression (PD), humid low apices (PL, <30 cm elevated over the depression) and mesic high apices (PH, 30-60 cm elevated over the depression). About 25 % of the polygon areas were low apices, 10 % high apices, and two thirds (65 %) depressions.

The uniform depression area of the polygons adjacent to the measuring-sites was about 10 * 10 m wide. The vegetation of this microsite was dominated by *Carex stans* and *Dupontia fisheri* on the vascular plant side, and *Drepanocladus revolvens* as well as *Calliergon sarmentosum* on the moss side. Mosses altogether showed a coverage of 100 %, whereas vascular plants covered 80 % (Table 4.1.16). Lichens were absent, dicotyledons represented only 5 % of coverage.

Table 4.1.16. Vegetation and coverage of the depression of the polygonal tundra (PD).

	coverage (%)	group coverage (%)	total coverage (%)
<i>Carex stans</i>	60		
<i>Dupontia fisheri</i>	20		
		80	
<i>Salix reptans</i>	3		
<i>Caltha arctica</i>	1		
<i>Pedicularis albalabiata</i>	1		
		5	
<i>Drepanocladus revolvens</i>	60		
<i>Calliergon sarmentosum</i>	20		
<i>Plagomnium elatum</i>	10		
<i>Polytrichum strictum</i>	10		
		100	185

Compared with the tundra type of the southern tundra at Lake Labaz, the depressions of the polygonal tundra contained only low biomass and annual production values were low (Table 4.1.17). Aboveground biomass was 56 g DW*m⁻² (Becker 1997), representing only 43 % of the corresponding value at the depression microsite of the tussock tundra, which was the poorest microsite at the southern location. Also, the ratio of aboveground/belowground biomass illustrates the comparative poverty of the depression of the polygonal tundra. With a value of 0.017, it was lower than the corresponding value of the wet-sedge tundra, the lowest analysed at the southern locality. In contrast to all other microsites investigated, annual production and biomass at the depression of the polygonal tundra was the same. Hence the production/biomass ratio was 1, which was the highest value of all investigated microsites. In this special case, plots for vegetation analysis and biomass/production analysis were not identical, but closely neighboured. There were no dicotyledons in the plot sampled for biomass/production values (Becker, personal communication. See chapter 3.3 for method of sampling) As remarked above, the analysis of belowground biomass was associated with some technical constraints, which may have resulted in overestimates (see chapter 3.3).

Table 4.1.17. Biomass and production of polygonal tundra, depression (PD) (modified from Becker, 1997).

<i>biomass (g DW*m⁻²)</i>		<i>production (g DW*m⁻²*a⁻¹)</i>
<i>aboveground</i>	<i>belowground</i>	<i>aboveground</i>
56	3388	56

At humid low polygon apices, the total degree of plant coverage was not as high as at the depression microsite. The vegetation at the low apices showed an increasing abundance of dwarf-shrubs, in particular *Dryas punctata*, which accounted for a total of 20 % of the coverage (Table 4.1.18). Other dwarf-shrubs, monocotyledons and lichens were responsible for a total species richness more than twice as high than at the depression microsite. Total vascular plant cover was 56 %, whereas mosses accounted for 93 %. *Tomentypnum nitens* dominated on the moss side, representing as much as 75 % of the coverage.

Table 4.1.18. Vegetation and coverage of the low apex of the polygonal tundra (PL).

	<i>frequency (thalli/m²)</i>		
<i>Stereocaulon spec.</i>	29		
<i>Thamnozia vermicularis</i>	46		
<i>Dactylina arctica</i>	15		
<i>Peltigera aptosa</i>	15		
<i>Cetraria cucullata</i>	2		
		total=107	
	<i>coverage (%)</i>	<i>group coverage (%)</i>	<i>total coverage (%)</i>
<i>Dryas punctata</i>	20		
<i>Astragalus umbelatus</i>	6		
<i>Salix pulchra</i>	9		
<i>Salix reptans</i>	5		
<i>Polygonum viviparum</i>	1		
<i>Pedicularis albalabiata</i>	1		
		42	
<i>Carex arctosibirica</i>	9		
<i>Arctagrostis latifolia</i>	1		
<i>Dupontia fisheri</i>	1		
<i>Eriophorum angustifolium</i>	3		
		14	
<i>Tomentypnum nitens</i>	75		
<i>Hylocomium splendens</i>	6		
<i>Aulacomnium turgidum</i>	8		
<i>Polytrichum strictum</i>	4		
		93	149

The mesic microsite of the high apices showed the same total degree of coverage as the low apex microsite (Table 4.1.19). Although the species composition of both microsites was quite similar, several differences indicated that the high apex microsite was drier and more exposed than the low apex microsite: When moving upwards in micro-relief, the total coverage by mosses decreased from near to 100 % to 76 %, as did the total number of moss species from 4 to 2. Also, the total number of lichen thalli observed increased by 47 %. Both monocotyledons indicating wet conditions (*Dupontia fisheri*, *Eriophorum vaginatum*) disappeared.

Table 4.1.19. Vegetation and coverage of the high apex of the polygonal tundra (PH).

	frequency (thalli/m ²)		
<i>Cetraria cucullata</i>	42		
<i>Thamnia vermicularis</i>	38		
<i>Dactylina arctica</i>	33		
<i>Stereocaulon spec.</i>	18		
<i>Cetraria nivalis</i>	15		
<i>Peltigera aptosa</i>	11		
	total =157		
	coverage (%)	group coverage (%)	total coverage (%)
<i>Dryas punctata</i>	39		
<i>Salix pulchra</i>	10		
<i>Astragalus alpinus</i>	3		
<i>Astragalus umbellatus</i>	2		
<i>Minuartia biflora</i>	1		
<i>Saxifraga hirculus</i>	1		
		56	
<i>Carex arctosibirica</i>	14		
<i>Arctagrostis latifolia</i>	4		
		18	
<i>Tomentypnum nitens</i>	32		
<i>Hylocomium splendens</i>	44		
		76	150

5.1.2.2.1.2 Soils

The low-centre polygonal tundra at Lake Levinson-Lessing showed wet soils derived from loamy-sandy sediments and accumulation of poorly decomposed plant material (Soil Taxonomy: Pergelic Cryaquept, FAO: Cryic Histosol)(Gundelwein *et al.* 1997). The main soil characteristics of the investigated polygon sites are presented in Fig. 4.1.6 and Tables 4.1.20 and 4.1.21 (Due to logistical constraints on the duration of the field-stay, soil parameters of the high apex site have not been elaborated). Most noticeable, the organic surface layers were much thinner as compared to those of the Lake Labaz-region. In contrast to the maximum of 17 cm thickness of the organic mat at the depression of the tussock tundra, only 6 cm thickness was observed in the polygonal tundra. In the case of the central depression of the polygonal tundra, the organic horizon could be separated in a poorly -and an intermediately decomposed horizon. The underlying sandy horizon showed gleyic features and was very acidic. The carbon-content of the organic horizons was high at both sites in micro-relief, but highest at the depression microsite. In lower horizons, remarkable amounts of carbon could be found. Compared with the tundra types at Lake Labaz the carbon-content of the organic layers ranged near to that of the wet sedge tundra, but exceeded the values with respect to the sub-surface horizons. The C/N-ratio of the polygonal tundra was similar to that of the wet sedge tundra at Lake Labaz: A decrease from 30 (organic surface horizon) to 15 (sandy mineral horizon) was observed at the depression of the polygonal tundra, whereas the corresponding values at the low apex site were 26 and 13.3, respectively. These comparatively wide ratios can be taken as indication of poor turnover-rates of organic material in this wet and cold tundra type.

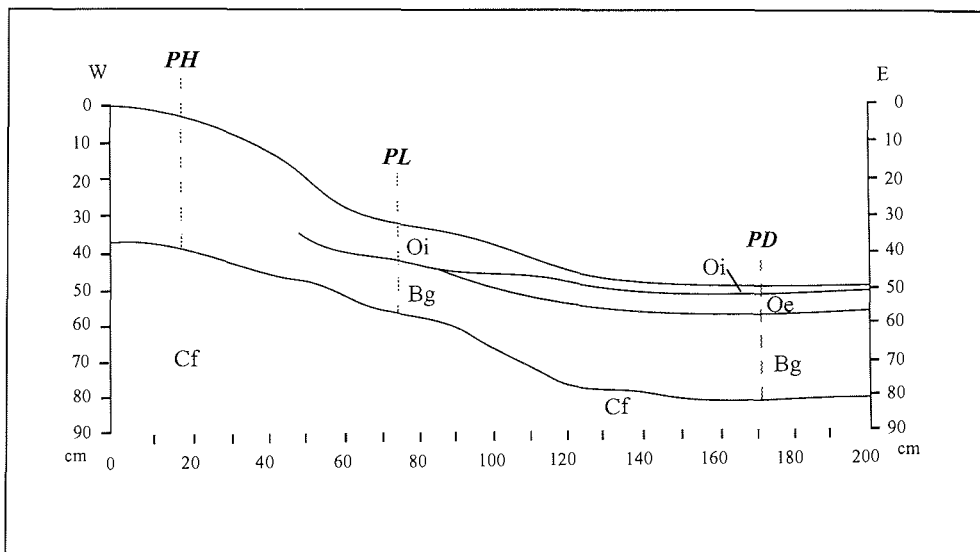


Fig. 4.1.6. Soil profile of the polygonal tundra showing the cross sections of the three microsites: high apex (PH), low apex (PL); depression (PD). No profile description can be given for the high apex microsite (see text).

Table 4.1.20. Soil characteristics of the depression of the polygonal tundra (**PD**) (modified from Gundelwein *et al.* 1997).

<i>horizon</i>	<i>depth</i> [cm]	<i>pH</i> (CaCl ₂)	<i>C</i> [% DW]	<i>N</i> [% DW]
Oi (poorly decomposed plant material)	0-2	5.0	18.0	0.6
Oe (intermediately decomposed plant material)	2-6	4.0	10.3	0.6
Bg (sandy mineral horizon with gleyic features)	6-35	4.3	6.0	0.4

Table 4.1.21. Soil characteristics of the low apex of the polygonal tundra (**PL**) (modified from Gundelwein *et al.* 1997).

<i>horizon</i>	<i>depth</i> [cm]	<i>pH</i> (CaCl ₂)	<i>C</i> [% DW]	<i>N</i> [% DW]
Oi (poorly decomposed plant material)	0-6	5.0	13.0	0.5
Bg (sandy mineral horizon with gleyic features)	6-25	4.6	4.0	0.3

5.1.2.2.1.3 Soil Microclimate

As demonstrated above for the spatially heterogeneous tussock tundra at Lake Labaz, also the low-centre polygonal tundra at Lake Levinson-Lessing also showed a variety of microclimatic conditions within its microsites. Mainly as a consequence of position in micro-relief, mean depth to water table dropped from less than 1 cm below the soil surface at the polygon depression to nearly 32 cm at the high apex over a horizontal distance of less than 2 m (Tables 4.1.22, 4.1.23, 4.1.24). Total amplitude of the water table position over the field season was found to be nearly identical at all microsites. After intensive rainfalls from 4.8.-7.8., the water table raised by about 7 cm, which in the case of the polygon depression led to water standing above the ground for 5 days (for graphs of soil microclimate see also appendix, Figs. A6, A7, A8).

Exposure, depth to water table, and a combination of plant cover and depth of active layer contributed to the differences of soil temperatures between microsites of the polygonal tundra, but differences were not as pronounced as in the tussock tundra. The coldest microsite (as indicated by soil temperature at 2 cm depth was the high apex showing a mean temperature of more than 1.5°K less than the depression, the warmest microsite. Also when looking at the mean soil temperatures in deeper horizons, the depression was the warmest microsite. While the high apex and the low apex showed almost identical mean soil temperatures close to the surface, the temperature amplitudes were different. Whereas the low apex showed the highest

amplitude of all microsites at 2 cm depth, it revealed the lowest at 20 cm depth. Contrary to this, the high apex showed the lowest amplitude of all microsites at 2 cm depth, but still the highest at 20 cm depth. These conditions were contrary to those of the investigated tundra type at Lake Labaz, where the wet sites were coldest and showed the narrowest amplitude of soil temperature over the profile. They may be explained by the high apex of the polygonal tundra being the most exposed microsite during a windy and cloudy season. Also, the insulating effect of the well developed mosslayer at the low apex microsite led to a high frost table at this microsite, resulting in the comparable low mean temperatures and temperature amplitudes in 10 and 20 cm depth. Additionally, the thermal buffer water may have a positive instead of a negative effect on the temperature regime of soils at this northern location already during late July and early August, resulting in the comparatively higher temperatures at all horizons of the depression microsite.

The increase of active layer depths in the polygonal tundra was not found as homogeneous as in the tundra types at Lake Labaz. Whereas the depth to permafrost increased only by 8.5 cm over the field season at the depression microsite, the corresponding value was 11 cm for the low apex and as much as 15 cm at the high apex. This corresponds to the general observation that drier sites thaw deeper and faster than their wet counterparts. Another important fact to mention when comparing the Lake Labaz-sites to the Lake Levinson-Lessing-sites is the as an average 20 cm deeper active layer in the southern tundra type.

Table 4.1.22. Soil temperatures, depth to permafrost and to water table at the depression of the polygonal tundra (PD) during the field-season at Lake Levinson-Lessing, 20.7.-12.8. 1996.

	soil temperatures (°C)					distance from soil surface (cm)	
	surface	2 cm	5 cm	10 cm	20 cm	permafrost	water table
mean	9.3	8.4	7.1	5.3	2.3	-28.9	-0.7
max.	21.6	17.6	12.8	8.4	3.2	-31.5	5
min.	2.4	2.4	2.4	2.4	0.8	-23	-7

Table 4.1.23. Soil temperatures, depth to permafrost and to water table at the low apex of the polygonal tundra (PL) during the field-season at Lake Levinson-Lessing, 20.7.-12.8. 1996.

	soil temperatures (°C)					distance from soil surface (cm)	
	surface	2 cm	5 cm	10 cm	20 cm	permafrost	water table
mean	9.5	7.0	5.4	4.0	0.9	-22.7	-8.0
max.	32.8	19.6	12.0	7.2	2.0	-26	-2
min.	1.2	1.2	1.2	1.2	0.0	-15	-14

Table 4.1.24. Soil temperatures, depth to permafrost and to water table at the high apex of the polygonal tundra (PH) during the field-season at Lake Levinson-Lessing, 20.7.-12.8. 1996.

	soil temperatures (°C)					distance from soil surface (cm)	
	surface	2 cm	5 cm	10 cm	20 cm	permafrost	water table
mean	8.6	6.8	5.7	4.7	2.2	-31	-31.7
max.	21.6	15.2	10.8	8.0	4.0	-37	-25
min.	2.0	2.0	2.0	2.4	0.4	-22	-35

5.1.2.2.1.4 Bacterial Biomass

Analysis of bacterial biomass in the polygonal tundra was performed by M. Bölker (unpublished data). The profile at the depression microsite showed a decrease of bacterial biomass with depth (Table 4.1.25). The highest value of $14.8 \mu\text{g C}\cdot\text{m}^{-2}\cdot\text{d}^{-1}$ was observed in the sample from 0-2 cm depth. This was about half the value of the uppermost sample from the wet sedge tundra at Lake Labaz. The bacterial biomass dropped only slightly in the lower organic horizon (Oe), still showing a value of $1.6 \mu\text{g C}\cdot\text{m}^{-2}\cdot\text{d}^{-1}$. The mineral horizon (Bg) still showed a biomass value of $6.2 \text{ mg CO}_2\cdot\text{m}^{-2}\cdot\text{h}^{-1}$, which was considerably higher than the value of the corresponding horizon from the wet sedge tundra at Lake Labaz.

Table 4.1.25. Total bacterial biomass (TBB) in various depths of the soil profile in polygonal tundra, depression (PD) (Bölker, unpublished data). Description of horizons from Gundelwein *et al.* 1997.

sample / depth (cm)	horizon	TBB ($\mu\text{g C}\cdot\text{g DW}^{-1}$)
0-2	Oi	14.76
2-6	Oe	11.58
6-35	Bg	6.23

The low apex microsite showed a decrease of the bacterial biomass with depth as well, but the differences between values were much smaller (Table 4.1.26). The biomass value of the uppermost horizon was as low as $3.6 \mu\text{g C}\cdot\text{m}^{-2}\cdot\text{d}^{-1}$, which is only about 25 % of the corresponding value from the depression microsite. Bacterial biomass decreased only slightly towards the lower horizons, showing values of about $2.1 \mu\text{g C}\cdot\text{m}^{-2}\cdot\text{d}^{-1}$ in the sample from 10-25 cm.

Bacterial biomass at the high apex microsite was not determined.

Table 4.1.26. Total bacterial biomass (TBB) in various depths of the soil profile in polygonal tundra, low apex (PL) (Bölter, unpublished data). Description of horizons from Gundelwein *et al.* 1997.

<i>sample / depth (cm)</i>	<i>horizon</i>	<i>TBB ($\mu\text{g C}\cdot\text{g DW}^{-1}$)</i>
0-5	Oi	3.61
5-10	Bg	3.31
10-25	Bg	2.07

5.2 *Experimental Results*

5.2.1 **Soil Respiration Studies**

5.2.1.1 *Experiments in the Field*

The soil respiration experiments performed in the scope of this study were designed to reveal quantitative as well as qualitative differences of the soil respiration process between tundra types and microsites. Therefore, experiments were performed at seven different microsites in three different tundra types, tussock tundra and wet sedge tundra (in the Southern Arctic Tundra at Lake Labaz), as well as low-centre polygonal tundra (in the Typical Arctic Tundra at Lake Levinson-Lessing). Three microsites were investigated in the tussock tundra, the tussock (TT), the moss hummock (TH), and the depression (TD). One site was under elaboration in the wet sedge tundra (WS). In the low-centre polygonal tundra, three microsites were investigated, the central depression (PD), the low apex (PL), and the high apex (PH). Soil and vegetation properties, microclimatic characteristics of these microsites and the scale of heterogeneity are described in the chapters “Characteristics of the experimental sites“ (4.1.1.2, and 4.1.2.2).

A total of 627 values (15 min. averages, see chapter 3.1.4) were recorded during about 41 diurnal experiments. Some diurnal experiments could not be performed for 24 h without interruption, mainly due to generator problems resulting from poor gasoline quality.

In order to identify microclimatic parameters generally controlling the soil respiration process of all investigated sites during the experimental periods, Spearman rank correlation of all soil respiration data with microclimatic site parameters was performed. The results of the correlation analysis identified water table to be the factor explaining most of the variation in soil respiration, closely followed by soil temperature at 2 cm depth (Table 4.2.1). As one consequence of this results, the obtained soil respiration values of the various tundra types and their microsites will be presented together with the courses of depth to water table and soil temperature at 2 cm depth (which will be abbreviated ST2 from here on) in the following paragraphs. Please note that ST2 and depth to water table values given in Tables are restricted to those taken simultaneously with the presented CO₂ effluxes.

Table 4.2.1. Spearman rank correlations (r_s) for all soil respiration data (15 min. averages, $n=627$) of all sites investigated with microclimatic parameters. * indicates correlation is significantly different from zero at $P<0.05$.

	<i>soil temperatures</i>						
	<i>surface</i>	<i>2 cm</i>	<i>5 cm</i>	<i>10 cm</i>	<i>20 cm</i>	<i>depth to water table</i>	<i>depth to permafrost</i>
soil respiration, all data, all sites	*0.566	*0.709	*0.673	*0.616	0.003	*-0.736	-0.092

5.2.1.1.1 Lake Labaz

Tussock tundra, tussock (TT)

At the beginning of the field season at Lake Labaz soil respiration rates observed were not measurable with the settings and performance of the instrumentation. Some modifications had to be made to the hydraulic system to make detection of these fluxes possible (see chapter 3.1.1). Depth to water table ranged between 21 cm and 23 cm below soil surface during experimental periods (Fig. 4.2.1 and Table 4.2.2). Soil respiration rates reaching a maximum of nearly $500 \text{ mg CO}_2 \cdot \text{m}^{-2} \cdot \text{h}^{-1}$ were recorded with an ST2 of 26.4°C during the last days of the measuring campaign. With a minimum observed ST2 of 5.2°C , the tussock microsite still showed soil respiration rates of about $400 \text{ mg CO}_2 \cdot \text{m}^{-2} \cdot \text{h}^{-1}$, the highest minimum rate of all microsites. The highest rates and the largest diurnal variations of soil respiration in the scope of this study were observed at this microsite.

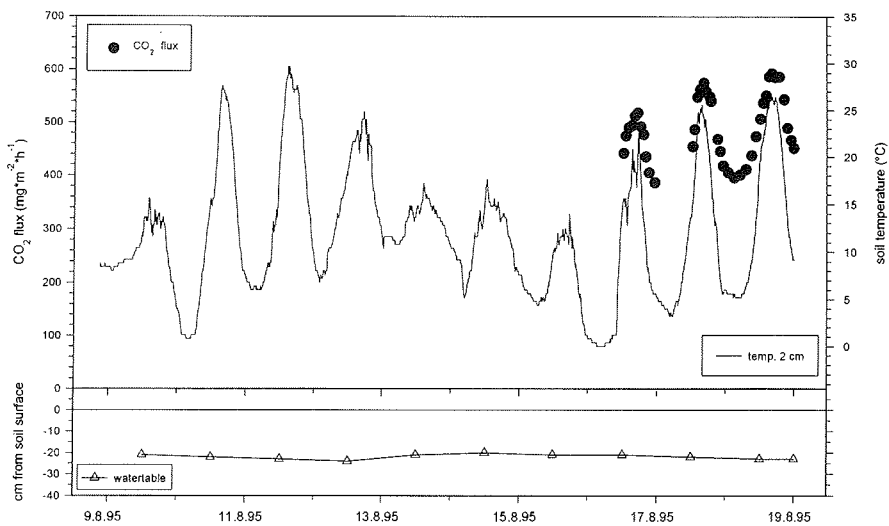


Fig. 4.2.1. 15 min. average values for CO₂-flux of soil respiration, soil temperature at 2 cm depth, and water table in tussock tundra, tussock (TT).

Table 4.2.2. Amplitudes and means of soil respiration, soil temperature at 2 cm depth, and water table of tussock tundra, tussock (TT), during periods of experiments.

	soil respiration (mg CO ₂ *m ⁻² *h ⁻¹)	soil temperature 2 cm (°C)	water table (cm from soil surface)
mean	490.6	15.8	-22.2
max	592.0	26.4	-21
min	395.2	5.2	-23

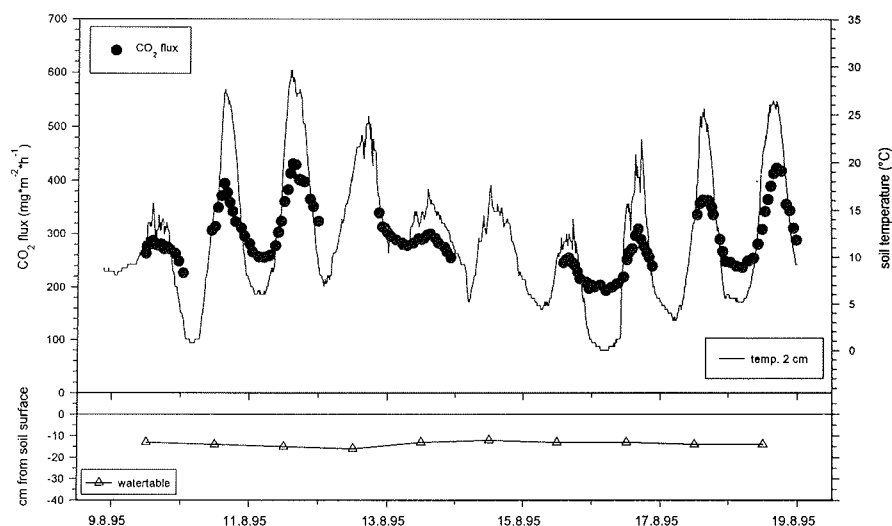


Fig. 4.2.2. 15 min. average values for CO₂-flux of soil respiration, soil temperature at 2 cm depth, and water table in tussock tundra, moss hummock (TH).

Table 4.2.3. Amplitudes and means of soil respiration, soil temperature at 2 cm depth, and water table in tussock tundra, moss hummock (TH), during periods of experiments.

	soil respiration (mg CO ₂ *m ⁻² *h ⁻¹)	soil temperature 2 cm (°C)	water table (cm from soil surface)
mean	297.7	14.6	-13.8
max	430.7	28.8	-12.6
min	209.0	3.2	-15.5

Tussock tundra, moss hummock (TH)

Depths to water table ranged between 12.6 cm and 15.5 cm below the soil surface during the experiment. Soil respiration rates at the moss hummock microsite of the tussock tundra showed large diurnal variations as well (Fig. 4.2.2). Maximum values of 430 mg CO₂*m⁻²*h⁻¹ were recorded at a ST2 of 28.8°C (Table 4.2.3). Minimum ST2 as low as 3.2°C led to soil respiration rates of more than 200 mg CO₂*m⁻²*h⁻¹.

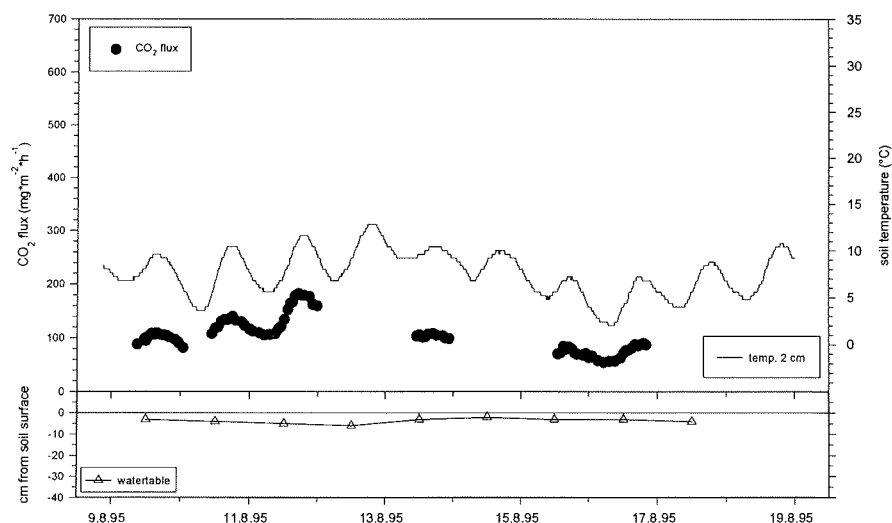


Fig. 4.2.3. 15 min. average values for CO₂-flux of soil respiration, soil temperature at 2 cm depth, and water table in tussock tundra, depression (TD).

Table 4.2.4. Amplitudes and means of soil respiration, soil temperature at 2 cm depth, and water table in tussock tundra, depression (TD), during periods of experiments.

	soil respiration (mg CO ₂ *m ⁻² *h ⁻¹)	soil temperature 2 cm (°C)	water table (cm from soil surface)
mean	106.7	7.7	-3.7
max	181.8	11.6	-2.5
min	54.0	2.0	-5.4

Tussock tundra, depression (TD)

Parallel with a water table ranging between 2.5 cm and 5.4 cm below soil surface (about 10 cm higher than at the moss hummock microsite), and ST2 of highest 11.6°C, maximum soil respiration rates of about 180 mg CO₂*m⁻²*h⁻¹ could be measured (Table 4.2.4). This value was a little less than the minimum rate observed at the moss hummock microsite with a ST2 of as low as 3.2°C. Minimum soil respiration rates at the depression microsite were found as low as 54 mg CO₂*m⁻²*h⁻¹ with a water table about 3 cm below the soil surface and ST2 of 2°C. At the depression microsite the modifying aspect of water table changes on a daily basis could be identified: maximum ST2-values on 13.8. were the same as on 10.8., but resulting CO₂ effluxes were considerably lower on the former day, when the water table position was some 2 cm closer to the soil surface than on the latter day. At the depression microsite of the

tussock tundra, absolute soil respiration rates were considerably lower and diurnal variations more attenuated than at the previously presented microsites (Fig. 4.2.3).

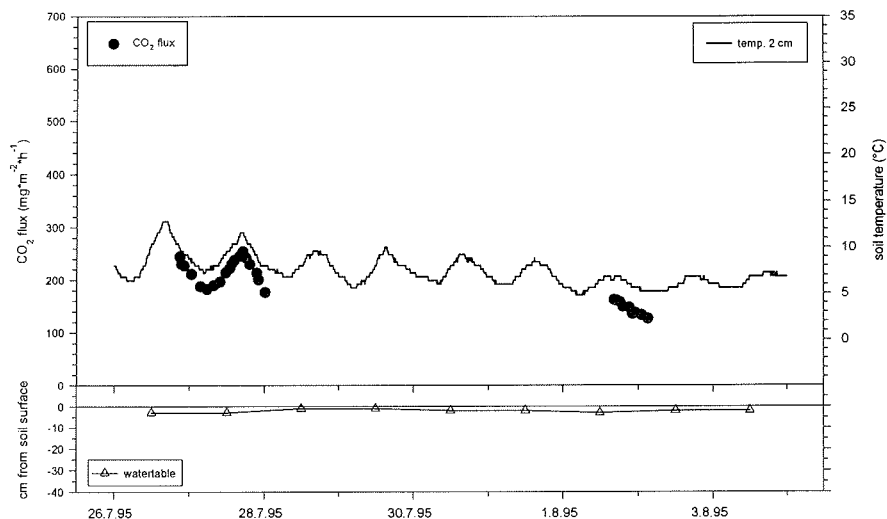


Fig. 4.2.4. 15 min. average values for CO₂-flux of soil respiration, soil temperature at 2 cm depth, and water table in wet sedge tundra (WS).

Table 4.2.5. Amplitudes and means of soil respiration, soil temperature at 2 cm depth, and water table in wet sedge tundra (WS), during periods of experiments.

	soil respiration (mg CO ₂ *m ⁻² *h ⁻¹)	soil temperature 2 cm (°C)	water table (cm from soil surface)
mean	194.4	8.3	-2.7
max	254.2	11.6	-2.0
min	125.9	5.2	-3.0

Wet sedge tundra (WS)

Three diurnal courses of soil respiration in wet sedge tundra (26.-27.7., 1.8.) showed a maximum CO₂ efflux rate of about 250 mg CO₂*m⁻²*h⁻¹ with a ST2 of 11.6°C (Fig. 4.2.4, Table 4.2.5). The high degree of vegetation cover shaded the soil surface and the constant water flow through this tundra type (see chapter 4.1.1.2.2) provided a thermal buffer, resulting in the lowest amplitude of ST2 in the wet sedge tundra. As a consequence, minimum CO₂ effluxes of 126 mg CO₂*m⁻²*h⁻¹ observed in combination with a ST2 of 5.2°C resulted in the lowest observed amplitude in soil respiration of only about 130 mg CO₂*m⁻²*h⁻¹. Depth to water table during the experimental periods was very stable and varied only between 2 cm and

3 cm below the soil surface. With a water table position of some 2.5 cm lower and the same maximum ST2, the depression microsite of the tussock tundra reached only about $180 \text{ mg CO}_2 \cdot \text{m}^{-2} \cdot \text{h}^{-1}$. Soil respiration rates towards the end of the measuring campaign were lower than during the first diurnal courses, due to slightly higher water table and lower temperatures.

A serious generator failure and resulting problems with the gas exchange device in the period from 28.7. to 1.8., as well as an unexpected end of the measuring campaign due to logistic problems, constrained the database of the wet sedge tundra at Lake Labaz.

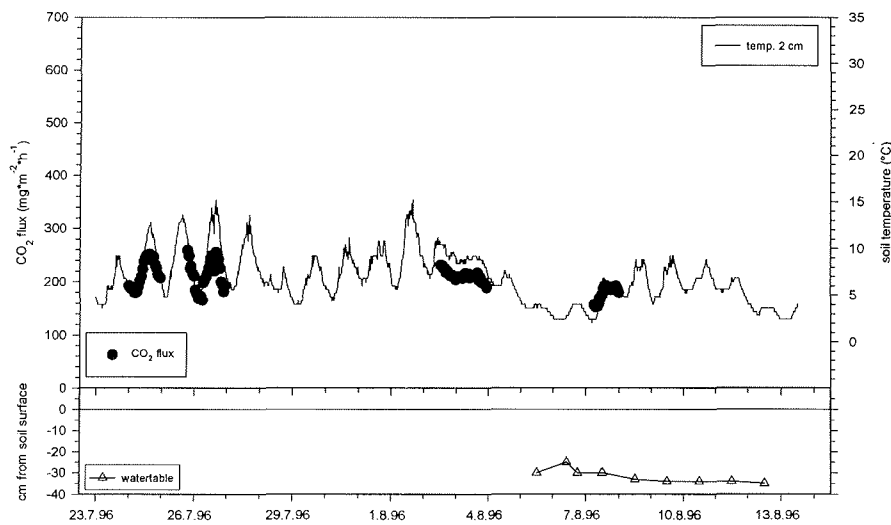


Fig. 4.2.5. 15 min. average values for CO_2 -flux of soil respiration, soil temperature at 2 cm depth, and water table in polygonal tundra, high apex (PH).

Table 4.2.6. Amplitudes and means of soil respiration, soil temperature at 2 cm depth, and water table in polygonal tundra, high apex (PH), during periods of experiments. See text for details.

	<i>soil respiration</i> ($\text{mg CO}_2 \cdot \text{m}^{-2} \cdot \text{h}^{-1}$)	<i>soil temperature 2 cm</i> ($^{\circ}\text{C}$)	<i>water table</i> (cm from soil surface)
mean	206.9	8.3	-30.5
max	258.9	14.8	-30.0
min	152.6	2.4	-31.5

5.2.1.1.2 Lake Levinson-Lessing

Polygonal tundra, high apex (PH)

Over the first two weeks of the measuring campaign in the polygonal tundra at Lake Levinson-Lessing, the soil water table at the high apex microsite was situated deeper than 35 cm below the soil surface and could not be registered (Fig. 4.2.5). A period of heavy rainfall during 4.-7.8. caused the water table to rise above the depth of the observation hole, and thus become measurable. When reading Table 4.2.6, it must be considered that the values for depth to water table refer only to the perceived period of the measuring campaign. The shading effect of the comparatively high degree of vascular plant cover (see Table 4.1.16) at this microsite resulted in a small amplitude for ST2. With the mean position of the water table lower than 30 cm and ST2 not exceeding 15°C, the high apex microsite showed maximum soil respiration values of about 260 mg CO₂*m⁻²*h⁻¹. The high apex microsite of the polygonal tundra thus reached only half of the maximum rates that could be observed at the comparably dry site of the tussock tundra at Lake Labaz. The diurnal variations of soil respiration were fairly attenuated as well: with minimum observed rates of about 150 mg CO₂*m⁻²*h⁻¹, the amplitude of CO₂ efflux was smaller than that of the wet sedge tundra at Lake Labaz, although the amplitude of ST2 was half as large there.

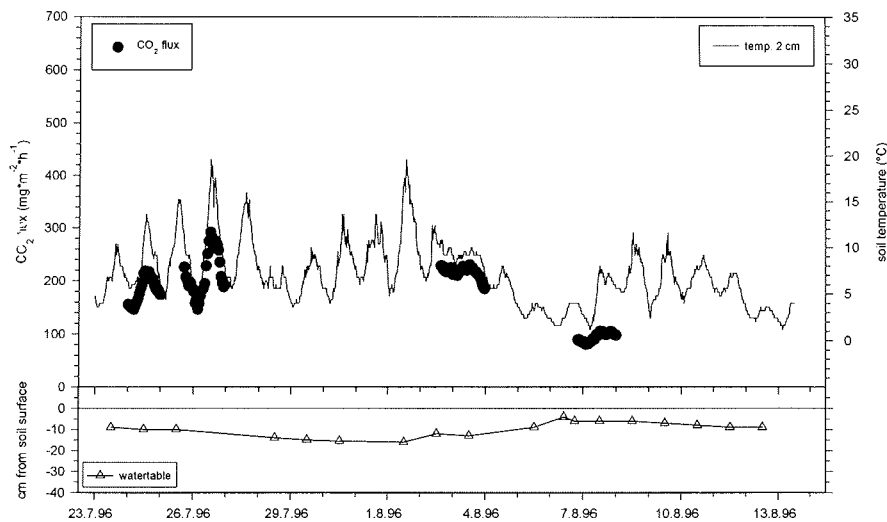


Fig. 4.2.6. 15 min. average values for CO₂-flux of soil respiration, soil temperature at 2 cm depth, and water table in polygonal tundra, low apex (PL).

Table 4.2.7. Amplitudes and means of soil respiration, soil temperature at 2 cm depth, and water table in polygonal tundra, low apex (PL), during periods of experiments.

	soil respiration (mg CO ₂ *m ⁻² *h ⁻¹)	soil temperature 2 cm (°C)	water table (cm from soil surface)
mean	178.1	8.1	-10.0
max	292.0	18.0	-6.0
min	80.0	1.2	-13.0

Polygonal tundra, low apex (PL)

The low apex microsite of the polygonal tundra was characterized by a water table ranging between 6 cm and 13 cm below soil surface (Table 4.2.7). ST2 values during the experimental periods ranged from as low as 1.2°C to 18°C, representing the widest range of all microsites at the northern location. Minimum soil respiration rates of 80 mg CO₂*m⁻²*h⁻¹ occurred together with the coldest ST2 and the highest water table position following heavy rainfalls from 4.-7.8. (Fig. 4.2.6). Maximum CO₂ effluxes of nearly 300 mg CO₂*m⁻²*h⁻¹, the highest measured in the polygonal tundra at Lake Levinson-Lessing, were recorded with the maximum observed ST2 and a depth to water table of about 12 cm. Depth to water table modified the total level of soil respiration at the low apex microsite beyond the effect of temperature alone, as indicated by the experiment from 6.-8.8..

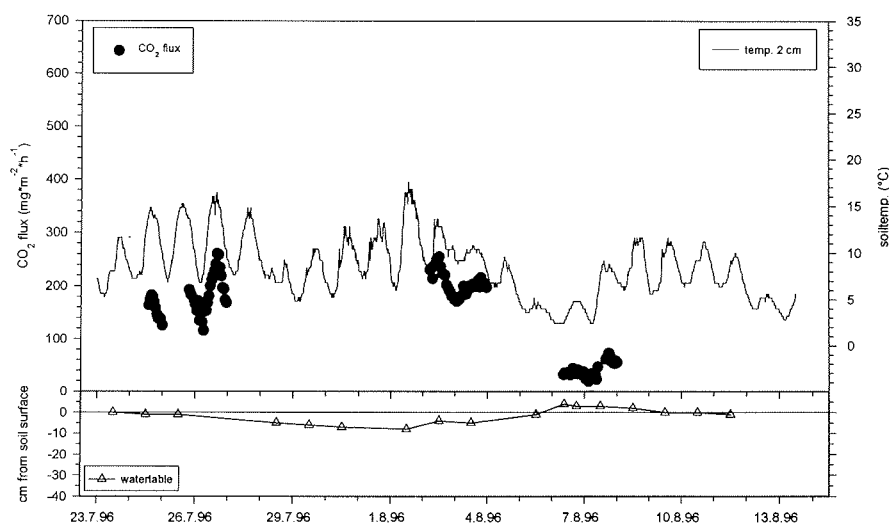


Fig. 4.2.7. 15 min. average values for CO₂-flux of soil respiration, soil temperature at 2 cm depth, and water table in polygonal tundra, depression (PD).

Table 4.2.8. Amplitudes and means of soil respiration, soil temperature at 2 cm depth, and water table in polygonal tundra, depression (PD), during periods of experiments.

	soil respiration ($\text{mg CO}_2 \cdot \text{m}^{-2} \cdot \text{h}^{-1}$)	soil temperature 2 cm ($^{\circ}\text{C}$)	water table (cm from soil surface)
mean	142.4	9.1	-1.1
max	260.5	15.6	3.9
min	19.2	2.4	-5.1

Polygonal tundra, depression (PD)

With depths to water table ranging from 5 cm below to 4 cm above soil surface, the central depression of the polygonal tundra was a special case among the sites presented above. Even with a water table several cm above the ground soil respiration values of about 20 to 80 $\text{mg CO}_2 \cdot \text{m}^{-2} \cdot \text{h}^{-1}$ could be obtained (Fig. 4.2.7). Although these flux rates were small, they were far from being negligible if compared to the maximum CO₂ effluxes observed at this microsite (Table 4.2.8). The phenomenon indicates that oxygen concentration in cold water was sufficient to maintain at least a considerable aerobic carbon turnover. Though the water table was situated that close below the soil surface at the depression microsite, ST2 values were found fairly high (15.6°C), resulting in maximum CO₂ effluxes of

260 mg CO₂*m⁻²*h⁻¹. This value was higher than the corresponding maximum of the high apex microsite and only little less than the maximum observed at the low apex microsite.

Summing up

Courses of soil respiration of a variety of tundra types and their microsites have been presented above, each one representing a specific microclimatic regime. It was shown that the absolute level of soil respiration rates was determined by the position of the water table, in particular at the wet and moist sites. Water table changes close to the soil surface resulted in comparatively large changes of soil respiration rates. Diurnal variations of soil respiration, however, reflected the soil temperature, particular the ST2. However, some hints were showing that also with similar or even the same depth to water table and ST2 the resulting soil respiration rates differed between microsites. It will be the goal of the modelling of the soil respiration process of all microsites to work out and elucidate differences in the response of the process to the controlling variables, and to possibly correlate these differences with site characteristics other than microclimatic parameters. The results and aspects of evaluation made possible by the modelling of soil respiration will be presented in the chapters 4.2.1.3.1 and 4.2.1.3.2.

5.2.1.2 Experiments in the Laboratory

The evaluation of a model describing the response of a process to more than one factor faces several constraints, in particular if each response is determined by a set of regression parameters. Co-occurrence of high water tables and colder ST2, as observed in most cases during field experiments, was furthermore complicating the task. Therefore, laboratory experiment on the effect of water table position on soil respiration were performed with microcosms from the different sites at a constant temperature of 5°C. The obtained model parameters were used as starting parameters for evaluating the combined temperature and water table models for the *in situ* soil respiration.

The response of soil respiration to water table position at a constant temperature of 5°C was systematically tested with seven microcosms originating from the different microsites (see chapter 3.1.3 for methodology).

All microcosms showed increasing soil respiration rates with a decreasing water table, as well as considerable rates also with a water table above the soil surface (Fig. 4.2.8). A strong increase of soil respiration rates with water table changes close to the soil surface was accompanied by smaller increases with such changes both above soil surface as well as in lower horizons in all samples, although this trend was most pronounced at the sample from the wet sedge tundra.

Differences between microcosms occurred with respect to the absolute level of soil respiration at a specific water table position and the increase of soil respiration within a given interval of water table change. Total soil respiration rates observed with the lowest water table position were highest in the microcosms from Lake Labaz. The highest rates were attained by the sample from the wet sedge tundra (WS), followed by those from the tussock tundra (TT, TH, TD). The microcosms from Lake Levinson-Lessing (PH, PL, PD) did not reach comparable rates, though they were an average of 5 cm higher. A trend towards higher maximum soil respiration rates from wet (third panel) over moist (second panel) to dry (upper panel) microsites was found for both tussock tundra and polygonal tundra, but could not be verified for the wet sedge tundra, which showed the highest value of all samples already with a water table of 17 cm below soil surface.

The microcosms from Lake Labaz showed higher sensitivity to water table changes at lower horizons as compared to those from Lake Levinson-Lessing. An increase of soil respiration with a falling water table was observed over the whole range of height of the microcosms from the tussock tundra, whereas soil respiration of the samples from the polygonal tundra tended towards insensitivity to water table changes at deeper horizons. As an exception, the microcosm from the wet sedge tundra at Lake Labaz also showed the tendency towards insensitivity at lower horizons. Also in contrary to the observations from above this sample, although from an extremely wet tundra, showed the highest soil respiration rate observed with a low water table. Thus, the microcosm from the wet sedge tundra showed the steepest response of soil respiration with a falling water table.

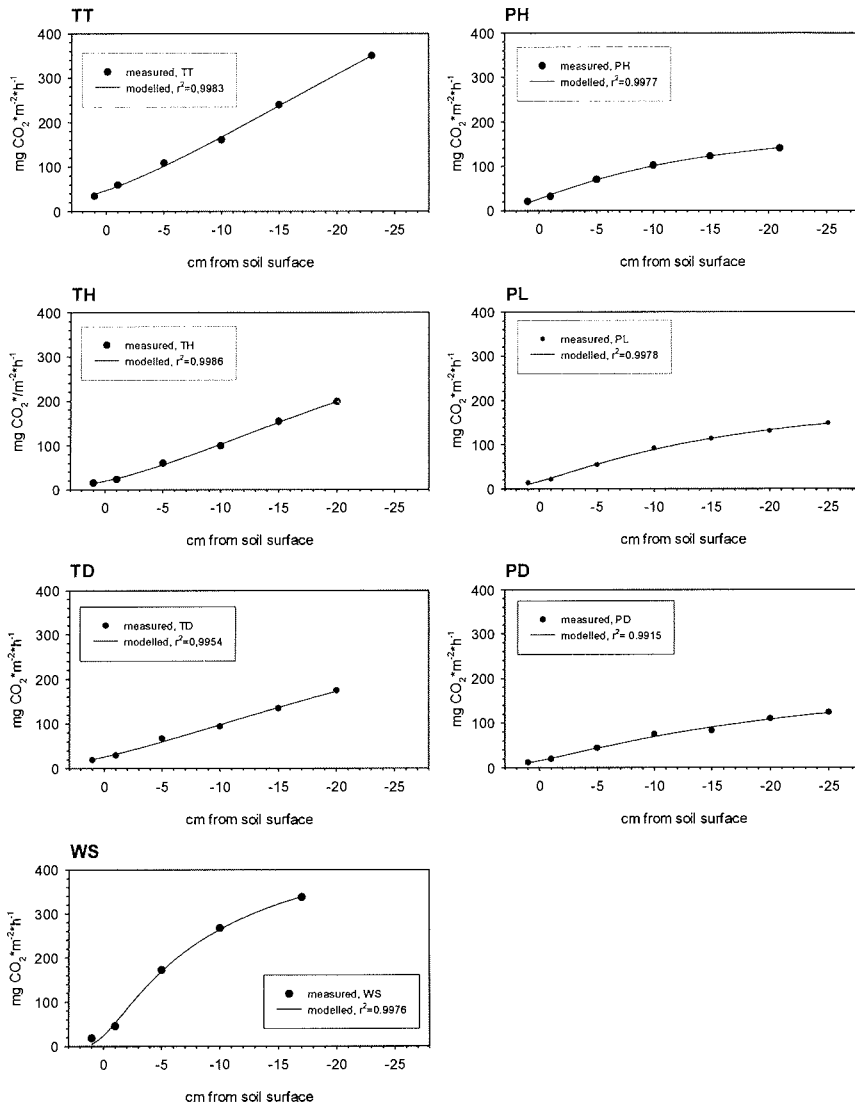


Fig. 4.2.8. Soil respiration ($\text{mg CO}_2 \cdot \text{m}^{-2} \cdot \text{h}^{-1}$) of microcosms under various water table conditions at a constant temperature of 5°C , measured datapoints and modelled with equation 7. Negative distances indicate levels below the soil surface.

In order to obtain a framework of regression parameter values that could be used for modelling the water table dependence of soil respiration rates observed in the field, the measured values from the laboratory experiments were fitted with equation 7 (Fig. 4.2.8). Correlation coefficients (r^2) were exceeding 0.99 in all cases (Table 4.2.9). Regression parameters showed clear differences between the samples from the polygonal tundra and the tussock tundra: Both, the “a“-parameter (mainly responsible for the level of the upper plateau) and the “b“-parameter (mainly responsible for the slope of the curve) were considerably higher in the samples from tussock tundra as compared to those from the polygonal tundra. The exceptional characteristic of the sample from the wet sedge tundra was elucidated by an “a“-parameter within the range of those from the polygonal tundra (i.e. insensitivity to changes of water table already close to the soil surface) and the lowest “b“-parameter of all samples (i.e. the steepest slope).

Table 4.2.9. Regression coefficients (r^2) and approximated parameters of equation 7 for the water table experiments.

<i>sample</i>	r^2	<i>a</i>	<i>b</i>
polygonal tundra, depression	0.9915	2.735	8.869
polygonal tundra, low apex	0.9978	2.723	6.449
polygonal tundra, high apex	0.9977	2.172	6.365
wet-sedge-tundra	0.9976	3.100	2.975
tussock tundra, depression	0.9954	3.327	15.11
tussock tundra, hummock	0.9986	3.855	13.19
tussock tundra, tussock	0.9983	3.618	18.69

5.2.1.3 Modelling of Soil Respiration in Tundra Systems

The results of the Spearman rank analysis (Table 4.2.1, chapter 4.2.1.1) suggested that depth to water table and soil temperature at 2 cm depth would be the best factors to include in a mathematical description of the CO₂ efflux from the investigated tundra types. For all seven sites the regression parameters of equations 5 and 7 were fitted to the observed soil respiration data as described in chapter 3.1.5. Regression coefficients (r^2) exceeding 0.9 could be obtained for all sites, except for the high apex microsite of the polygonal tundra (0.87, see Table 4.2.10). Furthermore, the slopes of the linear regression curves of modelled versus measured values were close to 1 in all cases. Also analysis of residuals revealed unbiased distributions in nearly all cases for both temperature- and depth to water table range, respectively (see Fig. 4.2.9 for an example of analysis of model quality for the model from the low apex microsite of the polygonal tundra (PL), for analysis of the quality of the other models see appendix, Figs. A9-A22). All these criteria indicated that mid-season soil respiration rates at the microsites investigated could be accurately described by their individual response to both soil temperature at 2 cm depth and depth to water table. Soil respiration rates measured were very well matched by the evaluated models (for graphs of model runs see appendix).

Table 4.2.10. Regression coefficients (r^2), standard errors of the estimate (STD of estimate) and n for the soil respiration models, as well as regression parameters for linear regression between modeloutput and measured values.

	soil respiration model		n	modelled versus measured	
	r^2	STD of estimate		a	b
tussock tundra, tussock (TT)	0.9319	16.5658	39	-1.0510	1.0021
tussock tundra, hummock (TH)	0.9130	9.1928	98	-0.8995	1.0029
tussock tundra, depression (TD)	0.9273	9.1928	80	-0.8176	1.0070
wet sedge tundra (WS)	0.9731	6.6201	28	-1.4142	1.0069
polygonal tundra, high apex (PH)	0.8650	6.6499	17*	-45.6534	1.2554
polygonal tundra, low apex (PL)	0.9782	9.4524	116	0.6244	0.9968
polygonal tundra, depression (PD)	0.9468	17.7226	120	-3.5168	1.0196

Note that n* for polygonal tundra, high apex refers to the combined temperature and depth to water table model only, the temperature part of the model was first fitted using an n of 107.

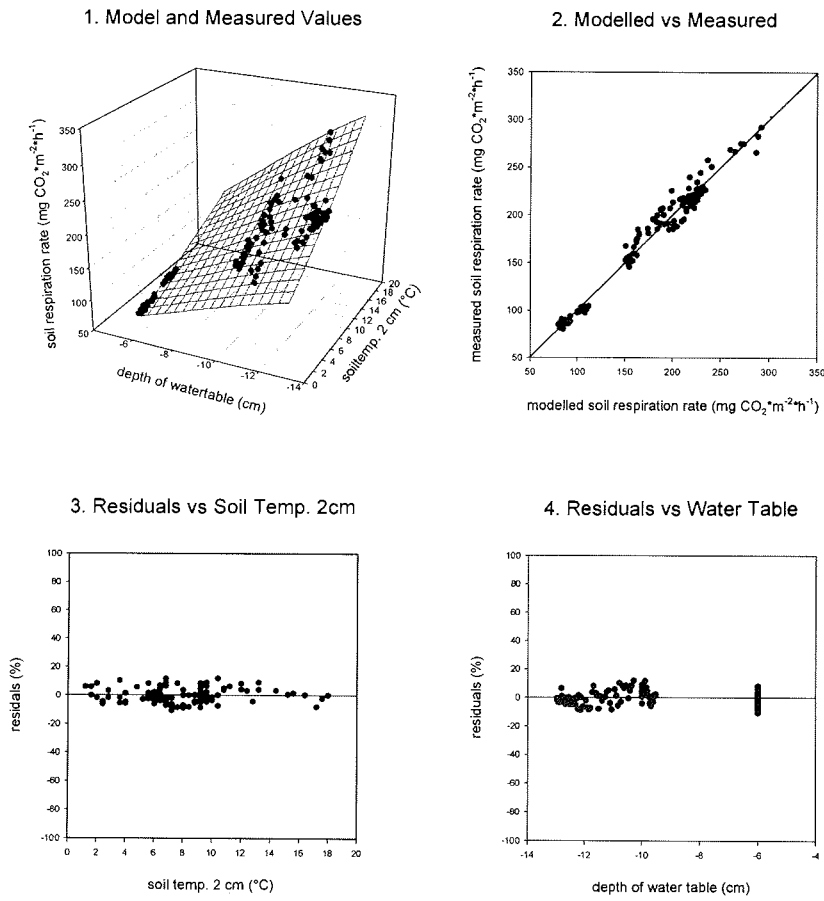


Fig. 4.2.9. Validated range of soil respiration model from polygonal tundra, low apex (PL) and measured values (graph 1), and analysis of model quality (Measured versus modelled values including linear regression (graph 2), relative residuals (% of modelled value) versus soil temperature at 2 cm depth (graph 3) and depth to water table (graph 4).

5.2.1.3.1 Balancing the CO₂ Efflux of Soil Respiration

As already mentioned when elucidating the theoretical background for ecological modelling (chapter 3.1.5), one of the advantages of a calibrated model is the possibility of most precise interpolation in the scope of balancing over the period of the field season where microclimatic conditions were observed. Thus, calculated soil respiration values cover all observed parameter combinations and therefore allow much better comparison between sites than the measured values alone. Table 4.2.11 shows means and amplitudes of soil respiration rates as well as of microclimatic conditions of every investigated site.

Table 4.2.11. Modeloutput of means and amplitudes of daily soil respiration rates ($\text{g CO}_2 \cdot \text{m}^{-2} \cdot \text{d}^{-1}$ and $\text{g C} \cdot \text{m}^{-2} \cdot \text{d}^{-1}$) over the period where microclimatic conditions were observed, as well as soil temperature, and depth to water table for the different microsites during this period.

	<i>Lake Labaz</i>				<i>Lake Levinson-Lessing</i>		
	<i>TT</i>	<i>TH</i>	<i>TD</i>	<i>WS</i>	<i>PH</i>	<i>PL</i>	<i>PD</i>
mean soil respiration							
($\text{g CO}_2 \cdot \text{m}^{-2} \cdot \text{d}^{-1}$)	10.9	6.7	2.6	4.0	4.7	4.3	3.8
($\text{g C} \cdot \text{m}^{-2} \cdot \text{d}^{-1}$)	3.0	1.8	0.7	1.1	1.3	1.2	1.0
min/max soil respiration							
($\text{g CO}_2 \cdot \text{m}^{-2} \cdot \text{d}^{-1}$)	8.4/14.9	4.8/10.2	1.3/4.9	3.0/7.3	3.7/5.1	1.5/9.3	0.8/11.3
($\text{g C} \cdot \text{m}^{-2} \cdot \text{d}^{-1}$)	2.3/4.1	1.3/2.8	0.4/1.3	0.8/2.0	1.0/1.4	0.4/2.5	0.2/3.1
rel. amplitude (% max)	44	54	73	59	27	84	93
mean soiltemp. 2 cm							
(°C)	12.0	11.5	7.6	7.4	6.8	7.3	8.7
min/max soiltemp. 2 cm							
(°C)	0.0/29.6	0.4/28.8	2.0/12.8	4.8/12.8	2.0/15.2	1.2/19.6	2.4/17.6
mean water table below soil surface (cm)	-21.8	-13.7	-3.7	-2.1	-32.1	-10.7	-2.4
min/max water table below soil surface (cm)	-24/-20	-16/-12	-6/-2	-3/-1	-35/-25	-16/-4	-8/4

Regarding daily means as well as maximum rates of soil respiration the tussock microsite of the tussock tundra showed by far the highest CO₂ efflux rates. The site lost an average of about $3 \text{ g C} \cdot \text{m}^{-2} \cdot \text{d}^{-1}$ from soil respiration over the summer season, with maximum rates of up to $4.1 \text{ g C} \cdot \text{m}^{-2} \cdot \text{d}^{-1}$. These fluxes were made possible by the highest observed mean and maximum values of ST2, as well as depths to water table of nearly 22 cm as an average. Although the microsite showed the highest amplitude of ST2 over the observed period, the amplitude of soil respiration was comparatively lower: minimum CO₂ efflux rates of $8.4 \text{ g CO}_2 \cdot \text{m}^{-2} \cdot \text{d}^{-1}$ were still higher than the maxima of most of the other sites. Relative amplitude of soil respiration was the second lowest observed.

In contrast to the high efflux rates of the tussock microsite, the depression microsite of the tussock tundra showed the lowest mean soil respiration rates of all sites, only 25 % of the value observed at the tussock microsite was reached here. A mean water table as high as 3.7 cm below soil surface limited total CO₂ effluxes. Also the amplitude of CO₂ efflux rates was the second lowest observed, 4.9 g CO₂*m⁻²*d⁻¹ and 1.3 g CO₂*m⁻²*d⁻¹ were obtained as maximum and minimum, respectively. This very low minimum efflux rate was observed with a minimum temperature somewhat higher than at both more exposed microsites of the tussock tundra, supporting once more the observation that depth to water table is limiting the absolute level of CO₂ efflux rates. Relative amplitude of soil respiration was found fairly high, indicating a considerable potential of the process over the observed parameter range.

The moss hummock microsite of the tussock tundra showed a mean water table position over the investigated period of nearly 14 cm below soil surface, thus situated about half distance between the water table positions of the tussock and the depression microsite. Daily means of soil respiration rates were reflecting this fact fairly accurately. Although amplitude as well as absolute values of ST2 at the moss hummock microsite were very similar to those of the tussock microsite, the absolute amplitude of CO₂ effluxes was lower, but the relative amplitude higher at the moss hummock microsite.

Although the mean water table in the wet sedge tundra was only 2.1 cm below soil surface, thus representing for the highest observed among all sites, daily means of soil respiration as well as minimum and maximum rates were observed considerably higher than at the depression microsite of the tussock tundra. A difference in the performance of the process of soil respiration is furthermore underlined by the fact that the mean ST2 was somewhat lower in the wet sedge tundra, too, as compared to the depression of the tussock tundra. Due to the fairly stable microclimatic conditions observed at the wet sedge tundra site, the relative amplitude of soil respiration was not found very high, but still in the same range as the value of the moss hummock microsite, which represented a much higher amplitude of conditions.

Although the high apex microsite of the polygonal tundra showed the lowest mean ST2 of all sites investigated, daily means of soil respiration were the highest found in this tundra type. Nevertheless, they represented for not even half of the value which was reached at the tussock microsite of the tussock tundra, which showed mean water table about 10 cm higher, but mean ST2 about twofold the value of the high apex. In contrast to the drier microsites of the tussock tundra, the high apex showed the lowest amplitude in soil respiration rates of all sites investigated, although water table position was found lowest at this microsite. Also the

relative amplitude was the lowest observed. A limiting effect of soil moisture on soil respiration rates at the high apex of the polygonal tundra has already been mentioned with the presentation of the data. Since position of water table was not observable over long periods of the measuring campaign, modelling was first performed with the temperature part of the model only (for graphs see appendix). A regression coefficient (r^2) of 0.794 (water+temperature model: 0.865) could be obtained for this model. Moreover, output of both models, temperature only and water+temperature, was nearly identical for the overlapping period. This suggests that depth to water table played only a very restricted role at the high apex microsite of the polygonal tundra.

The low apex microsite of the polygonal tundra showed daily means of soil respiration of $4.3 \text{ g CO}_2 \cdot \text{m}^{-2} \cdot \text{d}^{-1}$, which was only little less than at the high apex microsite. However, the difference in mean position of water table between the microsites was as much as about 21 cm. Although the mean water table of the low apex microsite was about comparable to the moss hummock microsite of the tussock tundra, a considerably higher amplitude of water table positions at the former site, in particular towards higher positions, led to a very high amplitude in soil respiration rates, particularly towards low rates, as well. Also the relative amplitude of CO_2 effluxes was the second highest observed, indicating a considerable potential of the process to changes of water table and soil temperature over the observed ranges.

The depression microsite of the polygonal tundra showed the highest amplitude of soil respiration rates observed among all investigated sites, in both absolute and relative terms. The minimum of only $0.8 \text{ g CO}_2 \cdot \text{m}^{-2} \cdot \text{d}^{-1}$ was observed with a water table position as high as 4 cm above the soil surface. Although the depth to water table never exceeded 8 cm and the maximum ST2 value was only 17.6°C , the maximum observed CO_2 efflux rate of $11.3 \text{ g CO}_2 \cdot \text{m}^{-2} \cdot \text{d}^{-1}$ was only surpassed by the tussock microsite of the tussock tundra, which maximum ST2 value was 12°C higher. If referring to mean values, the depression microsite showed the second lowest daily mean of soil respiration of all sites, which was accompanied by the second highest mean water table position as well. Although the mean ST2 value of the depression microsite was the highest observed in the polygonal tundra, the mean daily CO_2 efflux rate was the lowest found in this tundra type.

Analysis of the output of the soil respiration models elucidated that the absolute level of soil respiration at wet tundra sites was mainly determined by the position of the water table, thus reducing the role of soil temperature to be a modifier only. On a gradient towards drier microsites, i.e. position of water table deeper below soil surface, changes in water table position had a reduced effect and soil temperature determined the CO₂ efflux rates primarily. Additionally, the magnitude of respiring soil volume at drier sites provided higher soil respiration rates also with lower soil temperatures. With depths to water table exceeding 30 cm, effect of water table position was negligible and other factors like soil moisture seemed to control the magnitude of CO₂ efflux, again exceeding the effect of soil temperature. Consequently, relative amplitudes of soil respiration, indicating the potential of the process to change over the observed parameter range, was observed to be highest at sites with a water table close to the soil surface.

5.2.1.3.2 Performance of the Soil Respiration Process

Additionally to the absolute effect of temperature and water alone it could be seen already from the description of soil respiration fluxes that the response to both factors differed between sites. In the next section, the response to soil temperature and water table will be presented singularly on the basis of the evaluated models. Senseful curvefitting provided, model outputs are able to show the response to one of the factors only, with the effect of the other one filtered out. It has to be kept in mind though, that response to any factor still reflects an integrated picture of the many other parameters characterising a site (see also chapter 3.1.5). Since calculations on the basis of one part of the model with the other part switched-off will lead to an artificial scale of output values, the following Figures refer to relative fluxes, with the maximum response of all sites set to 100 %. Furthermore, to avoid parameter values exceeding the validated range of the models, calculations were performed over the observed parameter range only.

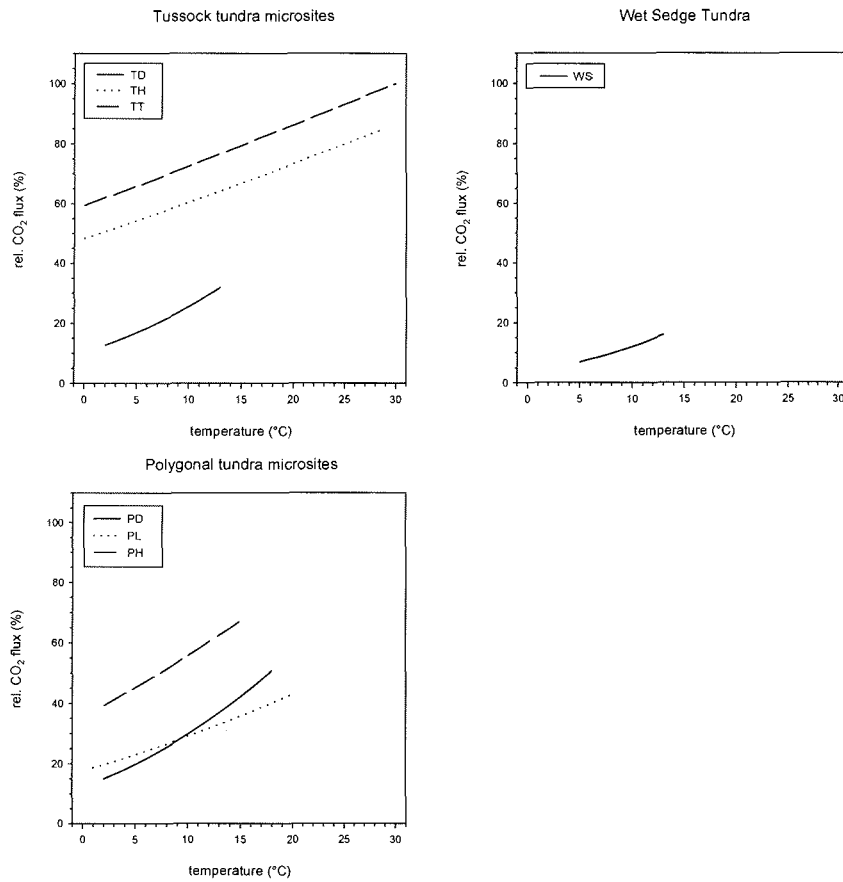


Fig. 4.2.10. Temperature response of the soil respiration process over the observed soil temperature range (2 cm depth) at each microsite. CO₂ fluxes from temperature model only, shown as relative soil respiration rates. Maximum response of all sites was set to 100 %.

5.2.1.3.2.1 Temperature Response

If the temperature response of soil respiration of the different microsites was plotted (Fig. 4.2.10), it became evident that differences between sites occurred referring to both the level of the response curve (absolute temperature response), as well as the slope of the response curve at a specific temperature (the relative temperature response). Concerning the level of temperature response, the tussock microsite of the tussock tundra showed highest soil respiration values over the whole range of soil temperature observed. The slope of the response curve appeared linear over the whole temperature range at the tussock microsite,

which was also valid for the moss hummock microsite. While the level of temperature response of the moss hummock microsite was found to be only slightly lower than at the tussock microsite, the slope of both curves was about identical.

The temperature response of soil respiration of the depression microsite of the tussock tundra showed about the same slope at low temperatures as both microsites mentioned above, but a fast increase of efflux rates towards higher temperatures, even over the restricted range of soil temperature observed. The level of temperature response of the depression microsite, however, was only 20 to 40 % of the rates the tussock microsite reached with the same temperatures.

Total CO₂ efflux rates from wet sedge tundra were even lower than from the depression microsite of the tussock tundra over a similar range of soil temperature. Increase of soil respiration rates towards higher temperatures was slower at the wet sedge tundra site, as compared to the depression microsite of the tussock tundra.

The pattern of the temperature response of soil respiration at the polygonal tundra microsites appeared more complex than the one observed at the tussock tundra microsites. Like at the dry site of the tussock tundra, the high apex showed the highest absolute temperature response of the polygonal tundra microsites. The increase of soil respiration rates with increasing temperature was about linear, the slope of the response curve was even steeper than observed at the tussock microsite.

Absolute response of soil respiration to temperature was about 50 % lower at the low apex microsite of the polygonal tundra as compared to the high apex microsite, but the relative temperature response increased more effectively towards higher temperatures, as indicated by the non-linear curve pattern.

The temperature response curve of the depression microsite of the polygonal tundra showed the strongest increase of relative temperature response towards higher temperatures. Additionally CO₂ efflux rates observed with low temperatures were not as pronounced lower compared with the more dry microsites of the same tundra type, as observed at the depression of the tussock tundra. Consequently, the absolute temperature response of the depression microsite at soil temperatures higher than 10°C exceeded the absolute response of the low apex microsite. While the depression microsite reached only 38 % of the soil respiration rate of the high apex at 2°C, it attained already 64 % at 15°C

5.2.1.3.2.2 *Relative Temperature Sensitivity*

Q_{10} values are widely accepted to express the temperature sensitivity of a process. Because the expression used for modelling the temperature response of soil respiration in this study was not simply exponential but allowed a change of temperature sensitivity with temperature, the Q_{10} can change over the temperature range observed. The absolute temperature sensitivity of the Q_{10} over an observed temperature range is therefore replaced by a relative temperature sensitivity, depending on temperature, in this study.

In particular because the sensitivity of the soil respiration process changes over the temperature range observed, continuous Q_{10} analysis can help to furthermore clarify the differences in temperature dependence between investigated sites.

The highest Q_{10} values and thus the highest relative sensitivity of soil respiration rate to temperature was reached by the three wet sites, tussock tundra, depression, wet sedge tundra, and polygonal tundra, depression (Fig. 4.2.11). Highest Q_{10} occurred at low temperatures at these sites with maximum values as high as 2.7, 3.4, and 2.5, respectively (Table 4.2.12). The wet sites also showed the steepest decrease of Q_{10} values with soil temperature over the observed range. A minimum Q_{10} value of 2.1 was calculated for a soil temperature of 12°C at the depression microsite of the tussock tundra. The corresponding minimum was 2.6 at the same temperature in the wet sedge tundra, and 2.0 at a temperature of 16°C at the depression of the polygonal tundra.

The decrease of Q_{10} with temperature was negligible at both the tussock- and the moss hummock microsite of the tussock tundra, which showed a Q_{10} of about 1.2. Similarly, the high apex and the low apex microsite of the polygonal tundra were close related in terms of absolute Q_{10} values as well as decrease of Q_{10} with temperature: Both sites showed absolute Q_{10} values around 1.6, which differed only by about 0.2 over a temperature range of about 12°C in the case of the high apex- and by about 0.3 over a temperature range of 17°C in the case of the low apex microsite.

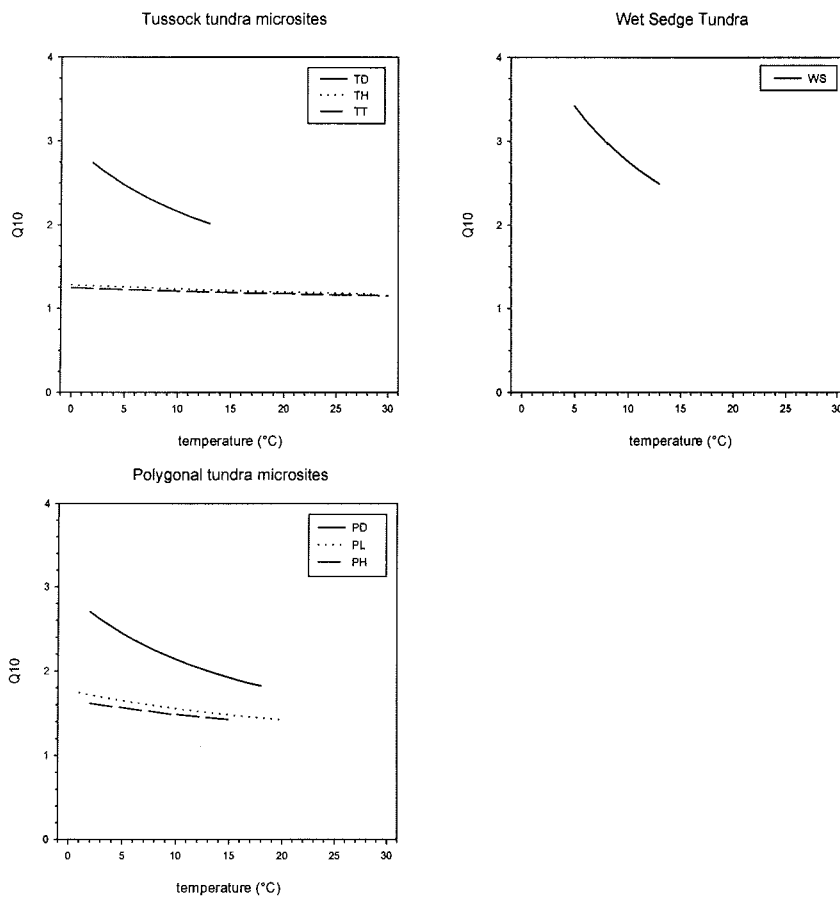


Fig. 4.2.11. Q_{10} -values of the soil respiration process over the observed temperature range at each site. Calculated from the approximated temperature models of the different microsites.

A closer look to the Q_{10} values at the mean soil temperatures at 2 cm depth observed at the sites during the field campaigns confirmed the pattern described above: The highest relative temperature sensitivity of soil respiration could be observed at the wet sites with Q_{10} values around 2.2 (TD and PD) or even 3 (WS). On a gradient towards the more dry sites, Q_{10} values were declining from 1.6 (PL) to 1.19 (TT).

Table 4.2.12. Q_{10} -values at mean soil temperature at 2 cm depth, as well as minimum and maximum Q_{10} -values observed at each site. Calculated from the approximated temperature models of the different microsites.

		Q_{10} at mean soil temperature 2 cm of site	max Q_{10} at soil temperature 2 cm of site	min Q_{10} at soil temperature 2 cm of site
TT	Q_{10} soiltemp. 2 cm (°C)	1.19 13	1.22 5	1.16 26
TH	Q_{10} soiltemp. 2 cm (°C)	1.22 13	1.27 3	1.17 29
TD	Q_{10} soiltemp. 2 cm (°C)	2.21 9	2.74 2	2.06 12
WS	Q_{10} soiltemp. 2 cm (°C)	2.99 8	3.42 5	2.58 12
PH	Q_{10} soiltemp. 2 cm (°C)	1.53 7	1.62 2	1.43 15
PL	Q_{10} soiltemp. 2 cm (°C)	1.61 7	1.74 1	1.45 18
PD	Q_{10} soiltemp. 2 cm (°C)	2.25 8	2.45 2	2.04 16

5.2.1.3.2.3 Response to Depth to Water Table

The response of soil respiration to depth to water table differed widely between the different microsites with respect to both relative CO₂ efflux level, as well as pattern of response at a given water table position (for whole response curves see also chapter 4.2.1.2). In contrast to the factor soil temperature, depth to water table observed in the field showed less overlapping ranges between sites, so that direct comparisons are more restricted.

The steepest response to water table positions close to the soil surface was observed at the wet sites, tussock tundra, depression, wet sedge tundra, and polygonal tundra, depression (Fig. 4.2.12). Within these first cm of water table changes, the wet sites reached absolute soil respiration rates of the same level like the drier sites did with water table positions several cm or even dm deeper. The steepest response of that kind as well as highest efflux rates among sites already with a water table very close to the soil surface could be observed at the wet sedge tundra site, an observation made in the laboratory as well. Both dry sites investigated,

tussock microsite of the tussock tundra as well as high apex microsite of the polygonal tundra were near to their level of insensitivity to water table changes at the range observed in the field. On the other hand, the high apex microsite still showed a considerable slope of the response curve with water table changes as deep as 25 cm to 35 cm. Whereas the moss hummock microsite of the tussock tundra tended towards insensitivity to water table changes over the observed range as well, the low apex microsite showed this tendency only at water table positions near to the lower end of the observed range.

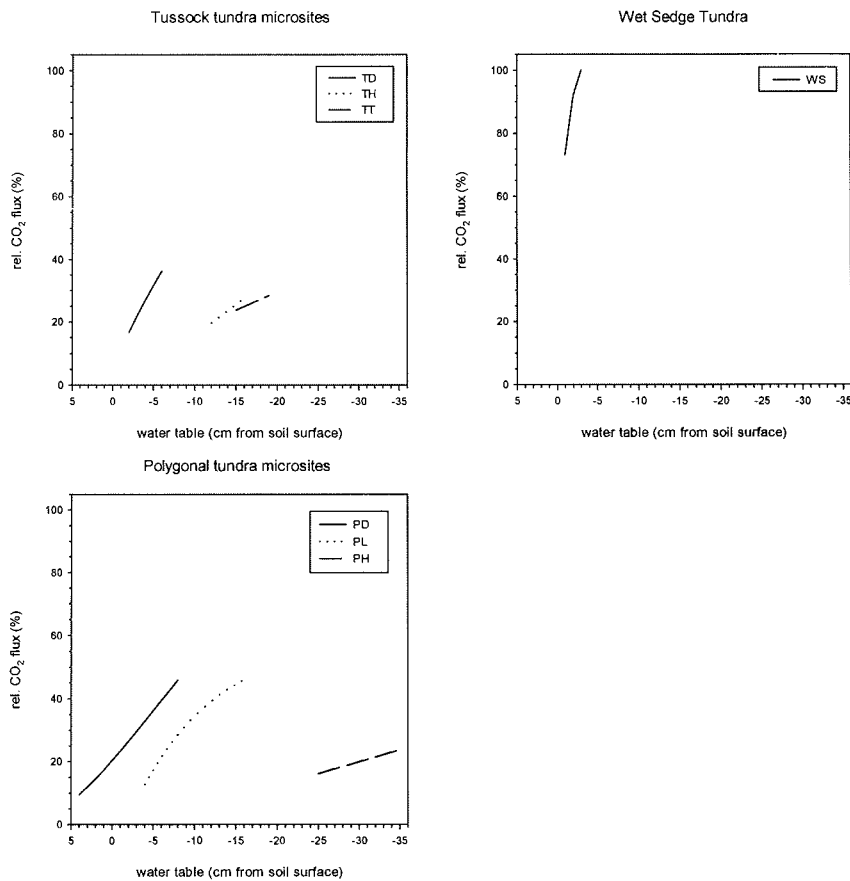


Fig. 4.2.12. Response of the soil respiration process to depth to water table over the observed water table range at each site. CO₂ fluxes from water model only, shown as relative soil respiration rates.

The slope of the response curve of the low apex microsite at water table positions closer to the soil surface was as steep or even steeper than the one of the depression microsite of the polygonal tundra. Due to the occurrence of water table positions as much as 4 cm above the soil surface at the depression microsite of the polygonal tundra, another feature of soil respiration response to water table could be seen here: The response curve showed a range of dropping sensitivity to water table changes towards water table positions above soil surface. CO₂ efflux rates were not observed to sharply decrease with the water table increasing above the soil surface at this microsite.

5.2.1.3.2.4 Identifying Patterns

As pointed out already in the scope of the laboratory experiments, one of the advantages of modelling is the parameterisation of reaction properties. The approximated parameters can be correlated with factors determining the reaction on a higher level than the one directly included in the model. This facilitates at least the delimitation of factor combinations or patterns responsible for an observed type of response, in the best case it can lead to the formation of indexes. In this study, the analysis of the approximated model parameters will be restricted to the correlations to site characteristics as presented in the chapters 4.1.1.2 and 4.1.2.2. To circumnavigate constraints by size of n , problems with normal distribution, as well as scale and character of the compared values, Spearman rank analysis was chosen to investigate correlations (see chapter 3.1.6).

In Table 4.2.13, the approximated parameters of the temperature and water table models of the different microsites are presented.

Table 4.2.13. Approximated parameters of equations 5 and 7 for the *in situ* soil respiration models from the different microsites.

	z	T_0	a	b
tussock tundra, tussock (TT)	33.2	153.7	3.15	3.15
tussock tundra, hummock (TH)	32.0	161.0	4.73	4.73
tussock tundra, depression (TD)	135.7	219.2	2.93	2.93
wet-sedge tundra (WS)	130.2	227.4	4.75	0.114
polygonal tundra, high apex (PH)	76.1	194.3	4.63	27.38
polygonal tundra, low apex (PL)	48.3	199.0	9.45	0.95
polygonal tundra, depression (PD)	153.3	218.8	2.63	17.79

The results of the Spearman rank analysis of the approximated model parameters with site characteristics are shown in Table 4.2.14. To facilitate a clear presentation of the results, the table was restricted to site characteristics with significant correlations only (for a detailed list of all site characteristic used in the correlation analysis see also appendix, Table A3).

An additional parameter, which has not been shown in the chapters “characteristics of the experimental sites“ was included in the correlation analysis: On the basis of the daily mean of soil respiration of every single microsite as calculated from the model runs (see Table 4.2.11, chapter 4.2.1.3.1) and the vascular plant production (Tables 4.1.3, 4.1.11, 4.1.17), a seasonal ratio of production per soil respiration was calculated. This ratio served as a rough indicator of the carbon balance of a site.

Most of the significant correlations observed referred to biological site characteristics. Only one microclimatic (mean depth to water table) and two soil physical parameters (carbon content and thickness of the organic layer) correlated significantly with model parameters.

The results of the Spearman rank correlation analysis showed that site characteristics correlated with “ T_0 “ could be found in the surroundings of production- and biomass parameters. Furthermore, correlations to carbon content of the uppermost horizon and in particular the seasonal ratio production/soil respiration suggested, that high “ T_0 “-values (i.e. a decrease of Q_{10} with temperature) were linked to patterns connected with low decomposition capability.

The “ z “-parameter (which determines the absolute level of the temperature response of soil respiration in an unbiased way, i.e. without effect on Q_{10}) showed highest correlation to the aboveground biomass. Since the correlation was negative, it indicated a stronger increase of soil respiration with temperature at sites with less biomass. The correlation of “ z “ to mean water table position suggested a connection to quantity of respiring soil volume.

Best correlations of the “ a “-parameter were obtained with the bacterial biomass of the uppermost horizon, as well as with biomass and production parameters. This indicated a link of the level of insensitivity of soil respiration to water table changes more to biological than to soil physical properties.

The slope of the water table response curve, as determined by the “ b “-parameter, showed significant negative correlations to bacterial biomass parameters and belowground biomass (The inverse relationship of “ b “ and soil respiration rates as pointed out above should be considered).

Table 4.2.14. Spearman rank correlations (r_s) for the approximated parameters of equation 5 and 7 with site properties. Only correlations significant at $P < 0.05$ are included, n varies between 5 and 7. * indicates correlation is significantly different from zero at $P < 0.05$.

	T_0	z	a	b
daily gross photosynthesis mosses	*1.000			
seasonal ratio production / soil respiration	*1.000			-0.800
bacterial biomass 0-2 cm			*0.900	*-0.900
bacterial biomass 2-5 cm	*0.900			-0.800
C-content uppermost horizon	*0.900			
aboveground biomass		*-1.000	0.800	
belowground biomass	0.800		0.800	*-1.000
annual production			0.800	
mean water table	*-0.786	0.714		
thickness of organic layer	0.714			

5.2.1.3.3 Simulating Scenarios for Soil Respiration

With the background of the different responses of soil respiration presented above, it appears fruitful to simulate other than the original microclimatic conditions to the different sites. This will elucidate differences between sites with respect to their soil respiration potential to changes in soil temperature or / and depth to water table. A total of six scenario calculations have been calculated with each of the models investigated for microsites additionally to the one modelled with the original microclimatic conditions of the soils: To show effects of single factors, soil temperature at 2 cm depth has been both increased and decreased by 4°C, and also depth to water table has been increased as well as decreased by 4 cm, subsequently. Additionally, model runs with two reasonable combinations of these parameters, first colder and wetter conditions (soil temperature at 2 cm depth decreased by 4°C, depth to water table increased by 4 cm) and second warmer and drier conditions (soil temperature at 2 cm depth increased by 4°C, depth to water table decreased by 4 cm) were performed. Only the latter two scenarios were included in the Figures, the results of the other simulations will be summarized in Table 4.2.15. Figures of two sites are presented here (Figs. 4.2.13 and 4.2.14), each one an example for a special type of response (for graphs showing simulation scenarios of the other sites see appendix, Figs. A23-A27).

Figure 4.2.13 shows an example of the response of soil respiration of a dry site (tussock microsite of the tussock tundra) in three scenarios of water table and soil temperature. Warmer, drier conditions resulted in higher soil respiration rates than with the original parameter combination, colder, wetter conditions in lower rates. Because all applied changes

of water table position still ranged within the relatively insensitive part of the water table response curve (see also Fig. 4.2.12), the differences between the three CO₂ efflux graphs were about stable over the modelled time period, despite differences in water table position. It was evident, though, that relatively lower soil respiration rates occurred during the period of relatively higher water table positions from 12.-15.8. with all scenarios, although it has to be considered that soil temperature at 2 cm depth during this period was lower as well.

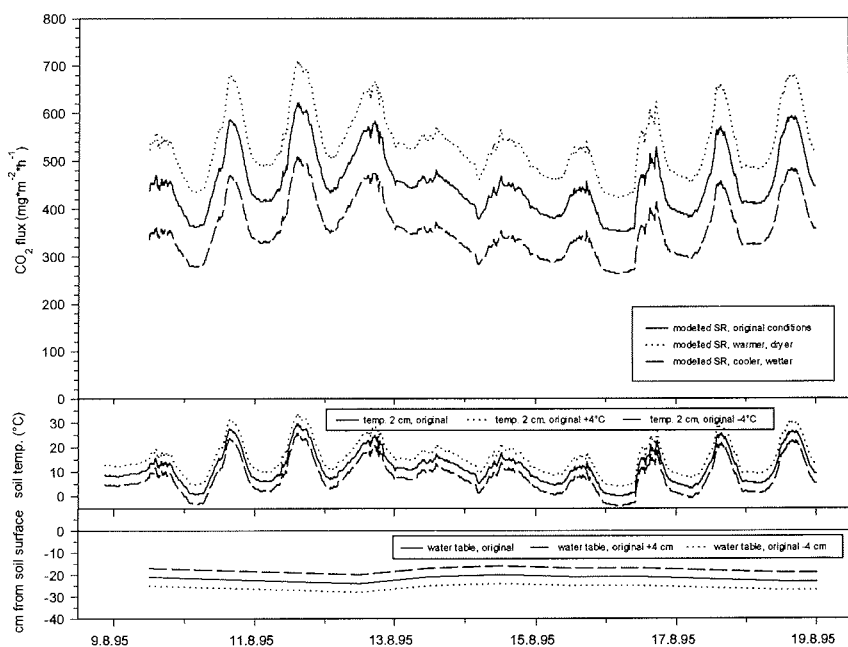


Fig. 4.2.13. Soil respiration in tussock tundra, tussock, modelled for three different scenarios: original parameter values, warmer and conditions (soil temperature 2 cm original +4°C, water table original -4 cm), and cooler wetter conditions (soil temperature 2 cm original -4°C, water table original +4 cm).

The response of the depression microsite of the polygonal tundra, an extremely wet site, to both the dry warm, and wet cold scenario was of different character (Fig. 4.2.14). Because water table position was at or even above the soil surface during the period around the 6.8. in all simulated scenarios (and thus in a part of the water table response curve approaching zero soil respiration), the resulting CO₂ effluxes of all simulations were very low and differences between them very small during this period. On 1.8, in contrary, water tables ranging from 12 cm to 4 cm below soil surface between scenarios resulted in maximum differences of soil respiration rates between scenarios. This range of water table positions is positioned in the most sensible part of the water table response curve (see also Fig. 4.2.12), so that the effect of water table can furthermore be amplified by the effect of soil temperature. This resulted in soil respiration rates higher than observed at the tussock microsite of the tussock tundra.

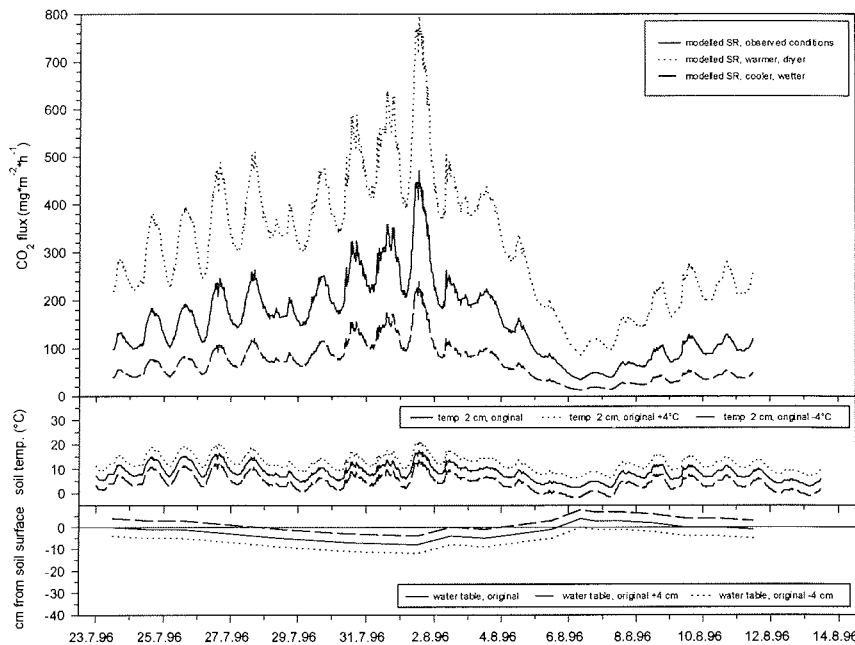


Fig. 4.2.14. Soil respiration in polygonal tundra, depression, modelled for three different scenarios: original parameter values, warmer and conditions (soil temperature 2 cm original +4°C, water table original -4 cm), and cooler wetter conditions (soil temperature 2 cm original -4°C, water table original +4 cm).

Table 4.2.15. Modelled daily means of soil respiration of microsites ($\text{g C}\cdot\text{m}^{-2}\cdot\text{d}^{-1}$) as with different scenarios of soil temperature and water table. Bold figures show percent of scenario calculations from daily soil respiration rates modelled with the original parameters values. ST2 = soil temperature at 2 cm depth ($^{\circ}\text{C}$); WT = water table (cm below soil surface); “+” and “-” = “original conditions +” and “original conditions -”, respectively.

	<i>ST2 and WT original</i>	<i>ST2 +4°C, WT original</i>	<i>ST2 -4°C, WT original</i>	<i>WT +4 cm, ST2 original</i>	<i>WT -4 cm, ST2 original</i>	<i>ST2 +4°C, WT -4 cm</i>	<i>ST2 -4°C, WT +4 cm</i>
TT	2.97 100	3.18 107	2.76 93	2.51 85	3.27 110	3.51 118	2.33 79
TH	1.82 100	1.96 108	1.67 92	1.17 64	2.35 129	2.54 140	1.08 59
TD	0.70 100	0.95 135	0.50 71	0.32 46	1.36 194	1.83 262	0.23 33
WS	1.10 100	1.65 150	0.69 63	0.76 69	1.49 135	2.23 202	0.48 43
PH	1.17 100	1.39 118	0.98 83	1.17 100	1.18 100	1.39 118	0.98 83
PL	1.17 100	1.40 119	0.97 83	0.82 70	1.46 125	1.74 149	0.68 58
PD	1.03 100	1.37 133	0.75 73	0.63 61	1.57 152	2.09 202	0.46 44

The total pattern of absolute and relative CO_2 effluxes as calculated with the simulated scenarios showed distinctive differences between sites (Table 4.2.15). With respect to changes in soil temperature, the highest relative potential of soil respiration was observed at the wet sedge tundra site, the lowest relative potential at the tussock microsite of the tussock tundra. The general trend was that the drier sites showed a lower relative potential of soil respiration to increase with temperature than the wet sites, like already seen when presenting the Q_{10} values. Also when referring to absolute values, the differences between the amounts of CO_2 emitted under original and altered conditions by the wet sedge tundra site was about two times the value attained by the tussock microsite. However, the absolute values of soil respiration was found to be highest at the tussock microsite of the tussock tundra with all temperature regimes applied.

With respect to changes of the position of the water table, the highest relative potential of soil respiration was reached by the depression microsite of the tussock tundra, whereas the high apex microsite of the polygonal tundra showed the lowest relative potential. The depression

microsite nearly doubled its CO₂ efflux rates with a lowering of the water table by 4 cm, whereas the high apex microsite showed no reaction at all with this scenario.

While the latter four scenarios were elucidating potentials of soil respiration to single effects, two more ecologically likely scenarios combine changes in both factors to simulate first a warmer drier season, and second a colder wetter season. By increasing the CO₂ efflux by the 2.5 fold in warmer drier conditions and reducing them to only a third in colder wetter conditions, the depression microsite of the tussock tundra showed the highest relative potential of soil respiration to these scenarios. Contrary, both drier sites, high apex microsite of the polygonal tundra as well as tussock microsite of the tussock tundra showed the least relative changes of CO₂ effluxes with the two combination scenarios (wetter colder, and drier warmer). It should be considered, however, that even with the distinctive increase of the CO₂ efflux rates of the depression microsite with warmer and drier conditions, the absolute amount of CO₂ emitted was only half the amount the tussock microsite reached in the same scenario.

If the three tundra systems would be “reassembled“ from their microsites again on the basis of the CO₂ effluxes presented in Table 4.2.15, no other heterogeneity than the one studied in the scope of this study provided, the pattern of CO₂ efflux rates would be modified again for both heterogeneous tundra types, tussock tundra and polygonal tundra. On the basis of the relative area shares of 50, 25, 25 % (depression, moss hummock, tussock) in tussock tundra, and of 65, 25, 10 % (depression, low apex, high apex) in polygonal tundra, as observed in the vicinity of the experimental sites, total CO₂ effluxes as calculated with the different scenarios would add to the values presented in Table 4.2.16. The high efflux rates of the dry sites were widely attenuated when observing tundra types rather than microsites, due to their relatively low area share. Consequently, absolute values of CO₂ efflux under original conditions were within the same range between tundra types, with tussock tundra still accounting for the maximum value. Relative temperature sensitivity was found highest in wet sedge tundra and lowest in polygonal tundra. Surprisingly, all tundra types showed uniform relative response to an increase or decrease of the water table position, but the tussock tundra still revealed highest absolute CO₂ efflux rates with both scenarios. The highest relative potential of soil respiration to change with both the warmer, drier as well as with the colder, wetter scenario could be found in wet sedge tundra, the lowest in tussock tundra. The polygonal tundra had an intermediate relative potential with these scenarios. In terms of absolute CO₂ effluxes, the tussock tundra showed the highest rates of the three compared tundra types with these

scenarios again, but the rates of the wet sedge tundra were found to be only slightly below that level with the warmer and drier scenario. Absolute rates of the polygonal tundra were found to be lowest among tundra types with the warmer drier scenario, but slightly higher than the rates of the wet sedge tundra with the colder wetter scenario.

Table 4.2.16. Modelled daily means of soil respiration of “reassembled“ tundra types ($\text{g C}\cdot\text{m}^{-2}\cdot\text{d}^{-1}$) as with different scenarios of soil temperature and water table. Bold figures show percent of scenario calculations from daily soil respiration rates modelled with the original parameters values. ST2 = soil temperature at 2 cm depth ($^{\circ}\text{C}$); WT = water table (cm below soil surface); “+“ and “-“ = “original conditions +“ and “original conditions -“, respectively.

	<i>ST2 and WT original</i>	<i>ST2 +4°C, WT original</i>	<i>ST2 -4°C, WT original</i>	<i>WT +4 cm, ST2 original</i>	<i>WT -4 cm, ST2 original</i>	<i>ST2 +4°C, WT -4 cm</i>	<i>ST2 -4°C, WT +4 cm</i>
tussock tundra	1.55 100	1.76 114	1.36 88	1.08 69	2.10 135	2.43 156	0.97 62
wet sedge tundra	1.10 100	1.65 150	0.69 63	0.76 69	1.49 135	2.23 202	0.48 43
polygonal tundra	1.08 100	1.38 128	0.83 77	0.73 68	1.50 139	1.93 179	0.57 53

5.2.2 Studies on CO₂ Fluxes of the Soil-Moss System Considering Moss Photosynthesis

As already pointed out in chapters 1, 3.1.2.2, 4.1.1.2, and 4.1.2.2 the soil-moss system formed a closely interwoven system in the investigated types of tundra. Separating the single parts for the purpose of CO₂ flux analysis would lead to artificial results (see chapter 3.1.2.2). Soil respiration measurements in the majority of field studies in tundra as well as in the previous chapters of this thesis included respiration of the photosynthetically active part of the moss layer. When covered by non-transparent chambers for longer periods, the magnitude of moss respiration may be altered, thus not representing the real conditions. Also, moss photosynthesis is able to buffer the CO₂ efflux of soil respiration to the atmosphere, a process which is hardly measurable when both systems are separated from each other. For this purposes, a transparent chamber was taken to examine for the net system flux of the soil-moss system (see chapter 3.1.2.2). Respiration of the soil-moss system was addressed by applying dark conditions for short periods only (i.e. about 15 min.). Moss photosynthesis was calculated from the difference between the net system flux and the respiration of the soil-moss system. This way of analysing respiration may offer a more realistic description of CO₂ effluxes from the biological “ground system“ of tundra.

In the following paragraphs, typical diurnal courses of CO₂ fluxes of the soil-moss systems are presented. Microsites chosen were the same as for the soil respiration experiments presented in the previous chapters. Subplots for the transparent chamber were situated as close as possible to the sub plots of the soil respiration chambers, to provide comparable conditions, and will also refer to the same microsite names and -descriptions. However, the two most dry microsites (tussock tundra, tussock, and polygonal tundra, high apex) had to be excluded for technical constraints (see chapter 3.1.2.2). In the case of the tussock microsite, it would anyway not have been possible to exclude vascular plants from the chamber, since mosses were hardly present between the shoots of the *Eriophorum vaginatum* cover.

To avoid confusion, the measured respiration will be referred to as “soil and moss respiration“ from here on. It should be considered, however, that apart from the fact that the moss receives radiation nearly continuously during the soil-moss system experiments, there was no structural difference to the set-up as performed in the soil respiration experiments.

In the following paragraphs gross moss photosynthesis, soil- and moss respiration and net system flux of the soil-moss system will be abbreviated GMP, SMR, and NSF, respectively.

5.2.2.1 Experiments in the Field

5.2.2.1.1 Lake Labaz

Tussock tundra, moss hummock (TH)

The sub plot of the moss hummock microsite for measurements of the soil-moss system was covered by the moss species *Hylocomium splendens* (90 %) and *Polytrichum strictum* (10 %), representing the two most dominant mosses at this microsite in their representative shares (see chapter 4.1.1.2.1.1). Depth to water table was 10 cm from soil surface over the day presented below (Fig. 4.2.15). The water content of the photosynthetically active parts of the mosses (0-1 cm) as analysed from samples near to the chamber was 88.6 % FW (775 % DW).

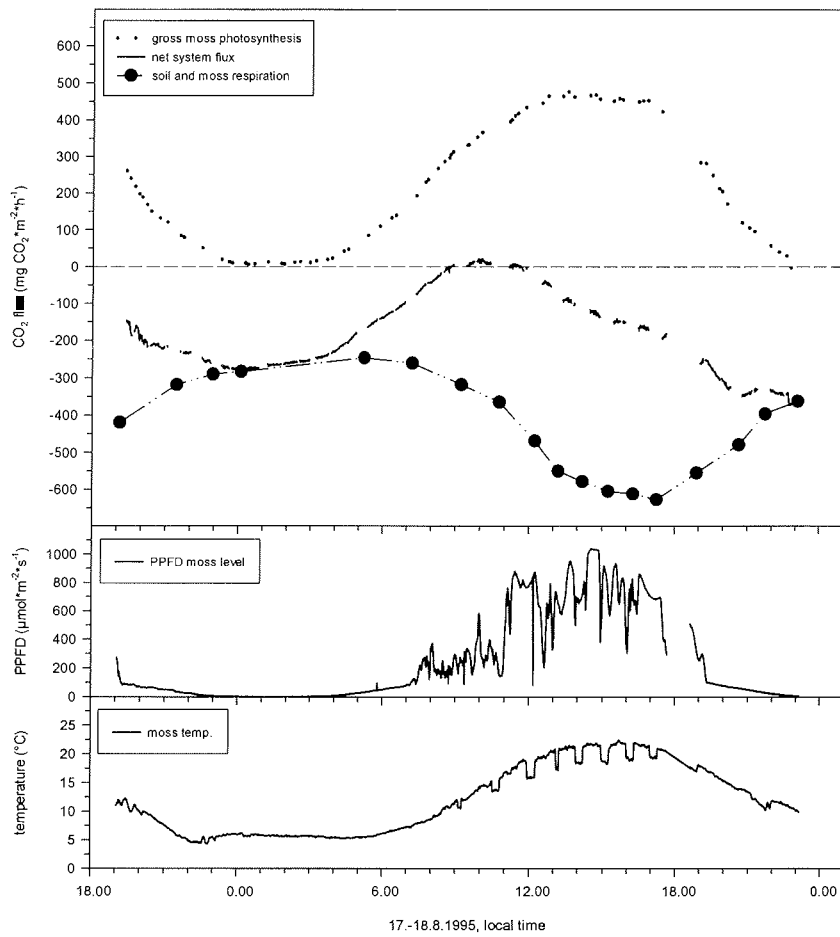


Fig. 4.2.15. CO₂-fluxes (net system flux, soil respiration, gross photosynthesis) and microclimatic conditions of the soil-moss system during a diurnal experiment from 17.-18.8.1995 in tussock tundra, moss hummock (TH). Depth to water table was -10 cm over the experimental period. Carbon losses of the soil-moss system are shown as negative fluxes, carbon gains as positive fluxes.

Table 4.2.17. Amplitudes and means of soil respiration, net soil-moss system flux, gross moss photosynthesis, moss temperature, and soil temperature at 2 cm depth during the diurnal experiment from 17.-18.8.1995 in tussock tundra, moss hummock (TH). Depth to water table was -10 cm over the experimental period. The daily total of PPFD at the moss level was $20.68 \text{ mol} \cdot \text{m}^{-2} \cdot \text{d}^{-1}$.

	<i>soil respiration</i> ($\text{mg CO}_2 \cdot \text{m}^{-2} \cdot \text{h}^{-1}$)	<i>net system flux</i> ($\text{mg CO}_2 \cdot \text{m}^{-2} \cdot \text{h}^{-1}$)	<i>gross moss photosynthesis</i> ($\text{mg CO}_2 \cdot \text{m}^{-2} \cdot \text{h}^{-1}$)	<i>PPFD at moss level</i> ($\mu\text{mol} \cdot \text{m}^{-2} \cdot \text{s}^{-1}$)	<i>moss temp.</i> ($^{\circ}\text{C}$)	<i>soiltemp. 2 cm</i> ($^{\circ}\text{C}$)
mean	-429.6	-182.5	185.2	239	11.7	13.5
max	-249.9	21.3	477.6	0	22.4	20.4
min	-626.9	-372.8	-4.0	1038	4.3	5.2

The 36 h experiment presented in Fig. 4.2.15 shows pronounced differences of microclimatic parameters controlling the CO_2 fluxes between day and night. Maximum PPFD values at moss level over the day reached more than $1000 \mu\text{mol} \cdot \text{m}^{-2} \cdot \text{s}^{-1}$, indicating extensive periods of irradiance (Table 4.2.17). Consequently, the moss temperatures were comparatively high with maximum values exceeding 22°C . During the about 4 h of darkness during night, moss temperatures around 5°C were observed. Soil temperature at 2 cm depth could not be shown for this experiment due to technical problems.

As a consequence of the ambient conditions, the three types of CO_2 fluxes presented showed pronounced diurnal courses as well, but maxima and minima were distinctively offset against each other. GMP followed the course of both PPFD and moss temperature, achieving rates as high as $480 \text{ mg CO}_2 \cdot \text{m}^{-2} \cdot \text{h}^{-1}$ during afternoon. The GMP curve did not show a further increase with an increase of PPFD above a level of about $300\text{-}400 \mu\text{mol} \cdot \text{m}^{-2} \cdot \text{s}^{-1}$. Over these periods the GMP rates were observed to be determined by the course of the moss temperature instead. Considerable assimilation rates during late evening and early morning furthermore indicates a high efficiency of the photosynthetic system already at low light levels.

The comparatively high level of soil respiration was made possible by the low water table position of 10 cm below soil surface. Maxima and minima of SMR was distinctively offset to the course of GMP. Following the course of soil temperature, maximum values of about $630 \text{ mg CO}_2 \cdot \text{m}^{-2} \cdot \text{h}^{-1}$ were achieved during late afternoon, minimum values of about $250 \text{ mg CO}_2 \cdot \text{m}^{-2} \cdot \text{h}^{-1}$ during early morning.

The NSF curve of the soil-moss system resulting from both processes shows that the soil-moss system lost CO_2 to the atmosphere during most of the day. Maximum losses of about $370 \text{ mg CO}_2 \cdot \text{m}^{-2} \cdot \text{h}^{-1}$ were attained during late evening, when comparatively high soil temperature resulted in considerable respiration rates and light was already ceasing. Lowest values of NSF even with a small trend towards sink function of the soil-moss system could be perceived during early morning hours, when rising irradiance already permitted considerable GMP, but soil respiration was low due to low soil temperatures.

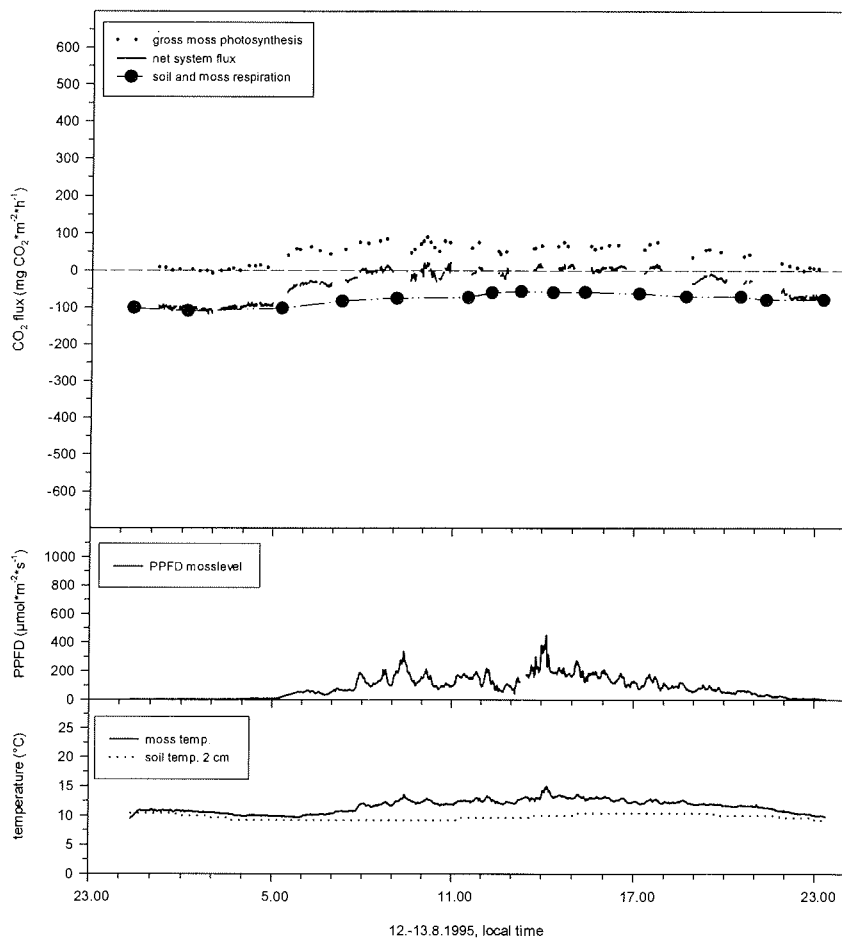


Fig. 4.2.16. CO₂-fluxes (net system flux, soil respiration, gross photosynthesis) and microclimatic conditions of the soil-moss system during a diurnal experiment from 12.-13.8.1995 in tussock tundra, depression (TD). Depth to water table was -1 cm over the experimental period. Carbon losses of the soil-moss system are shown as negative fluxes, carbon gains as positive fluxes.

Table 4.2.18. Amplitudes and means of soil respiration, net soil-moss system flux, gross moss photosynthesis, moss temperature, and soil temperature at 2 cm depth during a diurnal experiment from 12.-13.8.1995 in tussock tundra, depression (TD). Depth to water table was -1 cm over the experimental period. The daily total of PPFD at the moss level was $7.39 \text{ mol} \cdot \text{m}^{-2} \cdot \text{d}^{-1}$.

	soil respiration ($\text{mg CO}_2 \cdot \text{m}^{-2} \cdot \text{h}^{-1}$)	net system flux ($\text{mg CO}_2 \cdot \text{m}^{-2} \cdot \text{h}^{-1}$)	gross moss photosynthesis ($\text{mg CO}_2 \cdot \text{m}^{-2} \cdot \text{h}^{-1}$)	PPFD mosslevel ($\mu\text{mol} \cdot \text{m}^{-2} \cdot \text{s}^{-1}$)	moss temp. ($^{\circ}\text{C}$)	soiltemp. 2 cm ($^{\circ}\text{C}$)
mean	-75.6	-36.8	44.3	86	11.5	9.8
max	-55.6	21.9	95.1	449	15.0	10.4
min	-109.2	-117.5	-9.8	0	9.5	9.2

Tussock Tundra, depression (TD)

The moss vegetation of the sub plot for measurements on the soil-moss system at the depression microsite consisted of *Drepanocladus uncinatus* (80 %), *Polytrichum strictum* (10 %), and *Aulacomnium turgidum* (10 %), representing a typical community of this microsite (see chapter 4.1.1.2.1.1). The water content of the uppermost cm of the mosses as analysed from samples taken right beside the chamber was 90.3 % FW (934 % DW). Water table position was found 1 cm below soil surface on the day of the experiment, which was about the highest position of water table observed at this microsite.

The day showed overcast conditions (daily total of PPFD at 2 m was $6.8 \text{ mol} \cdot \text{m}^{-2} \cdot \text{d}^{-1}$) and consequently the diurnal amplitude of the microclimatic conditions was less pronounced than at the experiment at the moss hummock. Maximum PPFD values did not exceed $450 \mu\text{mol} \cdot \text{m}^{-2} \cdot \text{s}^{-1}$ (Fig. 4.2.16, Table 4.2.18). Darkness lasted for about 4-5 h during night. The moss temperatures ranged from 9.5°C to 15°C over the day. As a result of the high water table position, moss- and soil temperatures at 2 cm depth did not show a pronounced diurnal course and were comparatively low. While the minima of both temperatures were about identical during the second half of the night, the maximum temperature of the moss was found to be about 5°C higher than soil temperature at 2 cm depth during early afternoon.

SMR rates were small, mainly due to the high water table at this microsite. Because of the low amplitude of soil temperature they were on the same level over the day. Maximum values of $110 \text{ mg CO}_2 \cdot \text{m}^{-2} \cdot \text{h}^{-1}$ were perceived during late evening, minimum values of about $55 \text{ mg CO}_2 \cdot \text{m}^{-2} \cdot \text{h}^{-1}$ during early afternoon.

The assimilation rates of the moss community at this microsite were comparatively low at the actual conditions. A maximum rate of about $100 \text{ mg CO}_2 \cdot \text{m}^{-2} \cdot \text{h}^{-1}$ was observed, over night photosynthesis ceased for several hours. Since the GMP curve still reflected changes of the PPFD curve until about $300 \mu\text{mol} \cdot \text{m}^{-2} \cdot \text{s}^{-1}$, but not above, this suggests a light saturation level of the moss community around this level at temperatures between 10°C and 15°C .

The course of the NSF curve of the soil-moss system followed more or less the zero-line between net system loss and net system gain over most sunlit periods of the day, suggesting that the system was about balanced over this time. However, over wide periods of the night zero or near to zero GMP rates resulted in a sharp decrease of NSF rates towards the values of SMR.

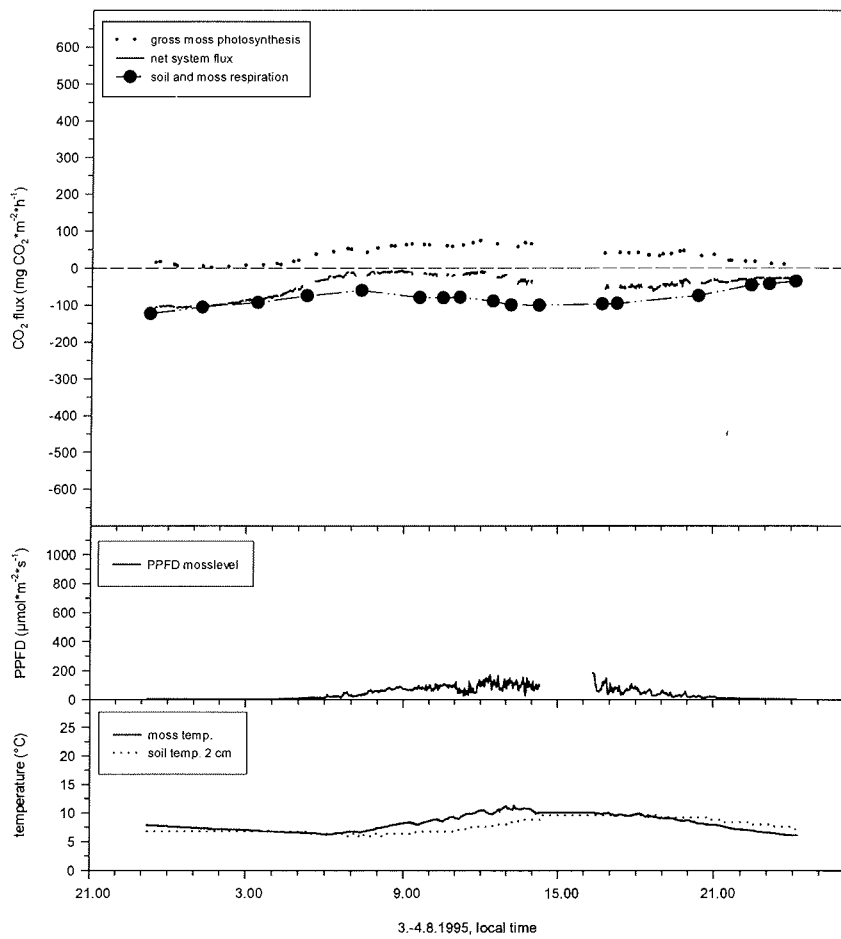


Fig. 4.2.17. CO₂-fluxes (net system flux, soil respiration, gross photosynthesis) and microclimatic conditions of the soil-moss system during a diurnal experiment from 3.-4.8.1995 in wet sedge tundra (WS). Depth to water table was -1 cm over the experimental period. Carbon losses of the soil-moss system are shown as negative fluxes, carbon gains as positive fluxes.

Table 4.2.19. Amplitudes and means of soil respiration, net soil-moss system flux, gross moss photosynthesis, moss temperature, and soil temperature at 2 cm depth during a diurnal experiment from 3.-4.8.1995 in wet sedge tundra (WS). Depth to water table was -1 cm over the experimental period. The daily total of PPFD at the moss level was $3.4 \text{ mol} \cdot \text{m}^{-2} \cdot \text{d}^{-1}$.

	soil respiration ($\text{mg CO}_2 \cdot \text{m}^{-2} \cdot \text{h}^{-1}$)	net system flux ($\text{mg CO}_2 \cdot \text{m}^{-2} \cdot \text{h}^{-1}$)	gross moss photosynthesis ($\text{mg CO}_2 \cdot \text{m}^{-2} \cdot \text{h}^{-1}$)	PPFD mosslevel ($\mu\text{mol} \cdot \text{m}^{-2} \cdot \text{s}^{-1}$)	moss temp. ($^{\circ}\text{C}$)	soiltemp. 2 cm ($^{\circ}\text{C}$)
mean	-81.1	-46.6	34.2	39.4	8.1	7.6
max	-35.9	-5.3	79.3	185	11.3	9.6
min	-123.2	-107.9	0.8	2	6.1	6

Wet sedge tundra (WS)

The sub plot of the transparent chamber in the wet sedge tundra was covered by mosses of the species *Drepanocladus uncinatus* only. As at the depression microsite of the tussock tundra, the water table was situated 1 cm below the soil surface on the day of the experiment, representing a comparatively high position for this type of tundra. The water content of directly neighboured moss samples was 94 % FW (1530 % DW). Some generator malfunction in the afternoon of the day resulted in a loss of data for about 2 h.

Compared to the day of experiment at the depression microsite of the tussock tundra, this day was sunny (total daily PPFD in 2 m was $26.4 \text{ mol} \cdot \text{m}^{-2} \cdot \text{d}^{-1}$). The irradiance observed at the moss level, however, was even more unfavourable for the mosses than at the one presented above, due to the high vascular plant cover in the wet sedge tundra (Fig. 4.2.17): Total daily PPFD at the moss level was $3.4 \text{ mol} \cdot \text{m}^{-2} \cdot \text{d}^{-1}$. Maximum values of only $185 \mu\text{mol} \cdot \text{m}^{-2} \cdot \text{s}^{-1}$ were observed over the day, several hours of darkness occurred during night (Table. 4.2.19). Soil temperatures at 2 cm depth were always below 10°C and showed a very attenuated diurnal course with an amplitude of not even 4°C . Maximum moss temperatures were only slightly higher, minima were the same as at 2 cm depth. The phase shift observed between both curves was about 5 h.

Maximum SMR rates of about $120 \text{ mg CO}_2 \cdot \text{m}^{-2} \cdot \text{h}^{-1}$ were perceived during early afternoon, but decreased to near $40 \text{ mg CO}_2 \cdot \text{m}^{-2} \cdot \text{h}^{-1}$ by the middle of the second night. The diurnal course was more pronounced than at the depression microsite of the tussock tundra, despite the even colder temperature regime observed in wet sedge tundra and the same position of water table.

GMP increased to rates of about $80 \text{ mg CO}_2 \cdot \text{m}^{-2} \cdot \text{h}^{-1}$ over the day, which was only little less than the maximum value obtained at the depression microsite of the tussock tundra with considerably higher PPFD values. This indicates comparatively low light saturation levels of the investigated moss species. Assimilation rates of the mosses at low irradiance during night indicates a sensitive photosynthetic response to light. Even at an irradiance level around $15 \mu\text{mol} \cdot \text{m}^{-2} \cdot \text{s}^{-1}$, a small difference in flux rates could be observed when the chamber was shaded.

The NSF of the soil-moss system was negative over the whole day investigated. Net system fluxes were identical with fluxes of soil respiration during the periods of the night when photosynthetic rates were close to zero. During these times, the soil-moss system lost CO_2 with rates of about $100 \text{ mg CO}_2 \cdot \text{m}^{-2} \cdot \text{h}^{-1}$. Minimum NSF of close below zero were obtained during early morning hours.

5.2.2.1.2 Lake Levinson-Lessing

Polygonal tundra, depression (PD)

Two experiments at the depression microsite of the polygonal tundra (performed at the same sub plot) will serve to clarify the mode of operation of different water table positions on the soil-moss system.

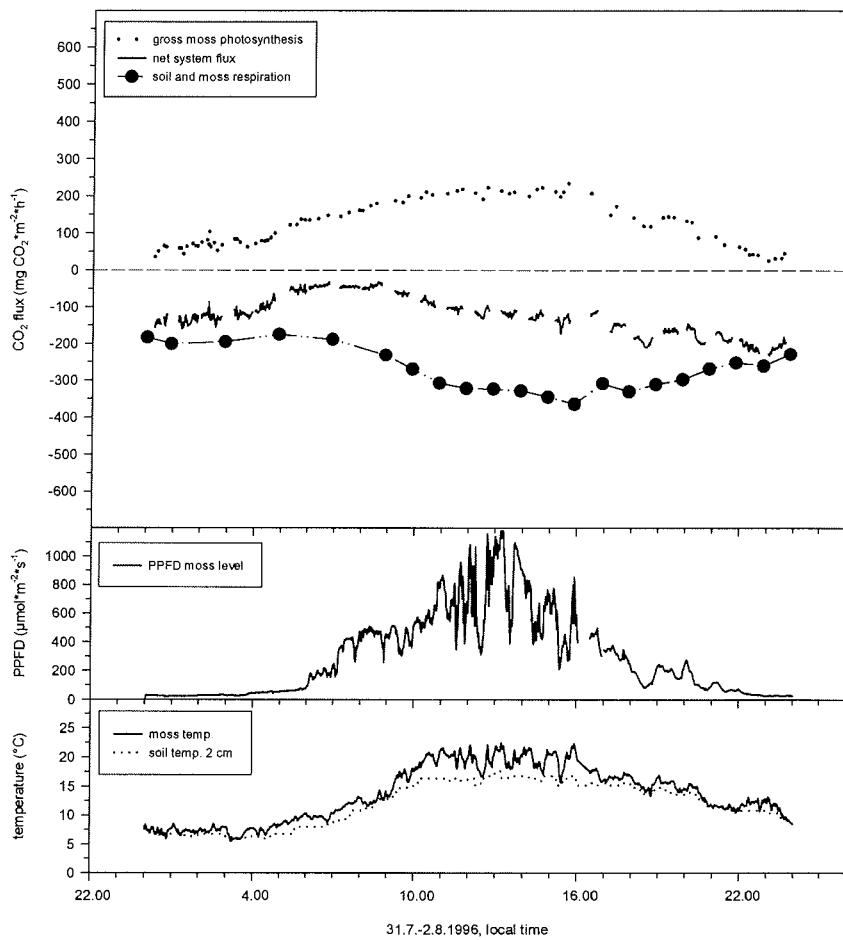


Fig. 4.2.18. CO₂-fluxes (net system flux, soil respiration, gross photosynthesis) and microclimatic conditions of the soil-moss system during a diurnal experiment from 31.7.-1.8.1996 (**experiment 1**) in polygonal tundra, depression (PD). Depth to water table was -7 cm over the experimental period. Carbon losses of the soil-moss system are shown as negative fluxes, carbon gains as positive fluxes.

Table 4.2.20. Amplitudes and means of soil respiration, net soil-moss system flux, gross moss photosynthesis, moss temperature, and soil temperature at 2 cm depth during a diurnal experiment from 31.7.-1.8.1996 (**experiment 1**) in polygonal tundra, depression (**PD**). Depth to water table was -7 cm over the experimental period. The daily total of PPFD at the moss level was $25.29 \text{ mol} \cdot \text{m}^{-2} \cdot \text{d}^{-1}$.

	<i>soil respiration</i> ($\text{mg CO}_2 \cdot \text{m}^{-2} \cdot \text{h}^{-1}$)	<i>net system flux</i> ($\text{mg CO}_2 \cdot \text{m}^{-2} \cdot \text{h}^{-1}$)	<i>gross moss photosynthesis</i> ($\text{mg CO}_2 \cdot \text{m}^{-2} \cdot \text{h}^{-1}$)	<i>PPFD mosslevel</i> ($\mu\text{mol} \cdot \text{m}^{-2} \cdot \text{s}^{-1}$)	<i>moss temp.</i> ($^{\circ}\text{C}$)	<i>soiltemp. 2 cm</i> ($^{\circ}\text{C}$)
mean	-270.9	122.3	132.7	293	13.5	11.9
max	-147.7	32.0	241.7	1179	22.4	17.6
min	-364.1	-231.5	22.3	3	5.5	6.0

Experiment 1 (31.7.-1.8.1996)

The sub plot for experiments on the soil-moss system at the depression of the polygonal tundra was covered by the moss species *Drepanocladus revolvens* (80 %) and *Calliergon sarmentosum* (20 %). The moss water content of comparable moss samples near to the chamber was 927 % DW. On the day of this experiment, the water table was as much as 7 cm below soil surface, which was the lowest water table observed at this site.

The day provided fair weather, clouds were rare (daily total of PPFD at 2 m was $28.3 \text{ mol} \cdot \text{m}^{-2} \cdot \text{d}^{-1}$). Since the vascular plant cover of the polygonal tundra was much more scattered than that in the wet sedge tundra, the moss layer was shaded only for short periods, the daily total of PPFD at the moss level was $25.29 \text{ mol} \cdot \text{m}^{-2} \cdot \text{d}^{-1}$. Maximum PPFD values ranged near to $1200 \mu\text{mol} \cdot \text{m}^{-2} \cdot \text{s}^{-1}$, and darkness was not reached during night (Fig. 4.2.18 and Table 4.2.20).

Moss temperature as well as soil temperature at 2 cm depth showed a pronounced diurnal course with maximum values of 22.4°C and 17.6°C , respectively. A phase shift between the two curves was hardly observable. As at the other sites, differences between both temperatures became negligible during night.

As a consequence of the low water table and large temperature amplitude, SMR revealed a conspicuous diurnal course, showing maximum values of more than $360 \text{ mg CO}_2 \cdot \text{m}^{-2} \cdot \text{h}^{-1}$ during late afternoon. Minimum SMR of about $150 \text{ mg CO}_2 \cdot \text{m}^{-2} \cdot \text{h}^{-1}$ could be observed around midnight.

Although PPFD values were comparatively low during night, GMP was apparent over the whole diurnal cycle. Maximum GMP rates of about $250 \text{ mg CO}_2 \cdot \text{m}^{-2} \cdot \text{h}^{-1}$ occurred during the middle of the day. Changes of irradiance were reflected by the GMP curve only up to a level of about $200 \mu\text{mol} \cdot \text{m}^{-2} \cdot \text{s}^{-1}$, suggesting a light saturation level of photosynthesis of the moss community around this value. Further increase of assimilation rate over the day followed the moss temperature curve.

The resulting NSF curve revealed the soil-moss system of the depression of the polygonal tundra to be a net source of CO_2 with the conditions described above. Due to the strong increase of soil respiration already early in the morning (due to low water table and homogeneity of soil temperature over the profile), the early morning trend of the NSF towards zero was sharp and short only. For the rest of the day, the soil-moss system lost CO_2 to the atmosphere with rates between 100 and $200 \text{ mg CO}_2 \cdot \text{m}^{-2} \cdot \text{h}^{-1}$.

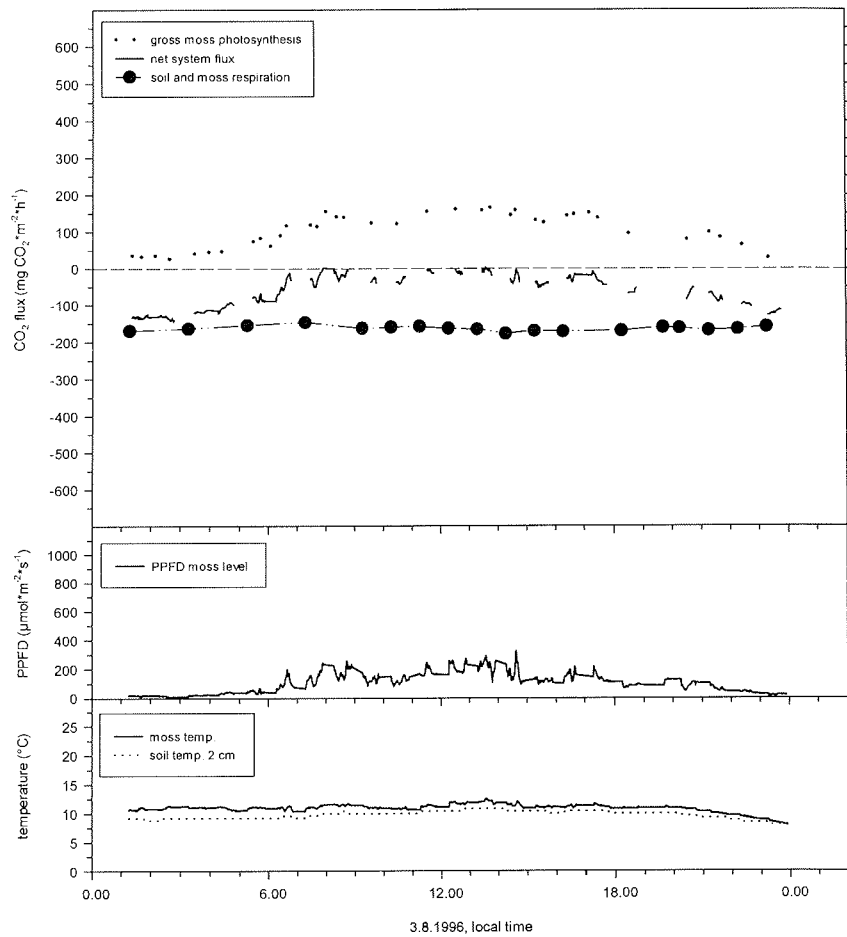


Fig. 4.2.19. CO₂-fluxes (net system flux, soil respiration, gross photosynthesis) and microclimatic conditions of the soil-moss system during a diurnal experiment on 3.8.1996 (**experiment 2**) in polygonal tundra, depression (**PD**). Depth to water table was -3 cm over the experimental period. Carbon losses of the soil-moss system are shown as negative fluxes, carbon gains as positive fluxes.

Table 4.2.21. Amplitudes and means of soil respiration, net soil-moss system flux, gross moss photosynthesis, moss temperature, and soil temperature at 2 cm depth during a diurnal experiment on 3.8.1996 (**experiment 2**) in polygonal tundra, depression (**PD**). Depth to water table was -3 cm over the experimental period. The daily total of PPFD at the moss level was $8.91 \text{ mol} \cdot \text{m}^{-2} \cdot \text{d}^{-1}$.

	<i>soil respiration</i> ($\text{mg CO}_2 \cdot \text{m}^{-2} \cdot \text{h}^{-1}$)	<i>net system flux</i> ($\text{mg CO}_2 \cdot \text{m}^{-2} \cdot \text{h}^{-1}$)	<i>gross moss photosynthesis</i> ($\text{mg CO}_2 \cdot \text{m}^{-2} \cdot \text{h}^{-1}$)	<i>PPFD mosslevel</i> ($\mu\text{mol} \cdot \text{m}^{-2} \cdot \text{s}^{-1}$)	<i>moss temp.</i> ($^{\circ}\text{C}$)	<i>soiltemp. 2 cm</i> ($^{\circ}\text{C}$)
mean	-163.1	-64.9	97.4	103	10.9	9.7
max	-146.9	2.2	173.5	322	12.5	10.8
min	-177.1	144.3	20.3	8	7.9	8

Experiment 2 (3.8.1996)

Conditions during the day of the second experiment at the same microsite differed from those presented above: The day was overcast (daily total of PPFD at 2 m was $9.7 \text{ mol} \cdot \text{m}^{-2} \cdot \text{d}^{-1}$) and the water table was situated 3 cm below soil surface. Water content of moss samples close to the chamber was determined to 1054 % DW.

Daily total of PPFD at the moss level was as low as $8.9 \text{ mol} \cdot \text{m}^{-2} \cdot \text{d}^{-1}$, maximum PPFD values did hardly exceed $300 \mu\text{mol} \cdot \text{m}^{-2} \cdot \text{s}^{-1}$. As on the day of experiment 1, no complete darkness occurred during night (Fig. 4.2.19). Consequently, the diurnal courses of both soil temperature at 2 cm depth and moss temperature was widely attenuated, showing an amplitude of about 3-4.5°C only (Table 4.2.21). Maximum soil temperatures at 2 cm depth ranged some 2°C below the corresponding moss temperature, but differences between both temperatures were minor during night.

Nearly no diurnal course of SMR could be observed, the total amplitude was only $30 \text{ mg CO}_2 \cdot \text{m}^{-2} \cdot \text{h}^{-1}$. Maximum rates ranged up to $180 \text{ mg CO}_2 \cdot \text{m}^{-2} \cdot \text{h}^{-1}$ only.

GMP did not cease over night, but still showed rates of about $20 \text{ mg CO}_2 \cdot \text{m}^{-2} \cdot \text{h}^{-1}$ with minimum PPFD values as low as $10 \mu\text{mol} \cdot \text{m}^{-2} \cdot \text{s}^{-1}$. Following a pronounced increase of assimilation rates with increasing irradiance in the morning, GMP did not show a considerable further intensification over the day. Consequently, maximum GMP rates ranged around $170 \text{ mg CO}_2 \cdot \text{m}^{-2} \cdot \text{h}^{-1}$ only.

NSF of the soil-moss system was observed to be negative for the whole day, but was close to zero during daylight. The soil-moss system lost CO_2 to the atmosphere with maximum absolute values of about $150 \text{ mg CO}_2 \cdot \text{m}^{-2} \cdot \text{h}^{-1}$ during night. Due to the evenness of SMR over the day, the NSF curve reflected the course of GMP.

Polygonal tundra, low apex (PL)

Like with the depression microsite of the polygonal tundra, two experiments from the low apex microsite (performed at the same sub plot) will serve to show the effect of different water table positions on the soil-moss system.

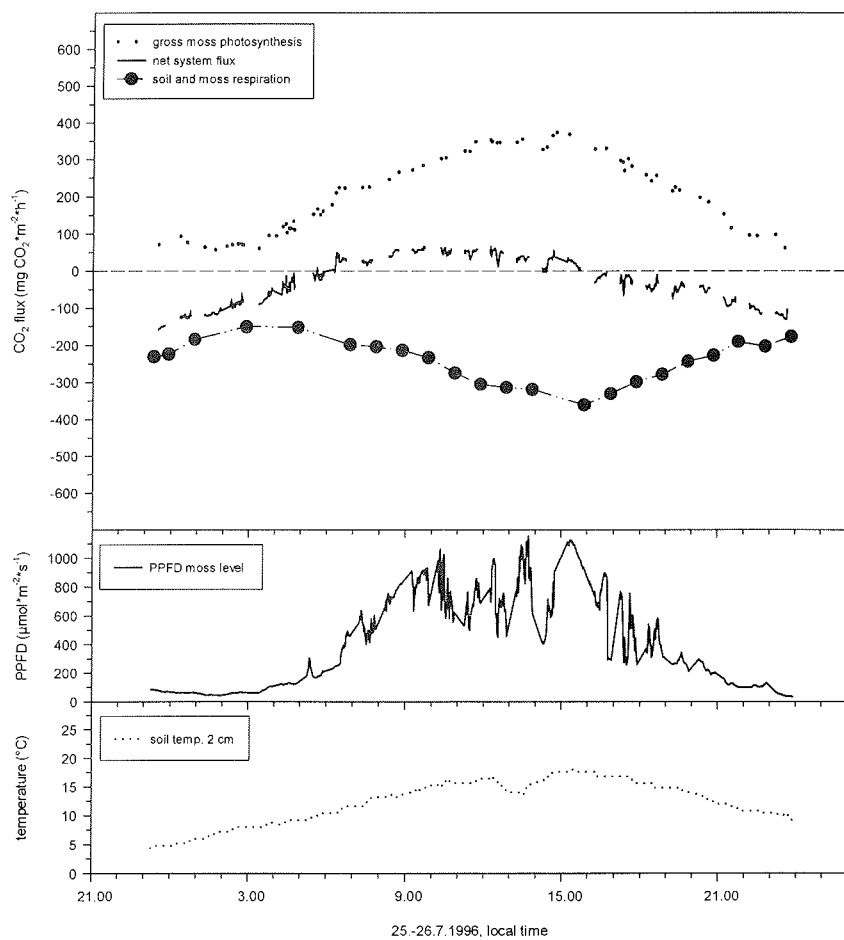


Fig. 4.2.20. CO₂-fluxes (net system flux, soil respiration, gross photosynthesis) and microclimatic conditions of the soil-moss system during a diurnal experiment from 25.-26.7.1996 (**experiment 1**) in polygonal tundra, low apex (PL). Depth to water table was -8 cm over the experimental period. Carbon losses of the soil-moss system are shown as negative fluxes, carbon gains as positive fluxes.

Table 4.2.22. Amplitudes and means of soil respiration, net soil-moss system flux, gross moss photosynthesis, moss temperature, and soil temperature at 2 cm depth during a diurnal experiment from 25.-26.7.1996 (**experiment 1**) in polygonal tundra, low apex (PL). Depth to water table was -8 cm over the experimental period. The daily total of PPFD at the moss level was $34.96 \text{ mol} \cdot \text{m}^{-2} \cdot \text{d}^{-1}$.

	<i>soil respiration</i> ($\text{mg CO}_2 \cdot \text{m}^{-2} \cdot \text{h}^{-1}$)	<i>net system flux</i> ($\text{mg CO}_2 \cdot \text{m}^{-2} \cdot \text{h}^{-1}$)	<i>gross moss photosynthesis</i> ($\text{mg CO}_2 \cdot \text{m}^{-2} \cdot \text{h}^{-1}$)	<i>PPFD mosslevel</i> ($\mu\text{mol} \cdot \text{m}^{-2} \cdot \text{s}^{-1}$)	<i>moss temp.</i> ($^{\circ}\text{C}$)	<i>soiltemp. 2 cm</i> ($^{\circ}\text{C}$)
mean	-241.5	-28.3	209.4	405	nd	12.2
max	-150.2	66.1	391.0	33	nd	18.0
min	-361.1	-157.8	53.3	1153	nd	4.4

Experiment 1 (25.-26.7.1996)

The dominating moss species at the low apex microsite was *Tomentypnum nitens*, which was also covering the chamber sub plot by 100 %. The water content of the moss, as analysed from samples right beside the chamber was 481% DW. Depth to water table was 8 cm on this particular day.

Fair weather with only single clouds in combination with the low vascular plant cover at the low apex microsite provided high irradiance at moss level for most of the day (Fig. 4.2.20). The daily total of PPFD at moss level was $34.96 \text{ mol} \cdot \text{m}^{-2} \cdot \text{d}^{-1}$, maximum values ranged above $1100 \mu\text{mol} \cdot \text{m}^{-2} \cdot \text{s}^{-1}$, and the observed minimum during night was still about $30 \mu\text{mol} \cdot \text{m}^{-2} \cdot \text{s}^{-1}$ (Table 4.2.22).

Due to a broken moss temperature sensor, only soil temperature at 2 cm depth can be presented for this day: The diurnal course of the curve was slightly offset to the radiation curve and showed maximum values of 18°C during early afternoon. During night the soil temperature at 2 cm depth decreased to about 4°C .

Low water table and high amplitude of soil temperature resulted in a clear diurnal course of SMR. Lowest absolute values of $150 \text{ mg CO}_2 \cdot \text{m}^{-2} \cdot \text{h}^{-1}$ could be observed during early morning, largest respiration rates as high as $360 \text{ mg CO}_2 \cdot \text{m}^{-2} \cdot \text{h}^{-1}$ occurred in the afternoon.

Clearly revealing the response of the moss to PPFD and temperature, the GMP curve showed maximum assimilation rates of near to $400 \text{ mg CO}_2 \cdot \text{m}^{-2} \cdot \text{h}^{-1}$ during early afternoon. Minimum photosynthetic rates of about $50 \mu\text{mol} \cdot \text{m}^{-2} \cdot \text{s}^{-1}$ at irradiances as low as $30 \mu\text{mol} \cdot \text{m}^{-2} \cdot \text{s}^{-1}$ were observed during night.

The NSF of the soil-moss system was positive from early morning to the afternoon. The increase of the NSF in the early morning was made possible by the time lag between the increase of GMP rates and absolute SMR rates. Due to the furthermore intensification of GMP over the day, the NSF was held positive also with higher SMR rates for several hours. When both GMP and SMR reached maximum absolute values during afternoon, the soil-moss system was still about balanced in terms of CO_2 fluxes. Due to the considerable GMP rates during night, the NSF curve was at no time matching the SMR curve and thus showed a minimum of about $160 \text{ mg CO}_2 \cdot \text{m}^{-2} \cdot \text{h}^{-1}$ only.

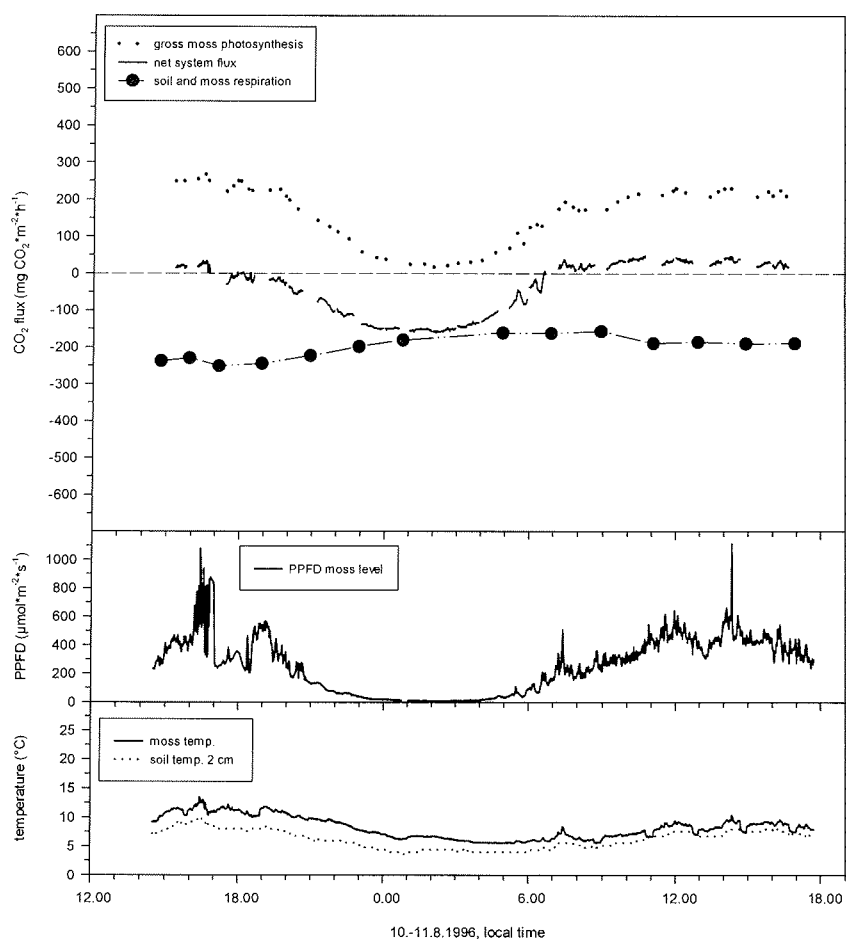


Fig. 4.2.21. CO₂-fluxes (net system flux, soil respiration, gross photosynthesis) and microclimatic conditions of the soil-moss system during a diurnal experiment from 10.-11.8.1996 (**experiment 2**) in polygonal tundra, low apex (**PL**). Depth to water table was -4 cm over the experimental period. Carbon losses of the soil-moss system are shown as negative fluxes, carbon gains as positive fluxes.

Table 4.2.23. Amplitudes and means of soil respiration, net soil-moss system flux, gross moss photosynthesis, moss temperature, and soil temperature at 2 cm depth during a diurnal experiment from 10.-11.8.1996 (**experiment 2**) in polygonal tundra, low apex (**PL**). Depth to water table was -4 cm over the experimental period. The daily total of PPFD at the moss level was 22.23 mol*m⁻²*d⁻¹.

	<i>soil respiration</i> (mg CO ₂ *m ⁻² *h ⁻¹)	<i>net system flux</i> (mg CO ₂ *m ⁻² *h ⁻¹)	<i>gross moss photosynthesis</i> (mg CO ₂ *m ⁻² *h ⁻¹)	<i>PPFD mosslevel</i> (μmol*m ⁻² *s ⁻¹)	<i>moss temp.</i> (°C)	<i>soiltemp.</i> 2 cm (°C)
mean	-199.9	-42.5	148.3	257	8.2	6.2
max	-156.6	48.5	275.9	1114	13.4	10.0
min	-251.5	-160.8	13.6	7	5.5	3.6

Experiment 2 (10.-11.8.1996)

The second experiment at the same sub plot of the low apex microsite of the polygonal tundra was performed on an overcast day with water table position only 4 cm below the soil surface. The water content of the mosses as analysed from samples close to the chamber was 521% DW. In contrast to the experiments presented above, this experiment was performed from early to late afternoon, instead from midnight to midnight (Fig. 4.2.21)

Irradiance levels on the day presented were generally around 500 μmol*m⁻²*s⁻¹ during daylight, only some cloudholes provided maximum values up to 1100 μmol*m⁻²*s⁻¹. Lowest PPFD values during night decreased below 10 μmol*m⁻²*s⁻¹. The daily total of PPFD at the moss level was 22.23 mol*m⁻²*d⁻¹ (Table 4.2.23).

Moss temperature and soil temperature showed a comparably attenuated diurnal course and showed no phase shift to each other. Minimum temperatures during night differed by about 2°C, whereas maximum temperatures over the day showed a difference of 3.4°C.

SMR values consequently showed an amplitude of about 100 mg CO₂*m⁻²*h⁻¹, only half of what has been observed in experiment 1. The maximum absolute rate of SMR (250 mg CO₂*m⁻²*h⁻¹) was as well about 100 mg CO₂*m⁻²*h⁻¹ lower than in experiment 1.

GMP showed a stable level of about 250 mg CO₂*m⁻²*h⁻¹ over daylight periods, not observed to be extensively modified by changes in irradiance level or temperature. GMP decreased to very low values over night, when PPFD values hardly reached 10 μmol*m⁻²*s⁻¹.

As a consequence of lower SMR rates than observed in experiment 1, but stable considerable GMP rates during daylight, NSF was positive again from early morning to late afternoon. Because of SMR lacking a diurnal course during the days observed, the NSF curve reflected the GMP curve fairly well. During the periods of the night with PPFD values close to zero, minimum NSF values of 160 mg CO₂*m⁻²*h⁻¹ closely matched SMR rates.

5.2.2.2 Moss Photosynthetic Performance

Already the diurnal courses of GMP of the different moss communities investigated suggested differences in photosynthetic response in particular to PPFD. Since the temperature range observed during apparent GMP was quite restricted in most cases, the photosynthesis models evaluated in the scope of balancing were rather incomplete in terms of temperature response. Therefore, only the light response curves are presented in Fig. 4.2.22 and the temperature range observed will be noted below each graph (for graphs of the evaluated photosynthesis models see appendix, Fig. A28). The line inserted represents the light regression of all GMP values included, not considering a modification by temperature.

All moss communities investigated showed high photosynthetic efficiency, i.e. a steep increase of gross photosynthesis with light. The moss species from the wet microsites at Lake Labaz, tussock tundra, depression, and wet sedge tundra, furthermore revealed a particular low light saturation level in the observed temperature range. Graphs suggest that *Drepanocladus uncinatus* and the connected species of the wet sedge tundra achieved light saturation already at about $100 \mu\text{mol}\cdot\text{m}^{-2}\cdot\text{s}^{-1}$ at temperatures around 10°C . Irradiance level in wet sedge tundra was not observed to increase above $300 \mu\text{mol}\cdot\text{m}^{-2}\cdot\text{s}^{-1}$, whereas values up to $800 \mu\text{mol}\cdot\text{m}^{-2}\cdot\text{s}^{-1}$ were attained at the depression microsite of the tussock tundra occasionally. Maximum photosynthetic rate of both moss communities was below $100 \text{mg CO}_2\cdot\text{m}^{-2}\cdot\text{h}^{-1}$ at the temperatures observed.

The moss community of the moss hummock of the tussock tundra, consisting of *Hylocomium splendens* and *Polytrichum strictum*, showed the highest maximum photosynthetic rates of up to $470 \text{mg CO}_2\cdot\text{m}^{-2}\cdot\text{h}^{-1}$. A steep increase of the response curve at low PPFD levels indicating high photosynthetic efficiency was followed by a light saturation level at about $400 \mu\text{mol}\cdot\text{m}^{-2}\cdot\text{s}^{-1}$. The broad temperature range of the moss hummock surface during daylight resulted in a scattering of data at light levels above $150 \mu\text{mol}\cdot\text{m}^{-2}\cdot\text{s}^{-1}$.

Tomentypnum nitens, the dominating moss at the low apex microsite of the polygonal tundra, achieved light saturation at a PPFD level around $250 \mu\text{mol}\cdot\text{m}^{-2}\cdot\text{s}^{-1}$ at temperatures between 6°C and 13°C . Since the graph suggests a maximum photosynthetic rate around $270 \text{mg CO}_2\cdot\text{m}^{-2}\cdot\text{h}^{-1}$, the initial slope of the response curve was steep, indicating high photosynthetic efficiency. Considerable scattering of data at high light levels already within a comparatively narrow temperature range suggests high temperature response of maximum photosynthetic rates.

In contrast, the much broader temperature range observed at the depression microsite of the polygonal tundra resulted in considerably less scattering of gross photosynthetic rates around

the maximum photosynthetic rate of about $220 \text{ mg CO}_2 \cdot \text{m}^{-2} \cdot \text{h}^{-1}$. The moss community at this site, consisting of *Drepanocladus revolvens* and *Calliergon sarmentosum* achieved light saturation level at about $350 \mu\text{mol} \cdot \text{m}^{-2} \cdot \text{s}^{-1}$. A less steep increase of the response curve than observed at the other sites indicated a smaller photosynthetic efficiency.

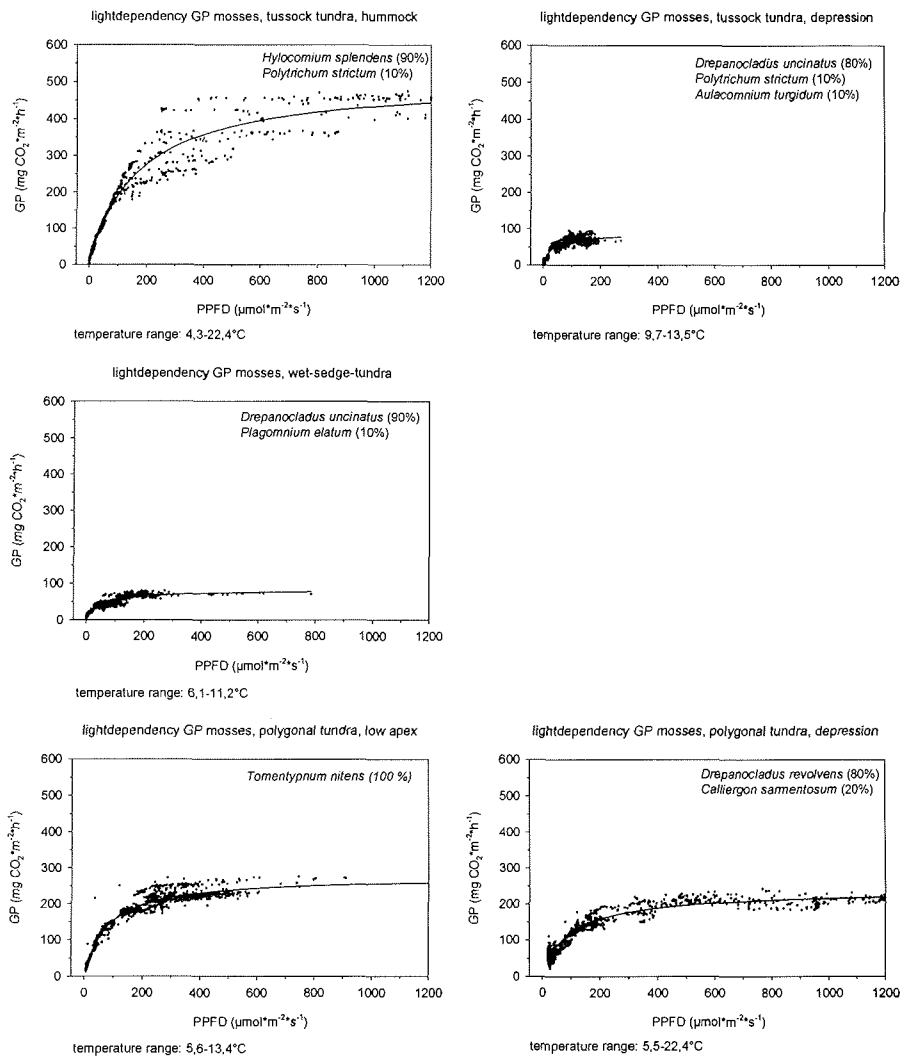


Fig. 4.2.22. Light dependence of gross mass photosynthesis (GP mosses) of the different moss communities. Measured values and regression line, fitted with equation 9. The moss temperature range of each experiment is noted below the graphs.

5.2.2.3 *Balancing the CO₂ Fluxes of the Soil-Moss System*

The CO₂ fluxes of the soil-moss system of the different microsites were balanced over the day on the basis of the experiments presented above. Therefore, gross moss photosynthesis of each moss community was modelled as a function of PPFD and moss temperature, in order to receive best interpolation of the photosynthetic curves. Gaps in the NSF curve were closed by adding the values of SMR to the modelled GMP values.

In Table 4.2.24, the absolute daily rates of SMR, GMP, NSF, and the relative reduction of SMR by GMP is presented for each microsite investigated in combination with the specific microclimatic conditions. Two diurnal experiments with different microclimatic conditions were included in two cases.

All soil-moss systems investigated showed a net loss of CO₂ over the observed periods, but some nearly reached the line of balancing in terms of CO₂ fluxes. The highest relative reduction of SMR by GMP was attained at the low apex microsite of the polygonal tundra (**PL**). The soil-moss system was about balanced in terms of CO₂ fluxes on the day of experiment 1 (25.7.1995). Highest irradiance sum at moss level of all experiments performed, and high moss temperatures (as indicated by the comparably high ST2; the moss temperature sensor was broken on that day) caused the highest GMP rate observed. Water table was higher, ST2 lower and consequently SMR rates were lower on the day of the second experiment at the low apex. The relative reduction of SMR by GMP ranked close behind the value attained during the first experiment. Lower moss temperatures and irradiance level resulted in comparatively reduced GMP rates as well.

The lowest relative reduction of SMR by GMP was achieved by the wet sedge tundra site (**WS**). Although SMR was particular low due to high water table and low ST2, lowest moss temperatures and irradiance sum of all experiments performed resulted in the lowest GMP observed.

The relative reduction of SMR by GMP at the depression of the tussock tundra (**TD**) was two times the value observed at the wet sedge tundra site, although total rates of SMR were about the same. The reason of the comparatively higher reduction value at the depression microsite could be found in the about 40 % higher GMP rates observed here.

The second lowest relative reduction of SMR by GMP of only 51 % could be observed at the hummock microsite of the tussock tundra (**TH**), although on the day of the experiment the second highest GMP value of all sites could be observed here. Highest absolute SMR rates of

all sites were made possible by highest ST2 values and lowest water table positions observed during experiments. The absolute value of NSF was by far lowest at the hummock microsite: Even though modified by the second highest GMP value observed, this site showed absolute net effluxes of a magnitude, most other sites did not achieve by SMR alone.

The relative reduction of SMR by GMP differed only by 10 % between the two experiments at the depression microsite of the polygonal tundra (**PD**), although the absolute NSF of experiment 1 was twice as high as of experiment 2. The 4 cm higher water table, as well as considerably lower moss- and soil temperatures and lower irradiance levels on the day of experiment 2 led to both particularly lower SMR and GMP rates in the case of the second experiment. Since the decrease was slightly biased towards SMR, both fluxes added to a comparatively more balanced NSF in the case of experiment 2.

Table 4.2.24. Soil and moss respiration (s + m respiration), gross moss photosynthesis and net soil-moss system flux ($\text{g C}\cdot\text{m}^{-2}\cdot\text{d}^{-1}$ and $\text{mg CO}_2\cdot\text{m}^{-2}\cdot\text{d}^{-1}$), percent reduction of soil respiration by gross moss photosynthesis, and microclimatic conditions for the diurnal experiments at different microsites.

	<i>TH</i>	<i>TD</i>	<i>WS</i>	<i>PL</i> (1)	<i>PL</i> (2)	<i>PD</i> (1)	<i>PD</i> (2)
s + m respiration ($\text{mg CO}_2\cdot\text{m}^{-2}\cdot\text{d}^{-1}$)	-9439	-1888	-1961	-5681	-4648	-6264	-3961
s + m respiration ($\text{g C}\cdot\text{m}^{-2}\cdot\text{d}^{-1}$)	-2.576	-0.515	-0.535	-1.55	-1.268	-1.709	-1.065
gross moss phot. ($\text{mg CO}_2\cdot\text{m}^{-2}\cdot\text{d}^{-1}$)	4798	1205	694	5611	4068	3345	2494
gross moss phot. ($\text{g C}\cdot\text{m}^{-2}\cdot\text{d}^{-1}$)	1.309	0.329	0.189	1.531	1.115	0.913	0.681
net soil-moss system flux ($\text{mg CO}_2\cdot\text{m}^{-2}\cdot\text{d}^{-1}$)	-4641	-682	-1267	-70	-561	-2919	-1407
net soil-moss system flux ($\text{g C}\cdot\text{m}^{-2}\cdot\text{d}^{-1}$)	-1.267	-0.186	-0.346	-0.019	-0.153	-0.797	-0.384
reduction of s +m respiration by gross moss phot. (%)	50.8	63.9	35.4	98.8	87.9	53.4	63.9
mean moss temp. (°C)	11.7	11.5	8.1	-	8.2	13.5	10.9
mean soiltemp. 2 cm (°C)	13.5	9.8	7.6	12.2	6.2	11.9	9.7
water table below soil surface (cm)	-10	-1	-1	-8	-4	-7	-3
daily total PPFD ($\text{mol}\cdot\text{m}^{-2}\cdot\text{d}^{-1}$)	20.68	7.40	3.40	34.96	22.23	25.29	8.91

5.2.3 Studies on CO₂ Fluxes of the Whole System

Two diurnal experiments on the CO₂ fluxes of the whole system (i.e. soil, moss, and vascular plants) of the depression of the polygonal tundra (PD) microsite will be presented in this paragraph. Their main purpose was to act as a framework for “assembling“ the contributions of the subsystems to the total CO₂ flux, through modelling of soil respiration and moss photosynthesis (see chapter 4.2.4). A sub plot with a representative vascular plant cover and moss cover (see Table 4.1.16) in close vicinity of both soil respiration chamber and soil-moss chamber was chosen for the experiments.

Experiment 1 (28.-29.7.1996)

The day of the experiment was cool and cloudy, with some sunny periods during afternoon. Mean air temperature at 2 m was about 10°C, mean soil temperature at 2 cm depth was 7.5°C (Table 4.2.25). The fairly attenuated diurnal course of these temperatures went nearly parallel and maxima were attained during late afternoon. Irradiance measured at 2 m height was characterized by values around 400 $\mu\text{mol}\cdot\text{m}^{-2}\cdot\text{s}^{-1}$ in the morning and values around 700 $\mu\text{mol}\cdot\text{m}^{-2}\cdot\text{s}^{-1}$ in the afternoon (Fig. 4.2.23). Minimum PPFD values hardly decreased below 20 $\mu\text{mol}\cdot\text{m}^{-2}\cdot\text{s}^{-1}$ during night. The daily total of PPFD at 2 m was 23.3 $\text{mol}\cdot\text{m}^{-2}\cdot\text{d}^{-1}$. Depth to water table was 4 cm.

Net system flux of the whole system was positive for about 19 of 24 hours. A steep increase and decrease occurred during early morning and late evening, respectively. NSF reached highest values of nearly 500 $\text{mg CO}_2\cdot\text{m}^{-2}\cdot\text{h}^{-1}$ during afternoon, parallel with high irradiances. During night the curve decreased to negative flux rates, but never matched the curve of system respiration

The diurnal amplitude of the system respiration was fairly attenuated. Maximum absolute efflux rates of 230 $\text{mg CO}_2\cdot\text{m}^{-2}\cdot\text{h}^{-1}$ occurred during late afternoon, minimum rates of about 140 $\text{mg CO}_2\cdot\text{m}^{-2}\cdot\text{h}^{-1}$ during early morning.

Table 4.2.25. Amplitudes and means of net system flux, system respiration, PPFD, air temperature at 2 m, and soil temperature at 2 cm depth during a diurnal experiment from 28-29.7.1996 (**experiment 1**) in the polygonal tundra, depression (PD). Depth to water table was -4 cm over the experimental period. The daily total of PPFD at 2 m was 23.3 mol*m⁻²*d⁻¹.

	<i>net system flux</i> (mg CO ₂ *m ⁻² *h ⁻¹)	<i>system respiration</i> (mg CO ₂ *m ⁻² *h ⁻¹)	<i>PPFD</i> (μmol*m ⁻² *s ⁻¹)	<i>air temperature</i> 2 m (°C)	<i>soil temperature</i> 2 cm (°C)
mean	222.3	-184.9	259	10.1	7.5
max	472.9	-136.3	805	13.0	10.4
min	-115.8	-229.7	16	7.6	4.8

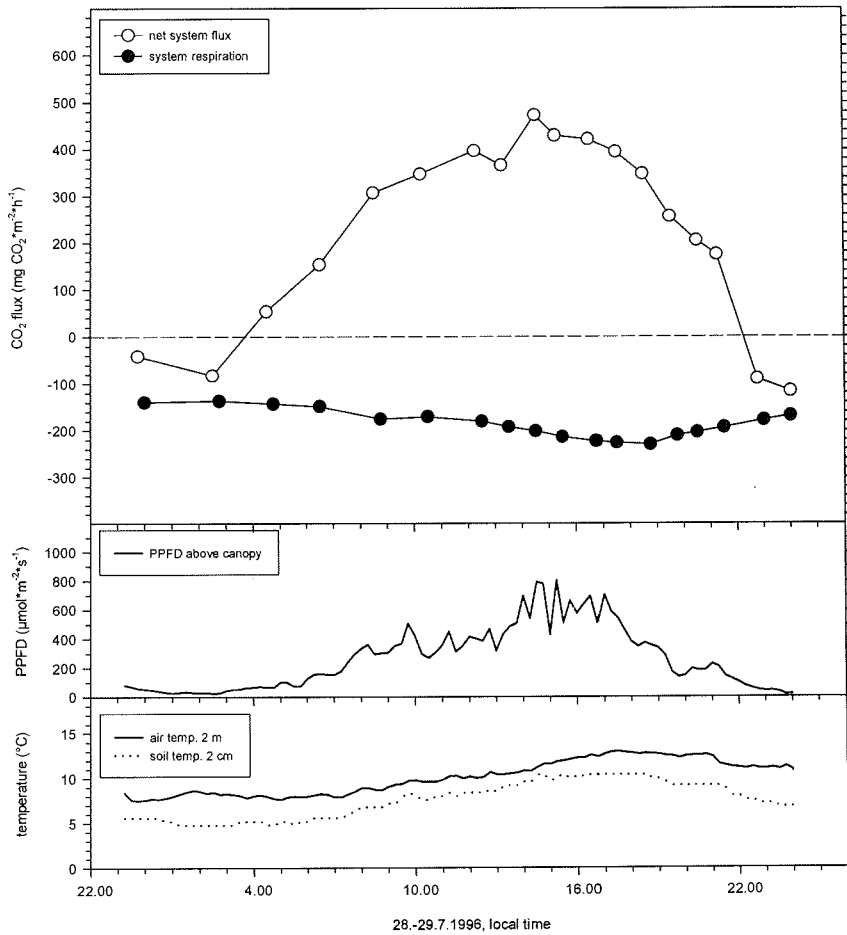


Fig. 4.2.23. CO₂-fluxes (net system flux, system respiration) and microclimatic conditions of the “whole system” of polygonal tundra, depression (PD), during a diurnal experiment from 28-29.7.1996 (**experiment 1**). Depth to water table was -4 cm over the experimental period. Carbon losses of the system are shown as negative fluxes, carbon gains as positive fluxes.

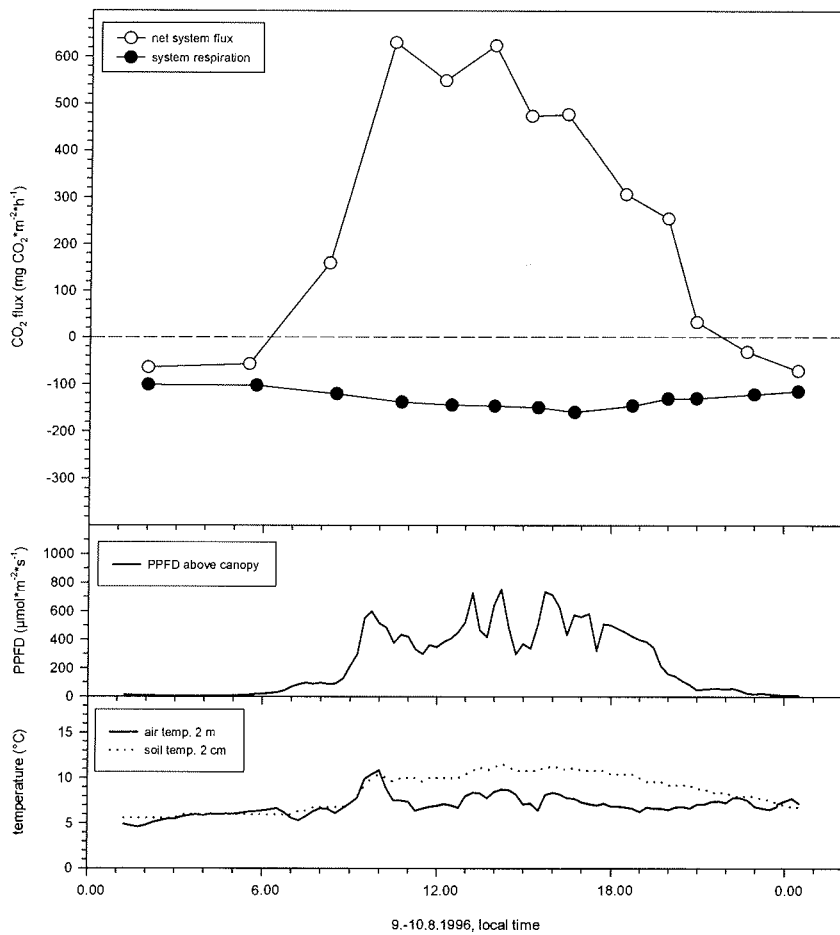


Fig. 4.2.24. CO₂-fluxes (net system flux, system respiration) and microclimatic conditions of the whole system of polygonal tundra, depression (PD), during a diurnal experiment on 9.-10.8.1996 (**experiment 2**). Depth to water table was -1 cm. Carbon losses of the system are shown as negative fluxes, carbon gains as positive fluxes.

Table 4.2.26. amplitudes and means of net system flux, system respiration, PPFD, air temperature at 2 m, and soil temperature at 2 cm depth during a diurnal experiment on 9.-10.8.1996 (**experiment 2**) in the polygonal tundra, depression (**PD**). Depth to water table was -1 cm over the experimental period. The daily total of PPFD at 2 m was $20.1 \text{ mol} \cdot \text{m}^{-2} \cdot \text{d}^{-1}$.

	<i>net system flux</i> ($\text{mg CO}_2 \cdot \text{m}^{-2} \cdot \text{h}^{-1}$)	<i>system respiration</i> ($\text{mg CO}_2 \cdot \text{m}^{-2} \cdot \text{h}^{-1}$)	<i>PPFD</i> ($\mu\text{mol} \cdot \text{m}^{-2} \cdot \text{s}^{-1}$)	<i>air temperature</i> 2 m ($^{\circ}\text{C}$)	<i>soil temperature</i> 2 cm ($^{\circ}\text{C}$)
mean	252.3	-131.2	237	7.0	8.5
max	630.6	-101.3	755	10.9	11.6
min	-72.1	-159.6	3	4.6	5.6

Experiment 2 (9.-10.8.1996)

The main difference between experiment 1 and 2 was that the position of the water table was 4 cm and 1 cm below soil surface, respectively. Although air temperature at 2 m was about 3°C colder on the day of experiment 2, soil temperature at 2 cm depth was found about 1°C higher on this day (Table 4.2.26). Soil temperature at 2 cm depth showed higher values than did air temperature at 2 m over most of the day (Fig. 4.2.24). While air temperature at 2 m reached its maximum already early in the morning, the maximum of soil temperature at 2 cm depth occurred during late afternoon. Irradiance was characterized by changes between cloudy and sunny periods, the daily total of PPFD of $20.1 \text{ mol} \cdot \text{m}^{-2} \cdot \text{d}^{-1}$ was very close to the value of experiment 1. Maximum PPFD values, however, reached only $759 \mu\text{mol} \cdot \text{m}^{-2} \cdot \text{s}^{-1}$ and minima during night were indicating darkness.

The diurnal course of system respiration was very attenuated, showing an amplitude of about $60 \text{ mg CO}_2 \cdot \text{m}^{-2} \cdot \text{h}^{-1}$ only. The absolute maximum of $160 \text{ mg CO}_2 \cdot \text{m}^{-2} \cdot \text{h}^{-1}$ was obtained during late afternoon.

Net system flux of the whole system of the depression of the polygonal tundra was positive for about 16 of 24 hours with the conditions described. Night NSF values were close to matching the rates of system respiration. Increase of NSF in the morning as well as decrease in the evening was very steep, daily maxima ranged up to $630 \text{ mg CO}_2 \cdot \text{m}^{-2} \cdot \text{h}^{-1}$.

5.2.4 Connecting the Subsystems

On the basis of the two diurnal experiments on CO₂ fluxes of the whole system in the depression of the polygonal tundra (PD), and the observed microclimatological parameters on that days, the contribution of the subsystems (soil, moss, vascular plants) was „reassembled“. Diurnal courses of soil respiration as well as moss photosynthesis were calculated on the basis of the corresponding models evaluated from measurements at sub plots of the same microsite. The three sub plots for the measurements of soil respiration, soil-moss system fluxes and whole-system fluxes were situated closely neighbored (i.e. less than 1 m from each other).

The microclimatic conditions of the depression of the polygonal tundra during 29.7. and 9.8. has already been introduced in the chapter 4.2.3.

The course of the net system flux of the whole system was most strongly influenced by the gross photosynthesis of the vascular plants (Figs. 4.2.25 and 4.2.26). Soil respiration accounted for nearly the total CO₂ efflux of the system, reducing the role of respiration of the aboveground parts of vascular plants to a minimum. No particular diurnal course of vascular plant respiration could be observed during both experiments. Both absolute level and diurnal amplitude of soil respiration was higher during experiment 1, as compared to experiment 2. Due to comparatively high gross photosynthetic rates of the mosses during the day, the soil-moss system was already about balanced for some hours during experiment 1. In combination with the lower soil respiration rates observed during experiment 2, the considerable gross photosynthetic rates of the mosses caused the soil-moss system to even act as a net sink for atmospheric CO₂ for an extended period. While during experiment 1 gross moss photosynthesis showed higher rates than gross vascular plant photosynthesis for several hours during night, both rates were about on the same level for the corresponding hours of experiment 2. During the periods when gross photosynthesis of the vascular plants nearly ceased, net system flux of the total system was mostly represented by the net system flux of the soil-moss system. Over the day, the absolute rates of gross vascular plant photosynthesis were about twice as high as the rates achieved by the gross moss photosynthesis. Already with irradiances of about $100\mu\text{mol}\cdot\text{m}^{-2}\cdot\text{s}^{-1}$, gross photosynthetic rates of the vascular plants exceeded the photosynthetic rates of the mosses.

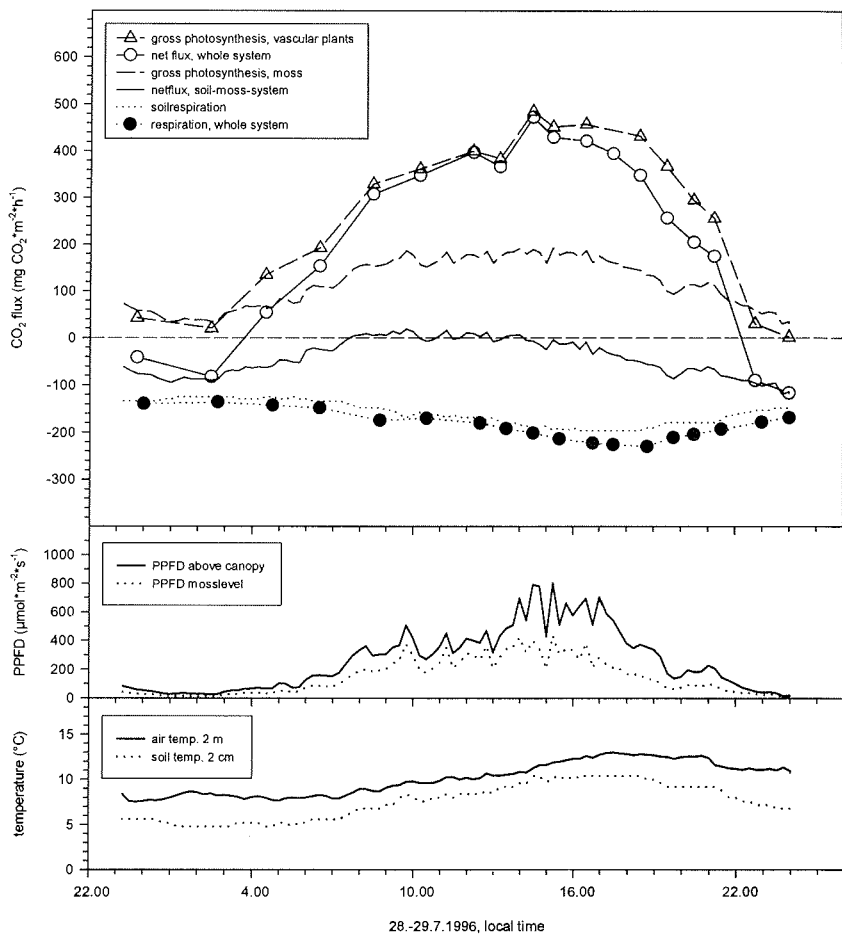
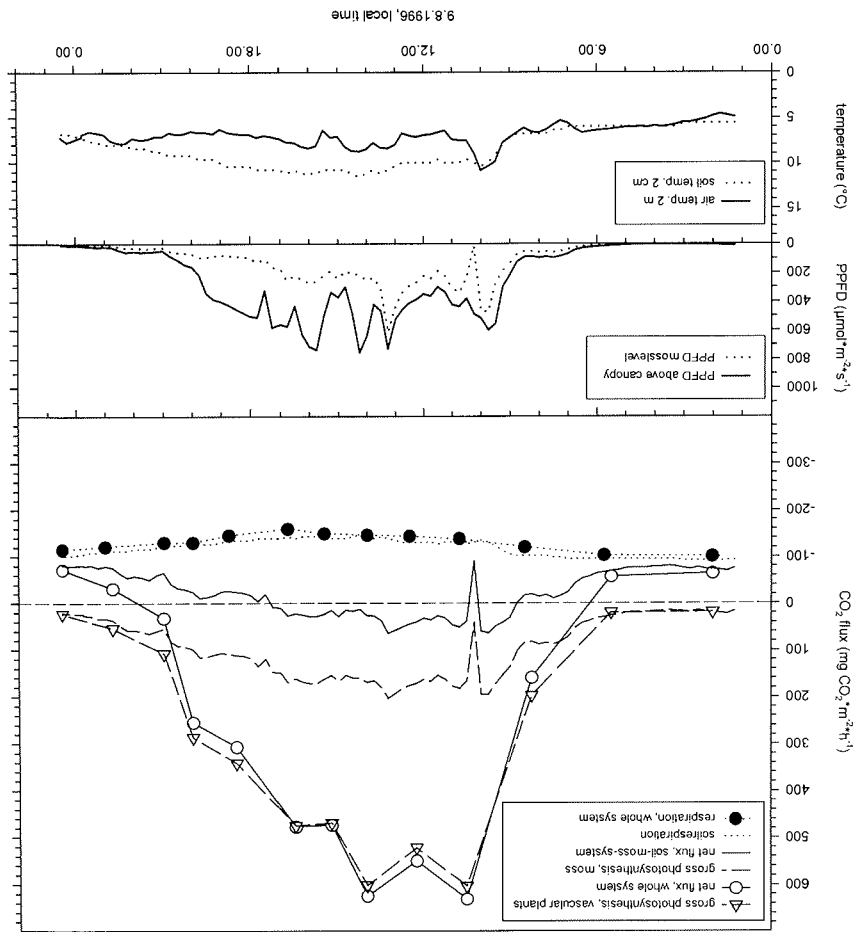


Fig. 4.2.25. CO₂-fluxes (mg CO₂*m⁻²*d⁻¹ and g C*m⁻²*d⁻¹) and microclimatic conditions at the depression microsite of the polygonal tundra (PD) during a diurnal experiment from 28.-29.8.1996 (experiment 1). Depth to water table was -4 cm.

Fig. 4.2.26. CO_2 -fluxes ($\text{mg CO}_2 \cdot \text{m}^{-2} \cdot \text{d}^{-1}$ and $\text{g C} \cdot \text{m}^{-2} \cdot \text{d}^{-1}$) and microclimatic conditions at the depression microsite of the polygonal tundra (PD) during a diurnal experiment from 9.-10.8.1996 (experiment 2). Depth to water table was -1 cm.



When the CO₂ fluxes of the subsystems were balanced over the day, differences between their contribution to the fluxes of the whole system as caused by different conditions became visible (Table 4.2.27). The net system flux of the whole system showed the depression of the polygonal tundra to be a strong sink for atmospheric CO₂ on both days presented here. The daily total of net system flux, however, was about 930 mg CO₂*m⁻²*d⁻¹ (16%) lower on 29.7. (experiment 1) as compared to 9.8. (experiment 2). Although irradiance and air temperature at 2 m was lower on the day of experiment 2, gross vascular plant photosynthesis was observed about 350 mg CO₂*m⁻²*d⁻¹ higher. On the other hand, moss photosynthesis was about 500 mg CO₂*m⁻²*d⁻¹ lower on this day, more than levelling this trend. The process responsible for the considerable difference of net system flux between both days was soil respiration: A water table position of only 1 cm below soil surface on 9.8. resulted in a CO₂ efflux by soil respiration of only about 2800 mg CO₂*m⁻²*d⁻¹, whereas it was observed as high as 3800 mg CO₂*m⁻²*d⁻¹ on 29.7. with a water table position of 4 cm below soil surface.

Table 4.2.27. Contribution of the subsystems to the total daily net system flux (mg CO₂*m⁻²*d⁻¹ and g C*m⁻²*d⁻¹) and microclimatic conditions for two diurnal experiments (29.7.1996 and 9.8.1996) at the depression microsite of the polygonal tundra (PD).

<i>polygonal tundra, depression</i>	<i>29.7.1996</i>		<i>9.8.1996</i>	
	<i>(experiment 1)</i>		<i>(experiment 2)</i>	
	<i>mg CO₂*m⁻²*d⁻¹</i>	<i>g C*m⁻²*d⁻¹</i>	<i>mg CO₂*m⁻²*d⁻¹</i>	<i>g C*m⁻²*d⁻¹</i>
net system flux	4762	1.30	5689	1.55
gross photosynthesis vascular plants	6185	1.69	6528	1.78
gross photosynthesis mosses	2774	0.76	2286	0.62
net flux soil-moss subsystem	-1025	-0.28	-530	-0.14
whole system respiration	-4251	-1.16	-3087	-0.84
aboveground respiration vascular plants	-452	-0.12	-271	-0.07
soil respiration	-3799	-1.04	-2816	-0.77
water table (cm below soil surface)		-4		-1
mean air temperature 2 m (°C)		10.1		7.0
mean moss temperature (°C)		8.6		8.9
mean soil temperature 2 cm (°C)		7.5		8.5
daily total PPFD 2 m (mol*m ⁻² *d ⁻¹)		22.38		20.50
daily total PPFD mosslevel (mol*m ⁻² *d ⁻¹)		12.44		10.04

As with the moss photosynthesis, the light response of gross photosynthesis of the vascular plant community (70 % *Carex stans*, 30 % *DuPontia fisheri*, see also Table 4.1.16) can be calculated from the balancing procedure (see above) and plotted (Fig. 4.2.27). The graph indicates a higher maximum photosynthetic rate than observed with the mosses. The light response model (equation 9), fitted with an r^2 of 0.89, suggests that no light saturation level was attained within the PPFD range observed. However, this result may not be very meaningful due to a sparse databasis and the lack of leaf temperatures.

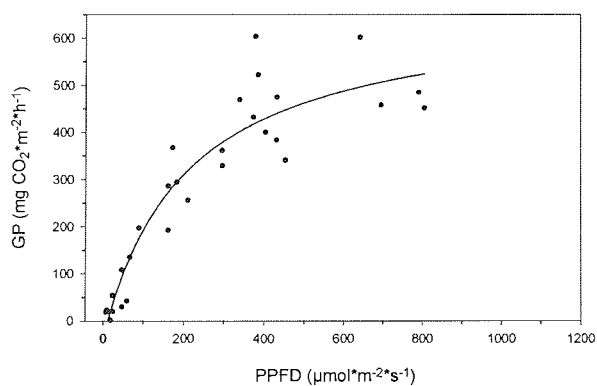


Fig. 4.2.27. Lightdependence of gross photosynthesis (GP) of the vascular plant community of the polygonal tundra, depression (PD). Calculated values and regression line, fitted with equation 9.

6 Discussion

6.1 Control of Soil Respiration in Tundra Systems

In tundra, huge carbon stocks are present in soils, in particular in organic surface layers (Everett 1981, Post *et al.* 1982, Gorham 1991). The thickness of the organic layers at the sites investigated in the scope of this study ranged from 5 to 17 cm, and showed relative carbon contents between 4.8 and 33.6 % DW. This adds to carbon contents of 15-25 kg*m⁻² (Gundelwein 1997), which appears comparable to studies on soil carbon of similar types of tundra in Alaska (Miller *et al.* 1983, Nadelhoffer 1997). Soil respiration is the process responsible for the release of carbon from this store to the atmosphere. The control of this process in different types of tundra and their microsites is an important factor for the understanding of the carbon balance of the tundra ecosystem (Billings *et al.* 1982, Oechel and Billings 1992). Spatial differences in the response of soil respiration to the controlling parameters reflect differences in the potential of sites to react to changes in their environment, e.g. in the scope of the anticipated climate change.

In this study, methods were applied allowing the correlation of soil respiration with the controlling parameters. The dynamic differential method of measuring gas-exchange *in situ* facilitated the making of a sufficient database to model the response of single sites to the controlling parameters. The obtained models served for drawing up response curves and for balancing of soil respiration. Furthermore, the approximated model parameters were used for correlation analysis of response characteristics with site characteristics of higher levels than directly included into the model. In the next paragraphs, spatial patterns of soil respiration quality and quantity will be discussed on the background of site characteristics.

Digression: components of soil respiration

The definition of the term soil respiration shall be clarified here. As Lundegård (1921) already defined, soil respiration is the CO₂ flux that can be measured at the soil-atmosphere interface, and that originates from microbial respiration as well as from root and rhizome respiration of vascular plants. In tundra and wetland studies, it furthermore includes the respiration of the (shaded) mosses (e.g. Peterson and Billings 1975, Billings *et al.* 1982, 1983, Pool and Miller 1982, Moore 1986, Moore and Knowles 1989, Oberbauer *et al.* 1991, 1992, 1996). Because soil and moss form a densely interwoven system in tundra, the removal of the mosses for the

purpose of measuring soil respiration would result in artificial CO₂ flux values (see chapter 3.1.2.1). While in the present study an attempt was made to achieve a more realistic interpretation of the contribution of the moss layer to the CO₂ efflux from the “soil system“ to the atmosphere (chapter 5.2), no differentiation could be made between microbial and root or rhizome respiration. However, the two latter processes are controlled by different factors than microbial respiration. While microbial respiration is an indicator of decomposition processes, root respiration reflects the effort of the plants to gather nutrients and to store carbon. Only a very restricted number of studies deal with estimating the contribution of root and rhizome respiration to soil respiration in tundra. The proportion of soil respiration accounted for by root and rhizome respiration has been estimated to range from 37 % (Flanagan and Bunnell 1981, from litter bag weight loss), over 30-70 % (Bunnell and Scouler 1975, model calculations), to 68 % (Billings *et al.* 1977, CO₂ gas exchange) in tundra. Lower contributions (below 20 %) of root and rhizome respiration to soil respiration were suggested by Oberbauer *et al.* (1992) in riparian tundra, based on modelling of microbial respiration measured in the laboratory. Their results were, however, based on assumptions that -critically viewed- change the real contribution of root and rhizome respiration to higher values.

Thus, root and rhizome respiration represents a considerable part of soil respiration in tundra systems. It has to be considered, that like in the case of soil and moss layer, also the separation from roots and rhizosphere for the purpose of measuring single CO₂ fluxes results in artificial values, since the function of both components is highly dependent on the structure of the intact system.

6.1.1 Microsite and Efflux Patterns

Previous studies have suggested that the controls of CO₂ efflux from wetland soils are complex and site specific (Peterson and Billings 1975, Billings *et al.* 1977, Svensson 1980, Luken and Billings 1985, Moore 1986). Also in this study, soil respiration rates showed wide differences between the tundra types and microsites investigated. Modelled daily means for the period July/August ranged from 2.6 g CO₂*m⁻²*d⁻¹ at the depression of the tussock tundra to 10.9 g CO₂*m⁻²*d⁻¹ at the tussock of the tussock tundra. These values are in the range of

Table 5.1. Literature review of (CO₂ gas exchanged based) field studies on soil respiration rates in tundra, and mean rates obtained in this study. (Values for Oberbauer *et al.* 1991, 1992, 1996 are means of July fluxes only).

site	microsite	soil respiration (g CO ₂ *m ⁻² *d ⁻¹)	source
tussock tundra, Southern Tundra zone, Taimyr Peninsula	tussock	10.9	this study
tussock tundra, Southern Tundra zone, Taimyr Peninsula	moss hummock	6.7	this study
tussock tundra, Southern Tundra zone, Taimyr Peninsula	depression	2.6	this study
wet sedge tundra, Southern Tundra zone, Taimyr Peninsula		4.0	this study
low centre polygonal tundra, Typical Tundra zone, Taimyr Peninsula	high apex	4.7	this study
low centre polygonal tundra, Typical Tundra zone, Taimyr Peninsula	low apex	4.3	this study
low centre polygonal tundra, Typical Tundra zone, Taimyr Peninsula	depression	3.8	this study
tussock tundra, northern foothills of the Brooks Range, Alaska	depression	5.0	Oberbauer et al. 1986
tussock tundra, northern foothills of the Philip Smith Mountains, Alaska		8.0	Oberbauer et al. 1991
water track tundra, northern foothills of the Philip Smith Mountains, Alaska		9.9	Oberbauer et al. 1991
riparian tundra, northern foothills of the Philip Smith Mountains, Alaska	Carex dominated	6.4	Oberbauer et al. 1992
riparian tundra, northern foothills of the Philip Smith Mountains, Alaska	Eriophorum dominated	5.0	Oberbauer et al. 1992
Cassiope dwarf-shrub heath, northern foothills of the Philip Smith Mountains, Alaska	moist	4.8	Oberbauer et al. 1996a
Cassiope dwarf-shrub heath, northern foothills of the Philip Smith Mountains, Alaska	dry	5.0	Oberbauer et al. 1996a

those from other studies in similar types of tundra (Table 5.1). The high value of the tussock in the tussock tundra of this study as compared to the values from Alaska may be due to very warm weather during field season at Lake Labaz (maximum soil temperatures at 2 cm depth at the tussock were up to 26°C).

Already the fact that the widest range of daily means in this study was observed in the same type of tundra, and within a distance of about 1 m, supports the theory that the greatest differences in CO₂ fluxes in wetlands occur on the microtopographic scale (Flanagan and Bunnell 1980, Waddington and Roulet 1996). No regular patterns were evident linking the observed CO₂ effluxes to the latitudinal gradient between Southern Arctic Tundra zone and Typical Arctic Tundra zone. The explanation for the wide range of soil respiration observed over the microtopographic scale is based on the combination of two facts. First, the correlation analysis clearly identified depth to water table and soil temperature at 2 cm depth to explain most of the variations observed in soil respiration. This was confirmed by the model quality and is in correspondence with other wetland studies (e.g. Svensson 1980, Peterson *et al.* 1984, Tenhunen *et al.* 1994, Oberbauer *et al.* 1996b). Second, the maximum differences in these parameters occurred on the microscale.

The highest rates of soil respiration were observed at sites with low water tables and high soil temperatures in the upper soil horizons (TT, TH, PL). The general pattern was furthermore that these two factors occurred in combination: A water table close to the soil surface caused lower temperatures in the uppermost horizons, whereas a lower water table permitted higher soil temperatures close to the soil surface. Consequently, the lowest soil respiration rates were observed at sites with high water table positions and the resulting lower soil temperatures (TD, WS, PD). Thus, the position of the water table at a site is the primary control of the magnitude of the CO₂ efflux from the soil, both directly and by affecting the soil temperature. There were, however, two exceptions from this general pattern. The wet sedge tundra (WS) showed the highest mean water table, but soil respiration rates were higher than at the depression of the tussock tundra with a slightly lower position of water table and an about comparable soil temperature range. This indicates between-site differences in the performance of the soil respiration process (see chapters 5.1.2, 5.1.3). The high apex of the polygonal tundra (PH) showed the by far lowest water table of all sites observed in this study, but soil respiration rates were only slightly higher as compared to the neighbouring low apex, with a water table about 20 cm higher. Efflux rates were also much lower than at the comparable site tussock of the tussock tundra with a mean water table position about 10 cm higher. This may

indicate that at this comparably dry site high apex, with an average water table position of below 30 cm, soil moisture was already limiting soil respiration. Oberbauer *et al.* (1991, 1996) have shown that such a limitation occurred during the second half of the growing season at tundra sites with low positions of the water table or with no observable water table. Silvola *et al.* (1996) observed the same pattern in boreal mires, when the water table dropped below 30-40 cm.

Another difference between sites refers to the diurnal course of soil respiration. Generally, the course of soil respiration followed the course of the soil temperature at 2 cm depth. Due to higher amplitudes of soil temperatures at 2 cm depth at sites with a low water table position (TT, TH), higher amplitudes of soil respiration occurred here. Sites with a constantly high position of the water table (TD, WS) showed only attenuated diurnal amplitudes, because of a restricted diurnal amplitude of soil temperatures. The latter effect is caused by the thermal buffer properties of water. The observed pattern is in correspondence with findings of Silvola *et al.* (1996) from boreal mires in Finland. In the present study, the absolute level on which the temperature induced oscillations of soil respiration occurred -as expressed by maxima and minima of soil respiration- was site specific as well. Minimum soil respiration rates at the tussock of the tussock tundra were only slightly lower than the maxima of the moss hummock, although the exposed tussock microsite showed the lowest observed minima in soil temperature at 2 cm depth. At sites with lower positions of the water table (TT, TH, PL) the absolute level of the oscillations caused by temperature was higher than at sites with higher positions of the water table (TD, WS, PD). This supports the theory of Oberbauer *et al.* (1992) that soil temperature is a factor which modifies the respiration rates permitted by prevailing water table in wet tundra types. The reason for this can be seen in the larger respiring soil volume which is available for respiration processes when the water table is at low positions (see chapter 5.1.2). Although effluxes were best correlated with the temperature at 2 cm depth, deeper soil horizons obviously contribute to the CO₂ efflux from tundra sites with low water tables as well.

6.1.2 The Factor Water Table

The position of the water table was the primary factor controlling soil respiration at the sites investigated in this study. This was clearly shown by the correlation analysis and the response curves derived from the soil respiration models. This result is in correspondence with other studies on soil respiration in wet tundra and bog systems (Billings *et al.* 1982, 1983, Peterson *et al.* 1984, Luken and Billings 1985, Moore 1989, Oberbauer *et al.* 1991, 1992, Ostendorf 1996). In this study, low water table positions resulted in higher CO₂ efflux rates, while water table positions close to the soil surface caused low CO₂ efflux rates. Billings *et al.* (1984) observed this effect in studies on tundra microcosms and presumed that the related controlling mechanism is oxygen diffusion limitation. These findings were supported by Whalen *et al.* (1996), who, based on micro-oxygen electrode measurements, suggests that moist tundra soils remain oxygenated to the water table with a rapid depletion of oxygen at or within 1 cm of the water table. Gebauer *et al.* (1996) found that the spatial variability of soil oxygen availability in tussock tundra and wet sedge tundra in Alaska was closely linked to the position of the water table and the physical properties of the involved soil horizons. The oxygen availability in less compact horizons (in particular organic horizons) was less strictly linked to the position of the water table, while water table changes in compact horizons (in particular mineral horizons) caused immediate changes in the availability of oxygen. This is in correspondence with the results of Flanagan and Veum (1974), who showed that organic horizons have higher oxygen content due to low bulk density and high aerated pore spaces. Peterson *et al.* (1984) showed that root respiration of the dominant vascular plants in tundra microcosms was not affected by the position of the water table indicating that it is rather the microbial population that is limited by low soil O₂ concentration.

It has been suggested that oxygen supply to microbes can be facilitated through plant roots (Armstrong 1967, Stuart *et al.* 1982). In this study, the occurrence of a red brown soil colour around vascular plant roots in deeper otherwise gleyic horizons e.g. of the wet sedge tundra, suggests that at least the microbes of the immediate rhizosphere may benefit from oxygen supply through plant roots. However, laboratory studies with oxygen-electrodes (Armstrong 1979, Flessa and Fischer 1992) have shown only very restricted effects, and field studies (Gebauer *et al.* 1996) have found no effect at all.

Thus, the high correlation of water table position and soil respiration rate observed in this study indicates the position of the water table to be a good predictor of soil aeration effects on

soil respiration. On the other hand, the soil respiration rates observed at the depression of the polygonal tundra (PD) suggest that even with positions of the water table above the soil surface considerable soil respiration rates of up to $100 \text{ mg CO}_2 \cdot \text{m}^{-2} \cdot \text{h}^{-1}$ may occur. This may be the share of the root and rhizome respiration. But also microbial respiration may occur under these conditions due to a combination of factors, like limited duration of flooding events (O_2 remaining in microenvironments of the soil), cold water temperatures (higher O_2 content of cold water), flowing water (constant O_2 supply), and probably also structure of the microbial community (more facultative anaerobic organisms at frequently flooded sites). The factor flowing water may in fact explain the higher soil respiration rates of the wet sedge tundra as compared to the depression of the tussock tundra with the same water table and soil temperatures.

The results of the laboratory experiments on the water table dependency of soil respiration (in microcosms) indicated that changes in soil respiration are most pronounced with water table changes closely below the soil surface. Changes of the water table position in deeper horizons do not alter the soil respiration rates much. With water table changes very close to or even above the soil surface, changes in soil respiration are less pronounced again. This is in correspondence with the results of Oberbauer *et al.* (1991) who found that soil moisture at the 0-5 cm depth was a better indicator of soil respiration than was soil moisture at greater depths. Furthermore, the results of both laboratory and field experiments showed that the response of soil respiration to depth to water table at all sites investigated can be very well expressed by an asymptotic function first introduced by Oberbauer *et al.* (1992). The application of a sigmoid function, which showed very high correlation coefficients for the laboratory data of this study as well, can be recommended for purposes with wider input ranges, like e.g. on the landscape scale. The function proved to be more robust to extrapolation.

Both models indicate the bulk of CO_2 released from the soils investigated to originate from the upper centimetres of the soil profile.

The response of soil respiration to water table differed between the sites investigated in this study. Permanently wet sites (TD, WS, PD) showed steeper response to water table changes as compared to the comparatively drier sites (TT, TH, PH). This is in correspondence with the results of Oberbauer *et al.* (1992), who, in a gradient study in riparian tundra in Alaska, also found steeper response of CO₂ efflux to changes in water table position towards the more waterlogged side of the transect. While Moore and Knowles (1989) and Oberbauer *et al.* (1991) assume these differences to be based on soil physical properties, in this study the correlation analysis suggests that steepness of soil respiration response to water table is determined by biological site characteristics. In detail, bacterial biomass of the uppermost soil horizons (0-2 cm, 2-5 cm), belowground biomass, and the seasonal ratio production / soil respiration, explained most of the between-site variations of the slope of the response to water table. This may indicate that the structure of the microbial community and the availability of carbon are the factors determining the steepness of the water table response of soil respiration. In a study on a toposequence of soils of the Imnavait watershed, Alaska, Cheng *et al.* (1996, c.f. Oberbauer *et al.* 1996b) found that carbon availability for microbial utilisation was higher at wet sites than at drier sites.

The drier sites of the present study were close to their level of insensitivity to water table changes at the range of positions observed in the field. However, even with water table positions up to 35 cm, soil respiration at the high apex of the polygonal tundra showed some response to changes of the water table, indicating the occurrence of soil respiration down to this depth. This is in contrast to the study of Oberbauer *et al.* (1992), who found that CO₂ efflux from riparian tundra was affected by decreasing water table only until depth to water table was about 10 cm. Silvola *et al.* (1996) suggested that in boreal mires in Finland soil respiration rates were not as much affected by changes in the position of the water table, if these changes occur below 20 cm depth. As indicated by the correlation analysis of the present study, the between-site pattern of the level of insensitivity to water table changes was linked to biological site characteristics. Apart from the bacterial biomass in the uppermost soil horizon (0-2 cm), differences in the level of insensitivity to water table changes were best explained by annual vascular plant production as well as aboveground and belowground biomass. This may indicate that besides the structure of the microbial community in particular the availability of carbon determines the level of insensitivity of soil respiration to water table changes.

From the described results, it can be concluded that the quantity, quality, and distribution of organic material as well as the related distribution of microbes in the soil profile determines a significant proportion of the patterns related to response of soil respiration to water table. Such relationships are suggested in decomposition studies from mires (e.g. Moore 1989, Szumigalski and Bayley 1996) and wet tundra types (e.g. Heal *et al.* 1981, Moorhead and Reynolds 1996). The final evaluation of the data set from the sites investigated in this project (e.g. fungal biomass, carbon fractionation) will probably complete the described patterns.

6.1.3 The Factor Temperature

Temperature has been frequently identified as a primary environmental control on soil respiration in tundra systems (Peterson and Billings 1975, Billings *et al.* 1977, Svensson 1980, Luken and Billings 1985, Moore 1986, Oberbauer *et al.* 1991, 1992, 1996), as was found in the present study. Although positive correlation between soil respiration and temperature has been shown in many studies (reviewed in Singh and Gupta 1977, Raich and Schlesinger 1992), there is no consensus on the type of the relationship. Linear (e.g. Witkamp 1966, Peterson and Billings 1975), exponential Arrhenius type (e.g. Howard and Howard 1979, Oberbauer *et al.* 1992), or even power relationships (Kucera and Kirkham 1971) have been used to describe the process. In this study, a principally exponential equation, which allows for a variable relative temperature sensitivity across the temperature range, was used to describe the temperature dependence of soil respiration (Lloyd and Taylor 1994). Besides the fact that the function provided a precise and unbiased explanation for the temperature induced variations of soil respiration, the option of a changing temperature sensitivity facilitated the revelation of additional patterns of temperature response (see below).

In the present study, the soil temperature at 2 cm depth served best to explain the temperature induced variations of soil respiration. The fact that soil temperatures close to the soil surface are better predictors of CO₂ efflux from tundra than soil temperatures of deeper horizons, is consensus in studies dealing with this topic (e.g. Peterson and Billings 1975, Billings *et al.* 1977, Svensson 1980, Luken and Billings 1985, Moore 1986, Oberbauer *et al.* 1991, 1992). This suggests that the majority of CO₂ released by soil respiration in tundra originates from the uppermost horizons. Billings *et al.* (1977) suggested that 60 to 80 % of the CO₂ efflux from soils at Barrow, Alaska, originates from the upper 5 cm of the soil.

The temperature response of soil respiration showed differences between the sites investigated. As with the response to depth to water table, the between-site differences in temperature response could not be attributed to the site position on the latitudinal gradient on Taimyr Peninsula, but to the position of the site in microrelief. The absolute level of temperature response was higher for the drier sites tussock and hummock of the tussock tundra (TT, TH), as well as for the high apex of the polygonal tundra (PH). According to what has been suggested in chapters 5.1.1 and 5.1.2, this pattern can be explained by the larger respiring soil volume of these sites. This theory is supported by the correlation analysis, which showed good correlation of the unbiased temperature response parameter (z) to the position of the water table. This would suggest the participation of deeper horizons in soil respiration at these sites. In a study on the quality of soil organic matter within the same project, Gundelwein (1997) suggests the occurrence of aerobic carbon turnover in these horizons from patterns obtained in XAD and density fractionation and lignin analysis.

The second pattern of temperature response is that the wet sites depression of the tussock tundra (TD), wet sedge tundra (WS), and the depression of the polygonal tundra (PD) showed steeper responses to temperature than did the drier sites. This indicates a greater temperature sensitivity of the soil respiration process at the wet sites. Moreover, the temperature sensitivity of soil respiration, as expressed by the Q_{10} , was not constant across the range of temperatures, but was greater at low temperatures than at high temperatures. Q_{10} values ranged from 1.2 at soil temperatures of 26°C to 3.4 at soil temperatures of 5°C. Similar patterns have been noted before (e.g. Slator 1906, Kanitz 1915, Kononova 1966, Flanagan and Veum 1974, Schleser 1982), yet were only rarely and recently considered in modelling studies of soil respiration or organic matter decomposition (Svensson 1980, Lloyd and Taylor 1992, Kirschbaum 1995, Kutsch and Kappen 1997). Lloyd and Taylor (1992) suggested that differences in the temperature response of different enzyme groups involved in the physiologically heterogeneous process of soil respiration cause differences in the temperature sensitivity of the process. Panikov (1997) showed that such patterns occur due to the response of different microbial populations with different life strategies or temperature adaptations. However, the findings of Oechel (1976), who observed higher Q_{10} values with decreasing temperatures in moss respiration, suggest that also a single species can show this pattern.

In the majority of studies mentioned, differences in the relative temperature sensitivity of different soils, microsites, or horizons at a given temperature have been attributed to methodological constraints or moisture limitations. Kirschbaum (1995) first assumed these

irregularities to reflect different inherent temperature sensitivities of different soils. Panikov (1997) suggested that differences in the trophic status of the environment may cause different relative temperature sensitivities. The use of individually fitted models for different microsites performed in the present study has revealed that the course of Q_{10} across the range of temperature can be attributed to site characteristics. The wet sites, depression of the tussock tundra (TD), wet sedge tundra (WS), and depression of the polygonal tundra (PD) showed the highest Q_{10} values as well as the sharpest decrease of Q_{10} with temperature. The drier sites tussock and hummock of the tussock tundra (TT, TH), as well as high and low apex of the polygonal tundra (PH, PL) showed lower Q_{10} values which were about constant across the temperature range observed. This observation is in correspondence with the results of Silvola *et al.* (1996), who found higher Q_{10} values at sites with water tables less than 20 cm below soil surface as compared to those sites with water tables below 20 cm depth. Svensson (1980) also observed higher Q_{10} values related to lower temperatures and higher soil moisture. He suggested that depletion of oxygen and oxygen diffusion rates limit soil respiration under these conditions. This may be an explanation for the results of this study as well, since low temperatures and high water tables occurred in combination at the wet sites investigated. The correlation analysis, however, revealed a clear pattern for Q_{10} values across the temperature range. Besides the significant correlation with the mean position of the water table, decreasing Q_{10} values with temperature were highly correlated with parameters indicating low composition capability, like the annual ratio of production / soil respiration and the carbon content of the uppermost horizon. This pattern suggests that high Q_{10} values at low temperatures can be explained by the availability of substrate in the uppermost soil layers, which immediately can be metabolized when the water table drops (and hence soil temperatures rise). This theory is supported by the findings of Silvola *et al.* (1985), who observed the greatest increase of soil respiration in drained peatland at sites with the poorly decomposed peats. Nadelhoffer *et al.* (1991) found that the quality of organic matter was even more important than soil temperature in controlling the rates of CO₂ efflux in a laboratory comparison of different arctic soils.

The Q_{10} values of the soil respiration process observed in this study (1.2 to 3.4) were representing the full range of what Raich and Schlesinger (1992) reported in a world-wide summary of soil respiration studies (1.3 to 3.3). Although the data base of this study is geographically limited, these corresponding ranges suggest the Q_{10} of soil respiration to be a site specific variable rather than a climate specific one.

6.1.4 Microsite and Soil Respiration Potential

Within the scope of the anticipated global warming, tundra areas are believed to be subject of the most pronounced changes (Solomon *et al.* 1985). The thermal and hydrological regimes of tundra soils are key factors determining the carbon balance of the tundra ecosystem (Maxwell 1992, Ostendorf *et al.* 1996), because they are the primary controls of CO₂ efflux from soils (Svensson 1980, Peterson *et al.* 1984, Tenhunen *et al.* 1994, Oberbauer *et al.* 1996b). The potential release of CO₂ from tundra soils would on the long-term result in a positive feedback on the global warming (Miller *et al.* 1983).

The potential of soil respiration to change in response to altered soil temperatures and water table positions showed wide differences between the investigated sites. The wet and cold sites (TD, WS, PD) showed the greatest relative changes of soil respiration rates to both altered soil temperatures and water table positions. In contrast, the drier and warmer sites (TT, TH, PH) showed nearly no changes of soil respiration rates with altered water table positions, and only small changes with altered soil temperatures. On the basis of what has been elaborated in the chapters 5.1.2 and 5.1.3, this pattern can readily be explained. With respect to changes of the water table position, the wet sites showed a current water table situated in the most sensible range of the water table response curve. Therefore, any change of the water table position had a maximum effect on CO₂ efflux from these sites. With respect to changes in soil temperature, the temperature sensitivity of soil respiration was higher at the wet sites than at the drier sites. Additionally, the relative temperature sensitivity of the soil respiration process at the wet sites was even higher at the comparatively colder temperatures which prevailed at these sites. The implication of these findings were clearly pointed out by Billings *et al.* (1982): any climate change that raises or lowers the water table will have profound effects on the magnitude of carbon loss in wet tundra systems, in particular in combination with increased soil temperatures.

In contrary, the drier sites showed water table positions at or close to their level of insensitivity to water table changes at the natural site. Consequently, changes in water table positions had no or very little effect on soil respiration rates at these sites. Temperature sensitivity of the soil respiration process, as expressed by the Q_{10} , was comparatively low. The

consequence was that altered temperature regimes did not change soil respiration rates as pronounced as at the wet sites.

Focusing on absolute instead of relative CO₂ efflux, the tussock of the tussock tundra (TT) showed the highest rates both with the original conditions as well as with all scenario calculations. The lowest absolute efflux rates with all but two scenarios were observed at the depression of the tussock tundra (TD). It is noteworthy, that the depression of the tussock tundra showed higher absolute CO₂ efflux rates than the dry site high apex of the polygonal tundra (PH), when the water table was lowered by 4 cm. The depression of the tussock tundra nearly doubled its CO₂ efflux rates with this scenario. This highlights the great potential of the wet sites also in terms of absolute efflux rates.

6.2 The Role of Moss Assimilation as a Buffer for CO₂ Effluxes from Tundra

Mosses represent an important growth form in tundra areas where they contribute significantly to biomass, production, and cover (Webber 1974, 1978, Rastorfer 1978, Hastings *et al.* 1989, Shaver and Chapin 1991). At the sites investigated in the scope of this study, moss coverage ranged from 71-100 %. In a sedge-moss meadow in Western Taimyr, for example, bryophytes comprise 91 % of the aboveground biomass (Wielgolaski, 1978). Chernov (1985) characterized the role of mosses in tundra to be the “environment-forming building-blocks of the vegetation“. The ground surface where mosses are found is an important interface controlling the transfer of energy and materials; thus mosses hold a key role as filters between the above- and belowground parts of the ecosystem as well as between ecosystem and atmosphere (Rosswall and Granhall 1980). Important aspects of tundra ecosystem function therefore depend on the physiological response, turnover, and production of mosses (Tenhunen *et al.* 1992). It was one aspect of this “filter“-mode of operation in the context of ecosystem function, that the moss investigations of this study focused on:

Soil and moss form a closely interwoven system in wet and humid tundra types (Everett *et al.* 1981). Moss photosynthesis can be regarded as a “filter“, reducing the CO₂ losses of the belowground parts of the system originating from soil respiration. Since soil and moss can hardly be separated without changing essential structural and microclimatic characteristics of both components, a method for analysis of the CO₂ fluxes of the structurally intact soil-moss system *in situ* was developed (see chapter 3.1.2.2) and successfully applied.

It is noteworthy to recall that there was no structural difference between the soil-moss system experiments and the soil respiration experiments. The only difference between both set-ups was that the mosses were unshaded for most of the time during the soil-moss system experiments.

6.2.1 Microsite and Moss Photosynthesis

Intrinsic Factors

The moss communities analysed in this study showed wide differences in their photosynthetic capacity with respect to maximum gross photosynthetic rate and light saturation levels.

At the wet and cold microsites at Lake Labaz, the depression of the tussock tundra (TD) and the wet sedge tundra (WS), the moss communities dominated by *Drepanocladus uncinatus* showed maximum photosynthetic rates below $100 \text{ mg CO}_2 \cdot \text{m}^{-2} \cdot \text{h}^{-1}$. Both moss communities achieved these maximum rates already at light levels below $100 \mu\text{mol} \cdot \text{m}^{-2} \cdot \text{s}^{-1}$ in combination with temperatures around 10°C . A maximum photosynthetic rate about twice as high was observed at the wet depression microsite of the polygonal tundra at Lake Levinson-Lessing (PD), dominated by the moss *Drepanocladus revolvens*. Light saturation was not achieved until $350 \mu\text{mol} \cdot \text{m}^{-2} \cdot \text{s}^{-1}$ at this site, most possibly due to moss temperatures up to 10°C higher than at the southern sites. Both moss communities of the drier microsites, the moss hummock of the tussock tundra (TH), as well as the low apex microsite of the polygonal tundra (PL), showed considerably higher maximum photosynthetic rates of $450 \text{ mg CO}_2 \cdot \text{m}^{-2} \cdot \text{h}^{-1}$, and $270 \text{ mg CO}_2 \cdot \text{m}^{-2} \cdot \text{h}^{-1}$, respectively. While the low apex microsite of the polygonal tundra, dominated by *Tomentypnum nitens*, achieved this value at light levels above $250 \mu\text{mol} \cdot \text{m}^{-2} \cdot \text{s}^{-1}$ in combination with temperatures between 10 and 13°C , the species of the moss hummock microsite of the tussock tundra, dominated by *Hylocomium splendens*, were light saturated at about $450 \mu\text{mol} \cdot \text{m}^{-2} \cdot \text{s}^{-1}$, presumably due to comparatively higher temperatures of up to 22°C .

Extrinsic Factors

Apart from the individual photosynthetic capacity, photosynthetic yield of the moss communities in this study was furthermore constrained by a number of microclimatic factors, whose combinations appeared to be site specific as well.

Water. In the scope of this study, the highest daily assimilation rates and the thickest mats of alive mosses were observed at the wet, but not waterlogged microsites TH and PL. Along a gradient of increasing water availability, moss biomass in tundra generally increases to a maximum at wet microsites, and decreases again towards the waterlogged microsites (Oechel and Sveinbjörnsson 1978, Hastings *et al.* 1989). This pattern is generally based on the poikylhydric character of the mosses, allowing no or only restricted morphological control on their water status, and thus being dependent on the availability of water during periods of photosynthetic activity. Mosses generally show a range of optimum water content for photosynthesis and a decrease of photosynthetic rates with decreasing water content until, at very low water contents, no gas exchange can be observed (e.g. Lee and Stewart 1971, Oechel and Collins 1976, Sveinbjörnsson and Oechel 1978). The water content of the mosses investigated in this study was found to be constantly high over the experimental periods, suggesting a sufficient water supply for the maintenance of photosynthetic rates at the natural site (Table 5.2). Generally, one can distinguish between two strategies of mosses in handling their water supply (summarized in Proctor 1982): In *endohydric* species, water is taken up from a substratum or underlying water table and conducted internally (by apoplastic or symplastic transport, or specialised empty conducting cells) to the photosynthetically most active parts. In *ectohydric* species, water is absorbed over the entire surface. In some cases, water can be moved upwards in external capillary spaces, like between adjacent shoots, between stem and leaf surface, or in papillae. In fact, both types represent extremes between which a range of intermediates can be found ("mixohydric").

All moss species investigated in this study were capable to use the soil water as water supply, as indicated by the maintenance of constantly high water contents independent of rain or dew events. The mosses of the depression microsites of tussock tundra and polygonal tundra, as well as of the wet sedge tundra, were mostly of ectohydric character (Collins 1977, Oechel and Sveinbjörnsson 1978). Although their photosynthetically most active tissues were situated some cm above the water table, they showed very high water contents in the field (Table 5.2). Thus, external conduction, as well as sorption and capillary effects of the intact moss layer seemed to result in water contents of the photosynthetic tissue that were generally much higher than the optimum water content for photosynthesis (WC_{opt}). Water contents of the species from the drier microsites, *Hylocomium splendens* (TH) and *Tomentypnum nitens* (PL), were considerably lower than those from the wetter microsites, but obviously still in the range of WC_{opt} . The observation that the uppermost parts of these mosses were situated about

4-10 cm above the water table, suggests the occurrence of an efficient water conduction in both species. While nothing is known about water conduction mechanisms in *Tomentypnum nitens*, previous studies on *Hylocomium splendens* have denied the possibility of effective water conduction in the field (Skre *et al.* 1983, Sonesson *et al.* 1992). Laboratory experiments, however, have shown that *Hylocomium splendens* can exhibit considerable values of external conduction (Mägdefrau 1935, recalculated in Proctor 1992), supporting the observations of the present study. The species co-occurring with *Hylocomium splendens* at the moss hummock microsite, *Polytrichum strictum*, represents a genus known to show the most effective endohydric conduction (Bazazz *et al.* 1970). In a study on moss species distribution in relation to mean water table, Bubier and Moore (1995) found *Polytrichum strictum* on average 35 cm above the water table. However, also in endohydric moss species, the water content of the photosynthetically most active tissue sharply decreases if the water table falls below a certain species dependent limit (Clymo and Hayward 1982), which was obviously not reached for the mosses of the present study.

Table 5.2. Literature review of optimum water contents (% DW) for assimilation (WC_{opt}) of some of the moss species investigated in this study, and range of water content as observed in the field (this study). Note that the water content of the mosses in this study is taken of a species mixture, of which the compared species was only a part.

species (microsite, this study)	WC field, this study (% DW)	WC_{opt} (% DW)	site	source
<i>Hylocomium splendens</i> (TH)	775	500-700	Abisko, Sweden	Sonesson <i>et al.</i> 1992
<i>Polytrichum strictum</i> (TH, TD)	775	200	Signy I., Antarctica	Collins 1977
<i>Tomentypnum nitens</i> (PL)	480-520	400-600	Alberta, Canada	Busby & Whitfield 1977
<i>Calliergon sarmentosum</i> (PD)	927-1054	600	Barrow, Alaska	Oechel & Collins 1976
<i>Drepanocladus revolvens</i> (PD)	927-1054			
<i>Drepanocladus uncinatus</i> (TD, WS)	934-1530	500	Signy I., Antarctica	Collins 1977

Many mosses show a decrease of photosynthetic rates at supra-optimal water contents (e.g. Oechel and Collins 1976, Dilks and Proctor 1979). This phenomenon, mainly caused by increasing diffusion resistance for CO₂ into and inside the moss tissue (Clayton-Greene *et al.* 1985), may be of importance for the photosynthetic rates of the mosses investigated in this study (see also below: CO₂-paragraph). Since the uppermost parts of the mosses at the wet microsites of the present study showed water contents two- or three times the value of WC_{opt}, photosynthetic rates were most likely below optimum. Oechel and Collins (1976) showed that the reduction of photosynthetic rate was about 10 % of maximum rate with a water content of about 200 % DW above WC_{opt} in *Calliergon sarmentosum*. Mosses of more mesic distribution, like *Politrichum alpinum* showed more pronounced reduction values in the same study. This suggests that also the comparatively lower supra-optimal water content observed with the mesic species *Hylocomium splendens* in the present study may have resulted in below optimum photosynthetic rates.

The measurement technique used in this study proved especially capable for maintaining the natural water conditions of the investigated species by examining the undisturbed moss carpet or cushion *in situ*. In any case, the water loss of intact colonies of mosses is widely restricted compared to single shoots (Gimingham and Smith 1971). Furthermore, the water supply during experimental periods is widely ensured, if the mosses stay in contact with their substratum, and/or neighbouring shoots.

Light. Along a gradient of increased water availability in tundra (see above: *Water*-paragraph), mosses progressively experience less light, due to a concomitant increase of the vascular plant canopy, which shades the moss layer (Oechel and Sveinbjörnsson 1978, Tenhunen *et al.* 1992, Tenhunen *et al.* 1994). At Lake Labaz, irradiance values at the mesic and more exposed moss hummock microsite (TH) ranged up to 1000 $\mu\text{mol}\cdot\text{m}^{-2}\cdot\text{s}^{-1}$, whereas irradiance showed a maximum of only 450 $\mu\text{mol}\cdot\text{m}^{-2}\cdot\text{s}^{-1}$ at the neighboured depression microsite (TD). The lowest maximum of PPFD (185 $\mu\text{mol}\cdot\text{m}^{-2}\cdot\text{s}^{-1}$) was observed in the wet sedge tundra, the wettest tundra type. Here, the highest aboveground vascular plant biomass was found, considerably shading the moss layer. In particular the moss species of the wet microsites investigated in this study (TD, WS) compensated for low light levels with high photosynthetic efficiency (i.e. a steep increase of photosynthetic rates already at low light levels) and low light saturation levels, a mechanism well known from other studies on the

light response of mosses from wet habitats (Kallio and Kärenlampi 1975, Collins 1977, Proctor 1981). In contrast, the light saturation level of the moss species from the moss hummock (TH) was much higher, with about 250-400 $\mu\text{mol}\cdot\text{m}^{-2}\cdot\text{s}^{-1}$ in combination with temperatures up to 22°C. The species, *Hylocomium splendens* and *Polytrichum strictum*, were thus capable to make use of the higher irradiance levels occurring at this microsite. At a subarctic birch forest site with irradiance levels rarely exceeding 200 $\mu\text{mol}\cdot\text{m}^{-2}\cdot\text{s}^{-1}$, Sonesson *et al.* (1992) found light saturation in *Hylocomium splendens* already at about 100 $\mu\text{mol}\cdot\text{m}^{-2}\cdot\text{s}^{-1}$. This indicates a wide adaptational range of the photosynthetic apparatus of this moss species to ambient conditions (but see also below: CO_2 paragraph), as has been observed in other moss species as well (Hickleton and Oechel 1976, Oechel and Sveinbjörnsson 1978).

Thus, mosses are able to achieve considerable photosynthetic rates even when situated below a canopy of vascular plants. Additionally, mosses even benefit from vascular plant cover to a certain extent: Moderate shading can reduce evaporation and thus maintain sufficient water content of mosses for assimilation over extended time periods (Clymo and Hayward 1982, Harley *et al.* 1989, Hastings *et al.* 1989, Murray *et al.* 1989a, Murray *et al.* 1989b).

The conditions in the polygonal tundra at Lake Levinson-Lessing were somewhat different to those of the Southern Tundra site. Due to the more scattered and lower vascular plant cover at the depression microsite of the polygonal tundra (PD, 85 %), as compared to the wet sedge tundra (WS, 109 %), maximum PPFD values near to 1200 $\mu\text{mol}\cdot\text{m}^{-2}\cdot\text{s}^{-1}$ were observed at the moss level during a clear day. Unlike the moss community at the wet depressions of the Southern Tundra sites (dominated by *Drepanocladus uncinatus*), the moss community at the depression of the polygonal tundra (dominated by *Drepanocladus revolvens*) achieved light saturation only at about 350 $\mu\text{mol}\cdot\text{m}^{-2}\cdot\text{s}^{-1}$. However, moss temperatures were about 20°C during experiments at the latter site, which was about 10°C higher than at the former sites. Light saturation values for both temperature ranges are in correspondence with observations on *Drepanocladus uncinatus* by Collins (1977). Thus, due to its photosynthetic characteristics, the moss community of the depression of the polygonal tundra (PD) could use the comparatively intense light conditions at their natural stand.

About the same comparatively high maximum irradiance values at moss level as at the depression were observed at the low apex microsite of the polygonal tundra (PL), which showed an even lower vascular plant cover (56 %) than the depression microsite. Since *Tomentypnum nitens*, the dominating moss species at this microsite, was light saturated at

about $270 \mu\text{mol}\cdot\text{m}^{-2}\cdot\text{s}^{-1}$ in combination with temperatures around 13°C , it was also able to benefit from the high irradiance level at its stand.

CO₂. The ambient absolute CO₂ concentration is a key factor for the photosynthesis of green plants through determining the level of assimilation rates. In the case of mosses, the role of the absolute CO₂ concentration for photosynthesis has to be discussed in particular from two points of view, the ambient CO₂ concentration of the mosses *in situ* (a), and the effect of increased CO₂ concentrations on the photosynthetic capacity of mosses (b).

(a) Several studies have shown the occurrence of CO₂ concentrations higher than the atmospheric ambient around the photosynthetically active sections of moss shoots (Silvola 1985, Sveinbjörnsson and Oechel 1992, Sonesson *et al.* 1992, Tarnawski *et al.* 1992). While in these studies it was only suggested that this CO₂ originates from soil respiration, the results of the present study clearly confirm this suggestions. In particular during periods when the net CO₂ flux of the soil-moss system was negative (i.e. a net efflux of CO₂ from the soil-moss system to the atmosphere), the immediate environment of the mosses can be expected to be considerably enriched in CO₂. Negative net CO₂ fluxes of the soil-moss system were observed during the majority of experimental periods of this study, resulting in a high potential of the mosses at most sites to benefit from the high CO₂ concentrations. The degree of enrichment, however, is dependent on the ratio soil respiration versus moss photosynthesis (the absolute magnitude of the net system flux). It has to be considered, though, that the intervals of positive net system fluxes, or of small negative rates of net system fluxes, respectively, were all observed during periods of otherwise favourable conditions for photosynthesis, mostly during early morning. This may limit the potential of the high CO₂ concentration for moss photosynthesis to shorter, but still considerable time periods at some microsites (e.g. PL). Wind is another factor reducing the absolute CO₂ concentrations in the immediate environment of the moss. Its influence on the dilution of CO₂ in the moss layer is controlled by wind speed (Silvola 1986) and boundary layer characteristics of the specific site as determined by its position in microrelief and the structure of the vascular plant canopy (Proctor 1984). Boundary layer characteristics have received little systematic studies, although there is evidence of its importance also in the context of evaporation (Gimingham and Smith 1971, Nobuhara 1979). Proctor (1980) suggests that evaporation from moss cushions sharply increases with the occurrence of wind speeds high enough to cause turbulences on the level of the moss shoots, a level dependent on surface roughness.

It is thus suggested that the diurnal course of the net CO₂ flux of the soil-moss system determines the ambient absolute CO₂ concentration of mosses *in situ*. The present study does not yield any absolute levels of this concentration, but the literature suggests that it ranges from about atmospheric ambient up to 3500 ppm (Table 5.3). However, the meaningfulness of these data may be limited, since all authors were working with air sample volumes probably too large to represent the air in the immediate vicinity of the moss shoots only.

Table 5.3. Literature review of absolute CO₂ concentration in the immediate environment of the photosynthetically active parts of mosses.

range of CO ₂ concentration (ppm)	cm below moss surface	source	species / site
350-1143	2	Sonesson <i>et al.</i> 1992	<i>Hylocomium splendens</i> , birch forest, northern Sweden
450-600	0	Silvola 1985	<i>Sphagnum</i> spp., central Finland
340-530	3	Sveinbjörnsson and Oechel 1992	<i>Pleurocium schreberii</i> , black spruce forest, central Alaska
600-3500	1	Tarnawski <i>et al.</i> 1992	<i>Grimmia antarctici</i> , Casey Station, Antarctica

(b) Most comprehensive studies on the photosynthesis of mosses have been carried out at “normal“ ambient CO₂ concentrations of about 350 ppm (e.g. Oechel and Sveinbjörnsson 1978, Johansson and Linder 1980), not considering the situation that mosses face concentrations higher than “normal“ ambient at their natural site. The results of this study clearly prompt to the need of a more field-orientated approach for measurements of moss photosynthesis considering the CO₂ factor. Due to the lack of absolute CO₂ concentration values in this study it is difficult to assess the photosynthetic capacity of the mosses investigated. From a limited base of literature it is clear that bryophytes are strongly CO₂ limited at ambient levels around 350 ppm and that saturation does not occur until about 2000 ppm during short term increase of CO₂ levels (Silvola 1985, Coxson and Mackey 1990, Adamson *et al.* 1990, Sonesson *et al.* 1992, Tenhunen *et al.* 1992). Referring to Green and Lange (1994), increased CO₂ concentrations will have three major effects on the photosynthesis of mosses. First, optimal temperatures for photosynthesis will increase. This can be favourable for the mosses at the more mesic microsites (TH, PL) of this study, which experience higher temperatures. Second, assimilation rates at PPF levels below light saturation will increase, a situation of which mosses below a canopy of vascular plants (e.g. WS in this study) can benefit. Third, higher PPF levels will be required for light saturation.

This effect, although probably also caused by the adaptational range of the species, can be seen in *Hylocomium splendens*, which showed a light saturation value about twice as high in this study as compared to a study of Sonesson *et al.* (1992) (see above: *Light*-paragraph). Additionally, the decrease of photosynthetic rates at supra-optimal water contents (see above; *Water*-paragraph) will not occur in combination with higher CO₂ concentrations (Silvola 1990). Since this effect is caused by the high diffusion resistance of the soaked thallus, higher CO₂ partial pressures can fasten the diffusion rates (Lange *et al.* 1984). This phenomenon can be of particular importance for the mosses of the wet microsites (TD, WS, PD) in this study, where an increased CO₂ concentration can counteract the negative effect of the very high water contents observed.

Temperature. Because of the very restricted temperature range observed during saturating light conditions in the field, not much can be said about differences in the temperature dependence of photosynthesis between the investigated moss communities. Moss temperatures were generally lower at wet microsites (TD, WS, PD) and higher at the more elevated microsites (TH, PL), as documented in the microclimatic characteristics of the experimental sites. However, at sites lacking extensive vascular plant cover like the depression of the polygonal tundra, moss temperatures could also rise up to 22°C occasionally. Response curves of assimilation rates to temperature are typically broad in mosses of polar distribution, and values range from 5 to 25°C in arctic mosses (Longton 1988). Moreover, optimum temperature range changes over the season within periods of several days, being highly dependent on the actual microclimate of the specific site (Oechel 1976, Oechel and Sveinbjörnsson 1978). The observation that the range of temperatures measured during experiments in this study match the range given in the literature suggests that the investigated mosses may have been at least in the range of their optimum temperature during experiments. On the other hand, the occurrence of scattered data around the level of maximum photosynthetic rates in the light response curves of some microsites (TH, PL, PD) indicates a considerable response of moss assimilation rates to temperature.

6.2.2 Microsite and Quantitative Aspects of Buffering

The relative daily reduction of the CO₂ efflux from soil and moss respiration by the gross photosynthesis of the mosses ranged between 35 and 99 % in this study. This result clearly shows the importance of moss photosynthesis in the context of tundra ecosystem CO₂ fluxes. The diurnal pattern and magnitudes of the CO₂ fluxes of the soil-moss systems observed in this study were similar to those modelled with the “Gas-Flux“-simulator for the tundra of the Imnavait Creek watershed, Alaska (Tenhunen *et al.* 1994). All soil-moss systems investigated in the present study showed a net loss of CO₂ to the atmosphere over the experimental periods. The absolute net system CO₂ losses of the soil-moss system ranged from 4650 mg CO₂*m⁻²*d⁻¹ at the moss hummock of the tussock tundra to 70 mg CO₂*m⁻²*d⁻¹ at the low apex of the polygonal tundra. This wide range occurred although the microclimatic conditions for both moss and soil at both of these microsites were comparable during the experimental periods. On the other hand, the net system flux observed at the very wet depression of the tussock tundra in the Southern Tundra zone was about the same as at the drier low apex site of the polygonal tundra in the Typical Tundra zone. This indicates the net CO₂ flux of the soil-moss system at the different microsites to be a site specific quantity, dependent on the individual ratio between soil respiration and moss photosynthesis.

The relative reduction of the CO₂ efflux from soil and moss respiration by the gross photosynthesis of the mosses showed no clear pattern as related to microclimatic site characteristics or magnitudes of the single CO₂ fluxes. It is obvious, however, that both fluxes, soil and moss respiration and moss photosynthesis, were in the same order of magnitude at each specific site, as expressed by the relative daily reduction values ranging from 35 -99 % between sites. Considering the ranges of daily soil and moss respiration rates (1900-9400 mg CO₂*m⁻²*d⁻¹) and gross moss photosynthesis (700-5600 mg CO₂*m⁻²*d⁻¹) between sites, the relative reduction values are fairly constant. Sites with high soil and moss respiration rates showed also high rates of moss photosynthesis, sites with low respiration rates achieved low photosynthetic yield.

One explanation for this pattern is based on the microclimate of the site: The multiple experiments performed at the same microsite identified the water table to have a large influence on the single CO₂ fluxes of the soil-moss system at a specific site. Soil respiration rates decreased with a rising water table, most substantially when the water table was closely

below the soil surface (see also chapter 5.1.2). However, besides this direct influence on soil respiration, a high water table also reduced the temperatures of the uppermost soil horizons as well as of the moss layer. Furthermore, the increased CO₂ concentration in the immediate environment of the moss will most probably be reduced due to lower CO₂ production by soil respiration (see above). Both factors led to a reduced photosynthetic yield of the mosses. Consequently, both contributors to the net CO₂ flux of the soil-moss system, soil respiration and moss photosynthesis, were reduced by a rising water table. The side to which the decrease was biased was dependent on the ratio between soil and moss temperature, and on the irradiance level of the very day in combination with the photosynthetic characteristics of the mosses. In the case of the two experiments at the low apex of the polygonal tundra, a higher water table resulted in a lower net CO₂ flux of the soil-moss system, whereas in the case of the experiments at the depression of the polygonal tundra a lower water table caused a lower net CO₂ flux.

Another reason for the relative similarity of soil respiration and moss photosynthesis at a specific site can be found in the species composition and the photosynthetic capacity of the moss communities: At the wet sites with low soil respiration rates, depression of the tussock tundra (TD), wet sedge tundra (WS), and depression of the polygonal tundra (PD), mosses with a low photosynthetic capacity occurred. The warmer and drier microsite with higher soil respiration rates, moss hummock of the tussock tundra (TH) and low apex of the polygonal tundra (PL), were covered by moss communities with higher photosynthetic capacity.

An important aspect of the soil-moss system in the context of ecosystem CO₂ fluxes is the position of the water table. As mentioned above, all mosses investigated in the scope of this study were capable to use the soil water as water supply. A lowering of the water table will result in an increase of both soil respiration rates and photosynthetic rates of the mosses (see above). The latter process, however, can only function as long as the mosses keep about their optimum water content. The water content of the photosynthetically most active tips of the moss shoots decreases sharply when the water table falls below a certain species dependent limit (Clymo and Hayward 1982). In this case, photosynthetic rates of most mosses will decrease sharply as well (e.g. Lee and Stewart 1971, Oechel and Collins 1976, Sveinbjörnsson and Oechel 1978). A lowering of the water table below a microsite-specific limit will thus have a double effect on the CO₂ fluxes of the soil-moss system. First, soil respiration rates will increase because of a larger respiring volume (see chapter 5.1.2). Second, the buffer

function of moss photosynthesis on the CO₂ efflux from soil respiration will be lost due to a ceasing of photosynthesis.

An additional aspect of the net CO₂ flux of the soil-moss system and the relative reduction of the CO₂ effluxes from the soil by the photosynthesis of the mosses is the recycling of carbon in the organic layer. In particular during periods of negative net CO₂ fluxes (i.e. a net efflux of CO₂ from the soil-moss system to the atmosphere), the predominant source of CO₂ for moss photosynthesis will be derived from soil respiration. The ratio of assimilated CO₂ originating from the atmosphere on one hand and soil respiration on the other hand will be determined by the magnitude of the net system flux (see also above), wind speed (Silvola 1986), and boundary layer characteristics of the site as determined by its position in microrelief and the structure of the vascular plant canopy. Systematic studies of this phenomenon have not been performed for moss carpets or turfs yet, but an estimate for the much more open structure of a deciduous forest based on isotopic ratios showed that the share of soil-respired carbon was 22 % in shade leaves of the lower tree canopy (Schleser and Jayasekera 1985). For the much denser structure of moss carpets and cushions an even higher share can be expected. This aspect has to be considered e.g. for dating the carbon age of peat profiles. In recent studies, decreasing carbon accumulation rates (as suggested by radiocarbon signals) in younger parts of profiles have been interpreted as a decrease of site productivity (e.g. Ikonen 1993, Kuhry and Vitt 1996). The findings of the present study suggest that this effect may also be based on the increased recycling of soil-respired carbon in a peat profile increasing in depth.

6.3 Tundra System CO₂ Fluxes: Contributions of the Subsystems

From the rather limited data base of “whole system“ CO₂ fluxes obtained in the scope of this study, only restricted conclusions can be drawn. The very wet site depression of the polygonal tundra was a strong sink for atmospheric carbon dioxide during the two diurnal experiments. Carbon was accumulated with rates of 1.3 and 1.6 g C*m⁻²*d⁻¹. This is in the range of the maximum daily accumulation rates Tenhunen *et al.* (1992) calculated for the tussock tundra of Imnavait Creek, Alaska.

The bulk of the CO₂ gain at the depression of the polygonal tundra was contributed by the photosynthesis of the vascular plants, 26 and 31 % of the total gain was due to moss photosynthesis. The regression suggests that vascular plant photosynthesis -mainly by *Carex stans* and *Dupontia fisheri*- was not light saturated until about 700 μmol*m⁻²*s⁻¹. However, the lack of leaf temperatures constrain the meaningfulness of these results. Oberbauer *et al.* (1996b) obtained *in situ* light saturation for *Carex bigelowii* at 15°C between 500 and 700 μmol*m⁻²*s⁻¹, which is in correspondence with several other studies on arctic vascular plants (Tieszen 1973, 1975, 1978b, Johnson and Tieszen 1976, Limbach *et al.* 1982, Semikhatova *et al.* 1992), and may also apply to the species investigated in this study. In any case, vascular plant photosynthesis saturated at higher irradiance levels as compared to moss photosynthesis, so that assimilation by the vascular plants can be constrained by overcast conditions (Tenhunen *et al.* 1994, 1995). The total daily PPFD values of both experiments were nevertheless too similar to deduce differences in assimilation rates from differences in irradiance. The theory of Semikhatova (1992) that about a quarter of the vascular plants' carbon gain in arctic areas may occur between 22:00 and 04:00 did clearly not apply for the late July and early August experiments of the present study, since photosynthetic rates of the vascular plants during these periods were almost negligible. The photosynthetic efficiency of the vascular plants was smaller than the one of the mosses (see chapter 5.2.1), resulting in a less steeper increase of vascular plant photosynthetic rates with light. This difference in response to low light levels explains the observation that moss photosynthetic rates exceeded those of vascular plants during nights. Another limiting factor to vascular plant photosynthesis is stomatal conductance. Diurnal observations of photosynthesis in tussock tundra in Alaska (Gebauer 1994) did not reveal significant stomatal closure. However, cold soil temperatures are known to cause decreases of stomatal conductance in high arctic plants (Dawson and Bliss

1989). This suggests that also at waterlogged sites, stomatal conductance may limit CO₂ uptake by vascular plants.

Aboveground vascular plant respiration accounted for only about 10 % of the whole system respiration at the depression of the polygonal tundra. This comparatively low value reflects the fact that in wet tundra systems 85 to 98 % of the biomass are belowground (Billings *et al.* 1977). The percentage of belowground biomass at the depression of the polygonal tundra was 98.3 % in this study, but no separation of living and dead roots was performed.

Moss photosynthesis had an important effect on the CO₂ efflux from the depression of the polygonal tundra, also with respect to whole system fluxes. The net system CO₂ flux of the soil-moss system was only slightly negative during two diurnal experiments, because 73 and 81 % of the CO₂ efflux originating from soil respiration was buffered by moss photosynthesis. The factor controlling the magnitude of net system CO₂ flux of the “whole system“ at the depression of the polygonal tundra was position of the water table. With a water table position at 1 cm below soil surface, the total carbon gain of the system was 1.6 g C*m⁻²*d⁻¹, whereas with a water table position of 4 cm below soil surface, only 1.3 g C*m⁻²*d⁻¹ was gained. The effect of water table induced variations in soil respiration on diurnal tundra net system flux may best be visualized as a shift of the zero line. The zero line, on which the carbon gain by assimilation can add on, decreases with lower water table positions (due to higher soil respiration rates), and increases with higher water table positions (due to lower soil respiration rates). Oberbauer *et al.* (1996b) showed these zero point shifts -due to changes in soil water table and soil temperature- to be in the same order of magnitude as day to day variations of assimilation rates -due to aboveground climatic effects. The observed pattern is also in correspondence with the findings of Tenhunen *et al.* (1992), who showed that changes in the net CO₂ system flux of tussock tundra in Alaska was best explained by changes in soil water table and irradiance.

Thus, overall diurnal carbon balance of wet tundra is depending on the interplay of irradiance, soil water table and soil temperature.

6.4 Tundra Carbon Budgets: a Matter of Scaling

The dependence of any description on the scale of the measurement is one of the fundamental paradoxes in physics, and applies for ecology in the same manner. The data presented and discussed here are based on a time scale of days and a spatial scale of square centimetres. Any conclusions that derive from upscaling these data are constrained by the fact that not the single process determines the final result but their system specific linking (Levin 1993, Belovsky 1994). Nevertheless, this section aims to outline a framework of factors which have to be considered in the scope of tundra carbon budgets, when the scale is shifted upwards both in space and time.

Scaling in space

The CO₂ efflux by soil respiration of the different tundra types was calculated on the basis of the representative area shares of the investigated microsites. The obtained values, however, have to be regarded as estimates, since they are based on the obviously critical assumption that the investigated microsites covered the whole range of heterogeneity of the particular tundra type. Nonetheless, the overall pattern obtained may comprise some hints on the CO₂ efflux of different types of tundra. Due to relatively small area shares, the high daily CO₂ effluxes of the dry microsites were widely attenuated, when looking at tundra types rather than microsites. All tundra types showed about similar carbon losses by CO₂ efflux, ranging from 1.1 g C*m⁻²*d⁻¹ (polygonal tundra, wet sedge tundra) to 1.6 g C*m⁻²*d⁻¹ (tussock tundra). The highest absolute CO₂ losses in terms of soil respiration were calculated for the tussock tundra both with original microclimatic conditions and with a set of scenarios comprising altered soil temperatures and positions of water table. However, the highest relative potential of soil respiration to change under altered microclimatic scenarios was calculated for the wet sedge tundra. With a scenario suggested to occur in tundra as a consequence of the anticipated climate change (Rowntree 1997), comprising a soil temperature at 2 cm depth increased by 4°C and a water table position lowered by 4 cm, daily CO₂ efflux rates of the wet sedge tundra more than doubled in the present study, whereas the efflux in tussock tundra increased by only 56 %. This is in contrast to a study of Oechel *et al.* (1993), who stated that tussock tundra has the highest potential for carbon loss under conditions likely to occur with the anticipated climate change. The explanation for the high potential of the wet sedge tundra bases on its homogeneously wet character, without intermittent drier areas. The potential of soil

respiration to change with water table position and temperature is greatest at wet sites (see chapter 5.1.4), and consequently, in tundra types with the largest wet area shares.

It was not the aim of this study to realistically predict landscape fluxes. The strong point of chamber measurements -as clearly pointed out in this study- is on the side of revealing patterns of single processes. Landscape fluxes can be best determined by eddy correlation techniques (e.g. Fan *et al.* 1995, Baldocchi *et al.* 1996), which are on the other side not appropriate for assigning patterns to single processes. Chamber studies within the fetches of eddy correlation towers (e.g. Nordstrøm and Sommerkorn, unpublished data) proved to perfectly complement each other.

Scaling in time

The data of this study were captured during the second half of the summer season. No seasonal changes of CO₂ fluxes could be found within the about three weeks experimental period. Several reasons for seasonal changes of CO₂ fluxes exist in tundra. With reference to soil respiration, the position of the frost table at the beginning of the summer season is suggested to affect CO₂ efflux from soils through the same mechanism as water table (Oberbauer *et al.* 1996b). At the end of the season, when a frozen layer forms at the soil surface, frost may affect CO₂ efflux by restricting diffusion from still unfrozen lower horizons to the atmosphere (Zimov *et al.* 1996). The availability of carbon for microbial processes is thought to be greatly enhanced early in the season, due to frost-cracking of organic matter aggregates during winter and concomitant low turnover rates (Flanagan and Bunnell 1980, Schimel and Clein 1996).

Until recently, any upscaling of CO₂ fluxes to an annual scale in arctic areas was limited by a lack of winter observations. It was thus not possible to calculate yearly budgets. Within the last years, effort was undertaken to close this gap of knowledge. The results indicate that winter CO₂ efflux from tundra is considerable. Although the total magnitude of fluxes is comparatively small (Zimov *et al.* 1993, 1996), extremely high Q_{10} values at temperatures below 0°C (Sommerkorn, unpublished data), and very long winter seasons, let winter (October to May) CO₂ effluxes become an estimated share of 61 and 80 % of the yearly CO₂ efflux from tussock tundra and wet sedge tundra, respectively (Oechel *et al.* 1997). Even if these estimates may be high, due to wide interpolated periods, the clear implication of the findings is that estimates of the CO₂ efflux from tundra systems calculated earlier profoundly underestimated gaseous carbon loss on the yearly basis. However, no winter data exist for the sites investigated in this project, due to the lack of permanent stations and logistics.

In terms of “whole system“ CO₂ fluxes, seasonal changes mainly refer to phenology. Photosynthetic CO₂ uptake during early season depends on biomass development, i.e. on LAI, of deciduous and graminoid species (Tenhunen *et al.* 1994, Hahn *et al.* 1996). Although Semikhatova *et al.* (1992) report evergreen arctic shrubs to emerge from the snow with photosynthetic rates near to their mid season maximum, other studies (Gebauer, unpublished, c.f. Oberbauer 1996b) show that during the first days following snow melt photosynthetic rates are low. At the end of the season, evergreen species maintain high photosynthetic rates, while those of deciduous and graminoid species were reduced as compared to those at mid season (Tieszen 1975). This observation is explained by leaf senescence or cold hardening (Defoliart *et al.* 1988). Vascular plants also have strong seasonal changes in above- and belowground activity that influence the CO₂ efflux rates (McNulty and Cummins 1987). Moore (1989) suggested that such phenological trends were responsible for strong seasonal changes in CO₂ efflux from fen sites.

The remarks made in this section show that predicting overall carbon budgets on the basis of summer CO₂ fluxes is extremely error-prone, in particular in tundra areas. The need of continuous year-round measurements of CO₂ fluxes is evident.

Estimating the response of tundra carbon budgets to long-term climatic changes has furthermore to consider nutrient availability and cycling (Nadelhoffer *et al.* 1992, Jonasson *et al.* 1993), nutrient competition between plants and microbes (Michelsen *et al.* 1995, Jonasson *et al.* 1996), quality of litter and soil organic matter decomposition (Nadelhoffer *et al.* 1997), productivity and production/biomass ratios of vascular plants (Oechel and Billings 1992), changes in the vegetation structure (Callaghan and Jonasson 1995, Chapin *et al.* 1997), the fate of the thermal insulating and CO₂ efflux buffering moss carpets (Tenhunen *et al.* 1992), and the fate of the organic soil horizons under altered thermal and hydrological regimes (Kane *et al.* 1992).

Shifts of ecosystem structure and function in response to climate changes will occur on the same axes as existing patterns and gradients (Tenhunen *et al.* 1992). Microsites comprise the long-term information of biotic and abiotic regimes within their structure and function. Therefore, the spatial variability of CO₂ fluxes, as expressed by the different microsites investigated in the present study, can also be understood as a link to future projections.

Other carbon losses

When estimating total carbon losses from wet tundra some additional processes has to be considered. First of all, methane production is a major microbial process in wetlands (Matthews and Fung 1987). Northern wetlands (i.e. wet tundra, mires, bogs, and fens, north of 60°N) contribute with about 20 % to the methane emissions world-wide (Vourlitis and Oechel 1997). At a depression of the polygonal tundra, directly adjacent to the experimental site of the present study, Gundelwein (1997) has measured mean daily methane emissions of 76 mg CH₄*m⁻²*d⁻¹, whereas already at the low apex a mean of only 3 mg CH₄*m⁻²*d⁻¹ was obtained. This accounts for 5.5 % and 0.2 % of the gaseous carbon losses by CO₂ at these sites, respectively. Methane emissions are a sum of two processes. The production of methane is strictly limited to anaerobic horizons, whereas in higher aerobic horizons methane is oxidized again (Christensen 1993). As pointed out in chapter 5.1.2, the anaerobic soil zone in wet tundra types is about identical with the horizons below the water table (Whalen *et al.* 1996). The mean water table position of about 11 cm below the soil surface at the low apex of the polygonal tundra obviously provided sufficient aerated volume to reduce the methane production at this site to very low emission rates. This suggests that considerable carbon loss by methane emissions can occur in the wet sedge tundra and the depression of the tussock tundra as well, but would probably not contribute to the carbon loss of both moss hummock and tussock of the tussock tundra.

Methane emissions are believed to occur also during winter, although probably with only very patchy distribution (Whalen and Reeburgh 1988, Samarkin *et al.* 1993).

The second process to consider when calculating carbon budgets in wet tundra types is the lateral loss of dissolved organic matter (Koprivnjak and Moore 1992), presumably in form of highly mobile fulvic acids (Gundelwein 1997), or carbohydrates leached from plant roots (Topp and Pattey 1997). Kling *et al.* (1991) calculated this effect to account for carbon losses in the range of 20 % of those by soil respiration in tundra regions, in particular in downslope areas (Johnson *et al.* 1996). During massive flooding events following spring ablation, also plant detritus can be exported to aquatic systems (Chapin *et al.* 1980).

An often ignored loss of carbon from the plant-soil system is through herbivore grazing, e.g. by microtines, geese, reindeers and musk-ox. While the impact of the ungulates on vegetation seems to be highly variable in space (White *et al.* 1981), the impact of the microtine population varies drastically from year to year (Batzli 1981). Consequently, the effect of herbivore grazing on tundra systems is hard to quantify.

7 References

- Adamson, E., Post, A. and Adamson, H. (1990): Photosynthesis in *Grimmia antarctici*, an endemic Antarctic bryophyte, is limited by carbon dioxide. *Current Research in Photosynthesis* 4, 639-642.
- Albertsen, M. (1977): *Labor- und Felduntersuchungen zum Gasaustausch zwischen Grundwasser und Atmosphäre über natürlichen und verunreinigten Grundwassern*. Dissertation an der Christian-Albrechts-Universität Kiel.
- Aleksandrova, V. D. (1980): *The Arctic and Antarctic: Their Division into Geobotanical Areas*. Cambridge University Press, Cambridge, 247 pp.
- Allen, T. F. H. and Hoekstra, T. W. (1990): The confusion between scale-defined levels and conventional levels of organization in ecology. *Journal of Vegetation Sciences* 1, 5-12.
- Anderson, J. P. E. and Domsch, K. H. (1978): A physiological method for the quantitative measurement of microbial biomass in soils. *Soil Biology and Biochemistry* 10, 215-221.
- Armstrong, W. (1967): The relationship between oxydation-reduction potentials and oxygen diffusion levels in some waterlogged organic soils. *Journal of Soil Science* 18, 27-34.
- Armstrong, W. (1979): Aeration in higher plants. *Advances in Botanical Research* 7, 225-332.
- Arrhenius, S. (1915): *Quantative Laws in Biological Chemistry*. Bell, London, 164 pp.
- Bab'yeva, I. P. and Chernov, I. Y. (1983): Yeasts in the tundra soil of the Taimyr Peninsula (translated from Pochvovedeniye No.10, 60-64, 1982). *Soviet Soil Science* 39-43.
- Baldocchi, D., Valentini, R., Running, S., Oechel, W. C. and Dahlman, R. (1996): Strategies for measuring and modelling carbon dioxide and water vapour fluxes over terrestrial ecosystems. *Global Change Biology* 2, 159-168.
- Barry, R. G., Courtin, G. M. and Labine, C. (1981): Tundra climates. In: Bliss, L. C., Heal, O. W. and Moore, J. J. (eds.), *Tundra Ecosystems: a Comparative Analysis*. Cambridge University Press, Cambridge, pp 81-114.
- Batzli, G. O. (1982): Populations and energetics of small mammals in the tundra ecosystem. In: Bliss, L. C., Heal, O. W. and Moore, J. J. (eds.), *Tundra Ecosystems: a Comparative Analysis*, Cambridge University Press, Cambridge, pp 377-396.
- Bazazz, F. A., Paolillo, D. J. and Jagels, R. H. (1970): Photosynthesis and respiration of forest and alpine populations of *Polytrichum juniperinum*. *Bryologist* 73, 579-585.
- Becker, H. (1997): *Untersuchungen zur Biomasse typischer Boden-Vegetations-Komplexe von Permafroststandorten des Levinson-Lessing See Gebietes, Sibirien*. Unveröffentlichte Diplomarbeit am Institut für Bodenkunde der Universität Hamburg.
- Belovsky, G. E. (1994): How good must models and data be in ecology? *Oecologia* 100, 475-480.
- Billings, W. D. (1997): Challenges for the future: Arctic and alpine ecosystems in a changigng world. In: Oechel, W. C., Callaghan, T. V., Gilmanov, T., Holten, J. I., Maxwell, B. Molau, U. and Sveinbjörnsson B. (eds.), *Global Change and Arctic Terrestrial Ecosystems* (Ecological Studies 124). Springer, New York, pp 1-18.
- Billings, W. D., Luken, J. O., Mortensen, D. A. and Peterson, K. M. (1982): Arctic tundra: A source or sink for atmospheric carbon dioxide in a changing environment? *Oecologia* 53, 7-11.
- Billings, W. D., Luken, J. O., Mortensen, D. A. and Peterson, K. M. (1983): Increasing atmospheric carbon dioxide: possible effects on arctic tundra. *Oecologia* 58, 286-289.

- Billings, W. D., Peterson, K. M., Luken, J. O. and Mortensen, D. A. (1984): Interaction of increasing atmospheric carbon dioxide and soil nitrogen on the carbon balance of tundra microcosms. *Oecologia* 65, 26-29.
- Billings, W. D., Peterson, K. M., Shaver, G. R. and Trent, A. W. (1977): Root growth, respiration, and carbon dioxide evolution in an arctic tundra soil. *Arctic and Alpine Research* 9 (2), 129-137.
- Bliss, L. C., Heal, O. W. and Moore, J. J. (eds.) (1981): *Tundra Ecosystems: a Comparative Analysis*. Cambridge University Press, Cambridge, 813 pp.
- Bolshiyarov, D. Y. and Anisimov, M. A. (1995): Geomorphological studies and landscape mapping. In: Siegert, C. and Bolshiyarov, D. Y. (eds.), *Russian-German Cooperation: the Expedition Taimyr 1994* (Reports on Polar Research 175). Alfred Wegener Institute for Polar and Marine Research, Bremerhaven, pp 9-13.
- Bolshiyarov, D. Y. and Hubberten, H. W. (eds.) (1996): Russian-German cooperation: The expedition Taimyr 1995 and the expedition Kolyma 1995 of the ISSP Pushchino group (*Reports on Polar Research* 211). Alfred Wegener Institute for Polar and Marine Research, Bremerhaven, 208 pp.
- Bölter, M., Möller, R. and Dzomla, W. (1993): Determination of bacterial biovolume with epifluorescence microscopy: Comparison of size distributions from image analysis and size classifications. *Micron* 24, 31-40.
- Brunckhorst, H. (1994): Middendorfs sibirische Reise mit ergänzenden Beiträgen. *Schriftenreihe Nationalpark Schleswig-Holsteinisches Wattenmeer* (Nr. 4), Tönning, 314 pp.
- Bubier, J. L. and Moore, T.R (1995): Predicting methane emission from bryophyte distribution in northern Canadian peatlands. *Ecology* 76 (3), 677-693.
- Bunnell, F. L. and Dowding, P. (1974): ABISKO - a generalized decomposition model for comparisons between tundra sites. In: Holding, A. J., Heal, O. W., MacLean, S. F. and Flanagan, P. W. (eds.), *Soil Organisms and Decomposition in Tundra*. IBP Tundra Biome Steering Committee, Stockholm, pp 227-247.
- Busby, J. R. and Whitfield, D. W. A., (1977): Water potential, water content, and net assimilation of some boreal forest mosses. *Canadian Journal of Botany* 56, 1551-1558.
- Cernusca, A. (1991): Ecosystem research on grassland in the Austrian Alps and in the central Caucasus. In: Esser, G., Overdieck, D. (eds.), *Modern Ecology: Basic and Applied Aspects*. Elsevier, Amsterdam, pp 233-271.
- Chapin, F. S. III, Hobbie, S. E. and Shaver, G. R. (1997): Impacts of global change on composition of arctic communities. In: Oechel, W. C., Callaghan, T. V., Gilmanov, T., Holten, J. I., Maxwell, B. Molau, U. and Sveinbjörnsson B. (eds.), *Global Change and Arctic Terrestrial Ecosystems* (Ecological Studies 124). Springer, New York, pp 221-228.
- Chapin III, F. S., Jefferies, R. L., Reynolds, J. F., Shaver, G. R. and Svoboda, J. (1992): Arctic plant physiological ecology in an ecosystem context. In: Chapin III, F. S., Jefferies, R. L., Reynolds, J. F., Shaver, G. R. and Svoboda, J. (eds.), *Arctic Ecosystems in a Changing Climate*. Academic Press, San Diego, pp 441-451.
- Chapin III, F. S., Miller, P. C., Billings, W. D. and Coyne P. I. (1980): Carbon and nutrient budgets and their control in coastal tundra. In: Brown, J., Miller, P. C., Tieszen, L. L. and Bunnell, F. L. (eds.), *An Arctic Ecosystem: The Coastal Tundra at Barrow, Alaska*. Dowden, Hutchinson and Ross, Stroudsburg, Pennsylvania, pp 458-544.

- Cheng, W., Virginia, R. A., Oberbauer, S. F., Tenhunen, J. D., Gillespie, C. T. and Reynolds, J. F. (1996): Spatial and temporal variation in soil nitrogen microbial biomass, and respiration in an arctic catena (submitted).
- Chernov, Y. I. (1985): *The Living Tundra*. Cambridge University Press, Cambridge, 213 pp.
- Christensen, T. R. (1993): Methane emissions from arctic tundra. *Biogeochemistry* 21, 117-139.
- Clayton-Green, K. A., Collins, N. J., Green, T. G. A. and Proctor, M. C. F. (1985): Surface wax structure and function in leaves of Polytrichaceae. *Journal of Bryology* 13, 549-562.
- Clymo, R. S. and Hayward, P. M. (1982): The ecology of Sphagnum. In: Smith, A. J. E. (ed.), *Bryophyte Ecology*. Chapman and Hall, London, pp 229-289.
- Collins, N. J., (1977): The growth of mosses in two contrasting communities in the maritime Antarctic: Measurement and prediction of net annual production. In: Llano, G. A. (ed.), *Adaptations within Antarctic Ecosystems*. Smithsonian Institution, Washington, pp 921-933.
- Coxson, D. S. and Mackey, R. L. (1990): Diel periodicity of photosynthetic response in the subalpine moss *Pohlia wahlenbergii*. *Bryologist* 93, 417-422.
- Crawford, R. M. M. (ed.) (1997): *Disturbance and Recovery in Arctic Lands*. Kluwer Academic Publisher, Dordrecht, 621 pp.
- Dahlman, R. C. (1985): Modelling needs for the predicted responses to CO₂ enrichment; plants, communities and ecosystems. *Ecological Modelling* 29, 77-106.
- Dawson, T. E. and Bliss, L. C. (1989): Intraspecific variation in the water relations of *Salix arctica*, an arctic-alpine dwarf willow. *Oecologia* 79, 322-331.
- de Jong, E. and Schappert, H. J. V. (1972): Calculation of soil respiration and activity from CO₂-profiles in the soil. *Soil Science* 113, 328-333.
- de Jong, E., Redman, R.E. and Ripley, E. A. (1979): A comparison of methods to measure soil respiration. *Soil Science* 127, 300-306.
- Defoliart, L. S., Griffith, M., Chapin III, F. S. and Jonasson, S. (1988): Seasonal patterns of photosynthesis and nutrient storage in *Eriophorum vaginatum* L., an arctic sedge. *Functional Ecology* 2, 185-194.
- Dennis, J. G. (1977): Distribution patterns of belowground standing crop in Arctic tundra at Barrow, Alaska. *Arctic and Alpine Research* 9 (2), 113-127.
- Dennis, J. G. and Johnson, P. L. (1970): Shoot and rhizome standing crops of tundra vegetation at Barrow, Alaska. *Arctic and Alpine Research* 2, 253-266.
- Dennis, J. G., Tieszen, L. L. and Vetter, M. A. (1978): Seasonal dynamics of above- and belowground production of vascular plants at Barrow, Alaska. In: Tieszen, L. L. (ed.), *Vegetation and Production Ecology of an Alaskan Arctic tundra* (Ecological Studies 29). Springer, New York, 113-140.
- Dickson Regional Administration (1993): Climatic Data of the Taimyr Lake Station (in Russian). Monthly reports of the Russian hydro-meteorological committee 1962-92.
- Dierßen, K. (1990): *Einführung in die Pflanzensoziologie (Vegetationskunde)*. Wissenschaftliche Buchgesellschaft, Darmstadt, 241 pp.
- Dilks, T. J. K. and Proctor, M. C. F. (1979) Photosynthesis, respiration and water content in bryophytes. *New Phytologist* 82, 97-114.
- Domsch, K. H. (1961): Bodenatmung - Sammelbericht über Methoden und Ergebnisse. *Zentralblatt für Bakteriologie, Mikrobiologie und Parasitenkunde* 116, 33-78.
- Eckener, H., Italiaander, R. (1979): *Im Luftschiff über Länder und Meere*. W. Heyne Verlag, München, 303 pp.

- Edwards, N. T. (1989): Impact of herbicides on soil ecosystems. *CRC Critical Reviews in Plant Sciences* 8 (3), 221-257.
- Edwards, N. T. and Sollins, P. (1973): Continuous measurement of carbon dioxide evolution from partitioned forest floor components. *Ecology* 54, 406-412.
- Everett, K. R., Vassiljevskaya, V. D., Brown, J. and Walker, B. D. (1981): Tundra and analogous soils. In: Bliss, L. C., Heal, O. W. and Moore, J. J. (eds.), *Tundra ecosystems: a comparative analysis*. Cambridge University Press, Cambridge, pp 139-179.
- Fagerström, T. (1987): On theory, data and mathematics in ecology. *Oikos* 50 (2), 258-261.
- Fan, S.-M., Goulden, M.L., Munger, J.W., Daube, B.C., Bakwin, P.S., Wofsy, S.C., Amthor, J.S., Fitzjarrald, D.R., Moore, K.E. and Moore, T.R. (1995): Environmental controls on the photosynthesis and respiration of a boreal lichen woodland: a growing season of whole-ecosystem exchange measurements by eddy correlation, *Oecologia* 102, 443-452.
- Fang, C. and Moncrieff, J.B. (1996): An improved dynamic chamber technique for measuring CO₂ efflux from the surface of soil. *Functional Ecology* 10, 297-305.
- Fisher, E. L., Leonov, V. N., Nikolskaya, M. V., Petrov, O. M., Ratsko, A. P., Sulerzhitskiy, L. d., Cherkasova, M. M. (1990): The late Pleistocene in the central part of the North Siberian Lowland. *Polar Geography and Geology* 14, 313-325.
- Flanagan, P. W. and Bunnell, F. L. (1980): Microflora activities and decomposition. In: Brown, J., Miller, P. C., Tieszen, L. L. and Bunnell, F. L. (eds.), *An Arctic Ecosystem: the Coastal Tundra at Barrow, Alaska*. Dowden, Hutchinson and Ross, Stroudsburg, Pennsylvania, pp 291-334.
- Flanagan, P. W. and Veum, A. K. (1974): The influence of temperature and moisture on decomposition processes in tundra. In: Holding, A. J., Heal, O. W., MacLean, S. F. and Flanagan, P. W. (eds.), *Soil Organisms and Decomposition in Tundra*. IBP Tundra Biome Steering Committee, Stockholm, pp 249-278.
- Flessa, H. and Fischer, W. R. (1992): Plant induced changes in the redox potential of rize rhizospheres. *Plant and Soil* 143, 55-60.
- Franz, H. J. (1973): *Physische Geographie der Sowjetunion*. VEB, Leipzig.
- Frercks, W. (1954): Die Bodenatmung als Mittel zur Erfassung der Mikroorganismen-tätigkeit in Moor- und Heidesandböden, ein neues Verfahren zu ihrer Bestimmung und erste Ergebnisse. *Zeitschrift für Pflanzenernährung, Düngung und Bodenkunde* 66, 39-54.
- Gebauer, R. L. E. (1994): The effect of waterlogging on photosynthesis, nutrient status and growth of the arctic species *Eriophorum vaginatum* and *Eriophorum angustifolium*. PhD Thesis, San Diego State University, San Diego and University of California, Davis.
- Gebauer, R. L. E., Tenhunen, J. D. and Reynolds, J. F. (1996): Soil aeration in relation to soil physiological properties, nitrogen availability, and root characteristics within an arctic watershed. *Plant and Soil* 178, 37-48.
- Gimingham, C. H. and Smith, R. I. L. (1971): Growth form and water relations of mosses in the maritime Antarctic. *British Antarctic Survey Bulletin* 25, 1-21.
- Gorham, E. (1991): Northern peatlands: Role in the carbon cycle and probable response to climate warming. *Ecological Applications* 1, 182-195.
- Gould, S. J. and Lewantin, R. C. (1979): The spandrels of San Marco and the Panglossian paradigm: A critique of the adaptationist programme. *Proc. R. Soc. London B.* 205, 581-598.

- Grönlund, E. and Melander O. (1995): *Swedish-Russian Tundra Ecology-Expedition '94. A cruise report*. Swedish Polar Research Secretariat, Stockholm, 462 pp.
- Grosswald, M. G. (1989): Last glaciation in Siberia: Palaeogeographical and geomorphological problems. In: Polar Geomorphology: Second International Conference on Geomorphology. Abstract and papers. Materialien und Manuskripte zum Studiengang Geographie an der Universität Bremen, Heft 17, pp 14-15.
- Grulke, N.E., Riechers, G.H., Oechel, W.C., Hjelm, U. and Jaeger, C. (1990): Carbon balance in tussock tundra under ambient and elevated atmospheric CO₂. *Oecologia* 83, 485-494.
- Gundelwein, A. (1997): *Eigenschaften und Umsetzung organischer Substanz in nordsibirischen Permafrostböden*. Dissertation an der Universität Hamburg, 159 pp.
- Gundelwein, A., Becker, H., Müller-Lupp, T., Schmidt, N. (1997): Soils. In: Melles, M., Hagedorn, B. and Bolshiyarov, D. Y.(eds.), *Russian-German Cooperation: the Expedition Taimyr / Severnaya Zemlya 1996* (Reports on Polar Research 237). Alfred Wegener Institute for Polar and Marine Research, Bremerhaven, pp 11-14.
- Haber, W. (1958): Ökologische Untersuchung der Bodenatmung. *Flora* 146, 109-156.
- Hahn, S. C., Oberbauer, S. F., Gebauer, R., Grulke, N. E., Lange, O. L. and Tenhunen, J. D. (1996): Vegetation structure and aboveground carbon and nutrient pools in the Imnavait Creek watershed. In: J.F. Reynolds and J.D. Tenhunen (eds.), *Landscape Function and Disturbance in Arctic Ecosystems* (Ecological Studies 120). Springer, Berlin, pp 109-128.
- Harley, P.C., Tenhunen, J.D., Murray, K.J. and Beyers, J. (1989): Irradiance and temperature effects on photosynthesis of tussock tundra Sphagnum mosses from foothills of the Philip Smith Mountains, Alaska. *Oecologia* 79, 251-259.
- Hastings, S. J., Luchessa, S. A., Oechel, W. C. and Tenhunen, J. D. (1989): Standing biomass and production in water drainages of the foothills of the Philip Smith Mountains, Alaska. *Holarctic Ecology* 12 (3), 304-311.
- Heal, O. W., Flanagan, P. W., French, D. D. and MacLean, S. F. Jr. (1981): Decomposition and accumulation of organic matter in tundra. In: Bliss, L. C., Heal, O. W. and Moore, J. J. (eds.), *Tundra Ecosystems: a Comparative Analysis*. Cambridge University Press, Cambridge, pp 587-633.
- Hickleton, P. R. and Oechel, W. C. (1976): Physiological aspects of the ecology of *Dicranum fuscescens* in the subarctic. I: Acclimation and acclimation potential of CO₂ exchange in relation to habitat, light, and temperature. *Canadian Journal of Botany* 54, 1104-1119.
- Hochachka, P. W. and Somero, G. N. (1984): *Biochemical Adaptations*, Princeton University Press, Princeton, New Jersey.
- Howard, J. A. and Howard, D. M. (1979): Respiration of decomposing litter in relation to temperature and moisture. *Oikos* 33, 457-465.
- Ignatenko, I. V. (1971): Soils of the main types of tundra biocenoses in the Western Taimyr. In: Tikhomirov, B. A. and Polosova T. G. (eds.), *Biogeocenoses of Taimyr Tundra and their Productivity* (Vol. 5). Nauka, Leningrad, pp 57-107.
- Ikonen, L. (1993): Holocene development and peat growth of the raised bog Pesänsuo in SW-Finland. *Geological Survey of Finland Bulletin* 370, 234-245.
- Isayeva, L. L. (1984): Late Pleistocene glaciation of North-Central Siberia. In: Velishko, A. A., Wright, H. E. and Barnosky, C. W.(eds.), *Late Quaternary Environments of the Soviet Union*. University of Minnesota Press, Minnesota, pp 21-30.
- Jarvis, P. G. (1993): Prospects for bottom-up models. In: Ehleringer, J. R., Field, C. B., *Scaling Physiological Processes: Leaf to Globe*. Academic Press, San Diego, California, pp 117-126.

- Jenkinson, D. S., Adams, D. E. and Wild, A. (1991): Model estimates of CO₂ emissions from soil in response to global warming. *Nature* 351, 304-306.
- Joergensen, S. E. (1988): *Fundamentals of Ecological Modelling*. Elsevier, Amsterdam, 391 pp.
- Johansson, L.-G. and Linder, S. (1980): Photosynthesis of Sphagnum in different microhabitats on a subarctic mire. In: Sonesson, M. (ed.), *Ecology of a Subarctic Mire* (Ecological Bulletins 30). Swedish Natural Science Research Council, Stockholm, pp 181-190.
- Johnson, D. A. and Tieszen, L. L. (1976): Aboveground biomass allocation, leaf growth, and photosynthesis patterns in tundra plant forms in arctic Alaska. *Oecologia* 24, 159-173.
- Johnson, L. C., Shaver, G. R., Giblin, A. E., Nadelhofer, K. J., Rastetter, E. R., Laundre, J. A. and Murray, J. L. (1996): Effects of drainage and temperature on the carbon balance of tussock tundra microcosms. *Oecologia* 108, 737-748.
- Jonasson, S., Havström, M., Jensen, M. and Callaghan, T.V. (1993): In situ mineralization of nitrogen and phosphorus of arctic soils after perturbations simulating climatic change. *Oecologia* 95, 179-186.
- Jonasson, S., Vestergaard, P., Jensen, M. and Michelsen, A. (1996): Effects of carbohydrate amendments on nutrient partitioning, plant and microbial performance of a grassland-shrub ecosystem. *Oikos* 75, 220-226.
- Kallio, P. and Kärenlampi, L. (1975): Photosynthesis in mosses and lichens. In: Cooper, J. P. (ed.), *Photosynthesis and Productivity in Different Environments*. Cambridge University Press, Cambridge, pp 393-423.
- Kane, D. L., Hinzman, L. D., Ming-ko Woo and Everett, K. R. (1992): Arctic hydrology and climate change. In: Chapin III, F. S., Jefferies, R. L., Reynolds, J. F., Shaver, G. R. and Svoboda, J. (eds.), *Arctic Ecosystems in a Changing Climate*. Academic Press, San Diego, pp 35-57.
- Kanitz, A. (1915): *Temperatur und Lebensvorgänge*. Gebrüder Bornträger, Berlin.
- Kappen, L., Sommerkorn, M. and Schroeter, B. (1995): Carbon acquisition and water relations of lichens in polar regions - potentials and limitations. *Lichenologist* 27 (6), 531-545.
- Kershaw, K. A. (1978): The role of lichen in boreal tundra transition areas. *Bryologist* 81, 294-306.
- Khain, V. E. (1985): *Geology of the USSR*. Beiträge zur regionalen Geologie der Erde, Bd. 17, Gebr. Bornträger, Berlin.
- Kirschbaum, M. U. F. (1995): The temperature dependence of soil organic matter decomposition, and the effect of global warming on soil organic storage. *Soil Biology and Biochemistry* 27 (6), 753-760.
- Kling, G. W., Kipphut, G. W., Miller, M. C. (1991): Arctic lakes and streams as gas conduits to the atmosphere: Implications for tundra carbon budgets. *Science* 251, 298-301.
- Koepf, H. (1951): Laufende Messung der Bodenatmung im Freiland. *Landwirtschaftliche Forschung* 4, 186-194.
- Koestler, A. (1967): *The Ghost in the Machine*. Regnery, Chicago, 284 pp.
- Kononova, M. M. (1966): *Soil Organic Matter: Its Nature, its Role in Soil Formation and in Soil Fertility*. Pergamon Press, Oxford.
- Koprivnjak, J.-F. and Moore, T. R. (1992): Sources, sinks, and fluxes of dissolved organic carbon in subarctic fen catchments. *Arctic and Alpine Research* 24 (3), 204-210.
- Kucera, C. and Kirkham, D. (1971): Soil respiration studies in tallgrass prairie in Missouri. *Ecology* 52, 912-915.

- Kuhry, P. and Vitt, D.H. (1996): Fossil carbon/nitrogen ratios as a measure of peat decomposition. *Ecology* 77 (1), 271-275.
- Kutsch, W. L. (1994): *Untersuchungen zur Bodenatmung zweier Ackerstandorte im Bereich der Bornhöveder Seenkette*. Dissertation an der Christian-Albrechts-Universität Kiel, 136 pp.
- Kutsch, W. L., Kappen, L. (1997): Aspects of carbon and nitrogen cycling in soils of the Bornhöved Lake district II. Modelling the influence of temperature increase on soil respiration and organic carbon content in arable soils under different management. *Biogeochemistry* 39, 207-224.
- Lange, O. L., Beyschlag, B., Meyer, A. and Tenhunen, J. D. (1984): Determination of the photosynthetic capacity of lichens in the field- a method for measurement of light response curves at saturating CO₂ conditions. *Flora* 175, 283-293.
- Lee, J. A. and Stewart, G. R. (1971): Dessication injury in mosses. I. Intraspecific differences in the effect of moisture stress on photosynthesis. *New Phytologist* 70, 1061-1068.
- Levin, S. A. (1993) Concepts of scale at the local level. In: Ehleringer, J. R., Field, C. B. (eds.), *Scaling Physiological Processes: Leaf to Globe*. Cambridge University Press, Cambridge, pp 7-19.
- Limbach, W. E., Oechel, W. C. and Lowell, W. (1982): Photosynthetic and respiratory responses to temperature and light of three Alaskan tundra growth forms. *Holarctic Ecology* 5, 150-157.
- Lloyd, J. and Taylor, J. A. (1994): On the temperature dependence of soil respiration. *Functional Ecology* 8, 315-323.
- Londo, G. (1975): De decimale schaal for vegetatiekundlige opnamen van permanente Kwadraten. *Gorteria* 7 (7), 101-106.
- Longton, R. E. (1988): *The Biology of Polar Bryophytes and Lichens*. Cambridge University Press, Cambridge, 391 pp.
- Luken, J. O. and Billings, W. D. (1985): The influence of microtopographic heterogeneity on carbon dioxide efflux from a subarctic bog. *Holarctic Ecology* 8 (4), 306-312.
- Lundegård (1924): *Der Kreislauf der Kohlensäure in der Natur*. Gustav Fischer Verlag, Jena, 308 pp.
- Mägdefrau, K. (1935): Untersuchungen über die Wasserversorgung des Gametophyten und Sporophyten der Laubmoose. *Botanische Zeitschrift* 29, 337-375.
- Matthews, E. and Fung, I. (1987): Methane emissions from natural wetlands: Global distribution, area, and environmental characteristics of sources. *Global Biogeochemical Cycles* 1 (1), 61-86.
- Matveyeva, N. V. (1971): Dynamics of thawing of the active layer in the tundra of the Western Taimyr. In: Tikhomirov, B. A. and Polosova T. G. (eds.), *Biogeocenoses of Taimyr Tundra and their Productivity*, Vol. 4. Nauka, Leningrad, pp 45-56.
- Matveyeva, N. V. (1994): Floristic classification and ecology of tundra vegetation of the Taimyr Peninsula, northern Siberia. *Journal of Vegetation Science* 5, 818-828.
- Matveyeva, N. V., Parinkina, O. M., Chernov, Y. I. (1975): Maria Pronchitsheva Bay, USSR. In: Rosswall, T. and Heal, O. W. (eds.), *Structure and Function of Tundra Ecosystems* (Ecological Bulletins 20). Swedish Natural Science Research Council, Stockholm, pp 61-72.
- Maxwell, B. (1992): Arctic climate: Potential for change under global warming. In: Chapin III, F. S., Jefferies, R. L., Reynolds, J. F., Shaver, G. R. and Svoboda, J. (eds.), *Arctic Ecosystems in a Changing Climate*. Academic Press, San Diego, pp 11-34.

- McNulty, A. K. and Cummins, W. R. (1987): The relation between respiration and temperature in leaves of the arctic plant *Saxifraga cernua*. *Plant, Cell, and Environment* 10, 319-325.
- Melles, M. (ed.) (1994): *The Expedition Norilsk / Taimyr 1993 and Bunger Oasis 1993/94 of the AWI Research Unit Potsdam* (Reports on Polar Research 148). Alfred Wegener Institute for Polar and Marine Research, Bremerhaven, 80 pp.
- Melles, M., Hagedorn, B., Bolshiyarov, D. Y. (eds.) (1997): *Russian-German Cooperation: The Expedition Taimyr / Severnaya Zemlya 1996* (Reports on Polar Research 237). Alfred Wegener Institute for Polar and Marine Research, Bremerhaven, 170 pp.
- Michelsen, A., Schmidt, I. K., Jonasson, S., Dighton, J., Jones, H. E. and Callaghan, T. V. (1995): Inhibition of growth, and effects on nutrient uptake of arctic graminoids by leaf extracts- allelopathy or resource competition between plants and microbes? *Oecologia* 103, 407-418.
- Miller, P. C., Kendall, R. and Oechel, W. C. (1983): Simulating carbon accumulation in northern ecosystems. *Simulation* 40, 119-131.
- Moore, T. R. (1986): Carbon dioxide evolution from subarctic peatlands in eastern Canada. *Arctic and Alpine Research*. 18 (2), 189-193.
- Moore, T. R. (1989): Plant production, decomposition, and carbon efflux in a subarctic patterned fen. *Arctic and Alpine Research* 21 (2), 156-162.
- Moore, T. R. and Knowles, R. (1989): The influence of water table levels on methane and carbon dioxide emissions from peatland soils. *Canadian Journal of Soil Science* 69, 33-38.
- Moorhead, D. L. and Reynolds, J. F. (1996): Modelling decomposition in arctic ecosystems. In: J. F. Reynolds and J. D. Tenhunen (eds.), *Landscape Function and Disturbance in Arctic Ecosystems* (Ecological Studies 120), Springer -Verlag, Berlin, pp 347-367.
- Müller, H. H., Prokosch, P. and Syroechkovsky, E. E. (1993): Naturschutzgebiete auf Taimyr. WWF, Oslo, 38 pp.
- Murray, K.J., Harley, P.C., Beyers, J., Walz, H. and Tenhunen, J.D. (1989a): Water content effects on photosynthetic response of Sphagnum mosses from the foothills of the Philip Smith Mountains, Alaska. *Oecologia* 79, 244-250.
- Murray, K. J., Tenhunen, J. D. and Kummerow, J. (1989b): Limitations on Sphagnum growth and net primary production in the foothills of the Philip Smith Mountains, Alaska. *Oecologia* 80, 256-262.
- Nadelhoffer, K. J., Giblin, A. E., Shaver, G. R. and Laundre, J. A. (1991): Effects of temperature and substrate quality on element mineralization in six arctic soils. *Ecology* 72 (1), 242-253.
- Nadelhoffer, K. J., Giblin, A. E., Shaver, G. R. and Linkins, A. E. (1992): Microbial processes and plant nutrient availability in arctic soils. In: Chapin III, F. S., Jefferies, R. L., Reynolds, J. F., Shaver, G. R. and Svoboda, J. (eds.), *Arctic Ecosystems in a Changing Climate*. Academic Press, San Diego, pp 281-300.
- Nadelhoffer, K. J., Shaver, G. R., Giblin, A. and Rastetter, E. B. (1997): Potential impacts of climate change on nutrient cycling, decomposition, and productivity in arctic ecosystems. In: Oechel, W. C., Callghan, T., Gilmanov, T., Holten, J. I., Maxwell, B., Molau, U. and Sveinbjörnsson, B. (eds.), *Global Change and Arctic Terrestrial Ecosystems* (Ecological Studies 124). Springer, New York, pp 349-364.

- Nadelhoffer, K. J., Shaver, G. R., Giblin, A. and Rastetter, E. B. (1997): Potential impacts of climate change on nutrient cycling, decomposition, and productivity in arctic ecosystems. In: Oechel, W. C., Callaghan, T. V., Gilmanov, T., Holten, J. I., Maxwell, B. Molau, U. and Sveinbjörnsson B. (eds.), *Global Change and Arctic Terrestrial Ecosystems* (Ecological Studies 124). Springer, New York, pp 349-364.
- Nobuhara, H. (1979): Relationship between the number of shoots in a cushion and transpiration in *Bryum argenteum*. *Proceedings of the Bryological Society of Japan* 2, 91-92.
- Norin, B. N. and Ignatenko, I. V. (1975): Ary-Mas, USSR. In: Rosswall, T. and Heal, O. W. (eds.), *Structure and Function of Tundra Ecosystems* (Ecological Bulletins 20), Swedish Natural Science Research Council, Stockholm, pp 183-191.
- Nowak, E. (1995): Zum Naturschutz auf Taimyr zum Beginn der 90er Jahre. *Corax* 16, 187-203.
- Oberbauer, S. F., Cheng, W., Gillespie, C. T., Ostendorf, B., Sala, A., Gebauer, R., Virginia, R. A. and Tenhunen, J. D. (1996b), Landscape patterns of carbon dioxide exchange in tundra ecosystems. In: J. F. Reynolds and J. D. Tenhunen (eds.), *Landscape Function and Disturbance in Arctic Ecosystems* (Ecological Studies 120). Springer Verlag, Berlin, pp 223-256.
- Oberbauer, S. F., Gillespie, C. T., Cheng, W., Gebauer, R., Sala Serra, A. and Tenhunen, J. D. (1992): Environmental effects on CO₂ efflux from riparian tundra in the northern foothills of the Brooks Range, Alaska, USA. *Oecologia* 92, 568-577.
- Oberbauer, S. F., Gillespie, C. T., Cheng, W., Sala, A., Gebauer, R. and Tenhunen, J. D., (1996a): Diurnal and seasonal patterns of ecosystem CO₂ efflux from upland tundra in the foothills of the Brooks Range, Alaska, U.S.A.. *Arctic and Alpine Research* 28 (3), 328-338.
- Oberbauer, S. F., Oechel, W. C. and Riechers, G. H. (1986): Soil respiration of Alaskan tundra at elevated atmospheric carbon dioxide concentrations. *Plant and Soil* 96, 145-148.
- Oberbauer, S. F., Tenhunen, J. D. and Reynolds, J. F. (1991): Environmental effects on CO₂ efflux from water track and tussock tundra in arctic Alaska, U.S.A.. *Arctic and Alpine Research* 23 (2), 162-169.
- Oechel, W. C. (1976): Seasonal patterns of temperature response of CO₂ flux and acclimation in arctic mosses growing *in situ*. *Photosynthetica* 10, 447-456.
- Oechel, W. C. and Billings, W. D. (1992): Effects of global change on the carbon balance of arctic plants and ecosystems. In: Chapin III, F. S., Jefferies, R. L., Reynolds, J. F., Shaver, G. R. and Svoboda, J. (eds.), *Arctic Ecosystems in a Changing Climate*. Academic Press, San Diego, pp 139-168.
- Oechel, W. C., Callaghan, T. V., Gilmanov, T., Holten, J. I., Maxwell, B. Molau, U. and Sveinbjörnsson B. (eds.) (1997): *Global Change and Arctic Terrestrial Ecosystems* (Ecological Studies 124). Springer, New York, 493 pp.
- Oechel, W. C. and Collins, N. J. (1976): Comparative CO₂ exchange patterns in mosses from two tundra habitats at Barrow, Alaska. *Canadian Journal of Botany* 54, 1355-1369.
- Oechel, W. C. and Lawrence, W.T. (1985): Taiga. In: Chabot, B. F., Mooney, H. A. (eds.), *Physiological Ecology of North American Plant Communities*. Chapman and Hall, New York, pp 66-94.
- Oechel, W. C. and Sveinbjörnsson, B. (1978): Primary production processes in Arctic bryophytes at Barrow, Alaska. In: Tieszen, L. L. (ed.), *Vegetation and Production Ecology of an Alaskan Arctic Tundra*. Springer, New York, pp 269-298.

- Oechel, W. C., Hastings, S. J., Vourlitis, G., Jenkins, M., Reichers, G. and Grulke, N. (1993): Recent change of arctic tundra ecosystems from a net carbon dioxide sink to a source. *Nature* 361, 520-523.
- Oechel, W. C., Reichers, G., Lawrence, W. T., Prudhomme, T. I., Grulke, N. and Hastings, S.J. (1992): 'CO2LT' an automated, null-balance system for studying the effects of elevated CO₂ and global climate change on unmanaged ecosystems. *Functional Ecology* 6, 86-100.
- Oechel, W. C., Vourlitis, G. and Hastings, S. J. (1997): Cold season CO₂ emission from arctic soils. *Global Biogeochemical Cycles* 11 (2), 163-172.
- Ostendorf, B. (1996): Modelling the influence of hydrological processes on spatial and temporal patterns of CO₂ soil efflux from an arctic tundra catchment. *Arctic and Alpine Research* 28 (3), 318-327.
- Ostendorf, B., Quinn, P., Beven, K. and Tenhunen, J. D. (1996): Hydrological controls on ecosystem gas exchange in an arctic landscape. In: J. F. Reynolds and J. D. Tenhunen (eds.), *Landscape Function and Disturbance in Arctic Ecosystems* (Ecological Studies 120). Springer, Berlin, pp 370-386.
- Panikov, N. S. (1997): A kinetic approach to microbial ecology in arctic and boreal ecosystems in relation to global change. In: Oechel, W. C., Callaghan, T. V., Gilmanov, T., Holten, J. I., Maxwell, B. Molau, U. and Sveinbjörnsson B. (eds.), *Global Change and Arctic Terrestrial Ecosystems* (Ecological Studies 124). Springer, New York, pp 171-188.
- Parinkina, O. M. and Dokuchayev V. V. (1979): Decomposition of plant litter and cellulose in the tundra of the Taimyr Peninsula (translated from Pochvovedeniye No.11, 47-55, 1978). *Soviet Soil Science*, 676-684.
- Parkinson, K. J. (1981): An improved method for measuring soil respiration in the field. *Journal of Applied Ecology* 18, 221-228.
- Peterson, K. M. and Billings, W. D. (1975): Carbon dioxide flux from tundra soils and vegetation as related to temperature at Barrow, Alaska. *American Midland Naturalist* 94, 88-98.
- Peterson, K. M., Billings, W. D. and Reynolds, D. N. (1984): Influence of water table and atmospheric CO₂ concentration on the carbon balance of arctic tundra. *Arctic and Alpine Research* 16 (3), 331-335.
- Pfeiffer, E. M. and Hartmann, J. (1995): Characterisation of the organic matter in permafrost-affected soils. In: Siegert, C. and Bolshiyarov, D. Y. (eds.), *Russian-German Cooperation: the Expedition Taimyr 1994* (Reports on Polar Research 175). Alfred Wegener Institute for Polar and Marine Research, Bremerhaven, pp 36-41.
- Pfeiffer, E. M., Gundelwein, A., Nöthen, T., Becker, H. and Guggenberger, G. (1996): Characterization of the organic matter in permafrost soils and sediments of the Taimyr Peninsula, Siberia and Severnaya Zemlya, Arctic region. In: Bolshiyarov, D. Y., and Hubberten, H. W. (eds.), *Russian-German Cooperation: The Expedition Taimyr 1995 and the Expedition Kolyma 1995 of the ISSP Pushchino Group* (Reports on Polar Research 211). Alfred Wegener Institute for Polar and Marine Research, Bremerhaven, pp 46-63.
- Poole, D. K. and Miller, P. C. (1982): Carbon dioxide flux from three arctic tundra types in north-central Alaska, U.S.A.. *Arctic and Alpine Research* 14 (1), 27-32.
- Post, W. M., Emanuel, W. R., Zinke, P. J. and Stangenberger, A. G. (1982): Soil carbon pools and world life zones. *Nature* 298, 156-159.

- Post, W. M., Pastor, J., Zinke, P. J. and Strangenberger, A. B. (1985): Global patterns of soil nitrogen. *Nature*, 316, 616-617.
- Precht, H., Christophersen, J., Hensel, H., Larcher, W. (eds.) (1977): *Temperature and Life*. Springer, Berlin, 779 pp.
- Proctor, M. C. F. (1981): Physiological ecology of bryophytes. *Advances in Bryology* 1, 79-166.
- Proctor, M. C. F. (1982): Physiological ecology: water relations, light and temperature responses, carbon balance. In: Smith, A. J. E. (ed.), *Bryophyte Ecology*. Chapman and Hall, London, 333-381.
- Proctor, M.C.F. (1984): The experimental biology of Bryophyllum. 2. Structure and ecological adaptation. In: A.F. Dyer and J.G. Duckett (eds.), *Experimental Botany. An International Series of Monographs*. Academic Press, London, pp 9-37.
- Prokosch, P. (1995): Idee und Planung des Großen Arktis-Reservats. *Corax* 16, 208-212.
- Raich, J. W. and Schlesinger, W.H. (1992): The global carbon dioxide flux in soil respiration and its relationship to vegetation and climate. *Tellus* 44 (B), 81-99.
- Rastorfer, J. R. (1978): Composition and bryomass of the mosslayers of two wet-tundra-meadow communities near Barrow, Alaska. In: Tieszen, L. L. (ed.), *Vegetation and Production Ecology of an Alaskan Arctic Tundra*. Springer, New York, pp 169-183.
- Reynolds, J. F. and Acock, B. (1985): Predicting the response of plants to increasing carbon dioxide: A critique of plant growth models. *Ecological Modelling* 29, 107-129.
- Reynolds, J. F., Hilbert, D. W. and Kemp, P. R. (1993): Scaling ecophysiology from the plant to the ecosystem: A conceptual framework. In: Ehleringer, J. R., Field, C. B. (eds.), *Scaling Physiological Processes: Leaf to Globe*. Academic Press, San Diego, pp 127-140.
- Reynolds, J. F. and Tenhunen, J. D. (eds.) (1996): *Landscape Function and Disturbance in Arctic Ecosystems* (Ecological Studies 120). Springer, New York.
- Reynolds, J. F., Tenhunen, J. D., Leadley, P. W., Li, H., Moorhead, D. L., Ostendorf, B. and Chapin III, F. S. (1996): Patch and landscape models of arctic tundra: potentials and limitations. In: J. F. Reynolds and J. D. Tenhunen (eds.), *Landscape Function and Disturbance in Arctic Ecosystems* (Ecological Studies 120). Springer, Berlin, pp 293-324.
- Rieger, S. (1974): Arctic soils. In: Ives, J. D. and Barry, R. G. (eds.), *Arctic and Alpine Environments*. Methuen, London, pp 749-769.
- Romanenko, F. A. (1996): Relief of eastern foothills of the Byrranga range (a case of the Pronchischey Lake Northern coast, Taimyr). *Journal of Geomorphology (RAS)* 2, 93-99.
- Romell, L.G. (1922): Luftväxlingen i marken som ekologisk faktor. *Medd. Statens Skogsforsöksanstalt* 19, 2-10.
- Rosswall, T. and Granhall, U. (1980): Nitrogen cycling in a subarctic ombrotrophic mire. In: Sonesson, M. (ed.), *Ecology of a Subarctic Mire* (Ecological Bulletins 30). Swedish Natural Science Research Council, Stockholm, pp 209-234.
- Rosswall, T. and Heal, O. W. (eds.) (1975): *Structure and Function of Tundra Ecosystems* (Ecological Bulletins 20). Swedish Natural Science Research Council, Stockholm, 450 pp.
- Rowntree, P. R. (1997): Global and regional patterns of climate change: recent predictions for the Arctic. In: Oechel, W. C., Callaghan, T. V., Gilmanov, T., Holtén, J. I., Maxwell, B. Molau, U. and Sveinbjörnsson B. (eds.), *Global Change and Arctic Terrestrial Ecosystems* (Ecological Studies 124). Springer, New York, pp 82-109.

- Sachs, L. (1984): *Angewandte Statistik* (6. Auflage). Springer, Berlin, 552 pp.
- Safronova, I. N. and Sokolova, M. V. (1989): Comparative characteristics of four floras of the Byrranga Mountains (Taimyr) (in Russian). *Botanicheski Zhurnal* 74 (5), 718-731.
- Samarkin, V. A., Rivkina, E. M., Fedorov-Davidov, D. G. and Vecherskaya, M. S. (1993): CO₂ and CH₄ emissions of cryosols and subsoil permafrost and possible global climate change. Abstracts of the Symposium on Soil Processes and Management Systems, Greenhouse Gas Emissions and Carbon Sequestration, Columbus, Ohio, April 5-9, 1993.
- Samoilov, A. G. (1995): *Bowels of Taimyr Peninsula*. Norilsk, 203 pp.
- Schimel, J. P. and Clein, J. S. (1996): Microbial response to freeze-thaw cycles in tundra and taiga soils. *Soil Biology and Biochemistry* 28 (8), 1061-1066.
- Schleser, G. H. (1982): The response of CO₂ evolution from soils to global temperature changes. *Zeitschrift für Naturforschung* 27, 297-291.
- Schleser, G.H. and Jayasekera, R. (1985): d¹³C-variations of leaves in forests as an indication of reassimilated CO₂ from the soil. *Oecologia* 65, 536-542.
- Semikhatova, O. A., Gerasimenko, T. V. and Ivanova, T. I. (1992): Photosynthesis, respiration, and growth of plants in the Soviet Arctic. In: Chapin III, F. S., Jefferies, R. L., Reynolds, J. F., Shaver, G. R. and Svoboda, J. (eds.), *Arctic Ecosystems in a Changing Climate*. Academic Press, San Diego, pp 169-192.
- Šestak, Z., Catský, J. and Jarvis P. G. (1971): *Plant photosynthetic production, manual of methods*. Dr. W. Junk N. V., The Hague, 818 pp.
- Shaver, G. R. (1996): Integrated system research in Northern Alaska, 1947-1994. In: Reynolds, J. F. and Tenhunen, J. D. (eds.), *Landscape Function and Disturbance in Arctic Ecosystems* (Ecological Studies 120). Springer, Berlin, pp 19-34.
- Shaver, G. R. and Chapin, F. S. III (1991): Production:biomass relationships and element cycling in contrasting arctic vegetation types. *Ecological Monographs* 61, 1-31.
- Siegert, C. and Bolshiyarov, D.Y. (ed.) (1995): *Russian-German Cooperation: The Expedition Taimyr 1994* (Reports on Polar Research 175). Alfred Wegener Institute for Polar and Marine Research, Bremerhaven, 91 pp.
- Silvola, J. (1985): CO₂ dependance of photosynthesis in certain forest and peat mosses and simulated photosynthesis at various actual and hypothetical CO₂ concentrations. *Lindbergia* 11, 86-93.
- Silvola, J. (1986): Carbon dioxide dynamics in mires reclaimed for forestry in eastern Finland. *Annales Botanici Fennici* 23, 59-67.
- Silvola, J. (1990): Combined effects of varying water content and CO₂ concentration on photosynthesis in *Sphagnum fuscum*. *Holarctic Ecology* 13 (3), 224-228.
- Silvola, J., Välijoki, J. and Aaltonen, H. (1985): Effect of draining and fertilization on soil respiration at three ameliorated peatland sites. *Acta For. Fenn.* 191, 1-32.
- Singh, J. S. and Gupta, S. R. (1977): Plant decomposition and soil respiration in terrestrial ecosystems. *The Botanical Review* 43 (4), 449-528.
- Skre, O., Oechel, W. C. and Miller, P. M. (1983): Moss leaf water content and solar radiation at the moss surface in a mature black spruce forest in central Alaska. *Canadian Journal of Forestry Research* 13, 860-868.
- Slator, A. (1906): Studies in fermentation I. The chemical dynamics of alcoholic fermentation by yeast. *Journal of the Chemical Society* 89, 136-142.
- Solomon, A. M., Trabalka, J. R., Raichle, D. E. and Vorhees, E. D. (1985): The global cycle of carbon. In: Trabalka, J. R. (ed.), *Atmospheric Carbon Dioxide and the Global Carbon Cycle*. Nat. Tech. Info. Serv., Springfield, pp 1-13.

- Sommerkorn, M. (1995): Microbial communities and carbon turnover. In: Siegert, C. and Bolshiyarov, D. (eds.), *Russian-German Cooperation: The Expedition Taimyr 1994* (Reports on Polar Research 175). Alfred Wegener Institute for Polar and Marine Research, Bremerhaven, pp 41-52.
- Sommerkorn, M. (1996): Labaz Lake. In: Bolshiyarov, D. Y., and Hubberten, H. W. (eds.), *Russian-German Cooperation: The Expedition Taimyr 1995 and the Expedition Kolyma 1995 of the ISSP Pushchino Group* (Reports on Polar Research 211). Alfred Wegener Institute for Polar and Marine Research, Bremerhaven, pp 64-72.
- Sonesson, M., Gehrke, C. and Tjus, M. (1992): CO₂ environment, microclimate, and photosynthetic characteristics of the moss *Hylocomium splendens* in a subarctic habitat. *Oecologia* 92, 23-29.
- Spearman, W. (1904): The proof and measurement of association between two things. *American Journal of Psychology* 15, 72-101.
- Stuart, L., Oberbauer, S. and Miller, P. C. (1982): Evapotranspiration measurements in *Eriophorum vaginatum* tussock tundra in Alaska. *Holarctic Ecology* 5, 145-149.
- Sveinbjörnsson, B. and Oechel, W. C. (1992): Controls on growth and productivity of bryophytes: environmental limitations under current and anticipated conditions. In: Bates, J. W. and Farmer, A. M. (eds.), *Bryophytes and Lichens in a Changing Environment*. Clarendon Press, Oxford, pp 77-102.
- Svensson, B. H. (1980): Carbon dioxide and methane fluxes from the ombrotrophic parts of a subarctic mire. In: Sonesson, M. (ed.), *Ecology of a Subarctic Mire* (Ecological Bulletins 30). Swedish Natural Science Research Council, Stockholm, pp 235-250.
- Szumigalski, A.R. and Bayley, S.E. (1996): Decomposition along a bog to rich fen gradient in central Alberta, Canada. *Canadian Journal of Botany* 74, 573-581.
- Tarnawski, M., Melik, D., Roser, D., Adamson, E., Adamson, H. and Seppelt, R. (1992): In situ CO₂ levels in cushion and turf forms of *Grimmia antarctici* at Casey Station, East Antarctica. *Journal of Bryology* 17, 241-249.
- Tenhunen, J. D., Gillespie, C. T., Oberbauer, S. F., Sala, A. and Whalen, S. C. (1995): Climate effects on the carbon balance of tussock tundra in the Philip Smith Mountains, Alaska. *Flora* 190, 273-283.
- Tenhunen, J. D., Lange, O. L., Hahn, S., Siegwolf, R. and Oberbauer, S. F. (1992): The ecosystem role of poikilohydric tundra plants. In: Chapin III, F. S., Jefferies, R. L., Reynolds, J. F., Shaver, G. R. and Svoboda, J. (eds.), *Arctic Ecosystems in a Changing Climate*. Academic Press, San Diego, pp 213-237.
- Tenhunen, J. D., Siegwolf, R. T. W. and Oberbauer, S. F. (1994): Effects of phenology, physiology, and gradients in community composition, structure, and microclimate on tundra ecosystem CO₂ exchange. In: Schulze, E. D., Caldwell, M. M. (eds.), *Ecophysiology of Photosynthesis* (Ecological Studies 120). Springer, New York, 431-460.
- Tieszen, L. L. (1973): Photosynthesis and respiration in arctic tundra grasses: field light intensity and temperature responses. *Arctic and Alpine Research* 5, 239-251.
- Tieszen, L. L. (1975): CO₂ exchange in the Alaskan arctic tundra: Seasonal changes in the rate of photosynthesis of four species. *Photosynthetica* 9, 376-390.
- Tieszen, L. L. (ed.) (1978a): *Vegetation and Production Ecology of an Alaskan Arctic Tundra* (Ecological Studies 29). Springer, New York, 686 pp.

- Tieszen, L. L. (1978b): Photosynthesis in the principal Barrow, Alaska, species: a summary of field and laboratory responses. In: Tieszen, L. L. (ed.), *Vegetation and Production Ecology of an Alaskan Arctic Tundra* (Ecological Studies 29). Springer, New York, 241-268.
- Tikhomirov, B. A., Shamurin, V. F. and Aleksandrova, V. D. (1981): Phytomass and primary production of tundra communities, USSR. In: Bliss, L. C., Heal, O. W. and Moore, J. J. (eds.), *Tundra Ecosystems: a Comparative Analysis*. Cambridge University Press, Cambridge, pp 227-238.
- Topp, E. and Pattey, E. (1997): Soils as sources and sinks for atmospheric methane. *Canadian Journal of Soil Science* 77 (2), 167-178.
- Vasilyevskaya, V. D., Karavayev, N. A., Bogatyrev, L. G. and Ivanov, V. V. (1975): Agapa, USSR. In: Rosswall, T. and Heal, O. W. (eds.), *Structure and Function of Tundra Ecosystems* (Ecological Bulletins 20). Swedish Natural Science Research Council, Stockholm, pp 141-158.
- Vernikosky, V. A. (1996): Petrology and geochemistry of Taimyr riphean ophiolites. *Journal of Geology and Geophysics* 37 (1), 113-129.
- Vourlitis, G. L. and Oechel, W. C. (1997): The role of northern ecosystems in the global methane budget. In: Oechel, W. C., Callaghan, T. V., Gilmanov, T., Holten, J. I., Maxwell, B. Molau, U. and Sveinbjörnsson B. (eds.), *Global Change and Arctic Terrestrial Ecosystems* (Ecological Studies 124). Springer, New York, pp 266-289.
- Waddington, J.M. and Roulet, N.T. (1996): Atmosphere-wetland carbon exchanges: Scale dependency of CO₂ and CH₄ exchange on the developmental topography of a peatland. *Global Biogeochemical Cycles* 10 (2), 233-245.
- Walter, W. and Breckle, S. W. (1986): *Ökologie der Erde: Spezielle Ökologie der gemäßigten und arktischen Zonen Euro-Nordasiens* (Bd. 3). G. Fischer Verlag, Stuttgart, 587 pp.
- Washburn, A. L. (1979): *Geocryology. A survey of periglacial processes and environments*. Edward Arnold, London.
- Webber, P. J. (1978): Spatial and temporal variation of the vegetation and its production, Barrow, Alaska. In: Tieszen, L. L. (ed.), *Vegetation and Production Ecology of an Alaskan Arctic Tundra*. Springer, New York, pp 37-112.
- Whalen, S.C. and Reeburgh, W.S. (1988): A methane flux time series for tundra environments. *Global Biogeochemical Cycles* 2 (4), 399-409.
- Whalen, S. C., Reeburgh, W. S., Reimers, C. E. (1996): Control of methane emissions by microbial oxidation. In: Reynolds, J. F. and Tenhunen, J. D. (eds.), *Landscape Function and Disturbance in Arctic Ecosystems* (Ecological Studies 120). Springer, Berlin, pp 257-274.
- White, R. G., Bunnell, F. L., Gaare, E., Skogland, T. and Hubert, B. (1981): Ungulates on arctic ranges. In: Bliss, L. C., Heal, O. W. and Moore, J. J. (eds.), *Tundra Ecosystems: a Comparative Analysis*. Cambridge University Press, Cambridge, pp 397-483.
- Williams, P J., Smith, M. W. (1989): *The Frozen Earth: Fundamentals of Geocryology*. Cambridge University Press, Cambridge.
- Witkamp, M. (1966): Decomposition of leaf litter in relation to environment, microflora and microbial respiration, *Ecology* 47, 194-201.
- Witkamp, M. and Frank, M. L. (1969): Evolution of CO₂ from litter, humus and subsoil of a pine-stand. *Pedobiologia* 9, 358-365.
- Woodwell, D. M. and Dykeman, W. R. (1969): Respiration of a forest measured by carbon dioxide accumulation during temperature inversion. *Science* 154, 1031-1034.

- Wötzel, J. (1993): *Untersuchungen zur Freilandmessung der Bodenatmung mit dem dynamischen Verfahren*. Unveröffentlichte Diplomarbeit an der Christian-Albrechts-University Kiel, 81 pp.
- Yurtsev, B. A. (1994): Floristic division of the Arctic. *Journal of Vegetation Sciences* 5, 765-776.
- Zimov, S.A., Davidov, S.P., Voropaev, Y.V., Prosiannikov, S.F., Semiletov, I.P., Chapin, M.C. and Chapin, F.S. (1996): Siberian CO₂ efflux in winter as a CO₂ source and cause of seasonality in atmospheric CO₂. *Climatic Change* 33, 111-120.
- Zimov, S. A., Zimova, G. M., Davidov, S. P., Davidova, A. I., Voropaev, Y. V., Voropaeva, Z. V., Prosiannikov, S. F., and Prosiannikova, O. V. (1993): Winter biotic activity and production of CO₂ in Siberian soils: A factor in the greenhouse effect. *Journal of Geophysical Research* 98 (D3), 5017-5023.

Acknowledgements

During the past four years, many people and organizations have contributed to the realization of the research project presented in this dissertation. I wish to express my thanks to all of them.

The study was part of the multi-disciplinary German-Russian project "Environmental development of Central Siberia during Late Quaternary", involving the Alfred Wegener Institute of Polar and Marine Research, Potsdam, the Institute of Soil Science, University of Hamburg, the Institute for Polar Ecology, University of Kiel, as well as the Institute for Arctic and Antarctic Research, St. Petersburg. Research funds were provided by the German Ministry of Science and Technology (grant 03PLO14B).

I would like to express my sincere thanks to my Professor Dr. Ludger Kappen and to Priv.-Doz. Dr. Manfred Bölter, for their encouraging support and guidance and, most importantly, for leaving me the intellectual and financial space to develop and realize my own ideas. Their attitude to treat me as a colleague made this research fun and was a source of motivation for me.

My most special thanks go to my partner, Lis Sufke, who stood my months-long expeditions without complaints. Without your encouragement, your (admittedly not always pleasant but obviously necessary) kicks, and your skilfulness to organize life and manage children, this thesis would not be finished by now!

Organizing expeditions to Siberia in the middle of the 1990's requires an enormous amount of energy and patience. I wish to express my greatest thanks to those who made it possible for us to carry out these expeditions. In particular Dima Bolshiyarov and Mischa Anisimov from the Arctic and Antarctic Research Institute, St. Petersburg, but also the involved doctorate students and research assistants at the Alfred-Wegener-Institute, Potsdam, need to be mentioned at this place.

During three expeditions to Siberia, the breathtaking hospitality of the Russian people sometimes embarrassed us. My thanks are expressed -deputising for all our hosts- to Irina Kuzmina, who accommodated us in St. Petersburg during the long and hot days of custom negotiations in 1994 and 1995. At this place I also wish to thank Mischa Zhurbenko, who confirmed my lichen and vascular plant specimens, and who furthermore showed the St. Petersburg way of life to me.

I want to direct my thanks to the Dolgan people of the Lake Labaz region, in particular to the family of Aleksander and Avgusta Popov. The warm welcome they had in store for us in their land, and the offer to get insights into their way of life was an outstanding experience for me.

Living in field camps in the Arctic for months under sometimes adverse conditions demands more social attitudes of the participants than just the will to work together. I therefore wish to thank the following people for companionship and help in the field: Jens Hartmann, Julia Boike, Pier Paul Overduin, Dorothea Gintz, Sascha Derevyagin, Christine Siegert, Gerald Vannahme, Thomas Nöthen, Jenja Troshin, Nicole Schmidt, Birgit Hagedorn, Holger Becker, Thomas Müller-Lupp, Tobias Ebel, and Volodya Samarkin. My warmest thanks go to Andre Ivanov and his guitar. It was fun to share the Siberian experience with all of you.

During the field stays and the evaluation phase it was a great pleasure to cooperate with Andreas Gundelwein from the Institute of Soil Science in Hamburg. Thank you for the fruitful collaboration!

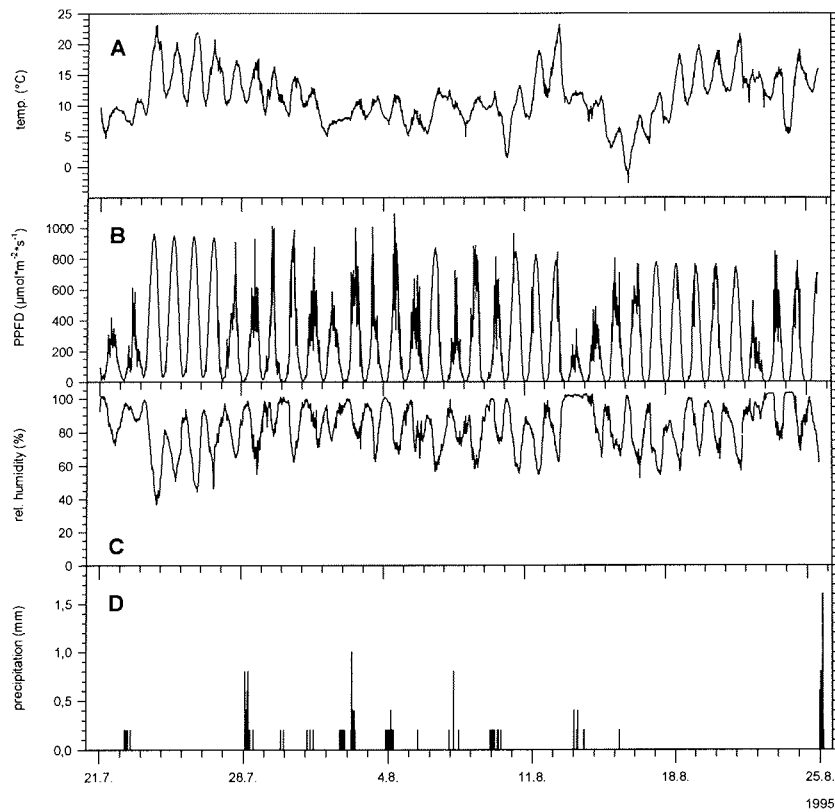
The warm and friendly atmosphere at the Institute of Polar Ecology in Kiel made everyday work easy for me. I am therefore grateful to all my colleagues. My particular thanks are directed to Florian Schulz, who helped me determining my moss specimens, and who furthermore had the talent to hit the critical points in methodological discussions. Without the qualified help of our technician Frank-Peter Rapp, the whole heap of technical equipment required for this study would have been nice to look at in the technical descriptions instead of being ready for the next field season. Thank you eF-Pi, what would I have done without you? Barbro Winkler, my office colleague, is particularly thanked for standing my numerous bad habits and giving the proper comments “from the background“. Dorothea Stübing is kindly thanked for her endurance in literature work.

Gratitude is furthermore expressed to Dr. Werner Kutsch for giving critical comments on an earlier version of the manuscript. Furthermore, this study benefited from valuable discussions with him during the early stages. I also owe particular thanks to Dr. Philip Wookey, Pier Paul Overduin, Jan Henning Steffen, Dr. Iris Werner, and Dr. Wilhelm Hagen for proof-reading parts of this thesis and correcting my English.

I acknowledge the bottomless support and encouragement of my mother during the whole period of my studies. Completion of this thesis would have been unthinkable without the chance to give our children under the loving care of Oma, MorMor and Opa. Birthe and Günther Sufke are furthermore thanked for accommodating me in the seclusion of their summer house during the critical last days of writing. My brother is thanked for igniting my interest on arctic landscapes through slides from his early travels.

My last thanks go to the Russian gasoline. If its quality had been any better, I would have captured even more data. It seems to be enough as it is, at least for me.

Appendix

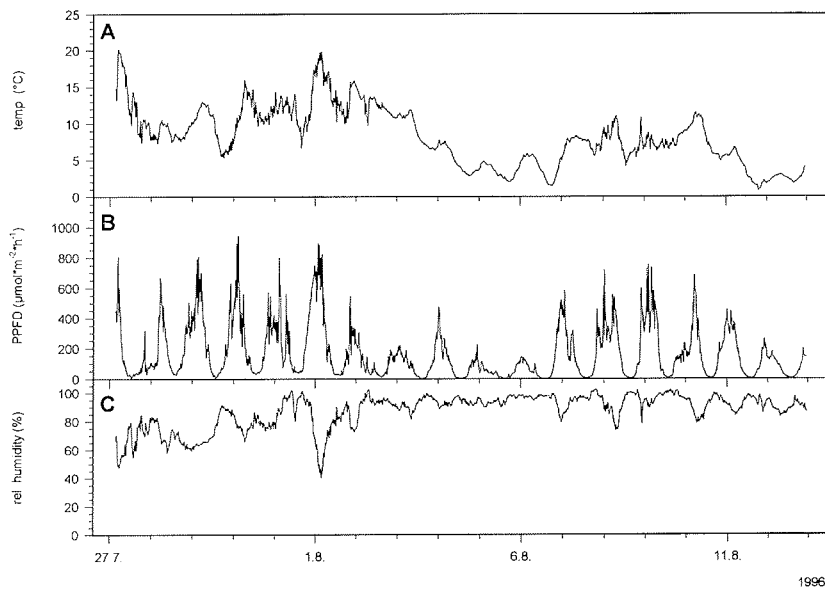


Mesoclimate, Lake Labaz, field season 1995.
A: ambient temperature, B: photosynthetic photon flux density,
C: relative humidity, D: precipitation

Fig. A1. Mesoclimate of the field season at Lake Labaz 1995.

Table A1. Daily means of ambient temperature and PPFD (2 m) during field season 1995 at Lake Labaz.

<i>date</i>	<i>daily means of ambient temperature (°C)</i>	<i>daily total of PPFD (mol*m⁻²*d⁻¹)</i>
21.07.95	8.1	13.6
22.07.95	8.9	14.0
23.07.95	16.0	39.4
24.07.95	15.4	40.3
25.07.95	16.2	39.4
26.07.95	15.2	36.5
27.07.95	13.6	21.8
28.07.95	13.5	20.2
29.07.95	12.1	20.4
30.07.95	11.7	24.5
31.07.95	10.3	20.1
01.08.95	6.9	18.0
02.08.95	9.0	26.4
03.08.95	9.6	18.3
04.08.95	9.4	26.4
05.08.95	7.1	17.9
06.08.95	9.3	31.0
07.08.95	10.2	12.8
08.08.95	9.3	25.3
09.08.95	9.4	18.3
10.08.95	8.3	33.1
11.08.95	12.9	29.4
12.08.95	16.2	25.7
13.08.95	11.4	6.8
14.08.95	9.8	13.0
15.08.95	4.5	20.0
16.08.95	3.9	24.4
17.08.95	8.3	28.4
18.08.95	12.3	27.7
19.08.95	14.5	24.0
20.08.95	14.8	23.6
21.08.95	15.6	25.7
22.08.95	13.8	10.8
23.08.95	12.7	18.1
24.08.95	12.4	20.8



Mesoclimate, Lake-Levinson-Lessing valley site, field season 1996.
 A: ambient temperature, B: photosynthetic photon flux density,
 C: relative humidity.

Fig. A2. Mesoclimate of the field season at Lake Levinson-Lessing 1996.

Table A2. Daily means of ambient temperature and PPFD (2 m) during field season 1996 at Lake Levinson-Lessing.

date	daily means of ambient temperature (°C)	daily total of PPFD (mol*m ⁻² *d ⁻¹)
28.07.96	9.6	12.7
29.07.96	10.2	23.3
30.07.96	9.8	21.3
31.07.96	11.8	19.6
01.08.96	13.7	28.3
02.08.96	13.1	11.1
03.08.96	11.3	8.2
04.08.96	6.5	9.7
05.08.96	3.7	4.7
06.08.96	4.0	4.5
07.08.96	5.2	14.4
08.08.96	7.9	18.5
09.08.96	6.9	20.1
10.08.96	9.0	14.8
11.08.96	5.7	14.0
12.08.96	2.2	7.2

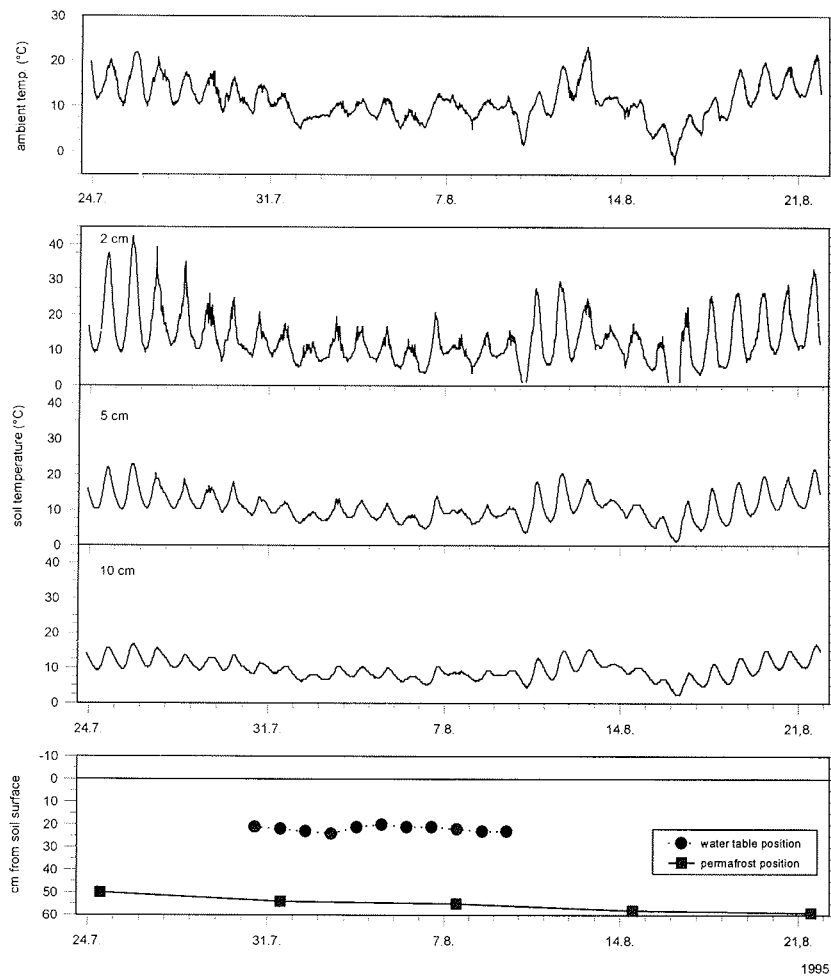


Fig. A3. Ambient temperature, soil temperatures, depth to water table and depth to permafrost in tussock tundra, tussock (TT), during field season 1995 at Lake Labaz.

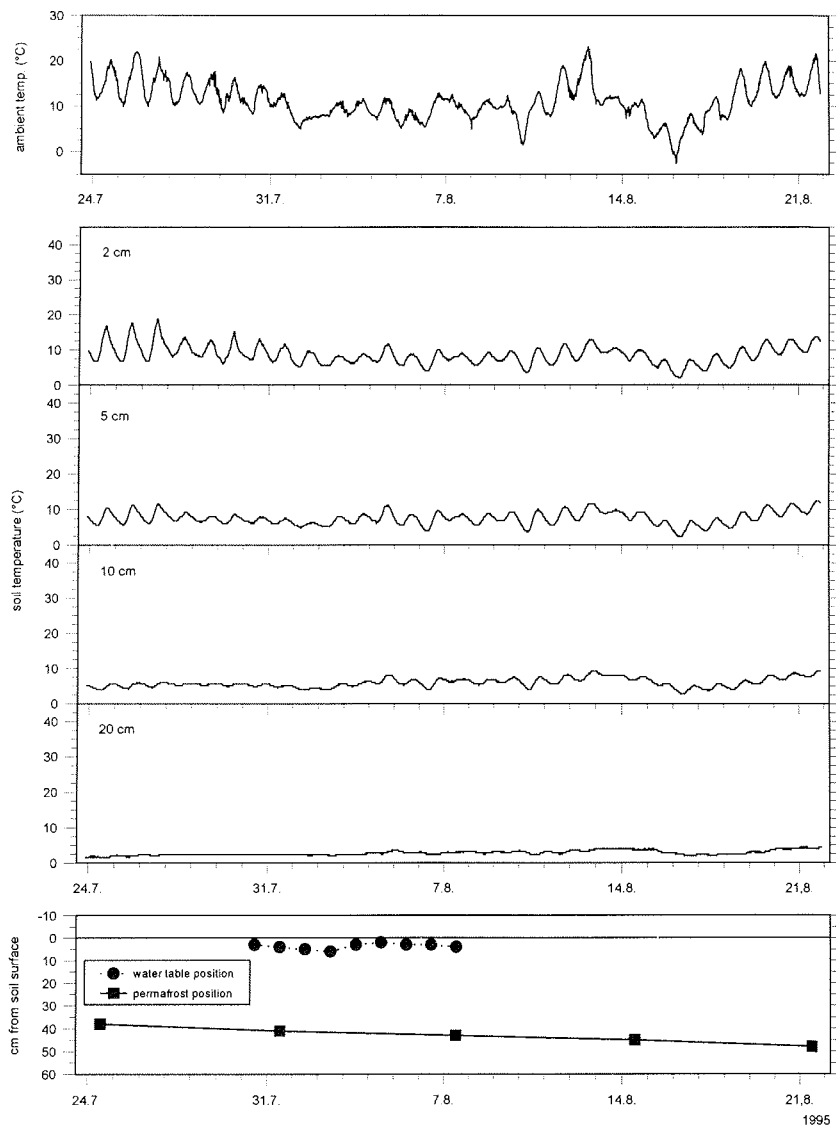


Fig. A4. Ambient temperature, soil temperatures, depth to water table and depth to permafrost in tussock tundra, depression (TD), during field season 1995 at Lake Labaz.

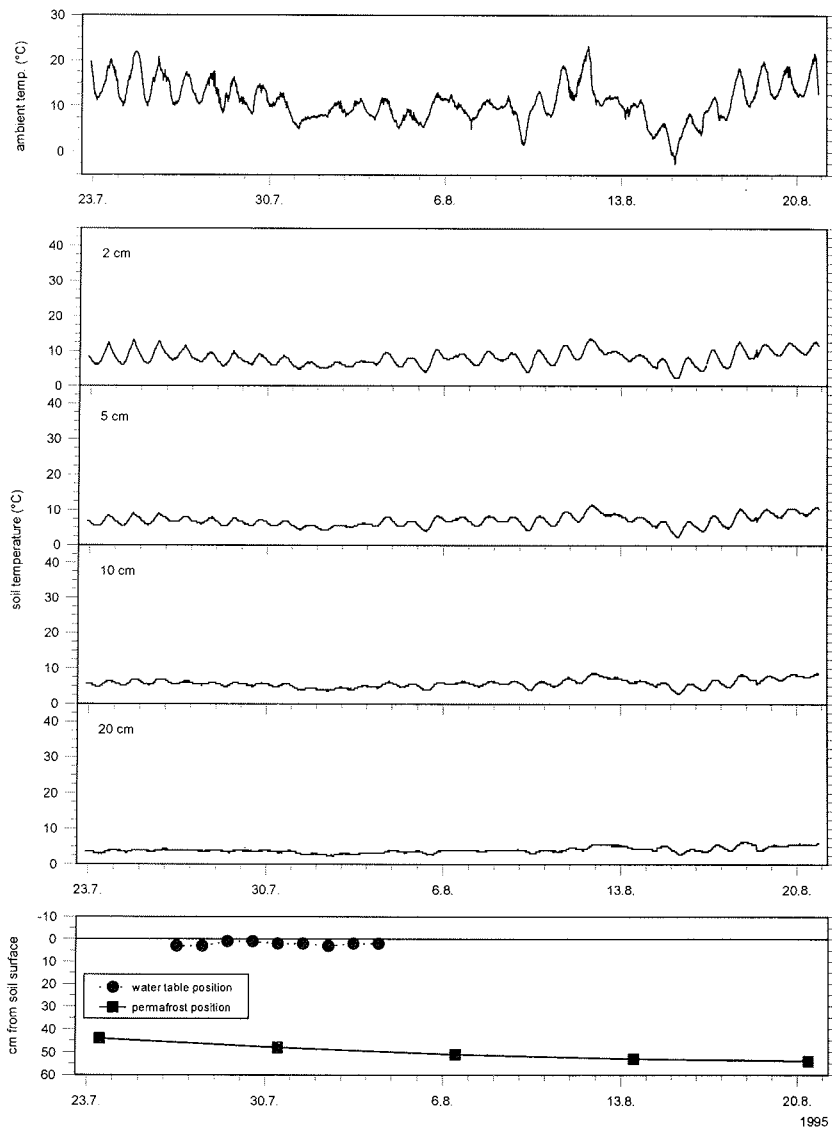


Fig. A5. Ambient temperature, soil temperatures, depth to water table and depth to permafrost in wet sedge tundra (WS) during field season 1995 at Lake Labaz.

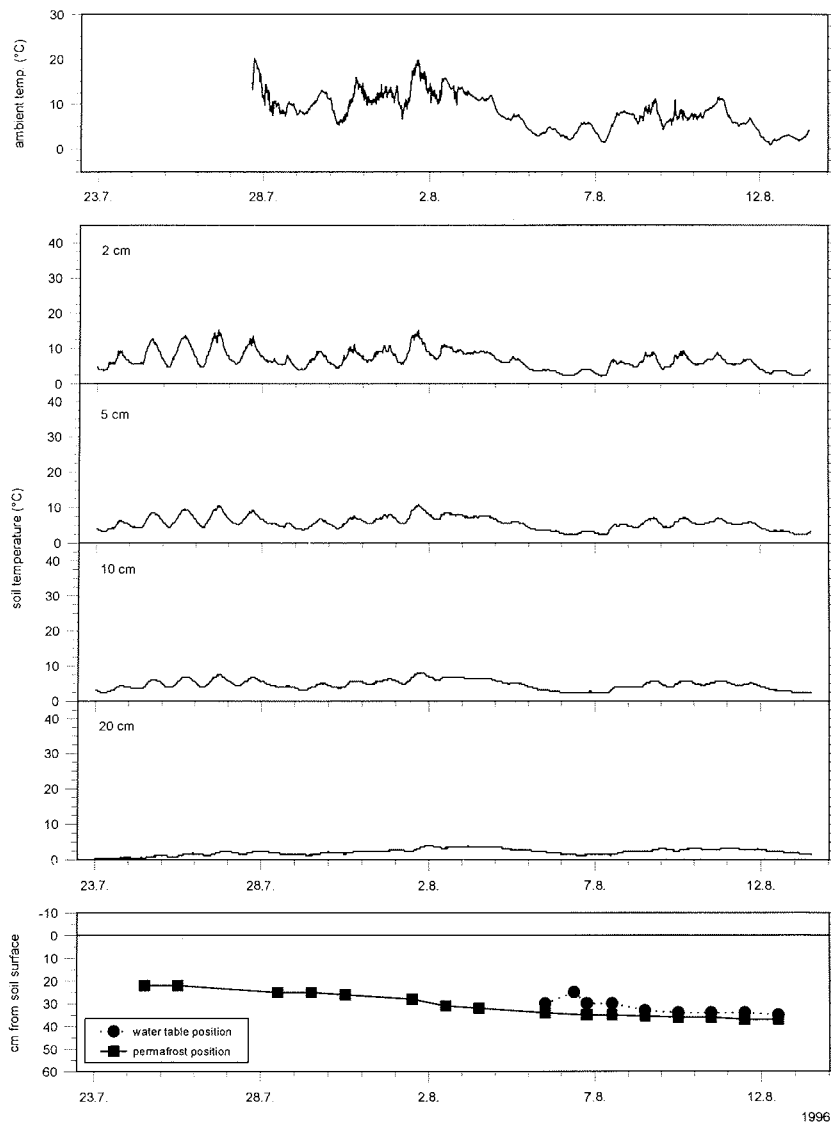


Fig. A6. Ambient temperature, soil temperatures, depth to water table and depth to permafrost in polygonal tundra, high apex (PH), during field season 1996 at Lake Levinson-Lessing.

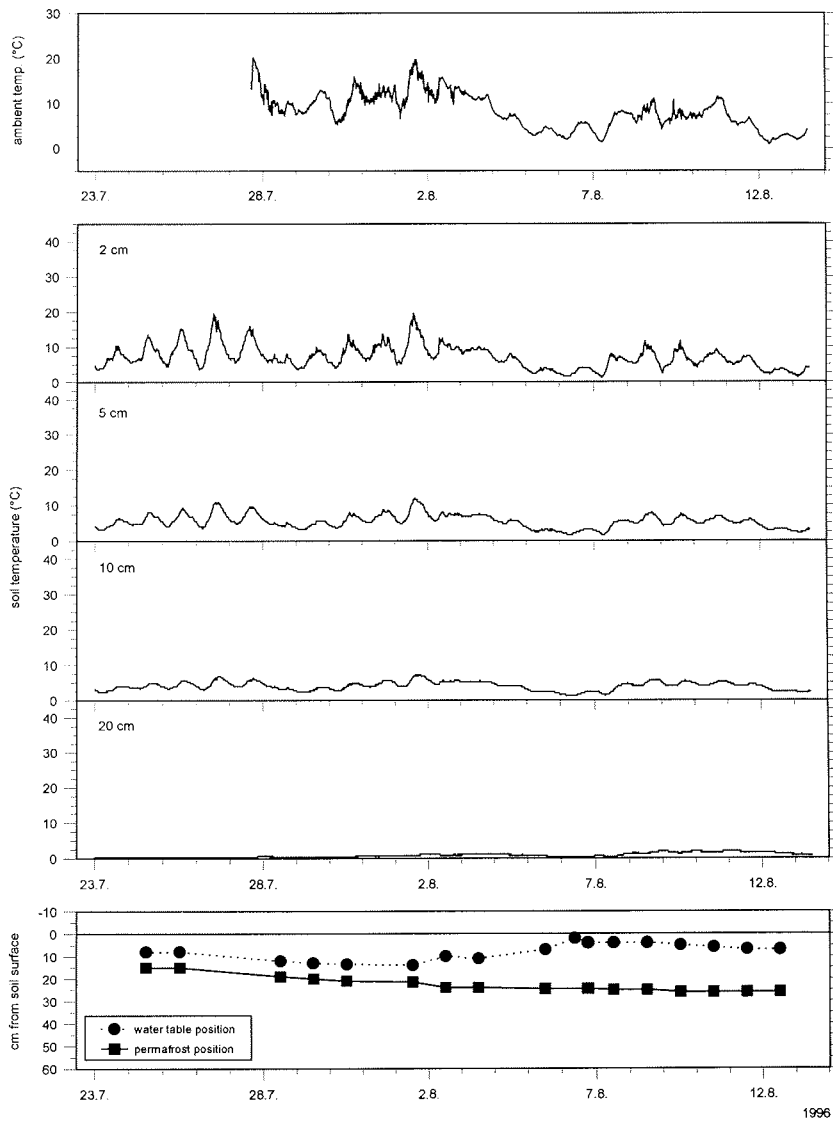


Fig. A7. Ambient temperature, soil temperatures, depth to water table and depth to permafrost in polygonal tundra, low apex (PL), during field season 1996 at Lake Levinson-Lessing.

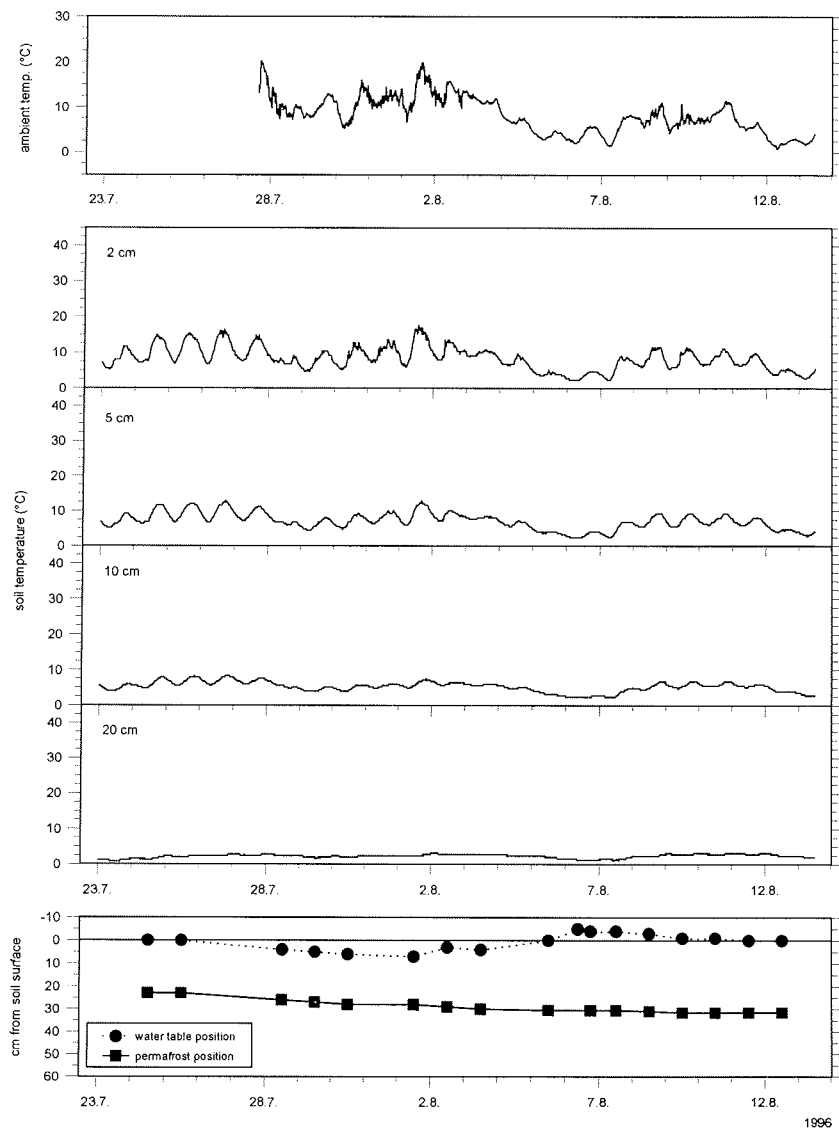


Fig. A8. Ambient temperature, soil temperatures, depth to water table and depth to permafrost in polygonal tundra, depression (PD), during field season 1996 at Lake Levinson-Lessing.

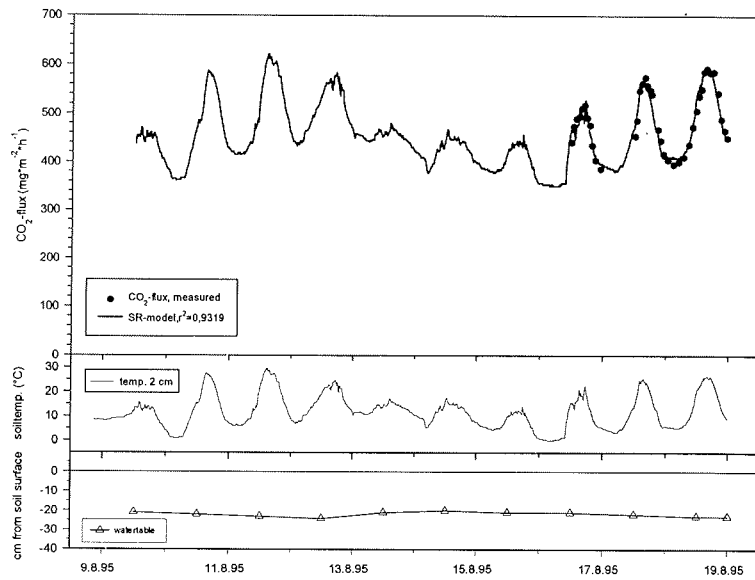


Fig. A9. Modelled course of soil respiration and measured soil respiration values in tussock tundra, tussock (TT), as well as soil temperature in 2 cm depth and depth to water table.

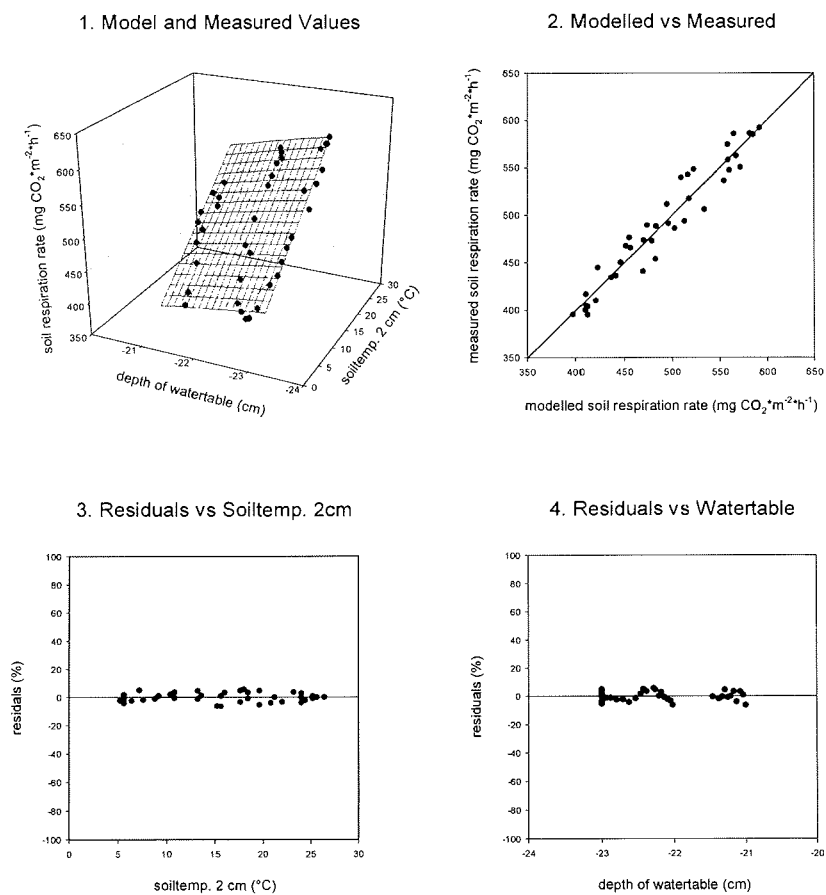


Fig. A10. Validated range of soil respiration model from tussock tundra, tussock (TT), and analysis of model quality (measured versus predicted values, relative model residuals versus soil temperature in 2 cm depth and depth to water table, respectively).

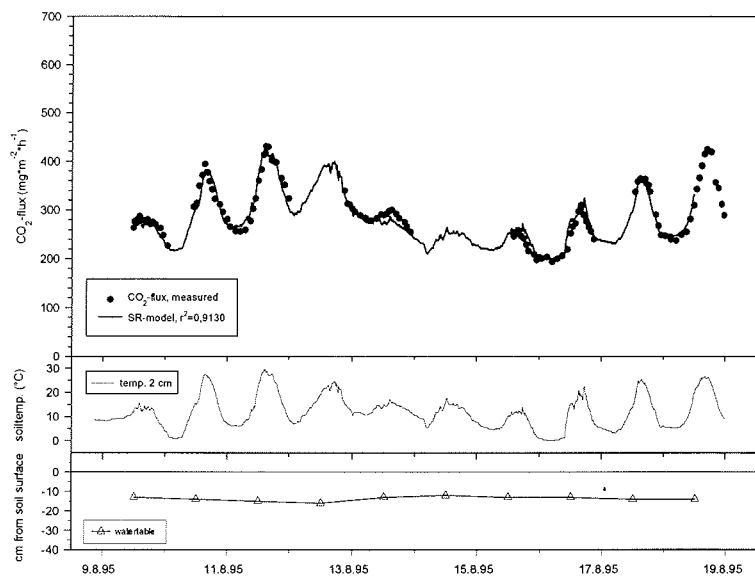


Fig. A11. Modelled course of soil respiration and measured soil respiration values in tussock tundra, moss hummock (TH), as well as soil temperature in 2 cm depth and depth to water table.

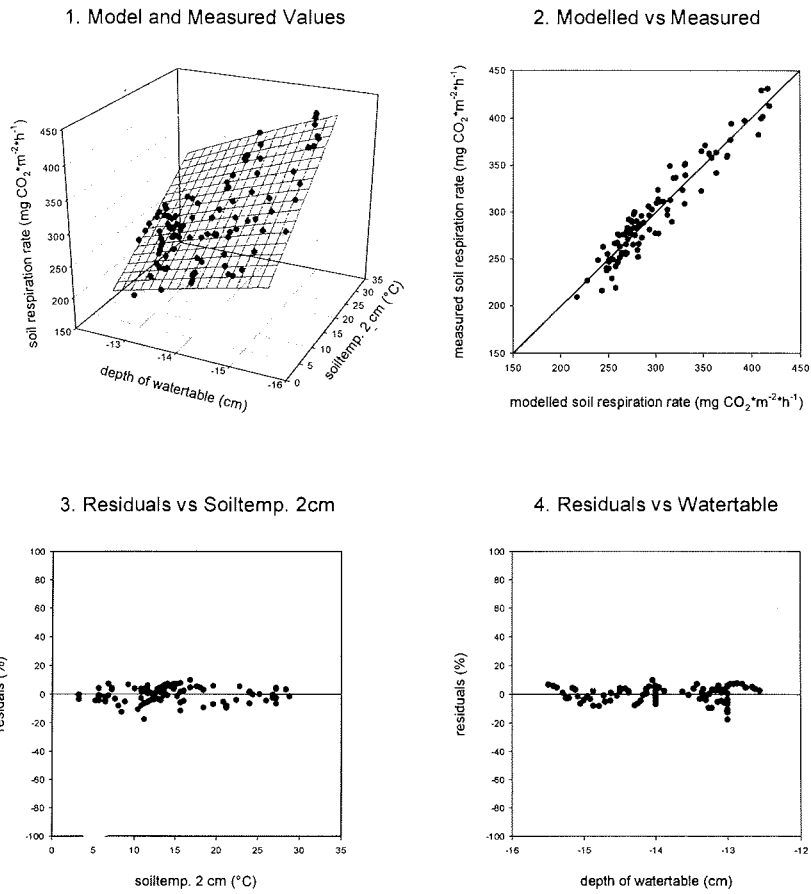


Fig. A12. Validated range of soil respiration model from tussock tundra, moss hummock (TH), and analysis of model quality (measured versus predicted values, relative model residuals versus soil temperature in 2 cm depth and depth to water table, respectively).

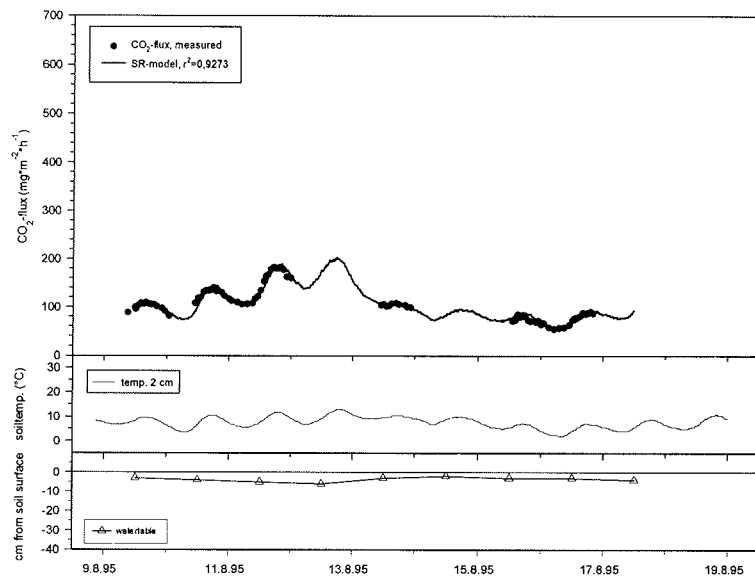


Fig. A13. Modelled course of soil respiration and measured soil respiration values in tussock tundra, depression (TD), as well as soil temperature in 2 cm depth and depth to water table.

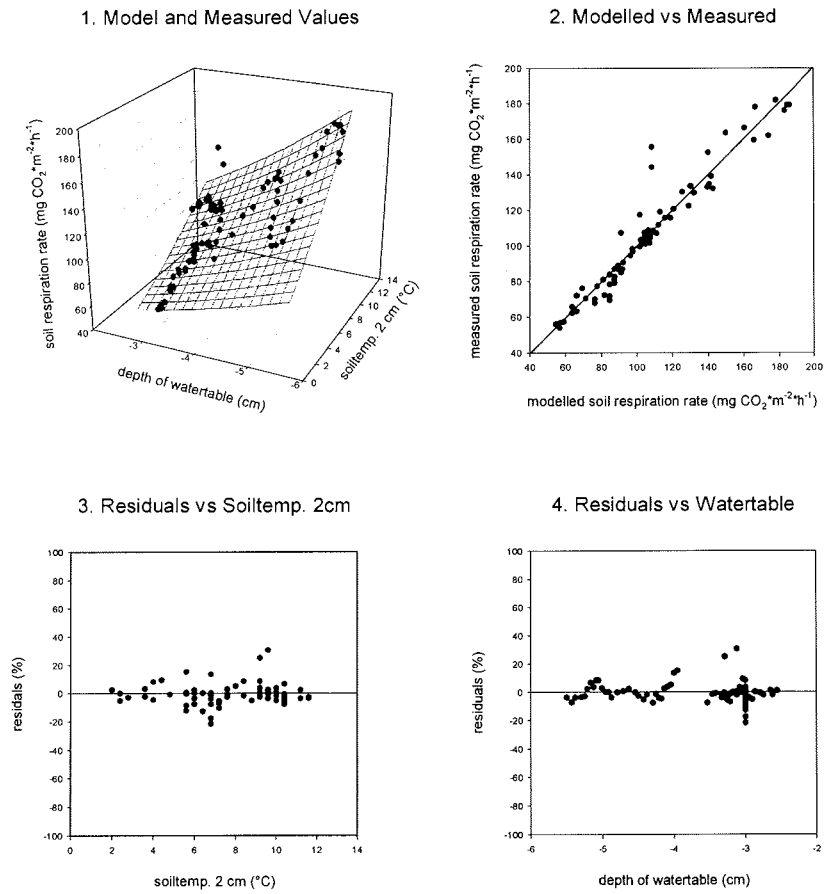


Fig. A14. Validated range of soil respiration model from tussock tundra, depression (TD), and analysis of model quality (measured versus predicted values, relative model residuals versus soil temperature in 2 cm depth and depth to water table, respectively).

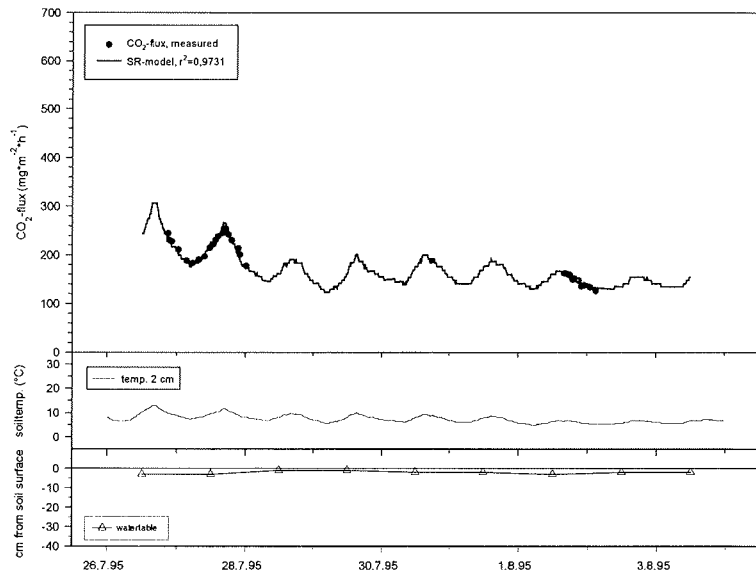


Fig. A15. Modelled course of soil respiration and measured soil respiration values in wet sedge tundra (WS), as well as soil temperature in 2 cm depth and depth to water table.

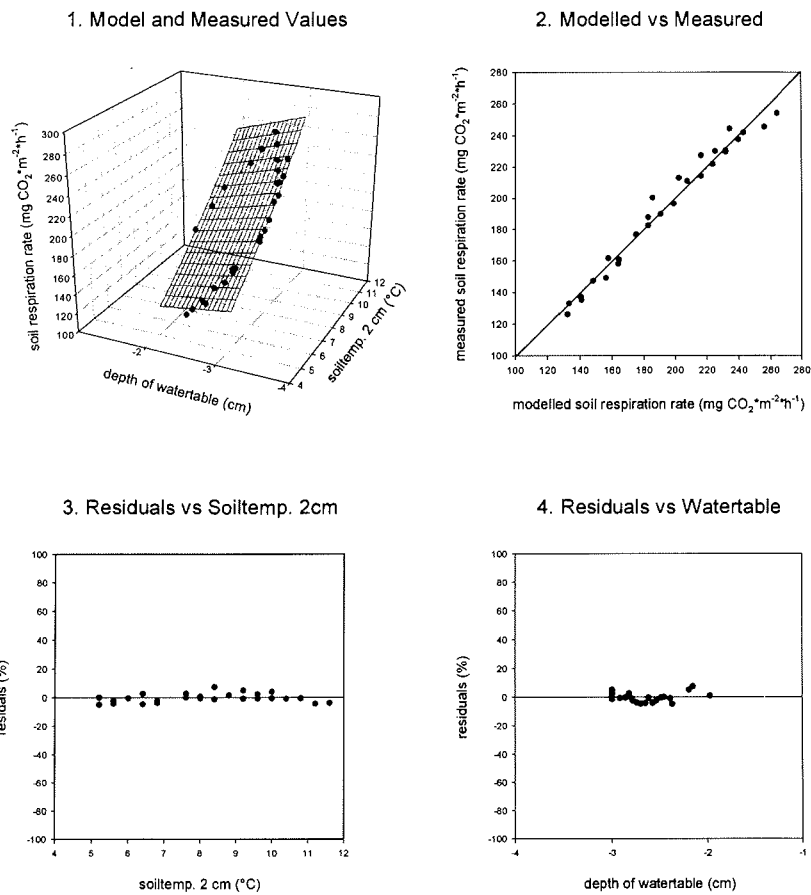


Fig. A16. Validated range of soil respiration model from wet sedge tundra (WS), and analysis of model quality (measured versus predicted values, relative model residuals versus soil temperature in 2 cm depth and depth to water table, respectively).

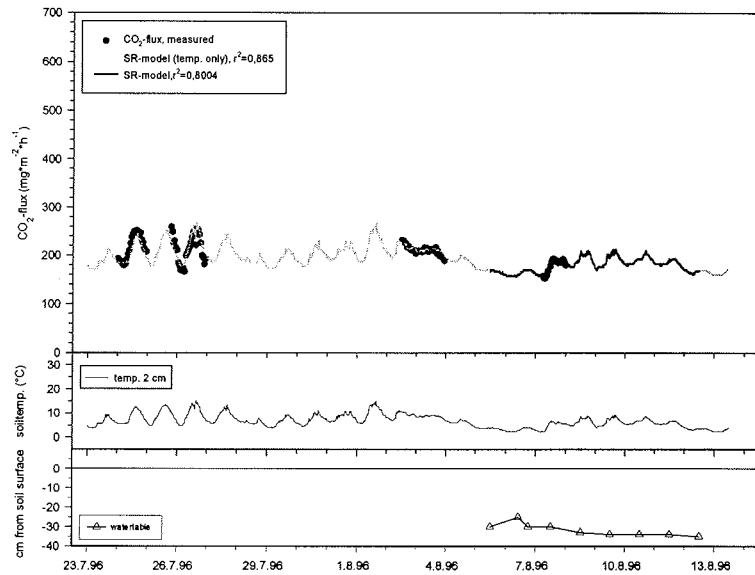


Fig. A17. Modelled course of soil respiration and measured soil respiration values in polygonal tundra, high apex (PH), as well as soil temperature in 2 cm depth and depth to water table.

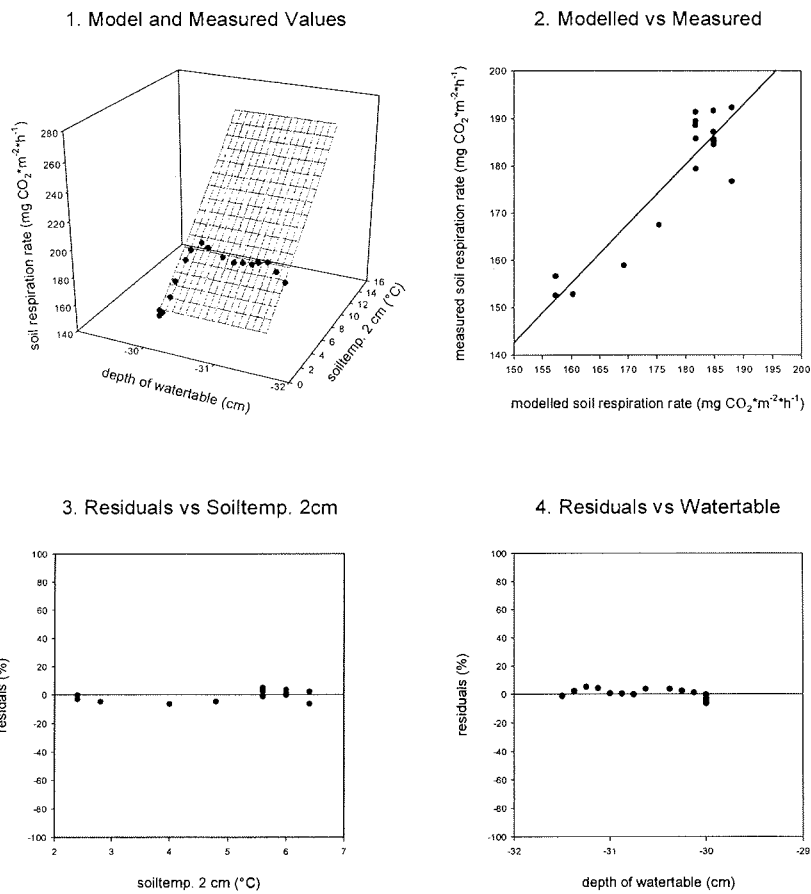


Fig. A18. Validated range of soil respiration model from polygonal tundra, high apex (PH), and analysis of model quality (measured versus predicted values, relative model residuals versus soil temperature in 2 cm depth and depth to water table, respectively).

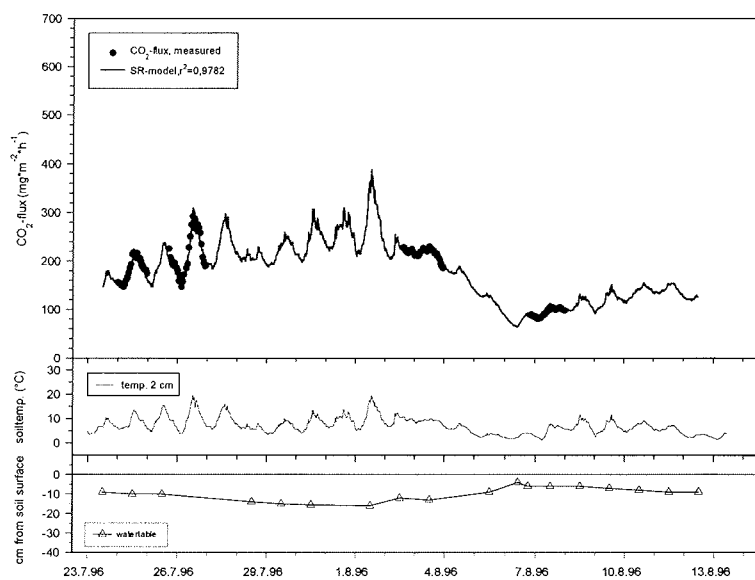


Fig. A19. Modelled course of soil respiration and measured soil respiration values in polygonal tundra, low apex (PL), as well as soil temperature in 2 cm depth and depth to water table.

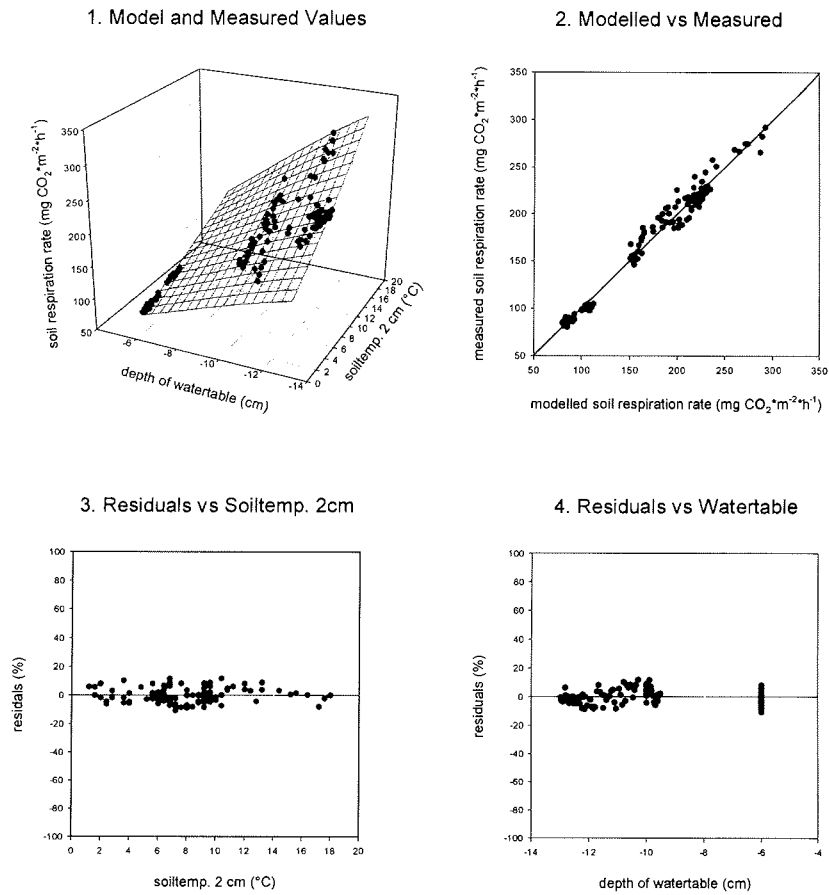


Fig. A20. Validated range of soil respiration model from polygonal tundra, low apex (PL), and analysis of model quality (measured versus predicted values, relative model residuals versus soil temperature in 2 cm depth and depth to water table, respectively).

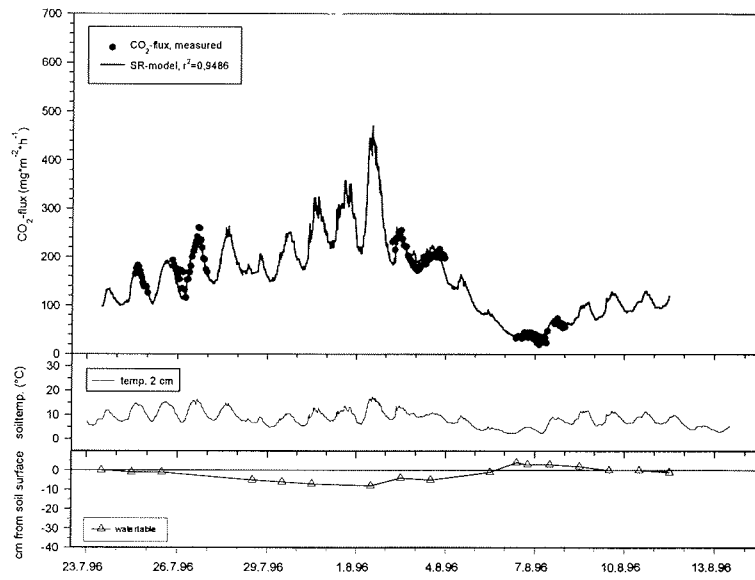


Fig. A21. Modelled course of soil respiration and measured soil respiration values in polygonal tundra, depression (PD), as well as soil temperature in 2 cm depth and depth to water table.

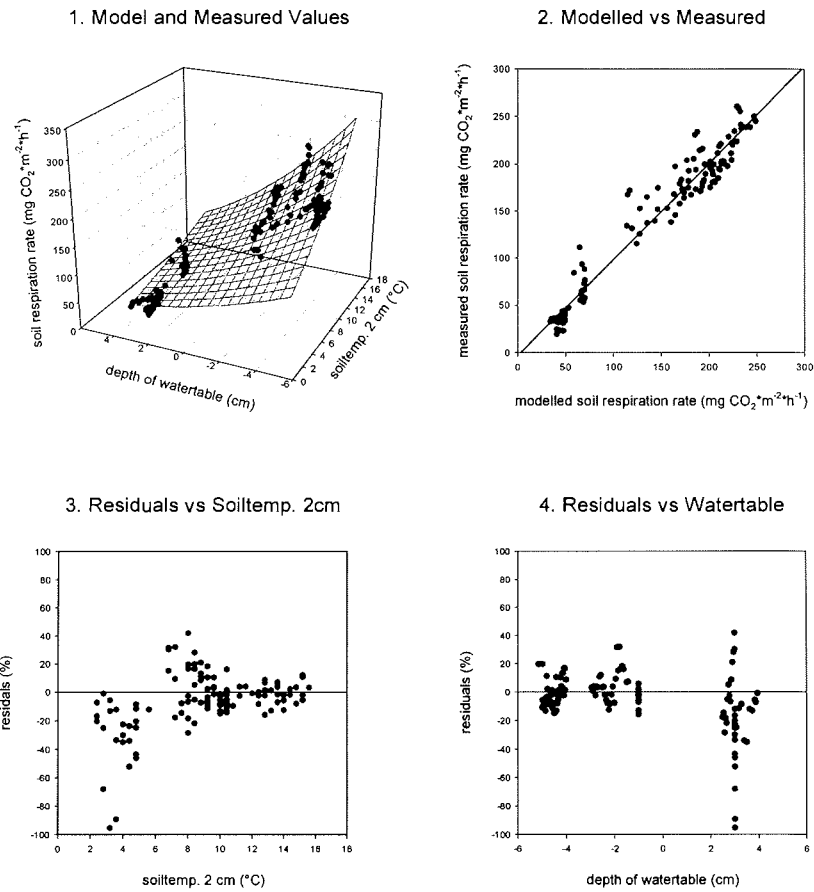


Fig. A22. Validated range of soil respiration model from polygonal tundra, depression (PD), and analysis of model quality (measured versus predicted values, relative model residuals versus soil temperature in 2 cm depth and depth to water table, respectively).

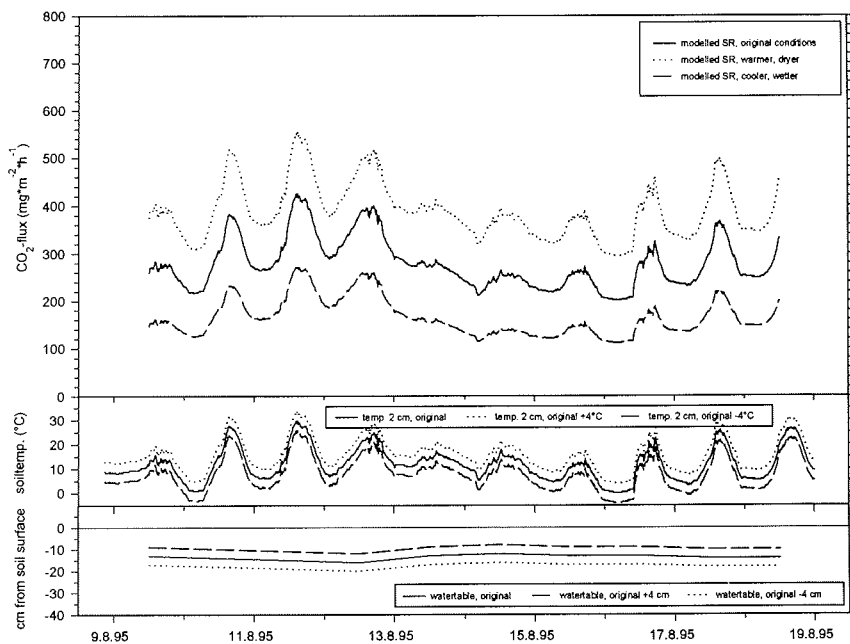


Fig. A23. Soilrespiration in tussock tundra, moss hummock (TH), modelled with three different scenarios: original parameter values, warmer and conditions (soiltemperature 2 cm original +4°C, water table original -4 cm), and cooler wetter conditions (soiltemperature 2 cm original -4°C, water table original +4 cm).

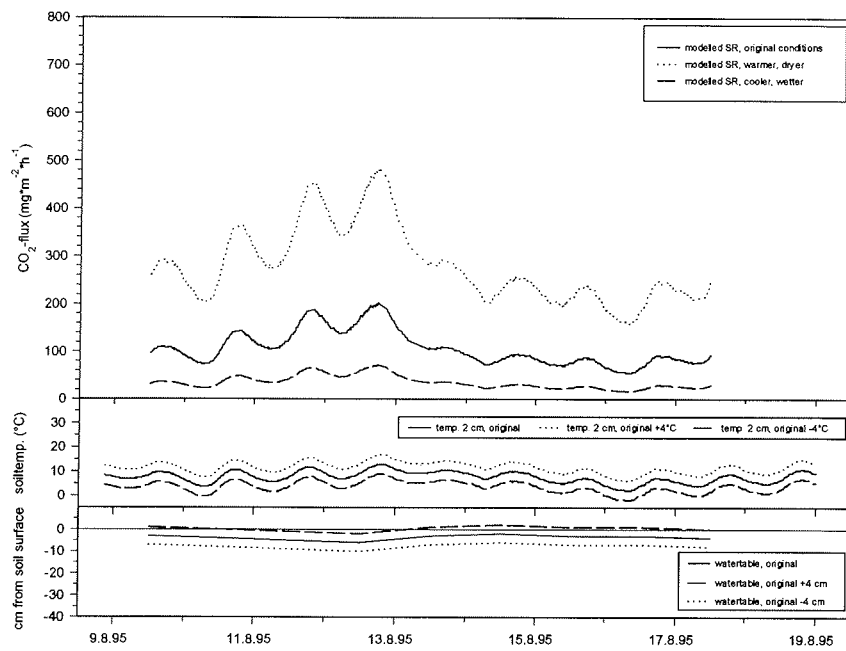


Fig. A24. Soilrespiration in tussock tundra, depression (TD), modelled with three different scenarios: original parameter values, warmer and conditions (soiltemperature 2 cm original +4°C, water table original -4 cm), and cooler wetter conditions (soiltemperature 2 cm original -4°C, water table original +4 cm).

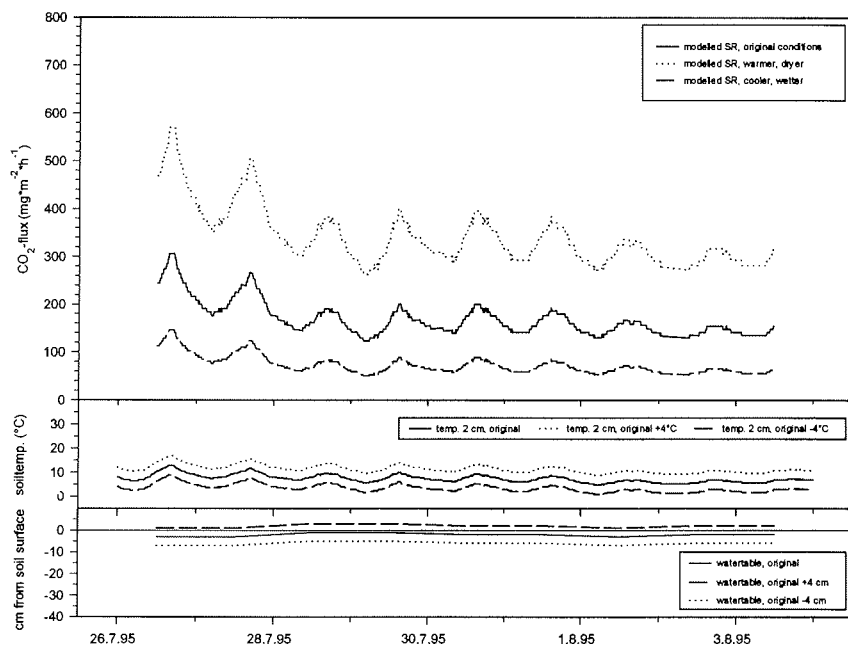


Fig. A25. Soilrespiration in wet sedge tundra (WS), modelled with three different scenarios: original parameter values, warmer and conditions (soiltemperature 2 cm original +4°C, water table original -4 cm), and cooler wetter conditions (soiltemperature 2 cm original -4°C, water table original +4 cm).

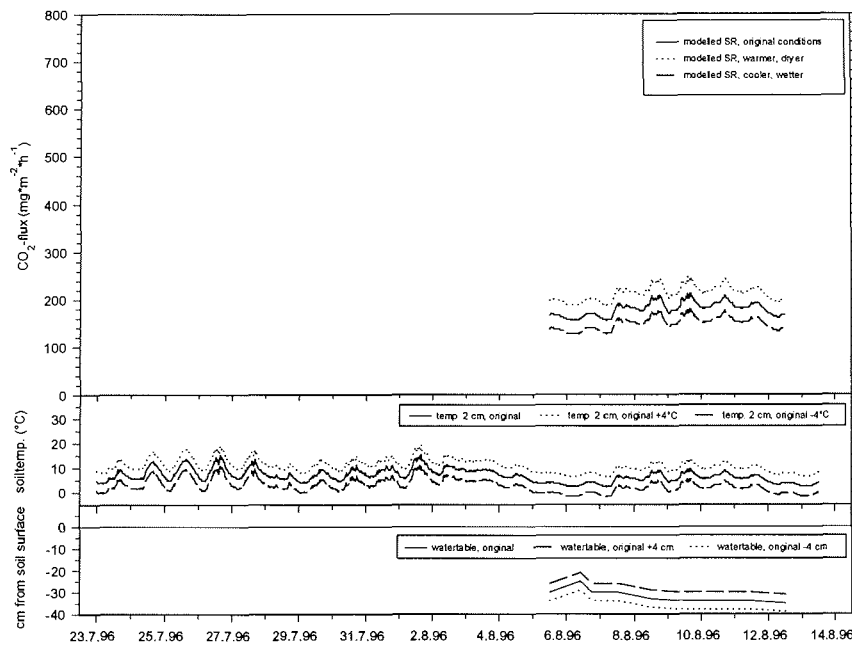


Fig. A26. Soilrespiration in polygonal tundra, high apex (PH), modelled with three different scenarios: original parameter values, warmer and conditions (soiltemperature 2 cm original +4°C, water table original -4 cm), and cooler wetter conditions (soiltemperature 2 cm original -4°C, water table original +4 cm).

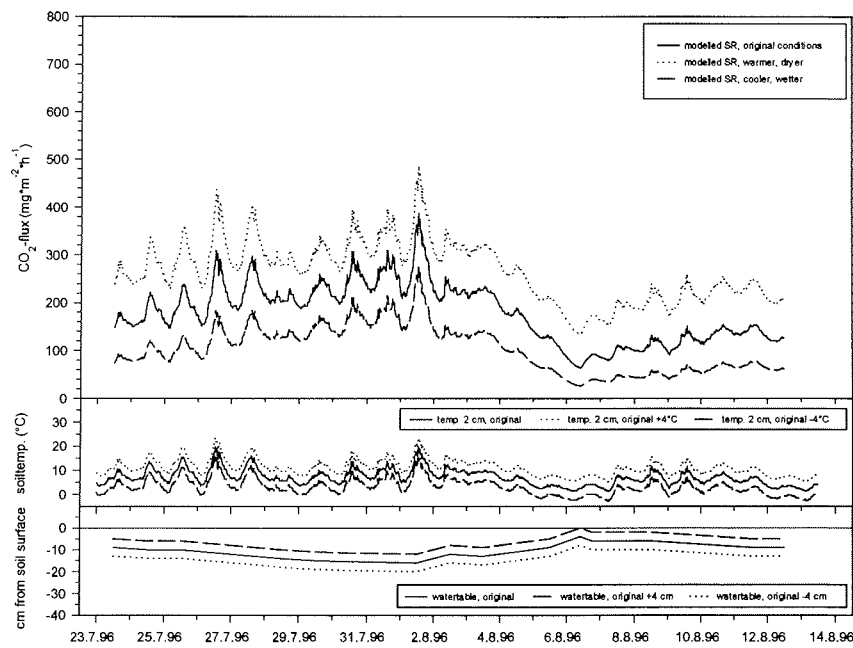


Fig. A27. Soilrespiration in polygonal tundra, low apex (PL), modelled with three different scenarios: original parameter values, warmer and conditions (soiltemperature 2 cm original +4°C, water table original -4 cm), and cooler wetter conditions (soiltemperature 2 cm original -4°C, water table original +4 cm).

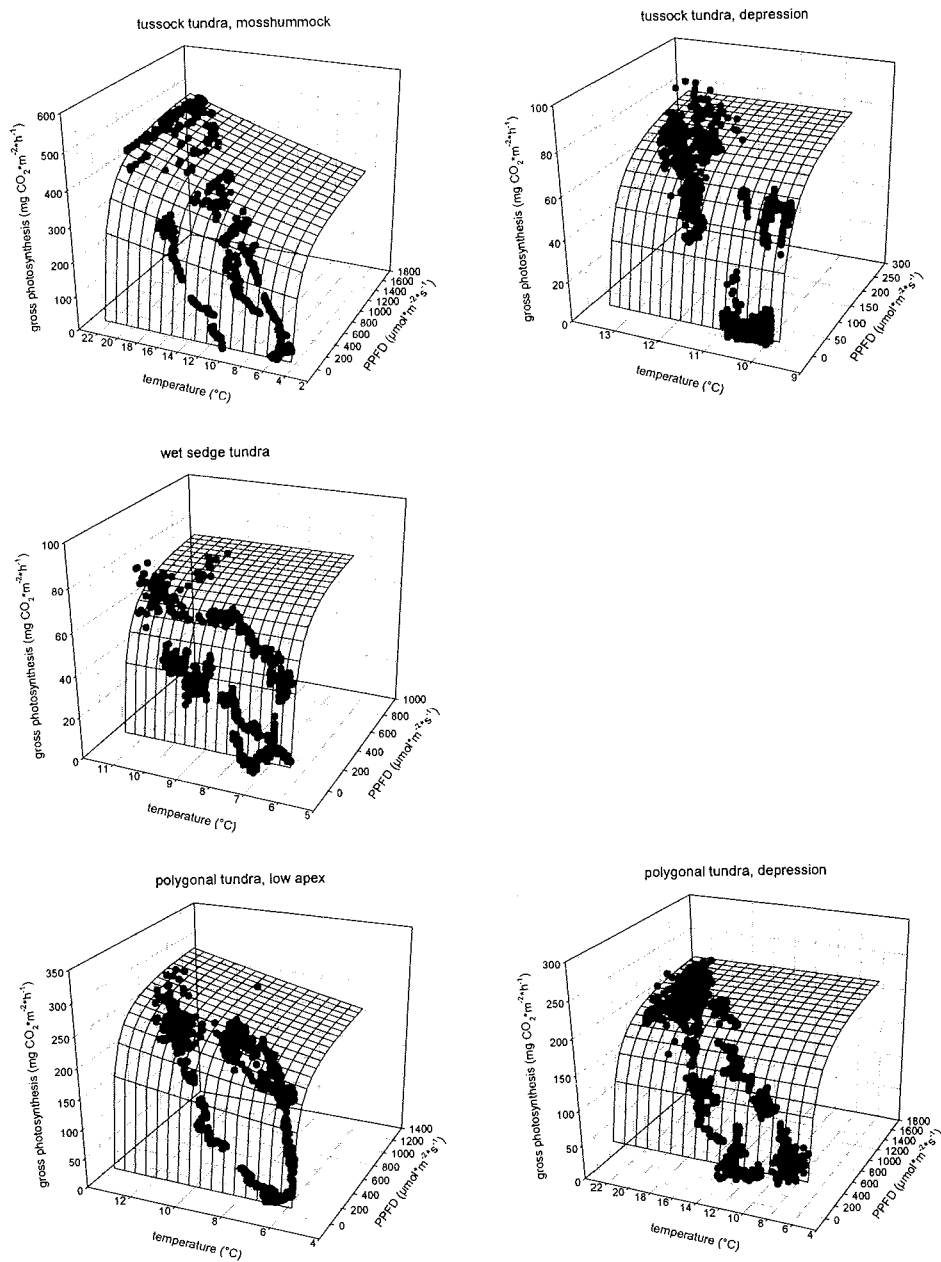


Fig. A28. Gross photosynthesis models of the different microsites. Graphs show dependence of gross moss photosynthesis on moss temperature and PPFD over the observed parameter range of each microsite.

Table A 3. Microsite characteristics used for the Spearman rank correlation analysis.

	<i>mean</i> <i>soil respiration</i> (mgCO ₂ /m ² d)	<i>mean</i> <i>soil temp.</i> (surface)	<i>mean</i> <i>soil temp.</i> (2cm)	<i>mean</i> <i>soiltemp.</i> (5cm)	<i>mean</i> <i>soil temp.</i> (10cm)	<i>mean</i> <i>water table</i> (cm)	<i>mean</i> <i>permafrost</i> (cm)	<i>thickness</i> <i>organic</i> <i>layer (cm)</i>
tussock tundra. tussock (TT)	10883	14.6	13.4	11	9.6	21.9	55.2	4
tussock tundra. moss hummock (TH)	6662	14.2	13	10.2	9.3	17.9	51	8
tussock tundra. depression (TD)	2565	12.9	8.6	7.5	5.9	3.7	43	17
wet sedge tundra (WS)	4033	9.2	8	7	5.8	2.1	50	13
polygonal tundra. high apex (PH)	4659	8.6	6.8	5.7	4.7	31.7	31	7
polygonal tundra. low apex (PL)	4299	9.5	7	5.4	4	8	22.7	9
polygonal tundra. depression (PD)	3790	9.3	8.4	7.1	5.3	0.7	28.9	5

continued

	<i>bulk density</i> <i>uppermost</i> <i>horizon (g/cm³)</i>	<i>carbon content</i> <i>uppermost horizon</i> <i>(% DW)</i>	<i>aboveground</i> <i>biomass vascular</i> <i>plants (gTG/m²)</i>	<i>belowground</i> <i>biomass vascular</i> <i>plants (gTG/m²)</i>	<i>bacterial</i> <i>biomass 0-2 cm</i> <i>(μgC/gDW)</i>
tussock tundra. tussock (TT)	0.4	11	369.6	4239	7.08
tussock tundra. moss hummock (TH)					
tussock tundra. depression (TD)	0.21	41.8	129.4	4310	7.02
wet sedge tundra (WS)	0.46	31.6	176.9	8360	29.38
polygonal tundra. high apex (PH)	0.46				
polygonal tundra. low apex (PL)	0.28	13.1			14.76
polygonal tundra. depression (PD)	0.35	17.5	55.84	3388	3.61

continued

	<i>bacterial</i> <i>biomass 2-5 cm</i> <i>(μgC/gDW)</i>	<i>annual production</i> <i>vascular plants</i> <i>(gTG/m²)</i>	<i>daily gross</i> <i>photosynthesis moss</i> <i>(mgCO₂/m²d)</i>	<i>vascular plant</i> <i>production/</i> <i>soil respiration</i>
tussock tundra. tussock (TT)	2.23	111.1		0.71
tussock tundra. moss hummock (TH)			4798	
tussock tundra. depression (TD)	13.23	41.6	1205	1.13
wet sedge tundra (WS)	16.21	156.5	694	2.71
polygonal tundra. high apex (PH)				
polygonal tundra. low apex (PL)	11.58		4068	
polygonal tundra. depression (PD)	3.31	55.84	2494	1.03

Folgende Hefte der Reihe „Berichte zur Polarforschung“ sind bisher erschienen:

- * **Sonderheft Nr. 1/1981** – „Die Antarktis und ihr Lebensraum“
Eine Einführung für Besucher – Herausgegeben im Auftrag von SCAR
- Heft Nr. 1/1982** – „Die Filchner-Schelfeis-Expedition 1980/81“
zusammengestellt von Heinz Köhnen
- * **Heft-Nr. 2/1982** – „Deutsche Antarktis-Expedition 1980/81 mit FS ‚Meteor‘“
First International BIOMASS Experiment (FIBEX) – Liste der Zooplankton- und Mikronektonnetzfüge
zusammengestellt von Norbert Klages.
- Heft Nr. 3/1982** – „Digitale und analoge Krill-Echolot-Rohdatenerfassung an Bord des Forschungsschiffes ‚Meteor‘“ (im Rahmen von FIBEX 1980/81, Fahrtabschnitt ANT III), von Bodo Morgenstern
- Heft Nr. 4/1982** – „Filchner-Schelfeis-Expedition 1980/81“
Liste der Planktonfänge und Lichtstärkemessungen
zusammengestellt von Gerd Hubold und H. Eberhard Drescher
- * **Heft Nr. 5/1982** – „Joint Biological Expedition on RRS ‚John Biscoe‘, February 1982“
by G. Hempel and R. B. Heywood
- * **Heft Nr. 6/1982** – „Antarktis-Expedition 1981/82 (Unternehmen ‚Eiswarte‘)“
zusammengestellt von Gode Gravenhorst
- Heft Nr. 7/1982** – „Marin-Biologisches Begleitprogramm zur Standorterkundung 1979/80 mit MS ‚Polar-
sirkel‘ (Pre-Site Survey)“ – Stationslisten der Mikronekton- und Zooplanktonfänge sowie der Bodenfischerei
zusammengestellt von R. Schneppenheim
- Heft Nr. 8/1983** – „The Post-Fibex Data Interpretation Workshop“
by D. L. Cram and J.-C. Freytag with the collaboration of J. W. Schmidt, M. Mall, R. Kresse, T. Schwinghammer
- * **Heft Nr. 9/1983** – „Distribution of some groups of zooplankton in the inner Weddell Sea in summer 1979/80“
by I. Hempel, G. Hubold, B. Kaczmaruk, R. Keller, R. Weigmann-Haass
- Heft Nr. 10/1983** – „Fluor im antarktischen Ökosystem“ – DFG-Symposium November 1982
zusammengestellt von Dieter Adelung
- Heft Nr. 11/1983** – „Joint Biological Expedition on RRS ‚John Biscoe‘, February 1982 (II)“
Data of micronekton and zooplankton hauls, by Uwe Piatkowski
- Heft Nr. 12/1983** – „Das biologische Programm der ANTARKTIS-I-Expedition 1983 mit FS ‚Polarstern‘“
Stationslisten der Plankton-, Benthos- und Grundschneppennetzfüge und Liste der Probenahme an Robben
und Vögeln, von H. E. Drescher, G. Hubold, U. Piatkowski, J. Plötz und J. Voß
- * **Heft Nr. 13/1983** – „Die Antarktis-Expedition von MS ‚Polarbjörn‘ 1982/83“ (Sommerkampagne zur
Atka-Bucht und zu den Kraul-Bergen), zusammengestellt von Heinz Köhnen
- * **Sonderheft Nr. 2/1983** – „Die erste Antarktis-Expedition von FS ‚Polarstern‘ (Kapstadt, 20. Januar 1983 –
Rio de Janeiro, 25. März 1983)“, Bericht des Fahrtleiters Prof. Dr. Gotthilf Hempel
- Sonderheft Nr. 3/1983** – „Sicherheit und Überleben bei Polarexpeditionen“
zusammengestellt von Heinz Köhnen
- * **Heft Nr. 14/1983** – „Die erste Antarktis-Expedition (ANTARKTIS I) von FS ‚Polarstern‘ 1982/83“
herausgegeben von Gotthilf Hempel
- Sonderheft Nr. 4/1983** – „On the Biology of Krill *Euphausia superba*“ – Proceedings of the Seminar
and Report of the Krill Ecology Group, Bremerhaven 12.–16. May 1983, edited by S. B. Schnack
- Heft Nr. 15/1983** – „German Antarctic Expedition 1980/81 with FRV ‚Walther Herwig‘ and RV ‚Meteor‘“ –
First International BIOMASS Experiment (FIBEX) – Data of micronekton and zooplankton hauls
by Uwe Piatkowski and Norbert Klages
- Sonderheft Nr. 5/1984** – „The observatories of the Georg von Neumayer Station“, by Ernst Augstein
- Heft Nr. 16/1984** – „FIBEX cruise zooplankton data“
by U. Piatkowski, I. Hempel and S. Rakusa-Suszczewski
- Heft Nr. 17/1984** – „Fahrtbericht (cruise report) der ‚Polarstern‘-Reise ARKTIS I, 1983“
von E. Augstein, G. Hempel und J. Thiede
- Heft Nr. 18/1984** – „Die Expedition ANTARKTIS II mit FS ‚Polarstern‘ 1983/84“,
Bericht von den Fahrtabschnitten 1, 2 und 3, herausgegeben von D. Fütterer
- Heft Nr. 19/1984** – „Die Expedition ANTARKTIS II mit FS ‚Polarstern‘ 1983/84“,
Bericht vom Fahrtabschnitt 4, Punta Arenas–Kapstadt (Ant-II/4), herausgegeben von H. Köhnen
- Heft Nr. 20/1984** – „Die Expedition ARKTIS II des FS ‚Polarstern‘ 1984, mit Beiträgen des FS ‚Valdivia‘
und des Forschungsflugzeuges ‚Falcon 20‘ zum Marginal Ice Zone Experiment 1984 (MIZEX)“
von E. Augstein, G. Hempel, J. Schwarz, J. Thiede und W. Weigel
- Heft Nr. 21/1985** – „Euphausiid larvae in plankton samples from the vicinity of the Antarctic Peninsula,
February 1982“ by Sigrid Marschall and Elke Mizdalski
- Heft Nr. 22/1985** – „Maps of the geographical distribution of macrozooplankton in the Atlantic sector of
the Southern Ocean“ by Uwe Piatkowski
- Heft Nr. 23/1985** – „Untersuchungen zur Funktionsmorphologie und Nahrungsaufnahme der Larven
des Antarktischen Krills *Euphausia superba* Dana“ von Hans-Peter Marschall

- Heft Nr. 24/1985** – „Untersuchungen zum Periglazial auf der König-Georg-Insel Südshetlandinseln/ Antarktika. Deutsche physiogeographische Forschungen in der Antarktis. – Bericht über die Kampagne 1983/84“ von Dietrich Barsch, Wolf-Dieter Blümel, Wolfgang Flügel, Roland Mäusbacher, Gerhard Stablein, Wolfgang Zick
- * **Heft-Nr. 25/1985** – „Die Expedition ANTARKTIS III mit FS ‚Polarstern‘ 1984/1985“ herausgegeben von Gotthilf Hempel.
- * **Heft-Nr. 26/1985** – „The Southern Ocean“; A survey of oceanographic and marine meteorological research work by Hellmer et al.
- Heft Nr. 27/1986** – „Spätpleistozäne Sedimentationsprozesse am antarktischen Kontinentalhang vor Kapp Norvegia, östliche Weddell-See“ von Hannes Grobe
- Heft Nr. 28/1986** – „Die Expedition ARKTIS III mit ‚Polarstern‘ 1985“ mit Beiträgen der Fahrtteilnehmer, herausgegeben von Rainer Gersonde
- * **Heft Nr. 29/1986** – „5 Jahre Schwerpunktprogramm ‚Antarktisforschung‘ der Deutschen Forschungsgemeinschaft.“ Rückblick und Ausblick. Zusammengefasst von Gotthilf Hempel, Sprecher des Schwerpunktprogramms
- Heft Nr. 30/1986** – „The Meteorological Data of the Georg-von-Neumayer-Station for 1981 and 1982“ by Marianne Gube and Friedrich Obleitner
- Heft Nr. 31/1986** – „Zur Biologie der Jugendstadien der Notothenioidei (Pisces) an der Antarktischen Halbinsel“ von A. Kellermann
- Heft Nr. 32/1986** – „Die Expedition ANTARKTIS IV mit FS ‚Polarstern‘ 1985/86“ mit Beiträgen der Fahrtteilnehmer, herausgegeben von Dieter Fütterer
- Heft Nr. 33/1987** – „Die Expedition ANTARKTIS-IV mit FS ‚Polarstern‘ 1985/86 – Bericht zu den Fahrtabschnitten ANT-IV/3–4“ von Dieter Karl Fütterer
- Heft Nr. 34/1987** – „Zoogeographische Untersuchungen und Gemeinschaftsanalysen an antarktischem Makroplankton“ von U. Piatkowski
- Heft Nr. 35/1987** – „Zur Verbreitung des Meso- und Makrozooplanktons in Oberflächenwasser der Weddell See (Antarktis)“ von E. Boysen-Ennen
- Heft Nr. 36/1987** – „Zur Nahrungs- und Bewegungsphysiologie von *Salpa thompsoni* und *Salpa fusiformis*“ von M. Reinke
- Heft Nr. 37/1987** – „The Eastern Weddell Sea Drifting Buoy Data Set of the Winter Weddell Sea Project (WWSP)“ 1986 by Heinrich Hoerber und Marianne Gube-Lehnhardt
- Heft Nr. 38/1987** – „The Meteorological Data of the Georg von Neumayer Station for 1983 and 1984“ by M. Gube-Lenhardt
- Heft Nr. 39/1987** – „Die Winter-Expedition mit FS ‚Polarstern‘ in die Antarktis (ANT V/1–3)“ herausgegeben von Sigrid Schnack-Schiel
- Heft Nr. 40/1987** – „Weather and Synoptic Situation during Winter Weddell Sea Project 1986 (ANT V/2) July 16–September 10, 1986“ by Werner Rabe
- Heft Nr. 41/1988** – „Zur Verbreitung und Ökologie der Seegurken im Weddellmeer (Antarktis)“ von Julian Gutt
- Heft Nr. 42/1988** – „The zooplankton community in the deep bathyal and abyssal zones of the eastern North Atlantic“ by Werner Beckmann
- Heft Nr. 43/1988** – „Scientific cruise report of Arctic Expedition ARK IV/3“ Wissenschaftlicher Fahrtbericht der Arktis-Expedition ARK IV/3, compiled by Jörn Thiede
- Heft Nr. 44/1988** – „Data Report for FV ‚Polarstern‘ Cruise ARK IV/1, 1987 to the Arctic and Polar Fronts“ by Hans-Jürgen Hirche
- Heft Nr. 45/1988** – „Zoogeographie und Gemeinschaftsanalyse des Makrozoobenthos des Weddellmeeres (Antarktis)“ von Joachim Voß
- Heft Nr. 46/1988** – „Meteorological and Oceanographic Data of the Winter-Weddell-Sea Project 1986 (ANT V/3)“ by Eberhard Fahrbach
- Heft Nr. 47/1988** – „Verteilung und Herkunft glazial-mariner Gerölle am Antarktischen Kontinentalrand des östlichen Weddellmeeres“ von Wolfgang Oskierski
- Heft Nr. 48/1988** – „Variationen des Erdmagnetfeldes an der GvN-Station“ von Arnold Brodscholl
- * **Heft Nr. 49/1988** – „Zur Bedeutung der Lipide im antarktischen Zooplankton“ von Wilhelm Hagen
- Heft Nr. 50/1988** – „Die gezeitenbedingte Dynamik des Ekström-Schelfeises, Antarktis“ von Wolfgang Kobarg
- Heft Nr. 51/1988** – „Ökomorphologie nototheniider Fische aus dem Weddellmeer, Antarktis“ von Werner Ekau
- Heft Nr. 52/1988** – „Zusammensetzung der Bodenfauna in der westlichen Fram-Straße“ von Dieter Piepenburg
- * **Heft Nr. 53/1988** – „Untersuchungen zur Ökologie des Phytoplanktons im südöstlichen Weddellmeer (Antarktis) im Jan./Febr. 1985“ von Eva-Maria Nöthig
- Heft Nr. 54/1988** – „Die Fischfauna des östlichen und südlichen Weddellmeeres: geographische Verbreitung, Nahrung und trophische Stellung der Fische“ von Wiebke Schwarzbach
- Heft Nr. 55/1988** – „Weight and length data of zooplankton in the Weddell Sea in austral spring 1986 (Ant V/3)“ by Elke Mizdalski
- Heft Nr. 56/1989** – „Scientific cruise report of Arctic expeditions ARK IV/1, 2 & 3“ by G. Krause, J. Meincke und J. Thiede

- Heft Nr. 57/1989** – „Die Expedition ANTARKTIS V mit FS ‚Polarstern‘ 1986/87“
Bericht von den Fahrtabschnitten ANT V/4–5 von H. Miller und H. Oerter
- * **Heft Nr. 58/1989** – „Die Expedition ANTARKTIS VI mit FS ‚Polarstern‘ 1987/88“
von D. K. Fütterer
- Heft Nr. 59/1989** – „Die Expedition ARKTIS V/1a, 1b und 2 mit FS ‚Polarstern‘ 1988“
von M. Spindler
- Heft Nr. 60/1989** – „Ein zweidimensionales Modell zur thermohalinen Zirkulation unter dem Schelfeis“
von H. H. Hellmer
- Heft Nr. 61/1989** – „Die Vulkanite im westlichen und mittleren Neuschwabenland,
Vestfjella und Ahlmannryggen, Antarktika“ von M. Peters
- * **Heft-Nr. 62/1989** – "The Expedition ANTARKTIS VII/1 and 2 (EPOS I) of RV 'Polarstern'
in 1988/89", by I. Hempel
- Heft Nr. 63/1989** – „Die Eisalgenflora des Weddellmeeres (Antarktis): Artenzusammensetzung und Biomasse
sowie Ökophysiologie ausgewählter Arten“ von Annette Bartsch
- Heft Nr. 64/1989** – "Meteorological Data of the G.-v.-Neumayer-Station (Antarctica)" by L. Helmes
- Heft Nr. 65/1989** – „Expedition Antarktis VII/3 in 1988/89“ by I. Hempel, P. H. Schalk, V. Smetacek
- Heft Nr. 66/1989** – „Geomorphologisch-glaziologische Detailkartierung
des arid-hochpolaren Borgmassivet, Neuschwabenland, Antarktika“ von Karsten Brunk
- Heft-Nr. 67/1990** – „Identification key and catalogue of larval Antarctic fishes“,
edited by Adolf Kellermann
- Heft-Nr. 68/1990** – „The Expedition Antarktis VII/4 (Epos leg 3) and VII/5 of RV 'Polarstern' in 1989“,
edited by W. Arntz, W. Ernst, I. Hempel
- Heft-Nr. 69/1990** – „Abhängigkeiten elastischer und rheologischer Eigenschaften des Meereises vom
Eisgefüge“, von Harald Hellmann
- Heft-Nr. 70/1990** – „Die beschalteten benthischen Mollusken (Gastropoda und Bivalvia) des
Weddellmeeres, Antarktis“, von Stefan Hain
- Heft-Nr. 71/1990** – „Sedimentologie und Paläomagnetik an Sedimenten der Maudkuppe (Nordöstliches
Weddellmeer)“, von Dieter Cordes.
- Heft-Nr. 72/1990** – „Distribution and abundance of planktonic copepods (Crustacea) in the Weddell Sea
in summer 1980/81“, by F. Kurbjeweit and S. Ali-Khan
- Heft-Nr. 73/1990** – „Zur Frühdiagenese von organischem Kohlenstoff und Opal in Sedimenten des südlichen
und östlichen Weddellmeeres“, von M. Schlüter
- Heft-Nr. 74/1990** – „Expeditionen ANTARKTIS-VIII/3 und VIII/4 mit FS ‚Polarstern‘ 1989“
von Rainer Gersonde und Gotthilf Hempel
- Heft-Nr. 75/1991** – „Quartäre Sedimentationsprozesse am Kontinentalhang des Süd-Orkey-Plateaus im
nordwestlichen Weddellmeer (Antarktis)“, von Sigrun Grünig
- Heft-Nr. 76/1990** – „Ergebnisse der faunistischen Arbeiten im Benthal von King George Island
(Südshetlandinseln, Antarktis)“, von Martin Rauscher
- Heft-Nr. 77/1990** – „Verteilung von Mikroplankton-Organismen nordwestlich der Antarktischen Halbinsel
unter dem Einfluß sich ändernder Umweltbedingungen im Herbst“, von Heinz Klöser
- Heft-Nr. 78/1991** – „Hochauflösende Magnetostratigraphie spätquartärer Sedimente arktischer
Meeresgebiete“, von Norbert R. Nowaczyk
- Heft-Nr. 79/1991** – „Ökophysiologische Untersuchungen zur Salinitäts- und Temperaturtoleranz
antarktischer Grünalgen unter besonderer Berücksichtigung des β -Dimethylsulfoniumpropionat
(DMSP) - Stoffwechsels“, von Ulf Karsten
- Heft-Nr. 80/1991** – „Die Expedition ARKTIS VII/1 mit FS ‚Polarstern‘ 1990“,
herausgegeben von Jörn Thiede und Gotthilf Hempel
- Heft-Nr. 81/1991** – „Paläoglazialologie und Paläozeanographie im Spätquartär am Kontinentalrand des
südlichen Weddellmeeres, Antarktis“, von Martin Melles
- Heft-Nr. 82/1991** – „Quantifizierung von Meereseigenschaften: Automatische Bildanalyse von
Dünnschnitten und Parametrisierung von Chlorophyll- und Salzgehaltsverteilungen“, von Hajo Eicken
- Heft-Nr. 83/1991** – „Das Fließen von Schelfeisen - numerische Simulationen
mit der Methode der finiten Differenzen“, von Jürgen Determann
- Heft-Nr. 84/1991** – „Die Expedition ANTARKTIS-VIII/1-2, 1989 mit der Winter Weddell Gyre Study
der Forschungsschiffe ‚Polarstern‘ und ‚Akademik Fedorov‘, von Ernst Augstein,
Nikolai Bagriantsev und Hans Werner Schenke
- Heft-Nr. 85/1991** – „Zur Entstehung von Unterwassereis und das Wachstum und die Energiebilanz
des Meereises in der Atka Bucht, Antarktis“, von Josef Kipfstuhl
- Heft-Nr. 86/1991** – „Die Expedition ANTARKTIS-VIII mit ‚FS Polarstern‘ 1989/90. Bericht vom
Fahrtabschnitt ANT-VIII / 5“, von Heinz Miller und Hans Oerter
- Heft-Nr. 87/1991** – „Scientific cruise reports of Arctic expeditions ARK VI / 1-4 of RV 'Polarstern'
in 1989“, edited by G. Krause, J. Meincke & H. J. Schwarz
- Heft-Nr. 88/1991** – „Zur Lebensgeschichte dominanter Copepodenarten (*Calanus finmarchicus*,
C. glacialis, *C. hyperboreus*, *Metridia longa*) in der Framstraße“, von Sabine Diel

- Heft-Nr. 89/1991** – „Detaillierte seismische Untersuchungen am östlichen Kontinentalrand des Weddell-Meeress vor Kapp Norvegia, Antarktis“, von Norbert E. Kaul
- Heft-Nr. 90/1991** – „Die Expedition ANTARKTIS-VIII mit FS „Polarstern“ 1989/90. Bericht von den Fahrtabschnitten ANT-VIII/6-7“, herausgegeben von Dieter Karl Fütterer und Otto Schrems
- Heft-Nr. 91/1991** – „Blood physiology and ecological consequences in Weddell Sea fishes (Antarctica)“, by Andreas Kunzmann
- Heft-Nr. 92/1991** – „Zur sommerlichen Verteilung des Mesozooplanktons im Nansen-Becken, Nordpolarmeer“, von Nicolai Mumm
- Heft-Nr. 93/1991** – „Die Expedition ARKTIS VII mit FS „Polarstern“, 1990. Bericht vom Fahrtabschnitt ARK VII/2“, herausgegeben von Gunther Krause
- Heft-Nr. 94/1991** – „Die Entwicklung des Phytoplanktons im östlichen Weddellmeer (Antarktis) beim Übergang vom Spätwinter zum Frühjahr“, von Renate Scharek
- Heft-Nr. 95/1991** – „Radioisotopenstratigraphie, Sedimentologie und Geochemie jungquartärer Sedimente des östlichen Arktischen Ozeans“, von Horst Bohrmann
- Heft-Nr. 96/1991** – „Holozäne Sedimentationsentwicklung im Scoresby Sund, Ost-Grönland“, von Peter Marienfeld
- Heft-Nr. 97/1991** – „Strukturelle Entwicklung und Abkühlungsgeschichte der Heimefrontfjella (Westliches Dronning Maud Land/Antarktika)“, von Joachim Jacobs
- Heft-Nr. 98/1991** – „Zur Besiedlungsgeschichte des antarktischen Schelfes am Beispiel der Isopoda (Crustacea, Malacostraca)“, von Angelika Brandt
- Heft-Nr. 99/1992** – „The Antarctic ice sheet and environmental change: a three-dimensional modelling study“, by Philippe Huybrechts
- * **Heft-Nr. 100/1992** – „Die Expeditionen ANTARKTIS IX/1-4 des Forschungsschiffes „Polarstern“ 1990/91“, herausgegeben von Ulrich Bathmann, Meinhard Schulz-Baldes, Eberhard Fahrbach, Victor Smetacek und Hans-Wolfgang Hubberten
- Heft-Nr. 101/1992** – „Wechselbeziehungen zwischen Schwermetallkonzentrationen (Cd, Cu, Pb, Zn) im Meewasser und in Zooplanktonorganismen (Copepoda) der Arktis und des Atlantiks“, von Christa Pohl
- Heft-Nr. 102/1992** – „Physiologie und Ultrastruktur der antarktischen Grünalge *Prasiola crispa* ssp. *antarctica* unter osmotischem Streß und Austrocknung“, von Andreas Jacob
- Heft-Nr. 103/1992** – „Zur Ökologie der Fische im Weddellmeer“, von Gerd Hubold
- Heft-Nr. 104/1992** – „Mehrkanalige adaptive Filter für die Unterdrückung von multiplen Reflexionen in Verbindung mit der freien Oberfläche in marinen Seismogrammen“, von Andreas Rosenberger
- Heft-Nr. 105/1992** – „Radiation and Eddy Flux Experiment 1991 (REFLEX I)“, von Jörg Hartmann, Christoph Kottmeier und Christian Wamser
- Heft-Nr. 106/1992** – „Ostracoden im Epipelagial vor der Antarktischen Halbinsel - ein Beitrag zur Systematik sowie zur Verbreitung und Populationsstruktur unter Berücksichtigung der Saisonalität“, von Rüdiger Kock
- Heft-Nr. 107/1992** – „ARCTIC '91: Die Expedition ARK-VIII/3 mit FS „Polarstern“ 1991“, von Dieter K. Fütterer
- Heft-Nr. 108/1992** – „Dehnungsbeben an einer Störungszone im Ekström-Schelfeis nördlich der Georg-von-Neumayer Station, Antarktis. – Eine Untersuchung mit seismologischen und geodätischen Methoden“, von Uwe Nixdorf.
- Heft-Nr. 109/1992** – „Spätquartäre Sedimentation am Kontinentalrand des südöstlichen Weddellmeeres, Antarktis“, von Michael Weber.
- Heft-Nr. 110/1992** – „Sedimentfazies und Bodenwasserstrom am Kontinentallhang des nordwestlichen Weddellmeeres“, von Isa Brehme.
- Heft-Nr. 111/1992** – „Die Lebensbedingungen in den Solekanälchen des antarktischen Meereises“, von Jürgen Weissenberger.
- Heft-Nr. 112/1992** – „Zur Taxonomie von rezenten benthischen Foraminiferen aus dem Nansen Becken, Arktischer Ozean“, von Jutta Wollenburg.
- Heft-Nr. 113/1992** – „Die Expedition ARKTIS VIII/1 mit FS „Polarstern“ 1991“, herausgegeben von Gerhard Kattner.
- * **Heft-Nr. 114/1992** – „Die Gründungsphase deutscher Polarforschung, 1865-1875“, von Reinhard A. Krause.
- Heft-Nr. 115/1992** – „Scientific Cruise Report of the 1991 Arctic Expedition ARK VIII/2 of RV „Polarstern“ (EPOS II)“, by Eike Rachor.
- Heft-Nr. 116/1992** – „The Meteorological Data of the Georg-von-Neumayer-Station (Antarctica) for 1988, 1989, 1990 and 1991“, by Gert König-Langlo.
- Heft-Nr. 117/1992** – „Petrogenese des metamorphen Grundgebirges der zentralen Heimefrontfjella (westliches Dronning Maud Land / Antarktis)“, von Peter Schulze.
- Heft-Nr. 118/1993** – „Die mafischen Gänge der Shackleton Range / Antarktika: Petrographie, Geochemie, Isotopengeochemie und Paläomagnetik“, von Rüdiger Hotten.
- * **Heft-Nr. 119/1993** – „Gefrierschutz bei Fischen der Polarmeere“, von Andreas P.A. Wöhrmann.
- * **Heft-Nr. 120/1993** – „East Siberian Arctic Region Expedition '92: The Laptev Sea - its Significance for Arctic Sea-Ice Formation and Transpolar Sediment Flux“, by D. Dethleff, D. Nürnberg, E. Reimnitz, M. Saarlo and Y. P. Sacchenko. – „Expedition to Novaja Zemlja and Franz Josef Land with RV. 'Dainie Zelensy'“, by D. Nürnberg and E. Groth.

- * **Heft-Nr. 121/1993** – „Die Expedition ANTARKTIS X/3 mit FS 'Polarstern' 1992“, herausgegeben von Michael Spindler, Gerhard Dieckmann und David Thomas.
- Heft-Nr. 122/1993** – „Die Beschreibung der Korngestalt mit Hilfe der Fourier-Analyse: Parametrisierung der morphologischen Eigenschaften von Sedimentpartikeln“, von Michael Diepenbroek.
- * **Heft-Nr. 123/1993** – „Zerstörungsfreie hochauflösende Dichteuntersuchungen mariner Sedimente“, von Sebastian Gerland.
- Heft-Nr. 124/1993** – „Umsatz und Verteilung von Lipiden in arktischen marinen Organismen unter besonderer Berücksichtigung unterer trophischer Stufen“, von Martin Graeve.
- Heft-Nr. 125/1993** – „Ökologie und Respiration ausgewählter arktischer Bodenfischarten“, von Christian F. von Dörrien.
- Heft-Nr. 126/1993** – „Quantitative Bestimmung von Paläoumweltparametern des Antarktischen Oberflächenwassers im Spätquartär anhand von Transferfunktionen mit Diatomeen“, von Ulrich Zielinski
- Heft-Nr. 127/1993** – „Sedimenttransport durch das arktische Meereis: Die rezente lithogene und biogene Materialfracht“, von Ingo Wollenburg.
- Heft-Nr. 128/1993** – „Cruise ANTARKTIS X/3 of RV 'Polarstern': CTD-Report“, von Marek Zwierz.
- Heft-Nr. 129/1993** – „Reproduktion und Lebenszyklen dominanter Copepodenarten aus dem Weddellmeer, Antarktis“, von Frank Kurbjeweit
- Heft-Nr. 130/1993** – „Untersuchungen zu Temperaturregime und Massenhaushalt des Filchner-Ronne-Schelfeises, Antarktis, unter besonderer Berücksichtigung von Anfrier- und Abschmelzprozessen“, von Klaus Grosfeld
- Heft-Nr. 131/1993** – „Die Expedition ANTARKTIS X/5 mit FS 'Polarstern' 1992“, herausgegeben von Rainer Gersonde
- Heft-Nr. 132/1993** – „Bildung und Abgabe kurzzeitiger halogener Kohlenwasserstoffe durch Makroalgen der Polarregionen“, von Frank Laturnus
- Heft-Nr. 133/1994** – „Radiation and Eddy Flux Experiment 1993 (REFLEX II)“, by Christoph Kottmeier, Jörg Hartmann, Christian Wamser, Axel Bochert, Christof Lüpkes, Dietmar Freese and Wolfgang Cohrs
- * **Heft-Nr. 134/1994** – „The Expedition ARKTIS-IX/1“, edited by Hajo Eicken and Jens Meincke
- Heft-Nr. 135/1994** – „Die Expeditionen ANTARKTIS X/6-8“, herausgegeben von Ulrich Bathmann, Victor Smetacek, Hein de Baar, Eberhard Fahrbach und Gunter Krause
- Heft-Nr. 136/1994** – „Untersuchungen zur Ernährungsökologie von Kaiserpinguinen (*Aptenodytes forsteri*) und Königspinguinen (*Aptenodytes patagonicus*)“, von Klemens Pütz
- * **Heft-Nr. 137/1994** – „Die känozoische Vereisungsgeschichte der Antarktis“, von Werner U. Ehrmann
- Heft-Nr. 138/1994** – „Untersuchungen stratosphärischer Aerosole vulkanischen Ursprungs und polarer stratosphärischer Wolken mit einem Mehrwellenlängen-Lidar auf Spitzbergen (79° N, 12° E)“, von Georg Beyerle
- Heft-Nr. 139/1994** – „Charakterisierung der Isopodenfauna (Crustacea, Malacostraca) des Scotia-Bogens aus biogeographischer Sicht: Ein multivariater Ansatz“, von Holger Winkler.
- Heft-Nr. 140/1994** – „Die Expedition ANTARKTIS X/4 mit FS 'Polarstern' 1992“, herausgegeben von Peter Lemke
- Heft-Nr. 141/1994** – „Satellitenaltimetrie über Eis – Anwendung des GEOSAT-Altimeters über dem Ekströmisien, Antarktis“, von Clemens Heidland
- Heft-Nr. 142/1994** – „The 1993 Northeast Water Expedition. Scientific cruise report of RV 'Polarstern' Arctic cruises ARK IX/2 and 3, USCG 'Polar Bear' cruise NEWP and the NEWLand expedition“, edited by Hans-Jürgen Hirche and Gerhard Kattner
- Heft-Nr. 143/1994** – „Detaillierte refraktionsseismische Untersuchungen im inneren Scoresby Sund Ost-Grönland“, von Notker Fechner
- Heft-Nr. 144/1994** – „Russian-German Cooperation in the Siberian Shelf Seas: Geo-System Laptev Sea“, edited by Heidemarie Kassens, Hans-Wolfgang Hubberten, Sergey M. Pryamikov und Rüdiger Stein
- * **Heft-Nr. 145/1994** – „The 1993 Northeast Water Expedition. Data Report of RV 'Polarstern' Arctic Cruises IX/2 and 3“, edited by Gerhard Kattner and Hans-Jürgen Hirche.
- Heft-Nr. 146/1994** – „Radiation Measurements at the German Antarctic Station Neumayer 1982-1992“, by Torsten Schmidt and Gert König-Langlo.
- Heft-Nr. 147/1994** – „Krustenstrukturen und Verlauf des Kontinentalrandes im Weddell Meer / Antarktis“, von Christian Hübscher.
- Heft-Nr. 148/1994** – „The expeditions NORILSK/TAYMYR 1993 and BUNGER OASIS 1993/94 of the AWI Research Unit Potsdam“, edited by Martin Melles.
- ** **Heft-Nr. 149/1994** – „Die Expedition ARCTIC' 93. Der Fahrtabschnitt ARK-IX/4 mit FS 'Polarstern' 1993“, herausgegeben von Dieter K. Fütterer.
- Heft-Nr. 150/1994** – „Der Energiebedarf der Pygoscelis-Pinguine: eine Synopse“, von Boris M. Culik.
- Heft-Nr. 151/1994** – „Russian-German Cooperation: The Transdrift I Expedition to the Laptev Sea“, edited by Heidemarie Kassens and Valeriy Y. Karpiy.
- Heft-Nr. 152/1994** – „Die Expedition ANTARKTIS-X mit FS 'Polarstern' 1992. Bericht von den Fahrtabschnitten / ANT-X / 1a und 2“, herausgegeben von Heinz Miller.
- Heft-Nr. 153/1994** – „Aminosäuren und Huminstoffe im Stickstoffkreislauf polarer Meere“, von Ulrike Hubberten.
- Heft-Nr. 154/1994** – „Regional und seasonal variability in the vertical distribution of mesozooplankton in the Greenland Sea“, by Claudio Richter.

- Heft-Nr. 155/1995** – "Benthos in polaren Gewässern", herausgegeben von Christian Wiencke und Wolf Arntz.
- Heft-Nr. 156/1995** – "An adjoint model for the determination of the mean oceanic circulation, air-sea fluxes und mixing coefficients", by Reiner Schlitzer.
- Heft-Nr. 157/1995** – "Biochemische Untersuchungen zum Lipidstoffwechsel antarktischer Copepoden", von Kirsten Fahl.
- ** Heft-Nr. 158/1995** – "Die Deutsche Polarforschung seit der Jahrhundertwende und der Einfluß Erich von Drygalskis", von Cornelia Lüdecke.
- Heft-Nr. 159/1995** – "The distribution of $\delta^{18}\text{O}$ in the Arctic Ocean: Implications for the freshwater balance of the halocline and the sources of deep and bottom waters", by Dorothea Bauch.
- * Heft-Nr. 160/1995** – "Rekonstruktion der spätquartären Tiefenwasserzirkulation und Produktivität im östlichen Südatlantik anhand von benthischen Foraminiferenvergesellschaftungen", von Gerhard Schmiedl.
- Heft-Nr. 161/1995** – "Der Einfluß von Salinität und Lichtintensität auf die Osmolytkonzentrationen, die Zellvolumina und die Wachstumsraten der antarktischen Eisdiatomeen *Chaetoceros* sp. und *Navicula* sp. unter besonderer Berücksichtigung der Aminosäure Prolin", von Jürgen Nothnagel.
- Heft-Nr. 162/1995** – "Meereistransportiertes lithogenes Feinmaterial in spätquartären Tiefseesedimenten des zentralen östlichen Arktischen Ozeans und der Framstraße", von Thomas Letzig.
- Heft-Nr. 163/1995** – "Die Expedition ANTARKTIS-XI/2 mit FS "Polarstern" 1993/94", herausgegeben von Rainer Gersonde.
- Heft-Nr. 164/1995** – "Regionale und altersabhängige Variation gesteinsmagnetischer Parameter in marinen Sedimenten der Arktis", von Thomas Frederichs.
- Heft-Nr. 165/1995** – "Vorkommen, Verteilung und Umsatz biogener organischer Spurenstoffe: Sterole in antarktischen Gewässern", von Georg Hanke.
- Heft-Nr. 166/1995** – "Vergleichende Untersuchungen eines optimierten dynamisch-thermodynamischen Meereismodells mit Beobachtungen im Weddellmeer", von Holger Fischer.
- Heft-Nr. 167/1995** – "Rekonstruktionen von Paläo-Umweltparametern anhand von stabilen Isotopen und Faunen-Vergesellschaftungen planktischer Foraminiferen im Südatlantik", von Hans-Stefan Niebler
- Heft-Nr. 168/1995** – "Die Expedition ANTARKTIS XII mit FS 'Polarstern' 1993/94. Bericht von den Fahrtabschnitten ANT XII/1 und 2", herausgegeben von Gerhard Kattner und Dieter Karl Fütterer.
- Heft-Nr. 169/1995** – "Medizinische Untersuchung zur Circadianrhythmik und zum Verhalten bei Überwinterern auf einer antarktischen Forschungsstation", von Hans Wortmann.
- Heft-Nr. 170/1995** – DFG-Kolloquium: Terrestrische Geowissenschaften - Geologie und Geophysik der Antarktis.
- Heft-Nr. 171/1995** – "Strukturentwicklung und Petrogenese des metamorphen Grundgebirges der nördlichen Heimefrontfjella (westliches Dronning Maud Land/Antarktika)", von Wilfried Bauer.
- Heft-Nr. 172/1995** – "Die Struktur der Erdkruste im Bereich des Scoresby Sund, Ostgrönland: Ergebnisse refraktionssismischer und gravimetrischer Untersuchungen", von Holger Mandler.
- Heft-Nr. 173/1995** – "Paläozoische Akkretion am paläopazifischen Kontinentalrand der Antarktis in Nordvictorialand – P-T-D-Geschichte und Deformationsmechanismen im Bowers Terrane", von Stefan Matzer.
- Heft-Nr. 174/1995** – "The Expedition ARKTIS-X/2 of RV 'Polarstern' in 1994", edited by Hans-W. Hubberten.
- Heft-Nr. 175/1995** – "Russian-German Cooperation: The Expedition TAYMYR 1994", edited by Christine Siebert and Dmitry Bolshiyarov.
- Heft-Nr. 176/1995** – "Russian-German Cooperation: Laptev Sea System", edited by Heidemarie Kassens, Dieter Piepenburg, Jörn Thiede, Leonid Timokhov, Hans-Wolfgang Hubberten and Sergey M. Priamikov.
- Heft-Nr. 177/1995** – "Organischer Kohlenstoff in spätquartären Sedimenten des Arktischen Ozeans: Terrigener Eintrag und marine Produktivität", von Carsten J. Schubert.
- Heft-Nr. 178/1995** – "Cruise ANTARKTIS XII/4 of RV 'Polarstern' in 1995: CTD-Report", by Jüri Sildam.
- Heft-Nr. 179/1995** – "Benthische Foraminiferenfaunen als Wassermassen-, Produktions- und Eisdriftanzeiger im Arktischen Ozean", von Jutta Wollenburg.
- Heft-Nr. 180/1995** – "Biogenopal und biogenes Barium als Indikatoren für spätquartäre Produktivitätsänderungen am antarktischen Kontinentalhang, atlantischer Sektor", von Wolfgang J. Bonn.
- Heft-Nr. 181/1995** – "Die Expedition ARKTIS X/1 des Forschungsschiffes 'Polarstern' 1994", herausgegeben von Eberhard Fahrbach.
- Heft-Nr. 182/1995** – "Laptev Sea System: Expeditions in 1994", edited by Heidemarie Kassens.
- Heft-Nr. 183/1996** – "Interpretation digitaler Parasound Echolotaufzeichnungen im östlichen Arktischen Ozean auf der Grundlage physikalischer Sedimenteigenschaften", von Uwe Bergmann.
- Heft-Nr. 184/1996** – "Distribution and dynamics of inorganic nitrogen compounds in the troposphere of continental, coastal, marine and Arctic areas", by María Dolores Andrés Hernández.
- Heft-Nr. 185/1996** – "Verbreitung und Lebensweise der Aphroditiden und Polynoiden (Polychaeta) im östlichen Weddellmeer und im Lazarevmeer (Antarktis)", von Michael Stiller.
- Heft-Nr. 186/1996** – "Reconstruction of Late Quaternary environmental conditions applying the natural radionuclides ^{230}Th , ^{10}Be , ^{231}Pa and ^{238}U : A study of deep-sea sediments from the eastern sector of the Antarctic Circumpolar Current System", by Martin Frank.
- Heft-Nr. 187/1996** – "The Meteorological Data of the Neumayer Station (Antarctica) for 1992, 1993 and 1994", by Gert König-Langlo and Andreas Herber.
- Heft-Nr. 188/1996** – "Die Expedition ANTARKTIS-XI/3 mit FS 'Polarstern' 1994", herausgegeben von Heinz Miller und Hannes Grobe.
- Heft-Nr. 189/1996** – "Die Expedition ARKTIS-VII/3 mit FS 'Polarstern' 1990", herausgegeben von Heinz Miller und Hannes Grobe.

- Heft-Nr. 190/1996** – "Cruise report of the Joint Chilean-German-Italian Magellan 'Victor Hensen' Campaign in 1994", edited by Wolf Arntz and Matthias Gorny.
- Heft-Nr. 191/1996** – "Leitfähigkeits- und Dichtemessung an Eisbohrkernen", von Frank Wilhelms.
- Heft-Nr. 192/1996** – "Photosynthese-Charakteristika und Lebensstrategie antarktischer Makroalgen", von Gabriele Weykam.
- Heft-Nr. 193/1996** – "Heterogene Reaktionen von N_2O_5 und HBr und ihr Einfluß auf den Ozonabbau in der polaren Stratosphäre", von Sabine Seisel.
- Heft-Nr. 194/1996** – "Ökologie und Populationsdynamik antarktischer Ophiuroiden (Echinodermata)", von Corinna Dahm.
- Heft-Nr. 195/1996** – "Die planktische Foraminifere *Neoglobobulimina pachyderma* (Ehrenberg) im Weddellmeer, Antarktis", von Doris Berberich.
- Heft-Nr. 196/1996** – "Untersuchungen zum Beitrag chemischer und dynamischer Prozesse zur Variabilität des stratosphärischen Ozons über der Arktis", von Birgit Heese.
- Heft-Nr. 197/1996** – "The Expedition ARKTIS-XI/2 of 'Polarstern' in 1995", edited by Gunther Krause.
- Heft-Nr. 198/1996** – "Geodynamik des Westantarktischen Riftsystems basierend auf Apatit-Spaltspuranalysen", von Frank Lisker.
- Heft-Nr. 199/1996** – "The 1993 Northeast Water Expedition. Data Report on CTD Measurements of RV 'Polarstern' Cruises ARKTIS IX/2 and 3", by Gereon Budéus and Wolfgang Schneider.
- Heft-Nr. 200/1996** – "Stability of the Thermohaline Circulation in analytical and numerical models", by Gerrit Lohmann.
- Heft-Nr. 201/1996** – "Trophische Beziehungen zwischen Makroalgen und Herbivoren in der Potter Cove (King George-Insel, Antarktis)", von Katrin Iken.
- Heft-Nr. 202/1996** – "Zur Verbreitung und Respiration ökologisch wichtiger Bodentiere in den Gewässern um Svalbard (Arktis)", von Michael K. Schmid.
- Heft-Nr. 203/1996** – "Dynamik, Rauigkeit und Alter des Meereises in der Arktis - Numerische Untersuchungen mit einem großskaligen Modell", von Markus Harder.
- Heft-Nr. 204/1996** – "Zur Parametrisierung der stabilen atmosphärischen Grenzschicht über einem antarktischen Schelfeis", von Dörthe Handorf.
- Heft-Nr. 205/1996** – "Textures and fabrics in the GRIP ice core, in relation to climate history and ice deformation", by Thorsteinn Thorsteinsson.
- Heft-Nr. 206/1996** – "Der Ozean als Teil des gekoppelten Klimasystems: Versuch der Rekonstruktion der glazialen Zirkulation mit verschiedenen komplexen Atmosphärenkomponenten", von Kerstin Fieg.
- Heft-Nr. 207/1996** – "Lebensstrategien dominanter antarktischer Oithonidae (Cyclopoida, Copepoda) und Oncaeididae (Poecilostomatoida, Copepoda) im Bellingshausenmeer", von Cornelia Metz.
- Heft-Nr. 208/1996** – "Atmosphäreneinfluß bei der Fernerkundung von Meereis mit passiven Mikrowellenradiometern", von Christoph Oelke.
- Heft-Nr. 209/1996** – "Klassifikation von Radarsatellitendaten zur Meereisererkennung mit Hilfe von Line-Scanner-Messungen", von Axel Bochert.
- Heft-Nr. 210/1996** – "Die mit ausgewählten Schwämmen (Hexactinellida und Demospongiae) aus dem Weddellmeer, Antarktis, vergesellschaftete Fauna", von Kathrin Kunzmann.
- Heft-Nr. 211/1996** – "Russian-German Cooperation: The Expedition TAYMYR 1995 and the Expedition KOLYMA 1995", by Dima Yu. Bolshiyakov and Hans-W. Hubberten.
- Heft-Nr. 212/1996** – "Surface-sediment composition and sedimentary processes in the central Arctic Ocean and along the Eurasian Continental Margin", by Ruediger Stein, Gennadij I. Ivanov, Michael A. Levitan, and Kirsten Fahl.
- Heft-Nr. 213/1996** – "Gonadenentwicklung und Eiproduktion dreier *Calanus*-Arten (Copepoda): Freilandbeobachtungen, Histologie und Experimente", von Barbara Niehoff.
- Heft-Nr. 214/1996** – "Numerische Modellierung der Übergangszone zwischen Eisschild und Eisschelf", von Christoph Mayer.
- Heft-Nr. 215/1996** – "Arbeiten der AWI-Forschungsstelle Potsdam in Antarktika, 1994/95", herausgegeben von Ulrich Wand.
- Heft-Nr. 216/1996** – "Rekonstruktion quartärer Klimaänderungen im atlantischen Sektor des Südpolarmeeres anhand von Radiolarien", von Uta Brathauer.
- Heft-Nr. 217/1996** – "Adaptive Semi-Lagrange-Finite-Elemente-Methode zur Lösung der Flachwassergleichungen: Implementierung und Parallelisierung", von Jörn Behrens.
- Heft-Nr. 218/1997** – "Radiation and Eddy Flux Experiment 1995 (REFLEX III)", by Jörg Hartmann, Axel Bochert, Dietmar Freese, Christoph Kottmeier, Dagmar Nagel and Andreas Reuter.
- Heft-Nr. 219/1997** – "Die Expedition ANTARKTIS-XII mit FS 'Polarstern' 1995. Bericht vom Fahrtabschnitt ANT-XII/3", herausgegeben von Wilfried Jokat und Hans Oerter.
- Heft-Nr. 220/1997** – "Ein Beitrag zum Schwerfeld im Bereich des Weddellmeeres, Antarktis. Nutzung von Altimetermessungen des GEOSAT und ERS-1", von Tilo Schöne.
- Heft-Nr. 221/1997** – "Die Expeditionen ANTARKTIS-XIII/1-2 des Forschungsschiffes 'Polarstern' 1995/96", herausgegeben von Ulrich Bathmann, Mike Lucas und Victor Smetacek.
- Heft-Nr. 222/1997** – "Tectonic Structures and Glaciomarine Sedimentation in the South-Eastern Weddell Sea from Seismic Reflection Data", by László Oszkó.

- Heft-Nr. 223/1997** – “Bestimmung der Meereisdicke mit seismischen und elektromagnetisch-induktiven Verfahren”, von Christian Haas.
- Heft-Nr. 224/1997** – “Troposphärische Ozonvariationen in Polarregionen”, von Silke Wessel.
- Heft-Nr. 225/1997** – “Biologische und ökologische Untersuchungen zur kryopelagischen Amphipodenfauna des arktischen Meereises”, von Michael Poltermann.
- Heft-Nr. 226/1997** – “Scientific Cruise Report of the Arctic Expedition ARK-XI/1 of RV ‘Polarstern’ in 1995”, edited by Eike Rachor.
- Heft-Nr. 227/1997** – “Der Einfluß kompatibler Substanzen und Kyroprotektoren auf die Enzyme Malatdehydrogenase (MDH) und Glucose-6-phosphat-Dehydrogenase (G6P-DH) aus *Acrosiphonia arctica* (Chlorophyta) der Arktis”, von Katharina Kück.
- Heft-Nr. 228/1997** – “Die Verbreitung epibenthischer Mollusken im chilenischen Beagle-Kanal”, von Katrin Linse.
- Heft-Nr. 229/1997** – “Das Mesozooplankton im Laptevmeer und östlichen Nansen-Becken - Verteilung und Gemeinschaftsstrukturen im Spätsommer”, von Hinrich Hanssen.
- Heft-Nr. 230/1997** – “Modell eines adaptierbaren, rechnergestützten, wissenschaftlichen Arbeitsplatzes am Alfred-Wegener-Institut für Polar- und Meeresforschung”, von Lutz-Peter Kurdelski.
- Heft-Nr. 231/1997** – “Zur Ökologie arktischer und antarktischer Fische: Aktivität, Sinnesleistungen und Verhalten”, von Christopher Zimmermann.
- Heft-Nr. 232/1997** – “Persistente chlororganische Verbindungen in hochantarktischen Fischen”, von Stephan Zimmermann.
- Heft-Nr. 233/1997** – “Zur Ökologie des Dimethylsulfoniumpropionat (DMSP)-Gehaltes temperierter und polarer Phytoplanktongemeinschaften im Vergleich mit Laborkulturen der Coccolithophoride *Emiliania huxleyi* und der antarktischen Diatomee *Nitzschia lecontei*”, von Doris Meyerdierks.
- Heft-Nr. 234/1997** – “Die Expedition ARCTIC '96 des FS ‘Polarstern’ (ARK XII) mit der Arctic Climate System Study (ACSYS)”, von Ernst Augstein und den Fahrteilnehmern.
- Heft-Nr. 235/1997** – “Polonium-210 und Blei-210 im Südpolarmeer: Natürliche Tracer für biologische und hydrographische Prozesse im Oberflächenwasser des Antarktischen Zirkumpolarstroms und des Weddellmeeres”, von Jana Friedrich.
- Heft-Nr. 236/1997** – “Determination of atmospheric trace gas amounts and corresponding natural isotopic ratios by means of ground-based FTIR spectroscopy in the high Arctic”, by Arndt Meier.
- Heft-Nr. 237/1997** – “Russian-German Cooperation: The Expedition TAYMYR / SEVERNAYA ZEMLYA 1996”, edited by Martin Melles, Birgit Hagedorn and Dmitri Yu. Bolshiyakov.
- Heft-Nr. 238/1997** – “Life strategy and ecophysiology of Antarctic macroalgae”, by Iván M. Gómez.
- Heft-Nr. 239/1997** – “Die Expedition ANTARKTIS XIII/4-5 des Forschungsschiffes ‘Polarstern’ 1996”, herausgegeben von Eberhard Fahrbach und Dieter Gerdes.
- Heft-Nr. 240/1997** – “Untersuchungen zur Chrom-Speziation im Meerwasser, Meereis und Schnee aus ausgewählten Gebieten der Arktis”, von Heide Giese.
- Heft-Nr. 241/1997** – “Late Quaternary glacial history and paleoceanographic reconstructions along the East Greenland continental margin: Evidence from high-resolution records of stable isotopes and ice-rafted debris”, by Seung-Il Nam.
- Heft-Nr. 242/1997** – “Thermal, hydrological and geochemical dynamics of the active layer at a continuous site, Taymyr Peninsula, Siberia”, by Julia Boike.
- Heft-Nr. 243/1997** – “Zur Paläoozeanographie hoher Breiten: Stellvertreterdaten aus Foraminiferen”, von Andreas Mackensen.
- Heft-Nr. 244/1997** – “The Geophysical Observatory at Neumayer Station, Antarctica. Geomagnetic and seismological observations in 1995 and 1996”, by Alfons Eckstaller, Thomas Schmidt, Viola Gaw, Christian Müller and Johannes Rogenhagen.
- Heft-Nr. 245/1997** – “Temperaturbedarf und Biogeographie mariner Makroalgen - Anpassung mariner Makroalgen an tiefe Temperaturen”, von Bettina Bischoff-Bäsmann.
- Heft-Nr. 246/1997** – “Ökologische Untersuchungen zur Fauna des arktischen Meereises”, von Christine Friedrich.
- Heft-Nr. 247/1997** – “Entstehung und Modifizierung von marinen gelösten organischen Substanzen”, von Berit Kirchhoff.
- Heft-Nr. 248/1997** – “Laptev Sea System: Expeditions in 1995”, edited by Heidemarie Kassens.
- Heft-Nr. 249/1997** – “The Expedition ANTARKTIS XIII/3 (EASIZ I) of RV ‘Polarstern’ to the eastern Weddell Sea in 1996”, edited by Wolf Arntz and Julian Gutt.
- Heft-Nr. 250/1997** – “Vergleichende Untersuchungen zur Ökologie und Biodiversität des Mega-Epibenthos der Arktis und Antarktis”, von Andreas Starbom.
- Heft-Nr. 251/1997** – “Zeitliche und räumliche Verteilung von Mineralvergesellschaftungen in spätquartären Sedimenten des Arktischen Ozeans und ihre Nützlichkeit als Klimaindikatoren während der Glazial/Interglazial-Wechsel”, von Christoph Vogt.
- Heft-Nr. 252/1997** – “Solitäre Ascidien in der Potter Cove (King George Island, Antarktis). Ihre ökologische Bedeutung und Populationsdynamik”, von Stephan Kühne.
- Heft-Nr. 253/1997** – “Distribution and role of microprotozoa in the Southern Ocean”, by Christine Klaas.
- Heft-Nr. 254/1997** – “Die spätquartäre Klima- und Umweltgeschichte der Bunge-Oase, Ostantarktis”, von Thomas Kulbe.

- Heft-Nr. 255/1997** – “Scientific Cruise Report of the Arctic Expedition ARK-XIII/2 of RV ‘Polarstern’ in 1997”, edited by Ruediger Stein and Kirsten Fahl.
- Heft-Nr. 256/1998** – “Das Radionuklid Tritium im Ozean: Meßverfahren und Verteilung von Tritium im Südatlantik und im Weddellmeer”, von Jürgen Sültenfuß.
- Heft-Nr. 257/1998** – “Untersuchungen der Saisonalität von atmosphärischen Dimethylsulfid in der Arktis und Antarktis” von Christoph Kleefeld.
- Heft-Nr. 258/1998** – “Bellingshausen- und Amundsenmeer: Entwicklung eines Sedimentationsmodells”, von Frank-Oliver Nitsche.
- Heft-Nr. 259/1998** – “The Expedition ANTARKTIS-XIV/4 of RV ‘Polarstern’ in 1997”, by Dieter K. Fütterer.
- Heft-Nr. 260/1998** – “Die Diatomeen der Laptevsee (Arktischer Ozean): Taxonomie und biogeographische Verbreitung” von Holger Cremer.
- Heft-Nr. 261/1998** – “Die Krustenstruktur und Sedimentdecke des Eurasischen Beckens, Arktischer Ozean: Resultate aus seismischen und gravimetrischen Untersuchungen”, von Estella Weigelt.
- Heft-Nr. 262/1998** – “The Expedition ARKTIS-XIII/3 of RV ‘Polarstern’ in 1997”, by Gunther Krause.
- Heft-Nr. 263/1998** – “Thermo-tektonische Entwicklung von Oates Land und der Shackleton Range (Antarktis) basierend auf Spaltspuranalysen”, von Thorsten Schäfer.
- Heft-Nr. 264/1998** – “Messungen der stratosphärischen Spurengase ClO, HCl, O₃, N₂O, H₂O und OH mittels flugzeuggetragener Submillimeterwellen-Radiometrie”, von Joachim Urban.
- Heft-Nr. 265/1998** – “Untersuchungen zu Massenhaushalt und Dynamik des Ronne Ice Shelves, Antarktis”, von Astrid Lambrecht.
- Heft-Nr. 266/1998** – “Scientific Cruise Report of the Kara Sea Expedition of RV ‘Akademik Boris Petrov’ in 1997”, edited by Jens Matthiessen and Oleg Stepanets.
- Heft-Nr. 267/1998** – “Die Expedition ANTARKTIS-XIV mit FS ‘Polarstern’ 1997. Bericht vom Fahrtabschnitt ANT-XIV/3” herausgegeben von Wilfried Jokat und Hans Oerter.
- Heft-Nr. 268/1998** – “Numerische Modellierung der Wechselwirkung zwischen Atmosphäre und Meereis in der arktischen Eisrandzone”, von Gerit Birnbaum.
- Heft-Nr. 269/1998** – “Katabatic wind and Boundary Layer Front Experiment around Greenland (KABEG ‘97)”, by Günther Heinemann.
- Heft-Nr. 270/1998** – “Architecture and evolution of the continental crust of East Greenland from integrated geophysical studies”, by Vera Schindwein.
- Heft-Nr. 271/1998** – “Winter Expedition to the Southwestern Kara Sea - Investigations on Formation and Transport of Turbid Sea-Ice”, by Dirk Dethleff, Peter Loewe, Dominik Weiel, Hartmut Nies, Gesa Kuhlmann, Christian Bahe and Gennady Tarasov.
- Heft-Nr. 272/1998** – “FTIR-Emissionsspektroskopische Untersuchungen der arktischen Atmosphäre”, von Edo Becker.
- Heft-Nr. 273/1998** – “Sedimentation und Tektonik im Gebiet des Agulhas Rückens und des Agulhas Plateaus (‘SETA-RAP’)”, von Gabriele Uenzelmann-Neben.
- Heft-Nr. 274/1998** – “The Expedition ANTARKTIS XIV/2”, by Gerhard Kattner.
- Heft-Nr. 275/1998** – “Die Auswirkung der ‘NorthEastWater’-Polynya auf die Sedimentation vor NO-Grönland und Untersuchungen zur Paläo-Ozeanographie seit dem Mittelwechsell”, von Hanne Notholt.
- Heft-Nr. 276/1998** – “Interpretation und Analyse von Potentialfelddaten im Weddellmeer, Antarktis: der Zerfall des Superkontinents Gondwana”. von Michael Studinger.
- Heft-Nr. 277/1998** – “Koordiniertes Programm Antarktisforschung”. Berichtskolloquium im Rahmen des Koordinierten Programms “Antarktisforschung mit vergleichenden Untersuchungen in arktischen Eisgebieten”, herausgegeben von Hubert Miller.
- Heft-Nr. 278/1998** – “Messung stratosphärischer Spurengase über Ny-Ålesund, Spitzbergen, mit Hilfe eines bodengebundenen Mikrowellen-Radiometers”, von Uwe Raffalski.
- Heft-Nr. 279/1998** – “Arctic Paleo-River Discharge (APARD). A New Research Programme of the Arctic Ocean Science Board (AOSB)”, edited by Ruediger Stein.
- Heft-Nr. 280/1998** – “Fernerkundungs- und GIS-Studien in Nordostgrönland”, von Friedrich Jung-Rothenhäusler.
- Heft-Nr. 281/1998** – “Rekonstruktion der Oberflächenwassermassen der östlichen Laptevsee im Holozän anhand aquatischen Palynomorphen”, von Martina Kunz-Pirung.
- Heft-Nr. 282/1998** – “Scavenging of ²³¹Pa and ²³⁰Th in the South Atlantic: Implications for the use of the ²³¹Pa/²³⁰Th ratio as a paleoproductivity proxy”, by Hans-Jürgen Walter.
- Heft-Nr. 283/1998** – “Sedimente im arktischen Meereis - Eintrag, Charakterisierung und Quantifizierung”, von Frank Lindemann.
- Heft-Nr. 284/1998** – “Langzeitanalyse der antarktischen Meereisbedeckung aus passiven Mikrowellendaten”, von Christian H. Thomas.
- Heft-Nr. 285/1998** – “Mechanismen und Grenzen der Temperaturanpassung beim Pierwurm *Arenicola marina* (L.)”, von Angela Sommer.
- Heft-Nr. 286/1998** – “Energieumsätze benthischer Filtrierer der Potter Cove (King George Island, Antarktis)”, von Jens Kowalke.
- Heft-Nr. 287/1998** – “Scientific Cooperation in the Russian Arctic: Research from the Barents Sea up to the Laptev Sea”, edited by Eike Rachor.

- Heft-Nr. 288/1998** – “Alfred Wegener. Kommentiertes Verzeichnis der schriftlichen Dokumente seines Lebens und Wirkens“, von Ulrich Wutzke.
- Heft-Nr. 289/1998** – “Retrieval of Atmospheric Water Vapor Content in Polar Regions Using Spaceborne Microwave Radiometry“, by Jungang Miao.
- Heft-Nr. 290/1998** – “Strukturelle Entwicklung und Petrogenese des nördlichen Kristallingürtels der Shackleton Range, Antarktis: Proterozoische und Ross-orogene Krustendynamik am Rand des Ostantarktischen Kratons“, von Axel Brommer.
- Heft-Nr. 291/1998** – “Dynamik des arktischen Meereises - Validierung verschiedener Rheologieansätze für die Anwendung in Klimamodellen“, von Martin Kreyscher.
- Heft-Nr. 292/1998** – “Anthropogene organische Spurenstoffe im Arktischen Ozean. Untersuchungen chlorierter Biphenyle und Pestizide in der Laptevsee, technische und methodische Entwicklungen zur Probenahme in der Arktis und zur Spurenstoffanalyse“, von Sven Utschakowski.
- Heft-Nr. 293/1998** – “Rekonstruktion der spätquartären Klima- und Umweltgeschichte der Schirmacher Oase und des Wohlthat Massivs (Ostantarktika)“, von Markus Julius Schwab.
- Heft-Nr. 294/1998** – “Besiedlungsmuster der benthischen Makrofauna auf dem ostgrönländischen Kontinentalhang“, von Klaus Schnack.
- Heft-Nr. 295/1998** – “Gehäuseuntersuchungen an planktischen Foraminiferen hoher Breiten: Hinweise auf Umweltveränderungen während der letzten 140.000 Jahre“, von Harald Hommers.
- Heft-Nr. 296/1998** – “Scientific Cruise Report of the Arctic Expedition ARK-XIII/1 of RV ‘Polarstern’ in 1997“, edited by Michael Spindler, Wilhelm Hagen and Dorothea Stübing.
- Heft-Nr. 297/1998** – “Radiometrische Messungen im arktischen Ozean - Vergleich von Theorie und Experiment“, von Klaus-Peter Johnsen.
- Heft-Nr. 298/1998** – “Patterns and Controls of CO₂ Fluxes in Wet Tundra Types of the Taimyr Peninsula, Siberia - the Contribution of Soils and Mosses“, by Martin Sommerkorn.

* vergriffen / out of print.

** nur noch beim Autor / only from the author.